3-Acetyl oleanolic acid (26)

รูป 24 ^{1}H-NMR สเปกตรัมของ 3-acetyl oleanolic acid (400 MHz) ใน CDCl$_3$
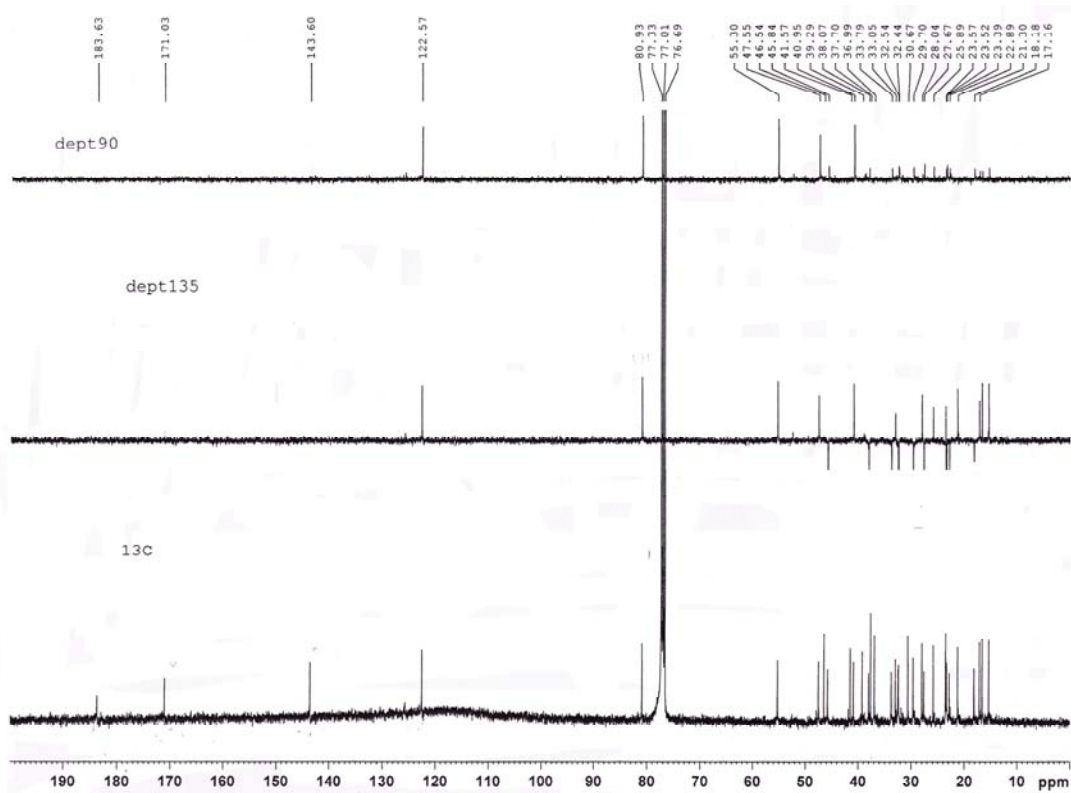
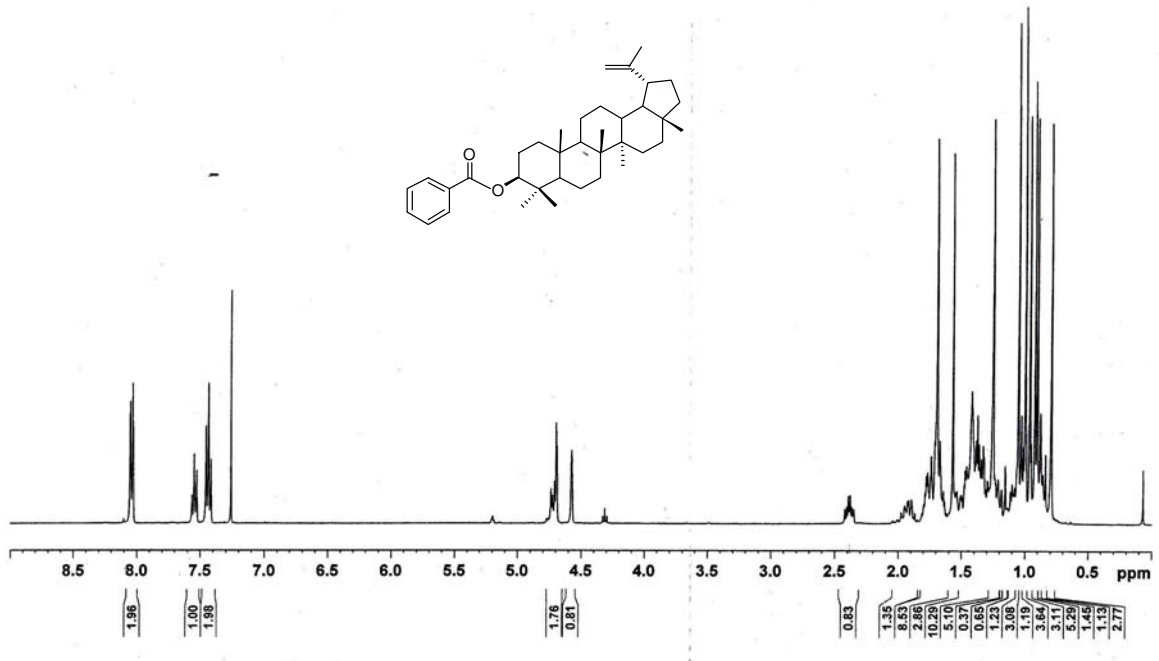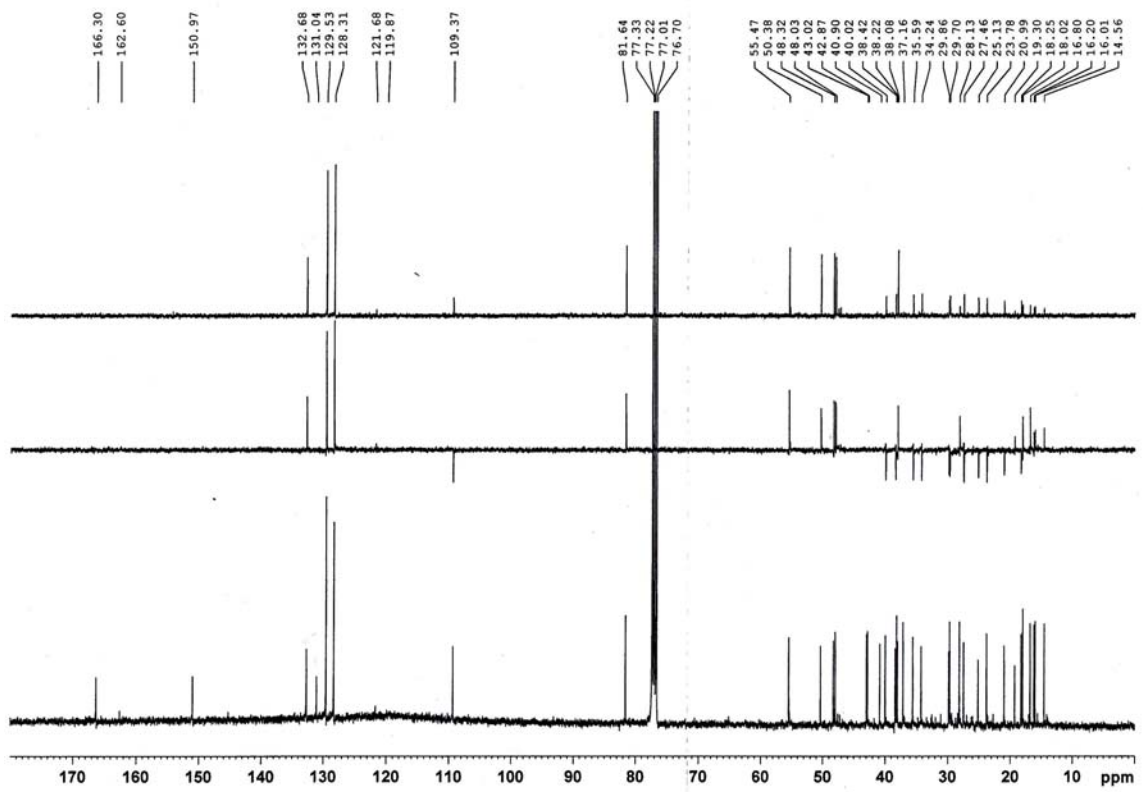**รูป 25** ^{13}C, Dept135, Dept90 NMR สเปกตรัมของ 3-acetyl oleanolic acid (100 MHz) ใน CDCl$_3$

Lupeol benzoate (16)

รูป 26 ^{1}H-NMR สเปกตรัมของ lupeol benzoate (400 MHz) ใน CDCl$_3$

รูป 27 ^{13}C, Dept135, Dept90 NMR สเปกตรัมของ lupeol benzoate (100 MHz) ใน CDCl$_3$

Lupeol cinnamate(17)
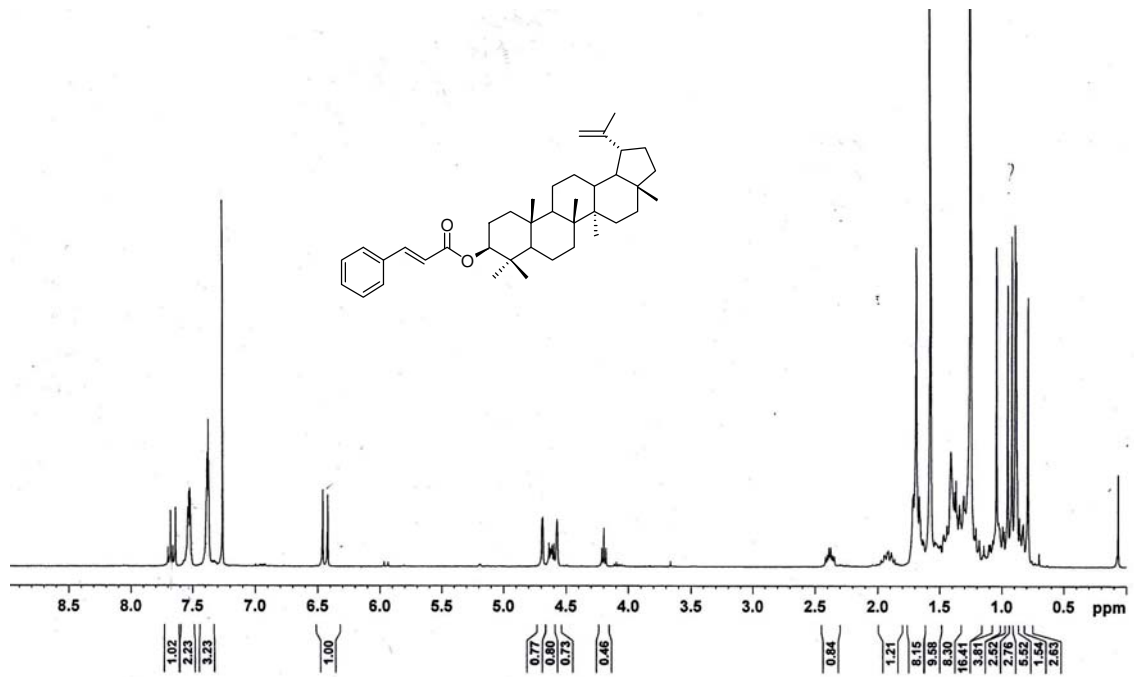
รูป 28 ^{1}H-NMR สเปกตรัมของ lupeol cinnamate (400 MHz) ใน CDCl$_3$
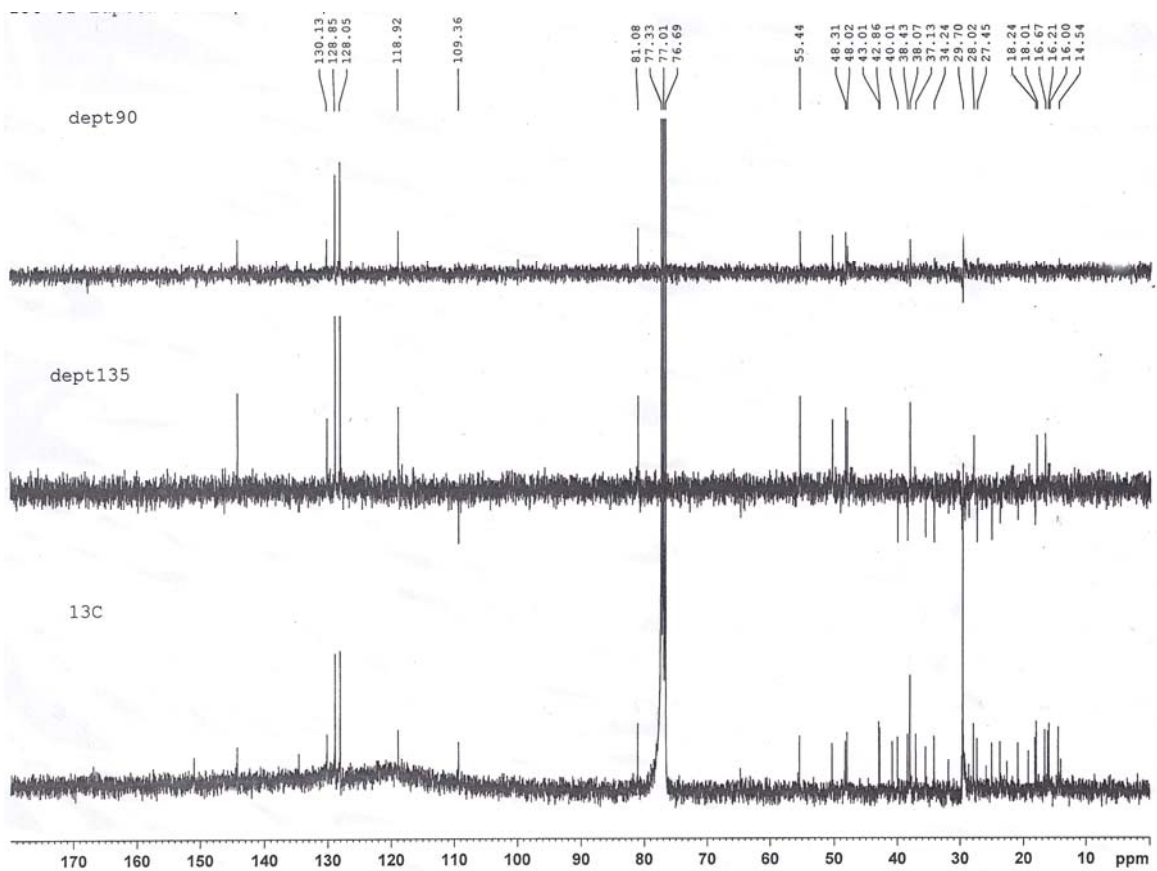
รูป 29 ^{13}C, Dept135, Dept90 NMR สเปกตรัมของ lupeol cinnamate (100 MHz) ใน CDCl$_3$
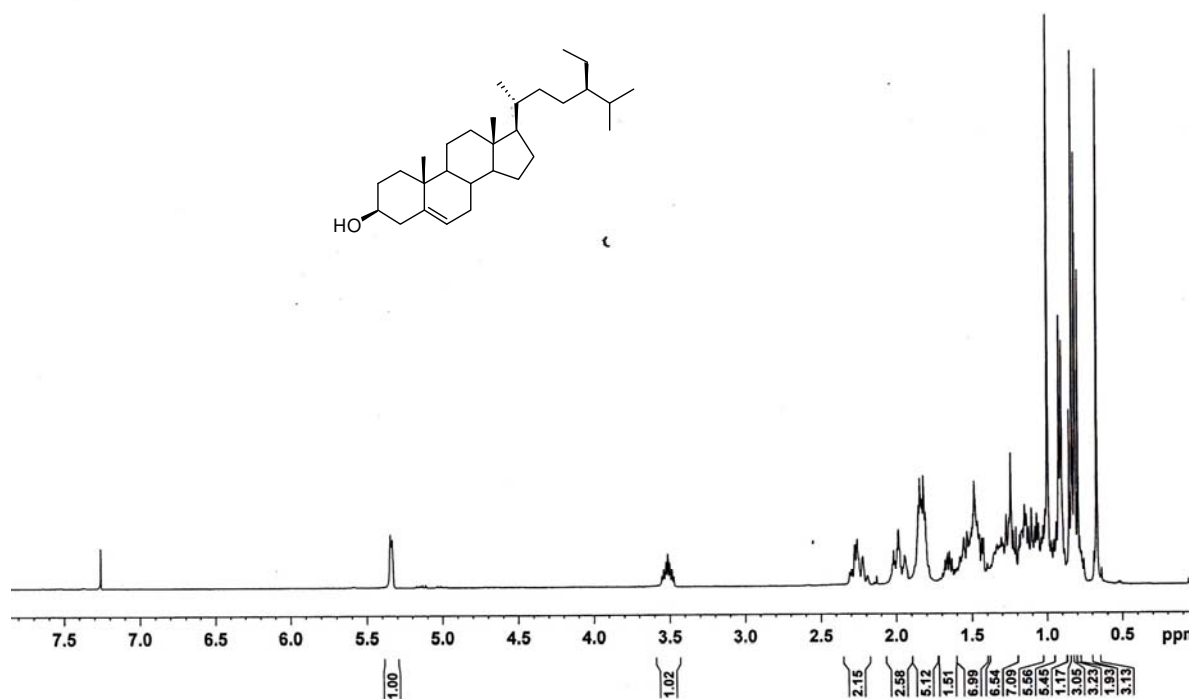
β-Sitosterol (9)

รูป 30 ¹H-NMR สเปกตรัมของ β-sitosterol (400 MHz) ใน CDCl₃
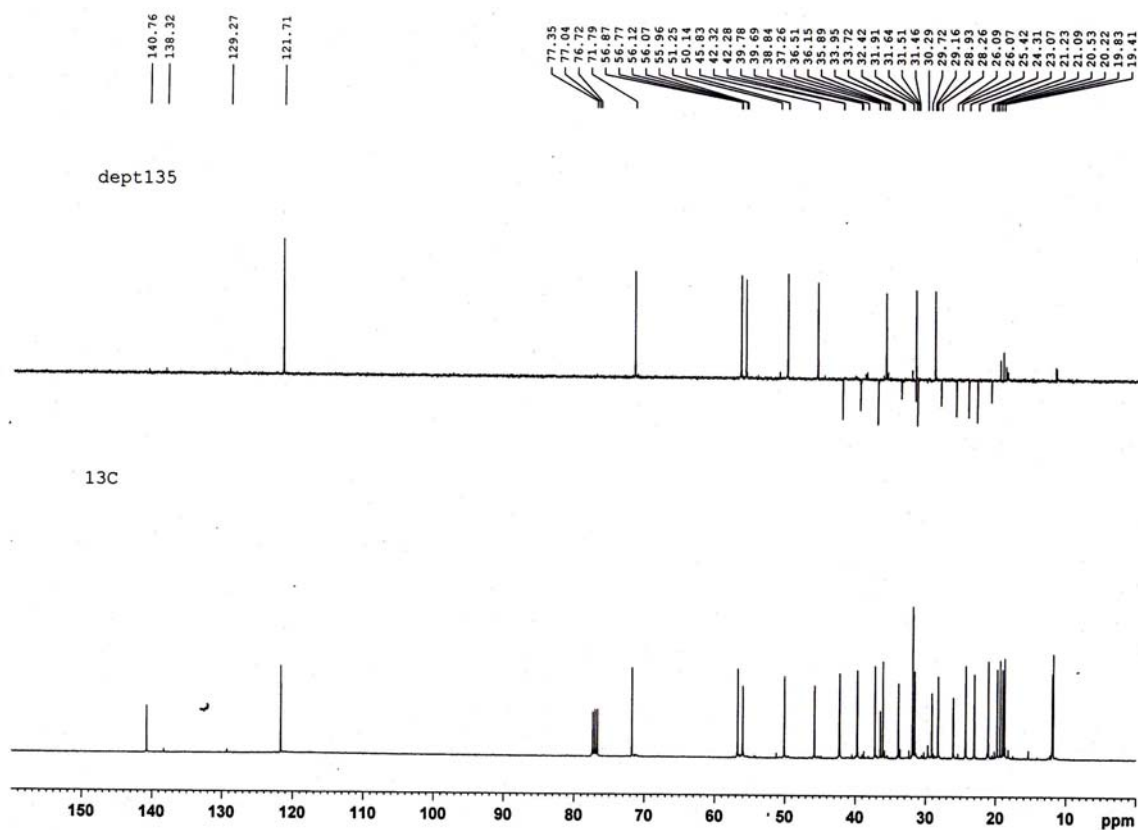
รูป 31 ¹³C, Dept135 NMR สเปกตรัมของ β-sitosterol (100 MHz) ใน CDCl₃

Stigmast-4-ene-3-one (15)
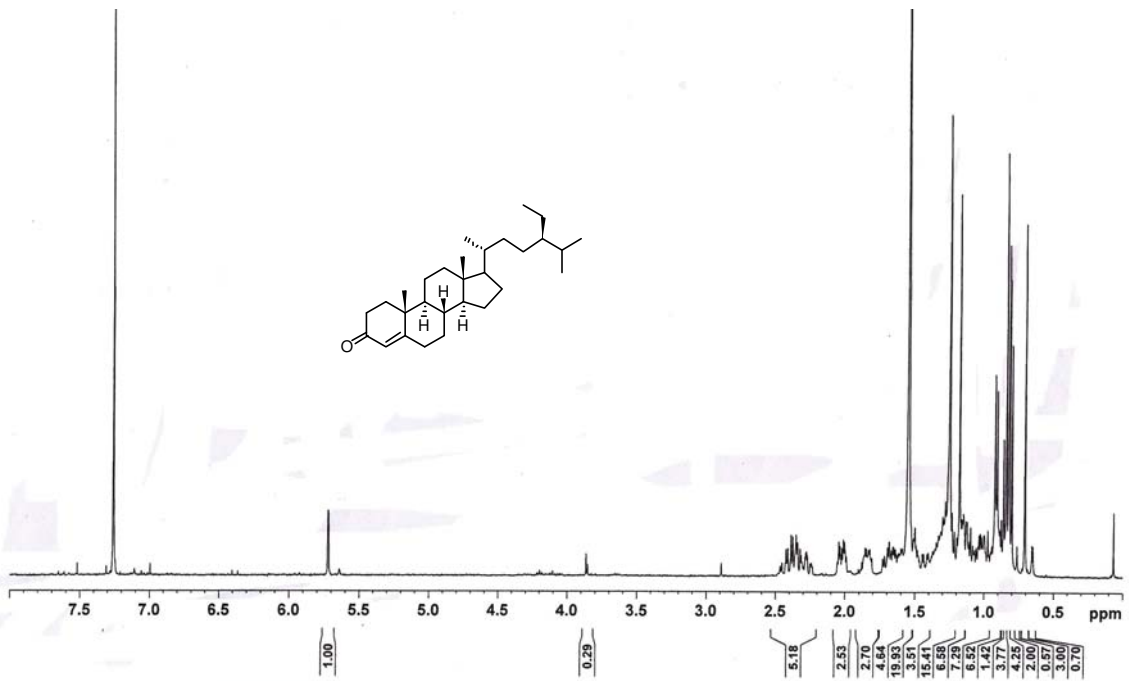
รูป 32 ^{1}H-NMR สเปกตรัมของ stigmast-4-ene-3-one (400 MHz) ใน CDCl$_3$
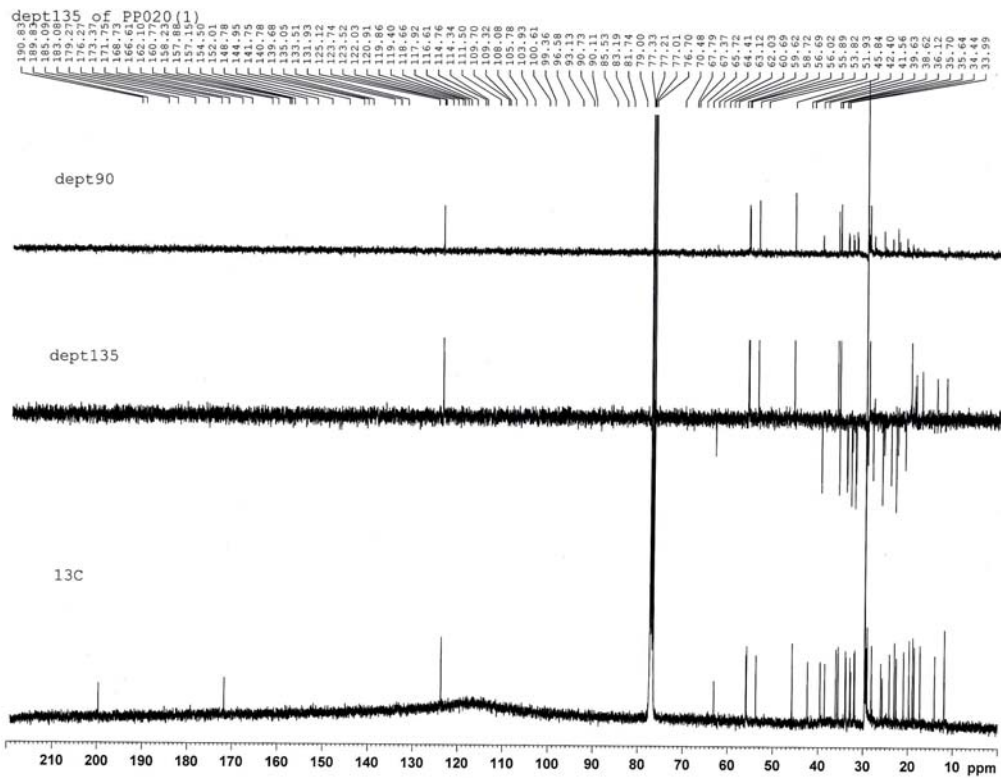
รูป 33 ^{13}C, Dept135 NMR สเปกตรัมของ stigmast-4-ene-3-one (100 MHz) ใน CDCl$_3$

β-Sitosterol benzoate (18)
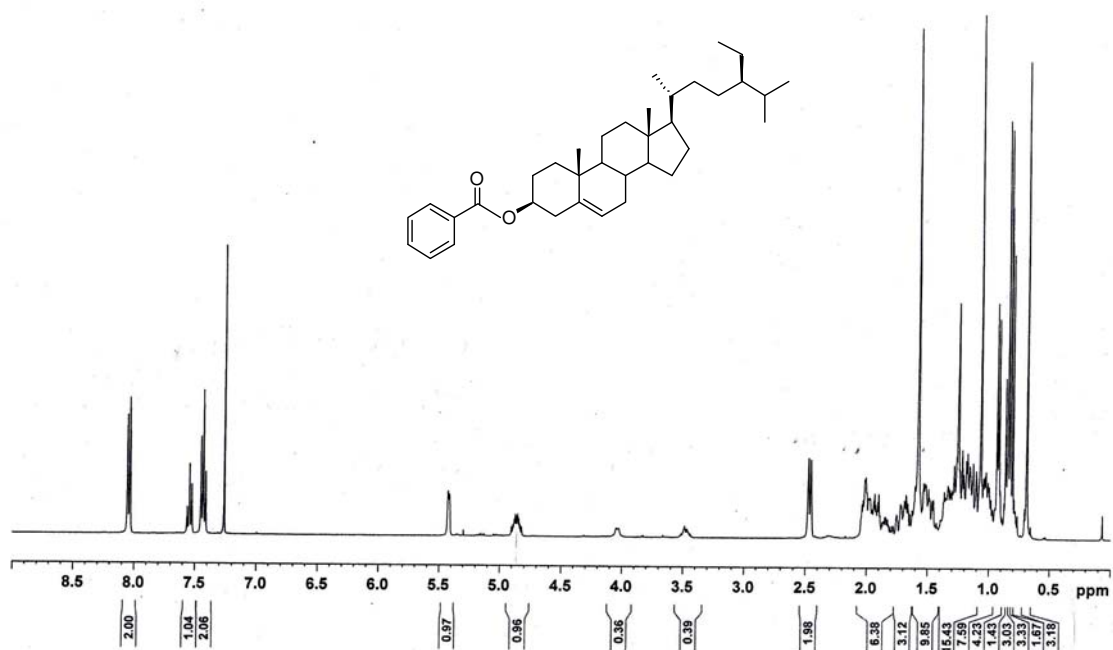
รูป 34 ^{1}H-NMR สเปกตรัมของ β-sitosterol benzoate (400 MHz) ใน CDCl$_3$
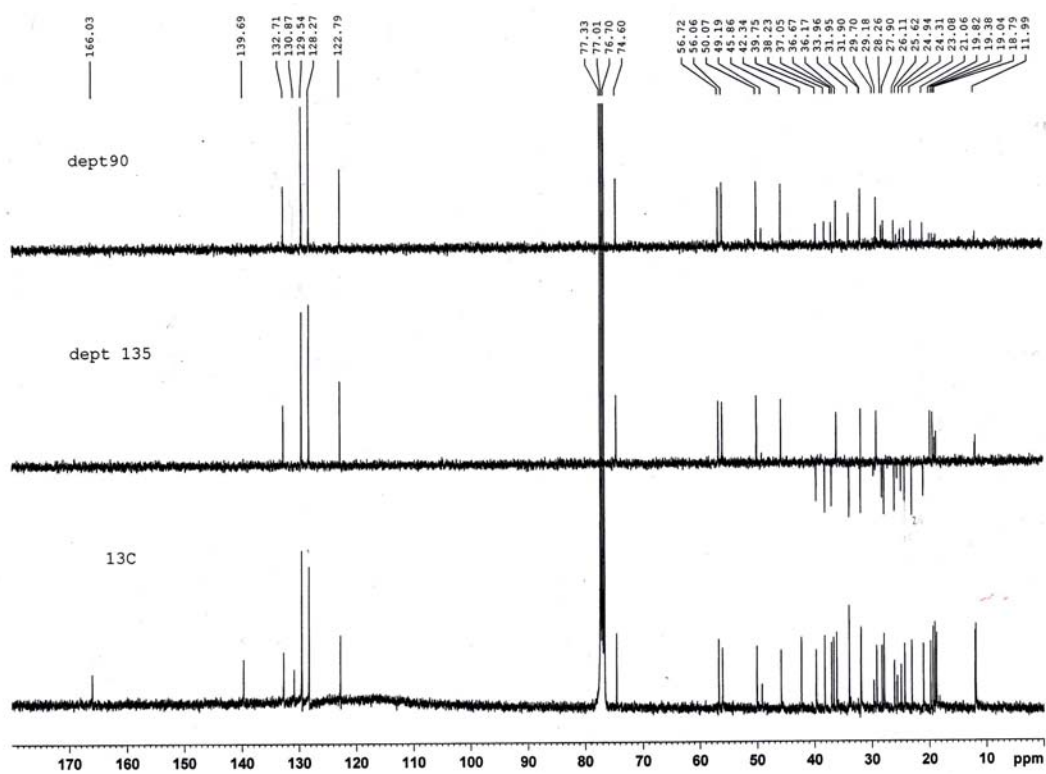
รูป 35 ^{13}C, Dept135 NMR สเปกตรัมของ β-sitosterol benzoate (100 MHz) ใน CDCl$_3$

β-Sitosterol cinnamate (19)
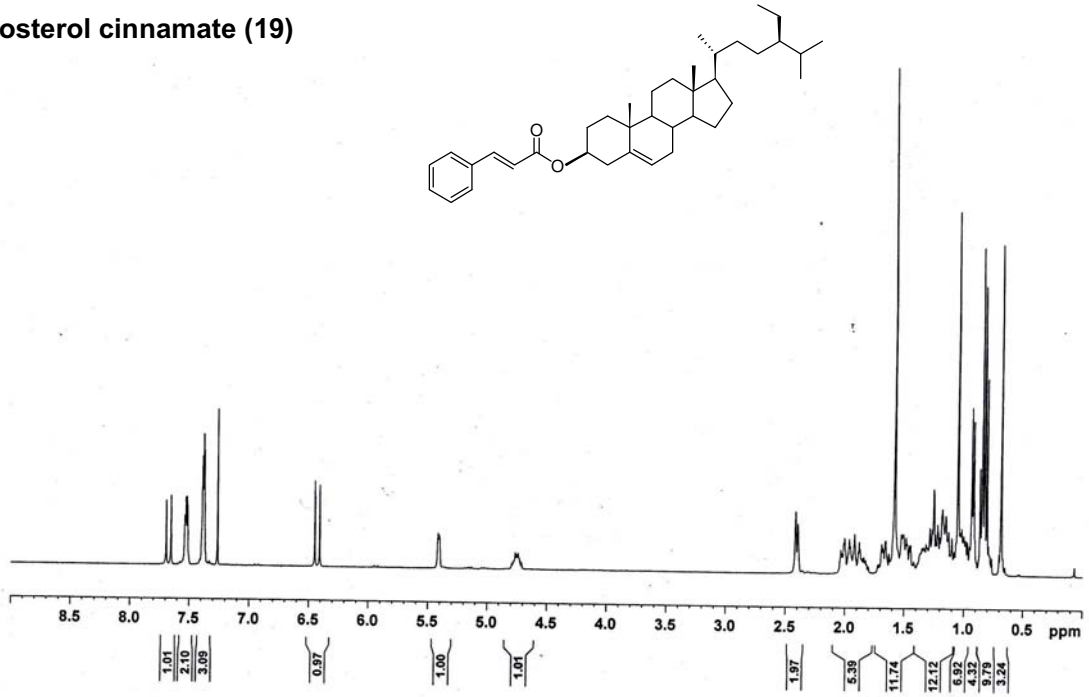
รูป 36 ^{1}H-NMR สเปกตรัมของ β-sitosterol cinnamate (400 MHz) ใน $CDCl_3$
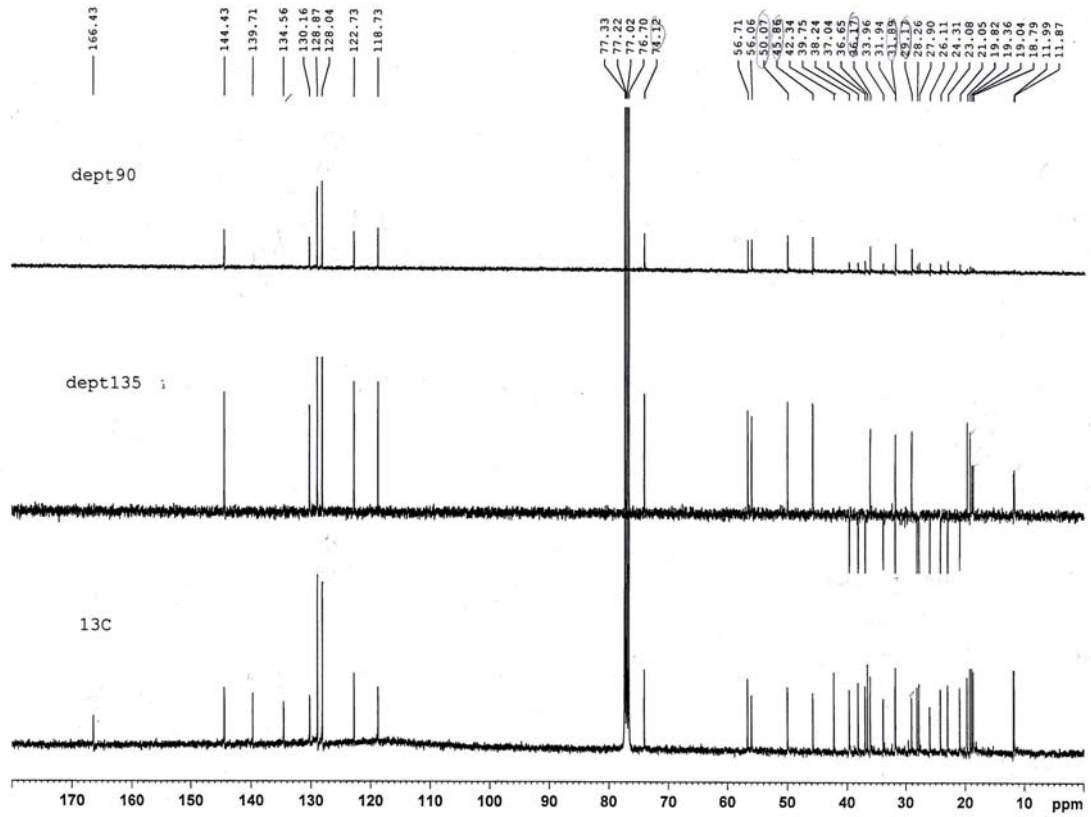
รูป 37 ^{13}C, Dept135 NMR สเปกตรัมของ β-sitosterol cinnamate (100 MHz) ใน $CDCl_3$

trans-Octadecyl ferulate (11)
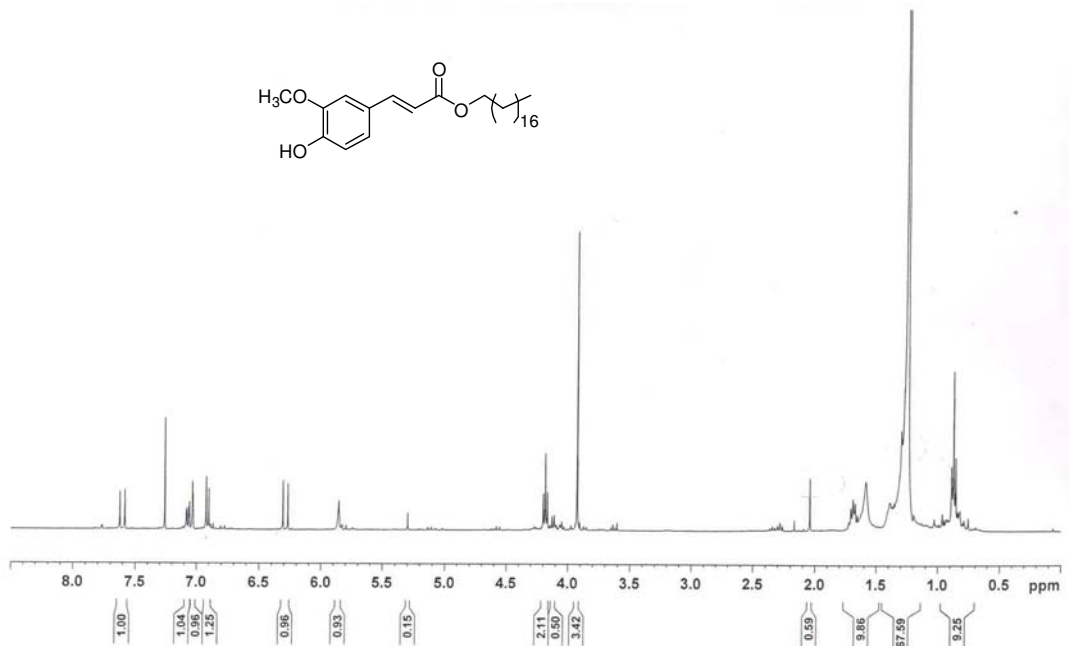
รูป 38 ^{1}H-NMR สเปกตรัมของ _trans_-octadecyl ferulate (400 MHz) ใน CDCl$_3$
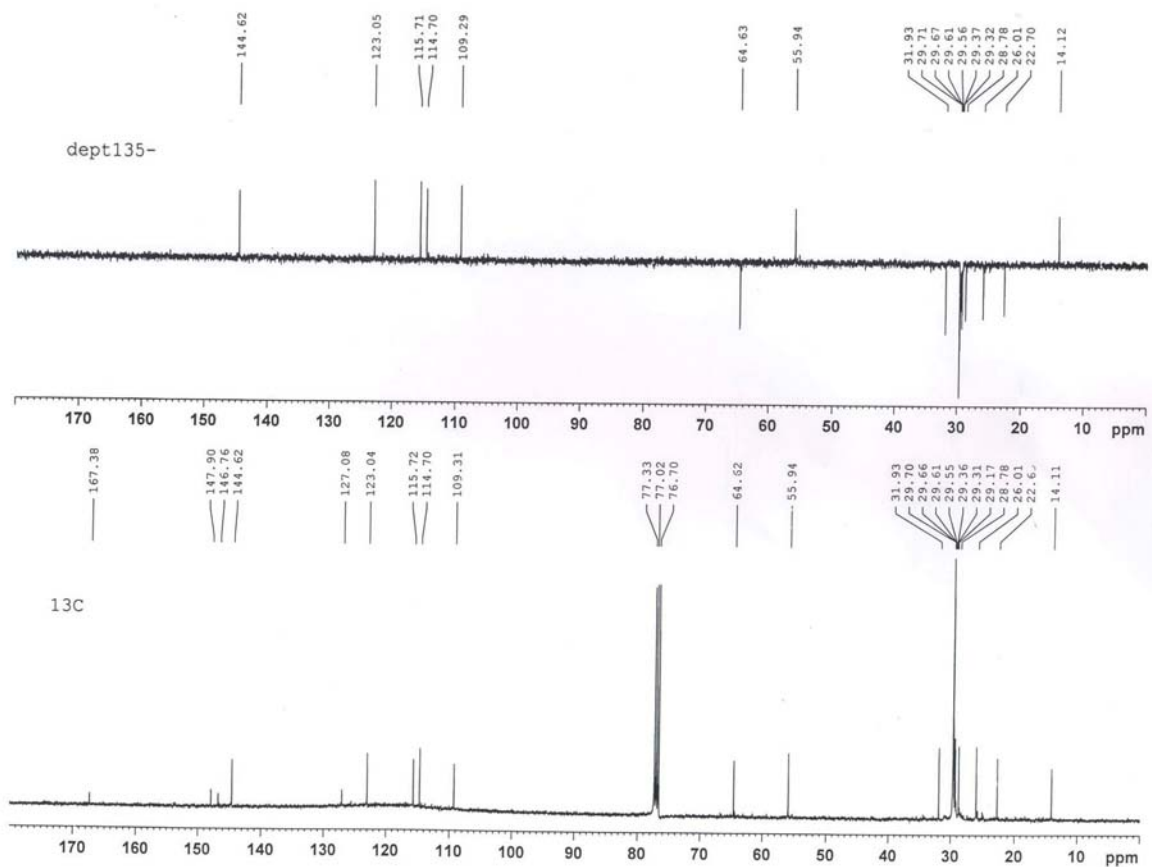
รูป 39 ^{13}C , Dept 135 สเปกตรัมของ _trans_-octadecyl ferulate (100 MHz) ใน CDCl$_3$

O-Acetyl-*trans*-octadecyl ferulate (10)
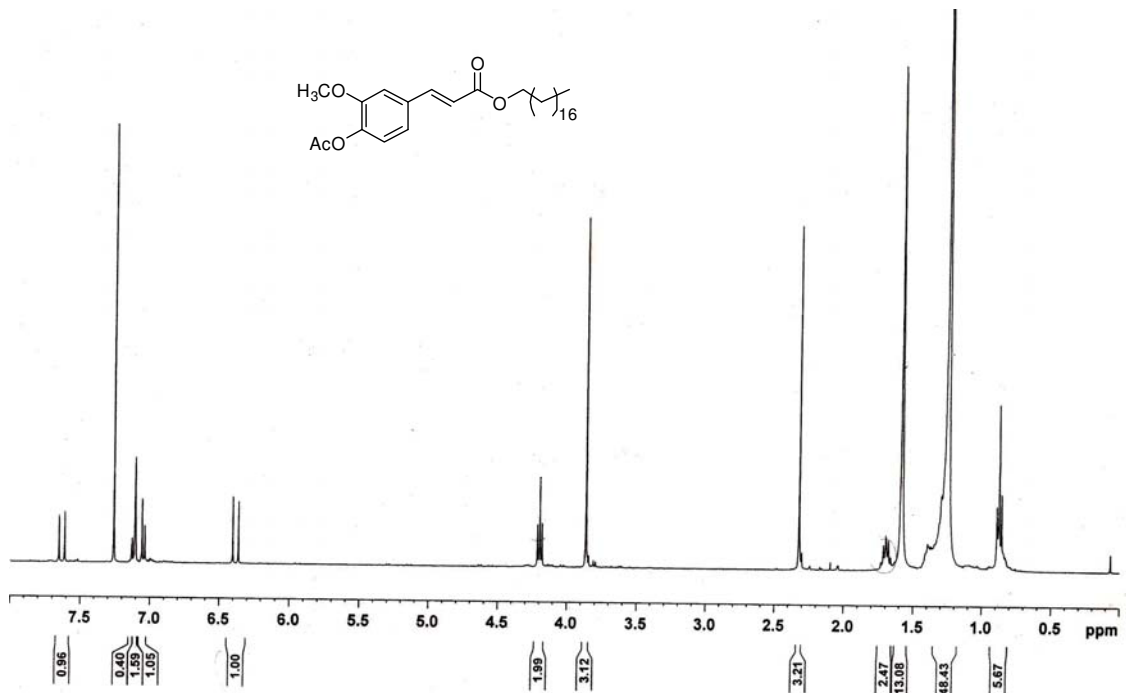
รูป 40 ^{1}H-NMR สเปกตรัมของ *O*-acetyl-*trans*-octadecyl ferulate (400 MHz) ใน CDCl$_3$
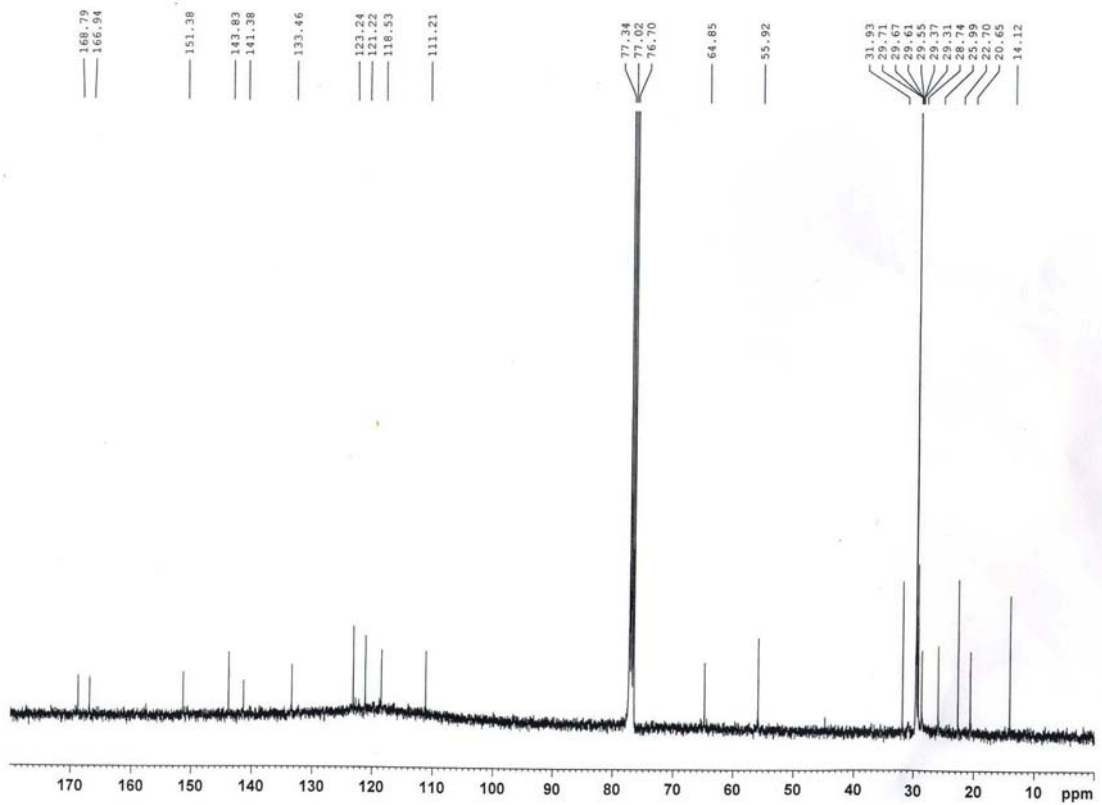
รูป 41 ^{13}C สเปกตรัมของ *O*-acetyl-*trans*-octadecyl ferulate (100 MHz) ใน CDCl$_3$

2,7-Dihydroxyxanthone (14)
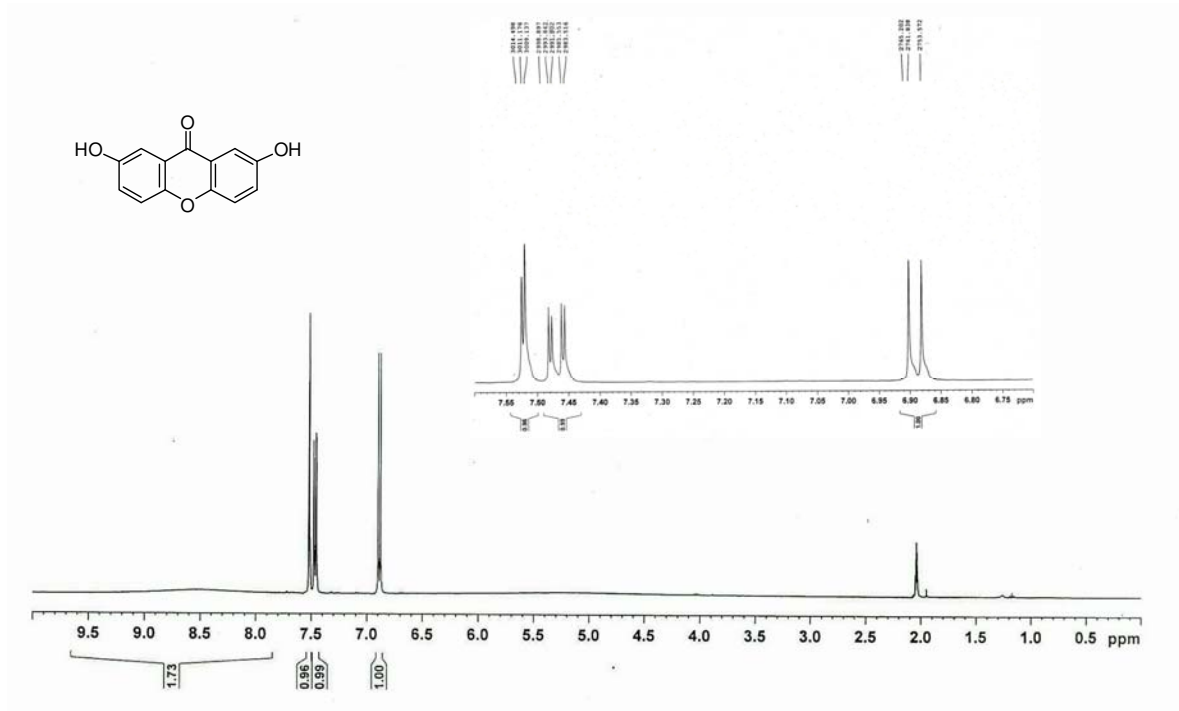
รูป 42 ^{1}H-NMR สเปกตรัมของ 2,7-dihydroxyxanthone (400 MHz) ใน acetone-d$_6$
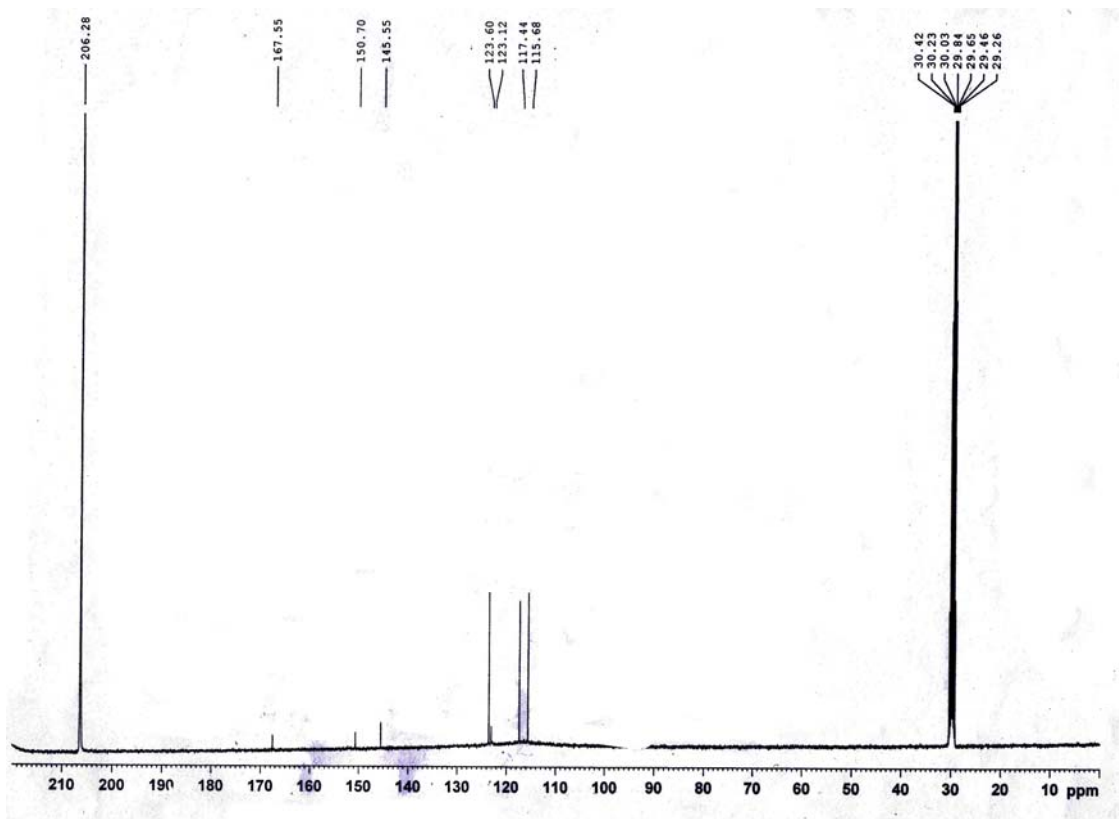
รูป 43 ^{13}C สเปกตรัมของ 2,7-dihydroxyxanthone (100 MHz) ใน acetone-d$_6$

Isolariciresinol (24)
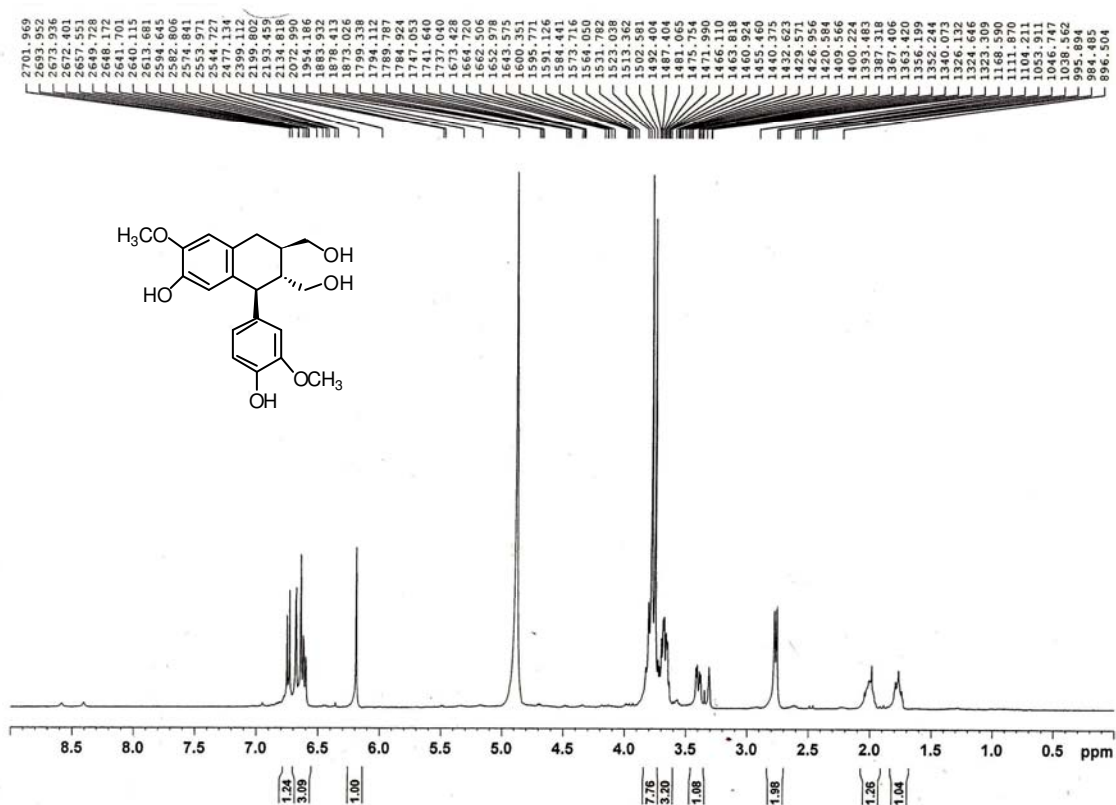
รูป 44 ^{1}H-NMR สเปกตรัมของ isolariciresinol (400 MHz) ใน CD_3OD
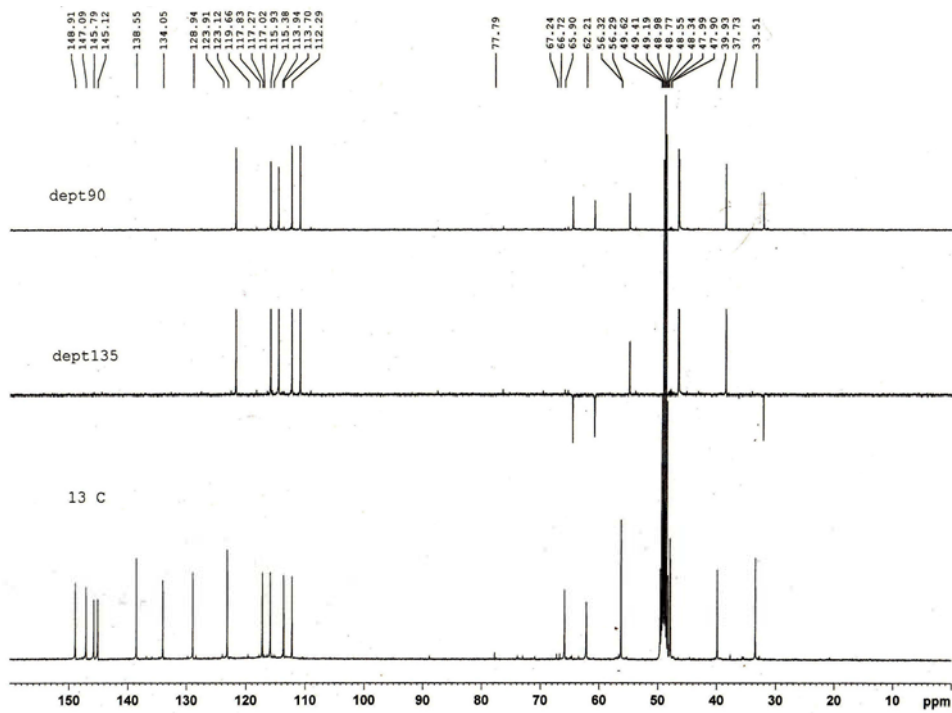
รูป 45 ^{13}C , Dept 135, Dept 90 สเปกตรัมของ isolariciresinol (100 MHz) ใน CD_3OD

Epicatechin (25)
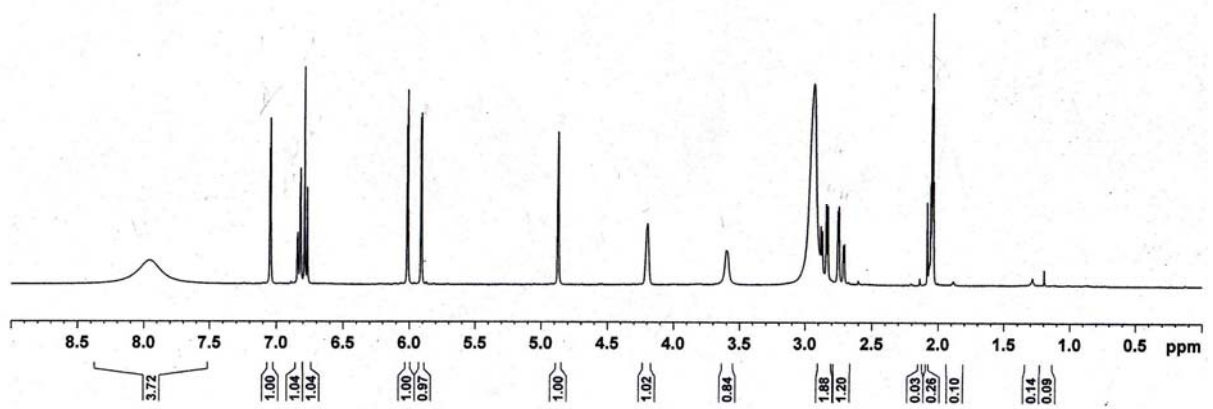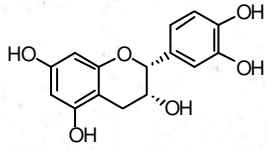
รูป 46 ^{1}H-NMR สเปกตรัมของ epicatechin (400 MHz) ใน acetone d$_6$
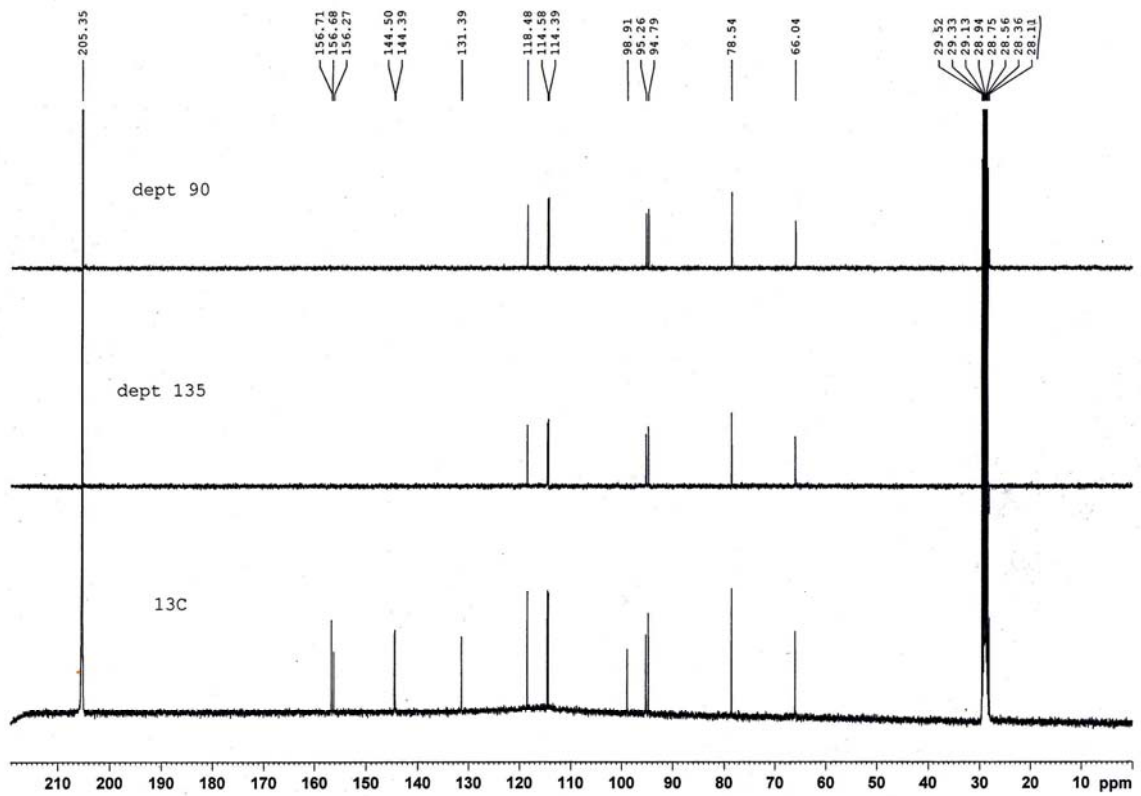
รูป 47 ^{13}C, Dept 135, Dept 90 สเปกตรัมของ epicatechin (100 MHz) ใน acetone-d$_6$

ผลสัมฤทธิ์ที่ได้จากโครงการวิจัย

1. ผลงานวิจัยที่ตีพิมพ์ในวารสาร

Alongkornsopit, J.; Wipasa, J.; Luangkamin, S.; Wongkham, W. Anticancer activity of ethyl acetate and n-butanol extracts from rhizomes of *Agagetes megacarpa* W.W. Smith. *African Journal of Biotechnology.* **2011**, 10 (17), 3455-3462.

2. ผลงานวิจัยที่ตีพิมพ์ในที่ประชุมวิชาการแบบ proceeding

2.1 Pringphrao, P.; Luangkamin, S. Partial synthesis of lupeol and β-sitosterol esters. *PACCON 2011 (Pure and Applied Chemistry International Conference),* Bangkok, Thailand, January 5-7, **2011**, P 690-693

2.2 Kornwongwan, P.; Luangkamin, S. Pentacyclic triterpenoids and steroids from the rhizomes of *Agapetes hosseana* Diels. *PACCON 2011 (Pure and Applied Chemistry International Conference),* Bangkok, Thailand, January 5-7, 2011, P 646-648

3. การเสนอผลงานในที่ประชุมวิชาการแบบ

3.1 Luangkamin, S.; Wongpornchai, S.; Phringphrao, P.; Thongthae, T.; Alongkornsopit, J.; Wongkham, W. Biological activities and Chemical Constituents from the Rhizomes of *Agapetes megacarpa*. . *34th Congress on Science and Technology,* Bangkok, Thailand, October 31-November 2, 2008.

3.2 Phringphrao, P.; Thammalangka, W.; Thongthae, T.; Luangkamin, S. Antioxidant Activity of Xanthone from *Agapetes megacarpa*. *PACCON 2009 (Pure and Applied Chemistry International Conference),* Naresuan University, Phitsanulok, Thailand, January 14-16, 2009.

3.3 Kornwongwan, P.; Luangkamin, S. Triterpenes from the leaves of *Agapetes hosseana* Diels. *35th Congress on Science and Technology,* Chonburi, Thailand, October 15-17, 2009.

4. ผลงานวิจัยที่คาดว่าจะตีพิมพ์

4.1 Luangkamin, S.; Pringphrao, P.; Wongpornchai, S. Triterpenoids from *Agapetes megacarpa* จะตีพิมพ์ใน *Achives of Parmacal Research*

4.2 Luangkamin,S.; Kornwongwan, P.; Wongpornchai, S. Chemical Constituent of Agapetes hosseana จะตีพิมพ์ใน *Achives of Parmacal Research*

เอกสารแนบ

Full Length Research Paper

Anticancer activity of ethyl acetate and *n*-butanol extracts from rhizomes of *Agapetes megacarpa* W.W. Smith

Jariya Alongkornsopit[1], Jiraprapa Wipasa[2], Suwaporn Luangkamin[3] and Weerah Wongkham[1]*

[1]Department of Biology, Faculty of Science, Chiang Mai University, Chiang Mai 50200, Thailand.
[2]Research Institute for Health Science, Chiang Mai University, Chiang Mai 50200, Thailand.
[3]Department of Chemistry, Faculty of Science, Chiang Mai University, Chiang Mai 50200, Thailand.

Agapetes megacarpa W.W. Smith, also known as Pratat Doi, is one of the commonly used medicinal herbs in northern Thailand. The water extract of the herb has been used for lactation and body shape-up by gestation women. Toxicity and antitumor activities of this herb have never been reported. The objective of this study was to examine the cytotoxic and antitumor activities of ethyl acetate and *n*-butanol partitioned extracts prepared from the rhizomes of this herb. The breast cancer cell lines, MCF-7 and MDA-MB231 and the lung cancer cell line NCI-H1299 were used. The cells were exposed to serial concentrations of the extracts in dimethylsulfoxide and dissolved in cell culture medium. Cytotoxic and antiproliferative assays were used employing the Sulforhodamine B method. The experiments showed that, none of the extracts expressed acute cytotoxicity to the cancer cells within 24 h. Antiproliferative effect was exhibited with time-and concentration-dependent manner after 5 days of exposure. Apoptotic induction on the cancer cell lines was analyzed by flow cytometry using Annexin-V-FITC/propidium iodide staining. Significant differences of apoptotic percentages were found from the exposed cells to both of the extract partitions when compared with the unexposed control cells. The results implied bioactive apoptotic induction by constituents contained in the more polar solvent partition.

Key words: *Agapetes megacarpa*, Pratat Doi, Thailand, cytotoxicity, antiproliferative, apoptosis, breast cancer, lung cancer, flow cytometry.

INTRODUCTION

Cancer is the second largest cause of death which killed 7.6 million people worldwide in 2005 (Danaei et al., 2005). The number is believed to become 9 million in 2015 and 11.5 million in 2030 (World Health Organization, 2007). There is an increasing interest to research and develop on new anticancer drugs, from both synthetic and natural sources (Mukherjee et al., 2001). Half of the drugs which have been approved recently are from natural sources (Kim and Park, 2002; Newman and

Cragg, 2007). Plants have been extensively used as natural sources to develop anticancer drugs because of their active constituents (Schwartsmann et al., 2002). Medicinal plants in Asian countries play an important role in cancer treatment and indeed, their chemical constituents and derivatives have been utilized for combating cancers over the last half-century (Newman et al., 2003).

The plants in the genus *Agapetes*, which are rich sources of pentacyclic triterpenes (Deng and Chen, 1991; Xuan, 2006), have been used as traditional medicine. The stems of *Agapetes saxicola*, *Agapetes megacarpa* and *Agapetes thailandica* are used for roborant in Thai folk medicine. *Agapetes lobbii* was reported to possess antioxidant properties (Tangkanakul et al., 2006) while

---

*Corresponding author. E-mail: w_wongkham@hotmail.com. Tel: +66 (0)53 94 3346 ext.1103. Fax: +66 (0)53 89 2259.

Agapetes neriifolia is applied as medicinal paste to treat fracture in Chinese people (Xuan, 2006). *Agapetes megacarpa* W.W. Smith, commonly known as Prathat doi belonging to the family Ericaceae, is a medicinal herb in the northern region of Thailand. The water extract of its rhizomes is utilized for gestation woman to increase lactation and also for maintaining the body-shape. However, phytochemical investigations of this species are still rare.

This study was aimed at the evaluation of the cytotoxicity and antiproliferative potential of the ethyl acetate and *n*-butanol extracts of *A. megacarpa* rhizomes. Their cytotoxic activity and antiproliferation were investigated on the non-small cell lung carcinoma cell line, NCI-H1299 and the human breast carcinoma cell lines, MCF-7 and MDA-MB231.

MATERIALS AND METHODS

Plant collection

A. megacarpa (AM) was collected from Doi Phahompok, Chiang Mai Thailand. The plant material was identified by curators of the herbarium at Queen Sirikit Botanic Garden, Chiang Mai. Voucher specimen was deposited to the herbarium with a systemic voucher code of Watthana-1443.

Rhizomes extraction

The fresh rhizomes of AM were collected, washed cleaned with tap water, cut into small pieces and weighted (2,186 g) before air-dried at 23 to 32°C for 5 to 7 days to get a consistent weight. The dried material was then, ground into a powder by an electric-grinder. The powder (773 g) was extracted with methanol using Soxhlet apparatus at 64.7°C. After evaporation of the methanol, the extract (113 g) was suspended in water and partitioned with ethyl acetate and *n*-butanol, respectively. Removal of the solvents from each fraction by an electrical evaporator and then freeze-drying yielded the partitioned extracts of ethyl acetate (AM-E, 18.46 g) and *n*-butanol (AM-N, 17.20 g). The partitioned extracts were stored at -20°C until needed.

Preparation of exposed solution

Concentrated stock solutions were prepared by adding a known weight of the partitioned extract to a known volume of dimethyl sulfoxide (DMSO). From each stock solution, 5 to 6 serially diluted working solutions were prepared. The exposed solutions were then, prepared prior to use by adding 1% of the working solutions to the known volume of appropriate medium to each cell type. The control solution contained 1% DMSO (v/v) in-well or the same volume of culture medium. The concentration of DMSO at 1% is non-toxic for cell viability.

Cell lines and culture

Human breast cancer cell line, MCF-7, was retrieved from a frozen stock of the Human and Animal Cell Technology Research Unit, Faculty of Science, Chiang Mai University. This cell line was continuously maintained from the stock cultured at the National Cancer Research Institute, Bangkok, Thailand. Another human breast cancer cell line, MDA-MB231 and the human lung cancer cell line, NCI-H1299, were purchased from the American Type Culture Collection (ATCC, USA). The culture media, DMEM, Leibovitz L-15 and RPMI-1640 (all from Gibco/Invitrogen, USA) were used for MCF-7, MDA-MB231 and NCI-H1299, respectively. The culture media were supplemented with 10% fetal bovine serum (FBS) (Gibco/Invitrogen, USA) and 100 ng/ml of penicillin and streptomycin (Sigma, USA). Cells in culture flasks (Nunc, USA) were incubated in the standard atmosphere of 95% relative humidity at 37°C and 5% CO_2.

The cytotoxicity assay

The cytotoxicity assay was performed by using the Sulforhodamine B (SRB) (Sigma, USA) colorimetric method on 96 wells culture-plate (Nunc, USA) to assess growth inhibition according to Vanicha and Kirtikara (2006). Briefly, the cell suspensions at 5,000 cells/well in 100 µl media were transferred into 2 sets of 3 plates. The media in a set of three wells basis on each plate was added with 100 µl of a dilution of the exposed mixture of AM-E or AM-N (in DMSO) and consequently, incubated for another 24 h. The exposed concentrations of the partitioned extracts were 5, 10, 20, 40, 60, 80 and 100 µg/ml. At the end of the exposed time, cells in each well were fixed by addition of 100 µl of cold (4°C) 10% (w/v) trichloroacetic acid (TCA) into the growth medium. Each plate was incubated at 4°C for 1 h before gently washed five times with tap water to remove TCA, the growth medium and dead cells. Plates were allowed to dry in air and to each well were added 50 µl of 0.057% (v/v) SRB dye in 1% acetic acid in deionized water and allowed to stand for 30 min at room temperature. At the end of the staining period, unbound SRB was removed by washing four times with 1% of an acetic acid solution. The plate was air-dried and 150 µl of 10 mM aqueous Tris base buffer of pH 10.5 was added to each well to dissolve the cell-bound dye. The plate was then shaken for 15 to 30 min on a gyratory shaker and the optical density (OD) was read at 510 nm in a microplate reader; control wells were used as blanks. Inhibition concentration at 50% of cell population or IC_{50} was calculated by using Priprobit program version 1.63 (Sakuma, 1998).

The antiproliferation assay

The antiproliferation assay aimed to study the basic pharmacological activities of the extracts. The experiments were carried out by using the SRB colorimetric method as mentioned earlier for the cytotoxicity assay except for the variation of exposed concentrations and exposed durations of the extract to the cells. Five plates of each cell line were prepared. On each plate, cells were exposed to a set of 6 serial concentrations of each extract varying between 10 to 100 µg/ml. These serial concentrations were used according to the value of the IC_{50} cytotoxic assay of each extract. The plates were incubated in standard CO_2 atmosphere and were taken each to the SRB assay at the end duration of 24, 48, 72, 96 and 120 h. The study was carried out by plotting the mean value of percentage cell proliferation of the exposed cells to the controls against the extract concentrations.

Apoptosis detection by Annexin V-FITC/propidium iodide staining

Annexin V staining for apoptosis detection was performed as previously described by Van et al. (1996). In brief, 10^5 cells/ml were seeded in 12 wells plates (corning) for 24 h. The exposed

Table 1. Cytotoxic activity of extracts from *A. megacarpa* on the human breast cancer cell lines, MCF-7 and MDA-MB-231, and the human lung cancer cell line, NCI-H1299.

Cell line	IC$_{50}$ (µg/ml)[a]	
	AM-E [b]	AM-N [c]
MCF-7	447.83	340.73
MDA-MB231	373.91	256.01
NCI-H1299	91.53	74.54

[a] IC$_{50}$, inhibition concentration at 50% effective level; [b]AM-E, ethyl acetate partition; [c]AM-N, *n*-butanol partition.

concentrations of each extract were prepared at 40 and 80 µg/ml and with 72 h exposure duration. At the end of incubation, cells were trypsinized and collected from each well into a 15 ml conical centrifuge tube and washed twice with 3 ml of the phosphate buffer saline (PBS) and centrifuged at 200 g. Cell pellet was resuspended in binding buffer (10 mM Hepes pH 7.4, 140 mM NaCl and 2.5 mM CaCl$_2$) containing Annexin V-FITC/propidium iodide (Invitrogen Carlsbad, CA, USA), and was incubated in the dark for 15 min at room temperature. The binding buffer was added to the stained cells and cells were analyzed immediately by FACS (BD Biosciences, San Jose, CA, USA) analysis. At least 10,000 counts were recorded in each analysis. Cells positive to Annexin V-FITC stained were considered as apoptotic cells.

Statistical analysis

All the experiments were carried out on triplicate basis and were presented as mean and standard deviation. Analysis of variance was performed by one way ANOVA, followed by Duncan test for pair wise comparison. The P-values less than 0.05 were considered to be statistically significant.

RESULTS AND DISCUSSION

The results of the cytotoxicity assay at 24 h of the exposed cells to the extracts are shown in Table 1. The criteria of cytotoxic activity for the crude extracts, as previously described by the American National Cancer Institute (NCI-USA), is an IC$_{50}$ < 30 µg/ml (Suffness and Pezzuto, 1990). The extracts from *A. megacarpa* in this study expressed a non-cytotoxic activity to both of the breast cancer cell lines, MCF-7 and MDA-MB231 with the IC$_{50}$ > 250 µg/ml. Selectively, very weak cytotoxic activities to the lung cancer cells, NCI-H1299, was expressed by both of the extracts, (AM-E and AM-N), at the IC$_{50}$ = 91.5 and 74.5 µg/ml, respectively. The IC$_{50}$ values in this experiment confirmed the non-toxic effects of *A. megacarpa* on the herbal remedies application by the northern Thai indigenous medicinal practitioners (Kornwongwan, 2006). Although, this herb has been used for a long time among the hill tribe people, there is no recorded data for clinical studies or for cytotoxic test against any cancer cell line.

The antiproliferative activity of the extracts on the cell lines was evaluated. Both partitioned extracts of the ethyl acetate (AM-E) (Figure 1) and the *n*-butanol (AM-N) (Figure 2), exhibited the antiproliferative activities to the cells in a time-and concentration-dependent manner. Time-dependent effects of AM-E on the breast cancer cells, MCF-7 and MDA-MB231 (Figure 1ab, respectively) were uniquely greater at 96 and 120 h than those on 24, 48 and 72 h. The effective time-dependent manner of AM-E was shown at 48 h and later was higher at 24 h on the lung cancer, NCI-H1299 (Figure 1c). The concentration-dependence of AM-E on the breast cancer cell, MCF-7 (Figure 1a), was notably shown at ≥ 10 µg/ml, while on MDA-MB231 it was at ≥ 40 µg/ml. On the lung cancer cells of NCI-H1299, the concentration effect of AM-E was clearly shown at ≥ 40 µg/ml (Figure 1c). Antiproliferative activity of the *n*-butanol partitioned extracts (AM-N) is shown in Figure 2. For the breast cancer cells, MCF-7 and MDA-MB231, the time-dependent activity of AM-N was exhibited at ≥ 72 h (Figure 2a) and ≥ 96 h (Figure 2b), respectively. At ≥ 48 h, the antiproliferation activity was observed on the lung cancer cells, NCI-H1299 (Figure 2c). The concentration-dependent manner of AM-N on the breast cancer cells, MCF-7, was not very clear (Figure 2a), while on MDA-MB231 (Figure 2b) as well as on the lung cancer cells, NCI-H1299 (Figure 2c) it was at ≥ 30 µg/ml.

Time-and concentration-dependent manner of the extract activities reflects the logical pharmacokinetics and pharmacodynamics on the cancer cells (Lees et al., 2004; Hsieh and Korfmacher, 2006). This is normally indicated in the cellular uptake across membrane and the metabolic disturbance within the cells (Le Coutre et al., 2004). These cellular pathways of activities are concerned with necessary signaling transduction through cytosol and nucleoplasm. The study of drug response and development of drug response model using these cell lines is the key to determine safety and hazardous levels and dosages of the extracts to which the cells are exposed (Sheiner et al., 1977, 1979).

Growth inhibition of the cancer cells due to the apoptotic induction was determined by using Annexin V-FICT/propidium iodide staining assay and was analyzed by flow cytometry. Investigation was carried out on both partitioned extracts (AM-E and AM-N) each at the exposed concentrations of 40 and 80 µg/ml for 72 h. The results indicated that, both partitions significantly induced apoptosis by concentration-dependent manner on all the investigated cell lines (Figure 3). The percentages of apoptotic cells induced by the two partitioned extracts were shown at the equivalent concentration. The effect of the AM-E expressed was significantly lesser than that of the AM-N in all the cancer cell lines. Apoptotic cells induced by AM-E of the equivalent concentrations were shown with similar percentage in all the cancer cell lines,
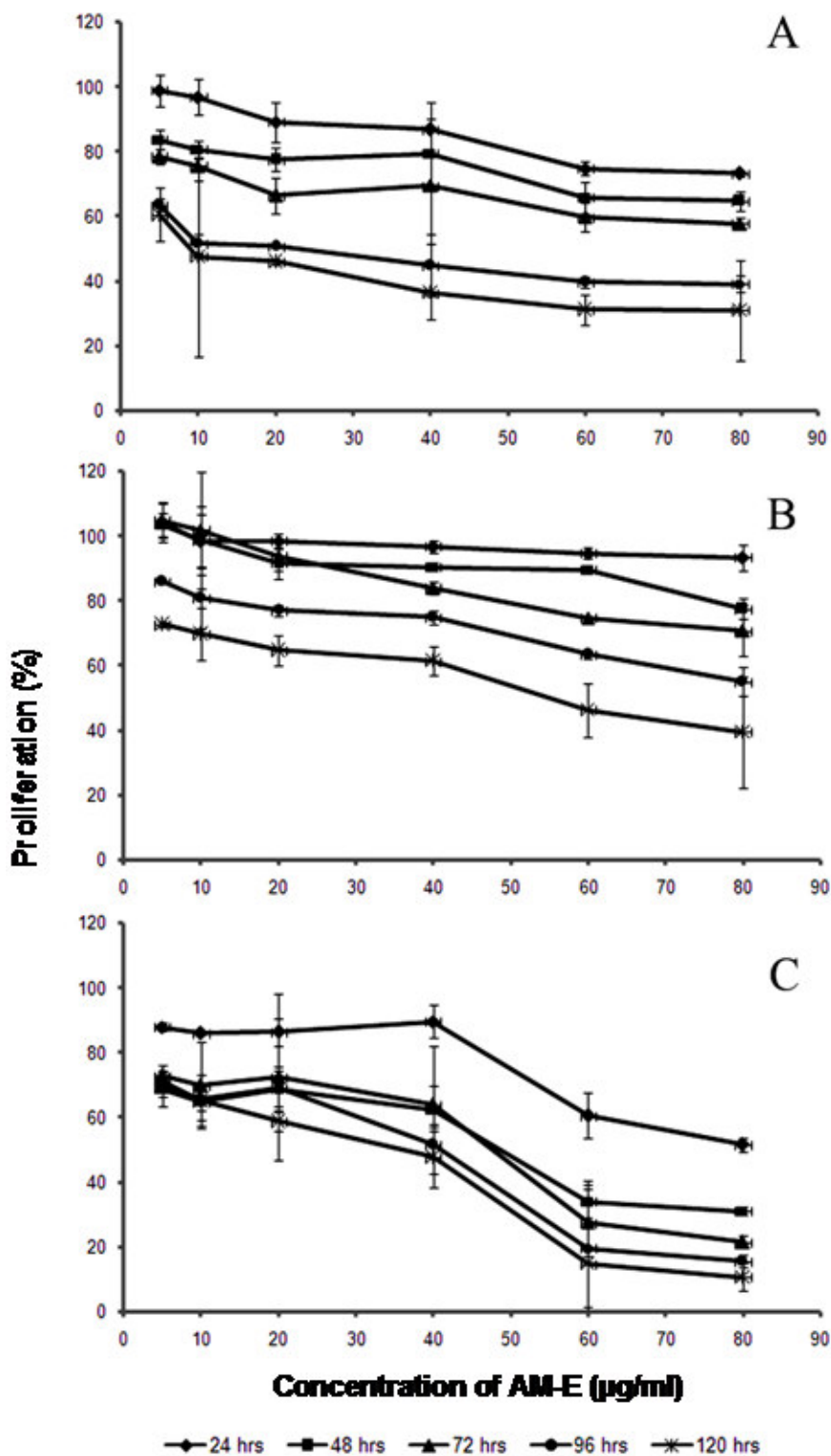
Figure 1. Antiproliferative effect of the ethyl acetate partition of *A. megacarpa* extract (AM-E) on the breast cancer cells, MCF-7 (A) and MDA-MD-231 (B) and the lung cancer cells, NCI-H1299 (C). The mean values of triplicates are performed with standard deviation bar.
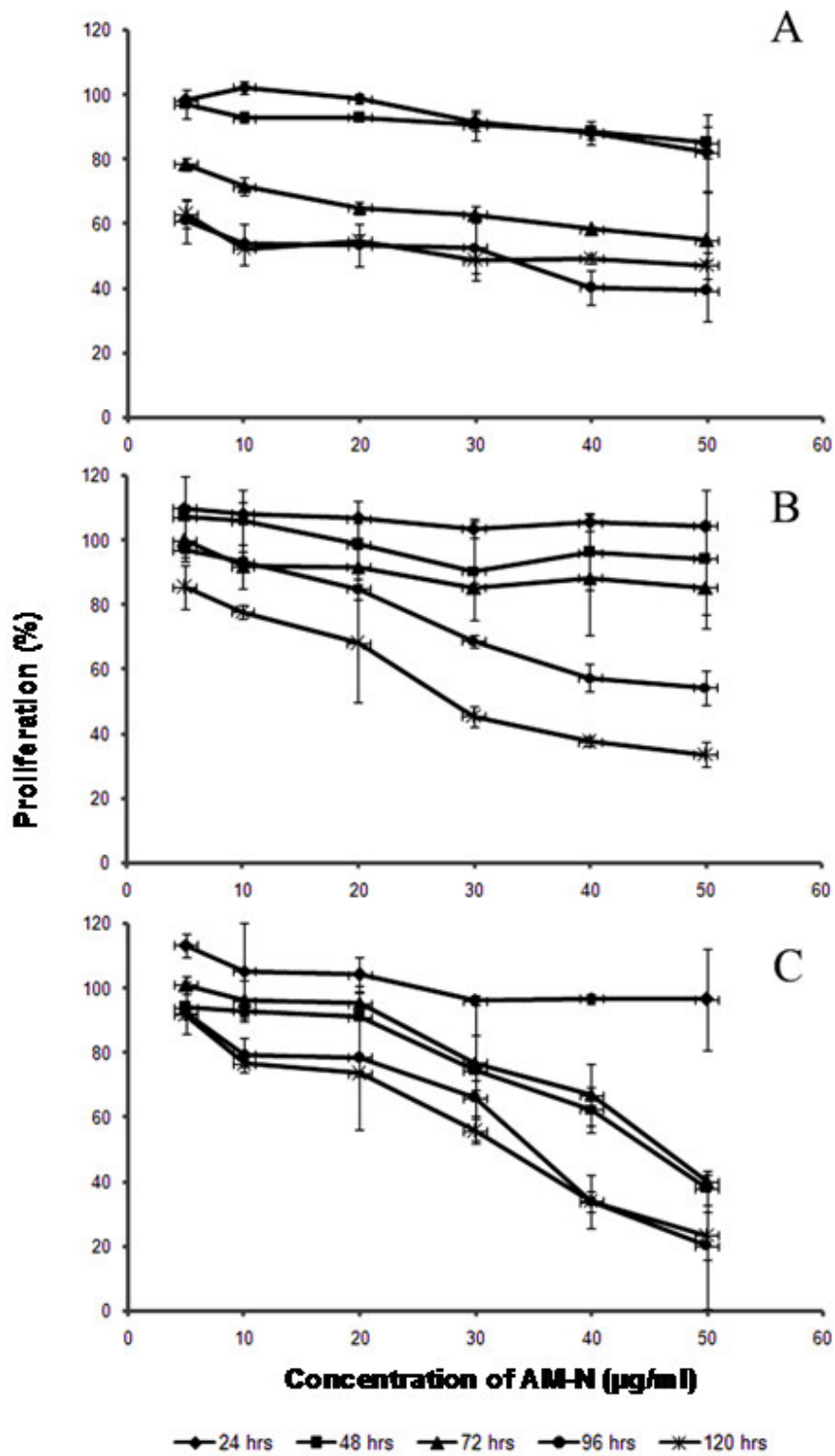
Figure 2. Antiproliferative effect of the *n*-butanol partition of *A. megacarpa* extract, AM-N, on the breast cancer cells, MCF-7 (A) and MDA-MD-231 (B) and the lung cancer cells, NCI-H1299 (C). The mean values of triplicates are shown with standard deviation bar.
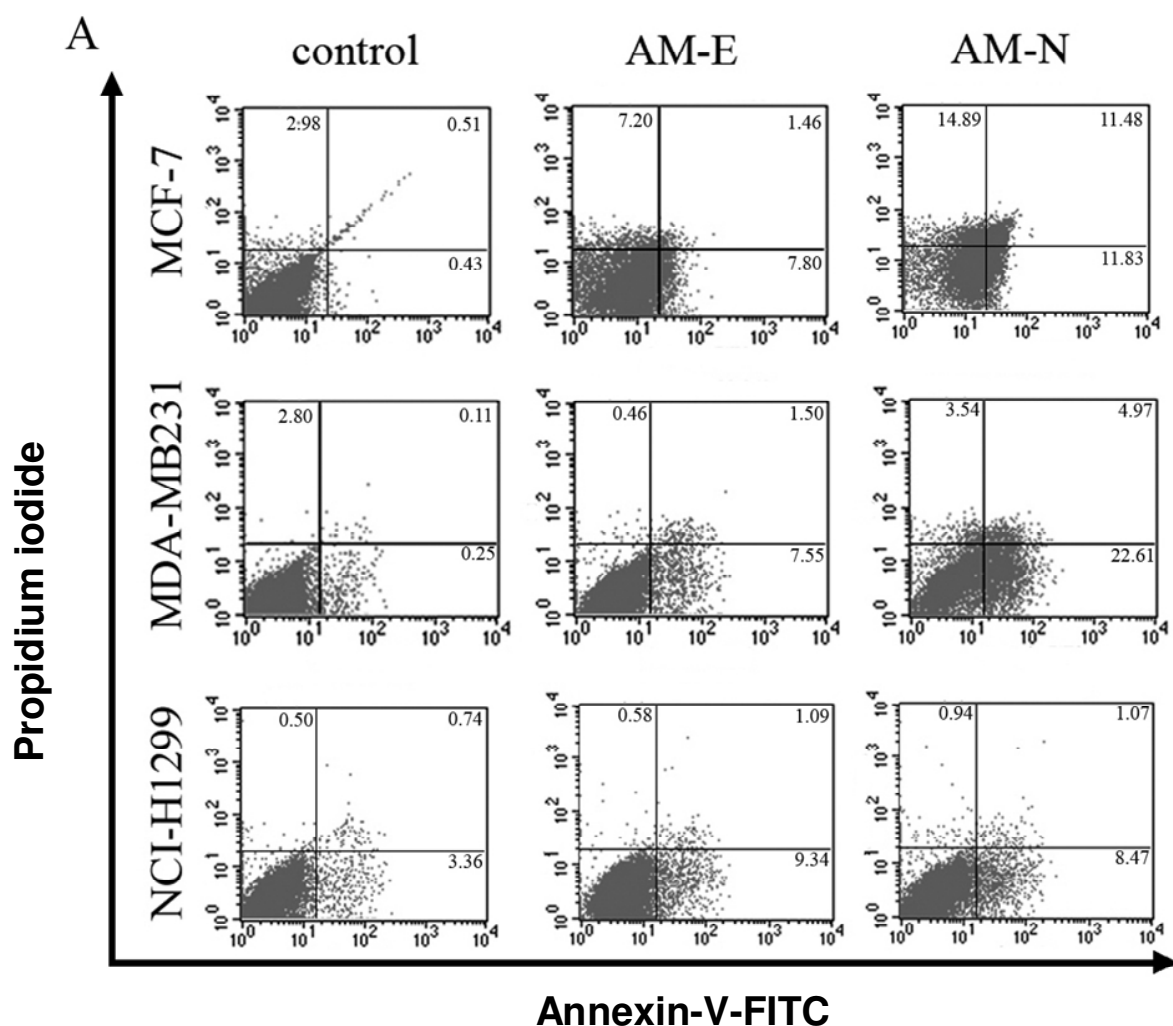
Figure 3. Apoptotic activities of the ethyl acetate partition (AM-E) and the *n*-butanol partition (AM-N), presented by flow cytometric dot-plot examples (A) and the mean percentage value of apoptotic cells (B to D) with standard deviation bars of triplicates. The concentration of the extracts were indicated in number (40 and 80 µg/ml) after the abbreviated name of partitions. Control groups were unexposed cells to the extract (1% DMSO). The small alphabets a-d, on the graph show statistical significant difference ($p \leq 0.05$).

while the AM-N induced more breast cancer cells (MCF-7 and MDA-MB231), than the lung cancer cells (NCI-H1299). This suggests that *A. megacarpa* was more active and selective for the induction of apoptosis on the human breast cancer cells than the human lung cancer cells.

The overall figures of the investigated activities of the two partitioned extracts of *A. megacarpa* were considered. The ethyl acetate partition (AM-E), expressed less effects than the *n*-butanol partition (AM-N), in all the studied activities. This indicates that, the active constituents obtained by the more polar solvent (*n*-butanol) in the extraction processes were responsible for the anticancer properties in this herb. The biological selective

activity of any compound might depend on the type of chemical composition and the concentration of active constituents as well as the types and developmental stages of the cancer (Lee et al., 2004). The different activities of the extracts to the two breast cancer cells may be due to the biological nature of the cell lines (Liu et al., 2001). MCF-7, the estrogen receptor possessing cells (ER+), expressed was less sensitive to the extract than the non-possessing estrogen receptor cells, MDA-MB-231. The activities of the extracts in breast cancer cells are probably evoked by the ER-mediated genomic pathway and the non-ER-mediated mechanisms (Zierau et al., 2002). This may also be because of the various physico-chemical properties of any individual component
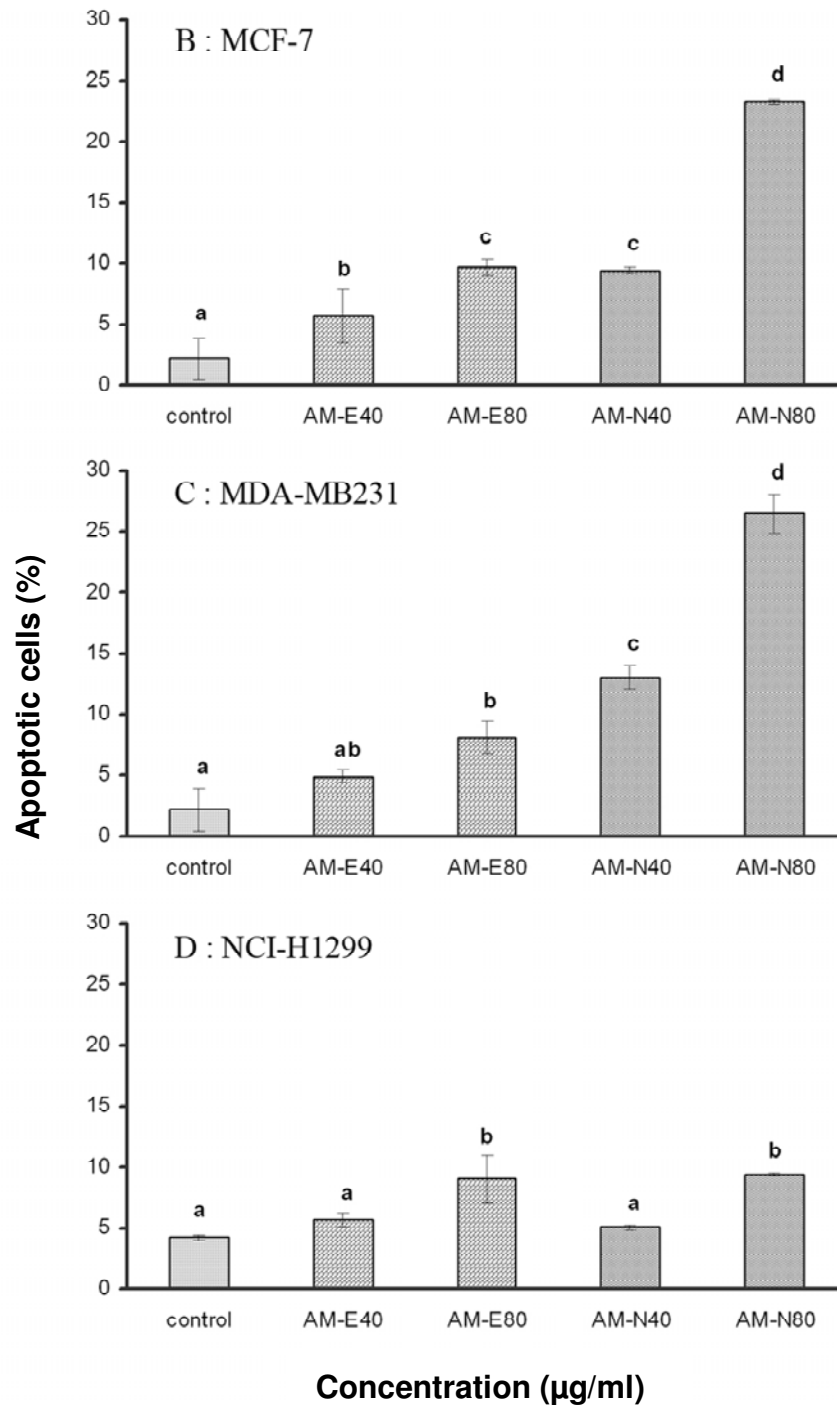
Figure 3. Contd.

of the extracts to the cells (Liske et al., 2002).

Although, some species of the herb in the genus *Agapetes* have been actually investigated, no specific active compounds have been reported so far on *A.* *megacarpa*. Several constituent have been identified from *A. obouata* (Chen et al., 1990), *A. hosseana* (Deng and Chen, 1991) and *A. neriifolia* (Xuan, 2006). Among those, the anticancer activities for β-sitosterol (Awad et

al., 2003; Park et al., 2007; Zhao et al., 2009), friedelanol (Kundu et al., 2000) and friedelin (Monkodkaew et al., 2009; Ding et al., 2010) have been shown. Those compounds were reported as cytotoxic to some cancer cells *in vitro*. Some of the compounds were from the non-polar constituents which differed from the activities of the extract from the polar fractions of this experiment. The results from this study, however, indicated for the first time, the apoptosis induction activities by the extracts from *A. megacarpa*. Further investigation is needed to identify the highly active compounds from this herb.

Acknowledgements

REFERENCES

Awad AB, Roy R, Fink CS (2003). Beta-sitosterol, a plant sterol, induces apoptosis and activates key caspases in MDA-MB-231 human breast cancer cells. Oncol. Rep. 10(2): 497-500.

Chen Y, Meng Y, Cheng X (1990). Chemical constituents of *Agapetes obouata* Huong SH. China J. Chinese Mater. Med. 15(9):549-551.

Danaei G, Vander Hoom S, Lopez A, Murray C, Ezzati M (2005). Causes of cancer in the world: comparative risk assessment of nine behavioural and environmental risk factors. Lancet, 366: 1784-1793.

Deng J, Chen Y (1991). Chemical constituents of Agapetes. (II). Chemical constituents of *Agapetes hosseana* Diels. Peop. Rep. China. 2(6): 757-760.

Ding Y, Liang C, Kim JH, Lee YM, Hyun JH, Kang HK, Kim JA, Min BS, Kim YH (2010). Triterpene compounds isolated from *Acer mandshuricum* and their anti-inflammatory activity. Bioorg. Med. Chem. Lett. 20(5): 1528-1531.

Hsieh Y, Korfmacher WA (2006). Increasing speed and throughput when using HPLC-MS/MS systems for drug metabolism and pharmacokinetic screening. Curr. Drug Metab. 7(5):479-489.

Kim J, Park EJ (2002). Cytotoxic anticancer candidates from natural resources. Curr. Med. Chem. Anticancer Agents, 2: 485-537.

Kornwongwan P (2006). Chemical constituents and biology activities from stems of *Agapetes megacarpa*. B.Sc. special problem, Chiang Mai University, Chiang Mai, Thailand, p. 95.

Kundu JK, Rouf ASS, Nazmul HM, Hasan CM, Rashid MA (2000). Antitumor activity of epifriedelanol from *Vitis trifolia*. Fitoterapia, 71(5): 577-579.

Le Coutre P, Kreuzer KA, Pursche S, Bonin MV, Leopold T, Baskaynak G, Dörken B, Ehninger G, Ottmann O, Jenke A, Bornhäuser M, Schleyer E (2004). Pharmacokinetics and cellular uptake of imatinib and its main metabolite CGP74588. Cancer Chemother. Pharmacol. 53: 313-323.

Lees P, Cunningham FM, Elliott J (2004). Principles of pharmacodynamics and their applications in veterinary pharmacology. J. Vet. Pharmacol. Ther. 27(6): 397-414.

Liske E, Hanggi W, Henneicke-von Zepelin HH, Boblitz N, Wustenberg P, Rahlfs VW (2002). Physiological investigation of a unique extract of black cohosh (*Cimicifuga racemosa rhizoma*): a 6-month clinical study demonstrates no systemic estrogenic effect. J. Womens Health Gend Based Med. 11: 163-174.

Liu J, Burdette JE, Xu H, Gu C, van Breemen RB, Bhat KP, Booth N, Constantinou AJ, Pezzuto JM, Fong HH, Famsworth NR, Bolton JL (2001). Evaluation of estrogenic activity of plant extracts for the potential treatment of menopausal symptoms. J. Agric. Food Chem. 49: 2472-2479.

Monkodkaew S, Loetchutinat C, Nuntasaen N, Pompimon W (2009). Identification and antiproliferative activity evaluation of a series of triterpenoids isolated from *Flueggea virosa* (Roxb. ex Willd.). Am. J. Appl. Sci. 6(10): 1800-1806.

Mukherjee AK, Basu S, Sarkar N, Ghosh AC (2001). Advances in cancer therapy with plant based natural products. Curr. Med. Chem. 8: 1467-1486.

Newman DJ, Cragg GM (2007). Natural products as sources of new drugs over the last 25 years. J. Nat. Prod. 70: 461-477.

Newman DJ, Cragg GM, Snader KM (2003). Natural products as sources of new drugs over the period 1981-2002. J. Nat. Prod. 66(7): 1022-1037.

Park C, Moon DO, Rhu CH, Choi BT, Lee WH, Kim GY, Choi YH (2007). Beta-sitosterol induces anti-proliferation and apoptosis in human leukemic U937 cells through activation of caspase-3 and induction of Bax/Bcl-2 ratio. Biol. Pharm. Bull. 30(7): 1317-1323.

Sakuma M (1998). Probit analysis of preference data. Appl. Entomol. Zool. 33: 339-347.

Schwartsmann G, Ratain MJ, Cragg GM, Wong JE, Saijo N, Parkinson DR, Fujiwara Y, Pazdur R, Newman DJ, Dagher R, Di Leone L (2002). Anticancer drug discovery and development throughout the world. J. Clin. Oncol. 20(18): 47S-59S.

Sheiner LB, Beal SL, Rosenberg B, Marathe VV (1979). Forcasting individual pharmacokinetics. Clin. Pharmacol. Ther. 26(3): 294-305.

Sheiner LB, Rosenberg B, Marathe VV (1977). Estimation of population characteristics of pharmacokinetic parameters from routine clinical data. J. Pharmacokin. Biopharm. 5: 445-479.

Suffness M, Pezzuto JM (1990). Assays related to cancer drug discovery. In: Hostettmann K (ed). Methods in Plant Biochemistry: Assays for Bioactivity, Vol. 6, Academic Press, London, pp. 71-133.

Tangkanakul P, Trakoontivakorn G, Auttaviboonkul P, Niyomvit B, Wongkrajang K (2006). Antioxidant activity of northern and northeastern Thai foods containing indigenous vegetables. Kasetsart J. Natural Sci. 40(suppl.): 47-58.

Van EM, Ramaekers FC, Schutte B, Reutelingsperger CP (1996). A novel assay to measure loss of plasma membrane asymmetry during apoptosis of adherent cells in culture. Cytometry, 24: 131-139.

Vanicha V, Kirtikara K (2006). Sulforhodamine B colorimetric assay for cytotoxicity screening. Nat. Prot. 1(3): 1112-1116.

World Health Organization (2007). The World Health Organization's fight against cancer: strategies that prevent, cure and care. WHO library cataloguing-in-publication data brochure. Printed in Switzerland. ISBN 9789241595438. P. 26.

Xuan H (2006). Chinese medicinal paste for treating fracture. Chinese Patent Application: CN 10011051 20051001.

Zhao Y, Chang SK, Qu G, Li T, Cui H (2009). β-sitosterol inhibits cell growth and induces apoptosis in SGC-7901 human stomach cancer cells. J. Agric. Food Chem. 57(12): 5211-5218.

Zierau O, Bodinet C, Kolba S, Wulf M, Vollmer G (2002). Antiestrogenic activities of *Cimicifuga racemosa* extracts. J. Steroid Biochem. Mol. Biol. 80: 125-130.

ANTIOXIDANT ACTIVITY OF XANTHONE FROM *AGAPETES MEGACARPA*

Phantiwa Phringphrao[1], Wimwipa Thammalangka[1], Worawit Thongthae[2] and Suwaporn Luangkamin*[1]

[1] *Department of Chemistry, Faculty of Science, Chiang Mai University, Chiang Mai, 50200*
[2] *Protected Area Regional Office 16, National Park Wildlife and Plant Conservation Department, Chiang Mai, 50100*
Email : suwaporn @ chiangmai.ac.th Tel: 053943341 ext 225

2,7-dihydroxyxanthone (**1**) was isolated from the rhizomes of *Agapetes megacarpa* (Prathat doi) together with four pentacyclictriterpenoids: lupeol (**2**), lupenone (**3**), 3-ketooleanane (**4**), fernenone (**5**) and *β*-sitosterol (**6**). Their structures were elucidated by analysis of their spectroscopic data and spectral data were compared with those reported in the literature[1-4]. Amongst these isolates, compounds (**1**) exhibited strong radical DPPH scavenging activity with IC_{50} value of 2.32 μg/ml.

2,7-dihydroxyxanthone (**1**)   lupeol (**2**)   lupenone (**3**)

3-ketooleanane (**4**)   fernenone (**5**)   *β*-sitosterol (**6**)
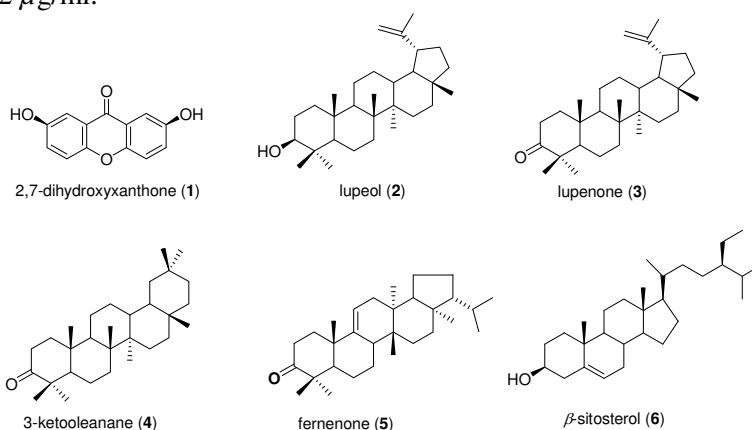
Keywords: *Agapetes megacarpa*, Prathat Doi, antioxidant, triterpene, xanthone

REFERENCES:
1. Tosa, H.; Iinuma, M.; Murakami, K.; Ito, T.; Tanaka, T.; Chelladurai, V.; Riswan, S.; *Phytochemistry*, **1997**, 45(1), 133-136.
2. Fotie, J.; Bohle, D.S.; Leimanis, M.L.; Geoffrey, E.; Rukunga, G.; Nkengfack, A.E.; *J. Nat. Prod.*, **2006**, 69, 62-67
3. Krishnavenj, K.S.; Srinivasa Rao, J.V.; *Fitoterapia*, **2000**, 71, 10-13.
4. Wu, F.; Koike, K.; Nikaido, T.; Ishii, K.; Ohmato, T.; Ikeda, K.; *Chemical & Pharmaceutical Bulletin*, **1990**, 38(8), 2281-2282.

Organic Chemistry
and
Medicinal Chemistry

Extraction and Biological Activities of *Parinari anamense* Hance

U. Polyium [1*], P. Ta-Ngam [2], and A. Thongnoi [3]

[1] Department of Chemistry, Faculty of Science and Technology, Rajamangala University of Technology Phra Nakhon, Bangkok Thailand 10800.
[2] Department of Biology, Faculty of Science and Technology, Rajamangala University of Technology Krungthep, Bangkok Thailand 10120.
[3] Thailand Institute of Scientific and Technological Research (TISTR) Pathum Thani, Thailand 12120.

*Corresponding author, e-mail : udomwish@hotmail.com

Abstract: Crude extracts from the stem bark of *Parinari anamense* Hance were assessed for their antioxidant activities tested using DPPH radical scavenging assay, total phenolic contents tested using the Folin–Ciocalteu method, antimalarial activity against *Plasmodium falciparum* using microculture radioisotope technique, cytotoxic activity against human mouth carcinoma (KB), human small cell lung cancer (NCI-H187) and breast cancer (MCF-7) cancer cell lines, tested using the resazurin microplate assay (REMA) and antimicrobial activity tested by the dilution method. The Results showed that a crude methanol extract exhibited free radical scavenging effect on the DPPH assay with IC_{50} value of 200 µg/ml, with the total phenolic contents of 42.70 mg GAE/g dw of standard BHT. Crude hexane extract exhibited inhibitory effect against *Plasmodium falciparum* and KB cancer cell lines with IC_{50} values of 3.25 and 34.12 µg/ml., respectively. Crude ethyl acetate extract exhibited inhibitory effect against KB and MCF-7 cancer cell lines with IC_{50} values of 19.03 and 47.70 µg/ml, respectively. A crude methanol extract exhibited inhibitory effect against NCI-H187 cancer cell lines with IC_{50} value of 48.51 µg/ml. The antimicrobial activities of crude hexane, ethylacetate and methanol extracts with MIC values of 15.60 - 62.50 µg/ml. These data support traditional uses of *P.anamense* in folk medicine

Introduction

Parinari anamense Hance is a plant of the Chrysobalanceae family and is typically found throughout Southeast Asia. In Thailand, it is locally known as Mapok tree.[1] Several parts of the *Parinari anamense* Hance are used in Thai traditional medicine as an Staple drink boiled water, Pradg, Itchy rash, Have a burning pain and Serum.[2] There are very few publications concerning the biological activities of *P.anamense*. Prayong[3] has shown that the cytotoxic activity of *P.anamense* in malignant human hepatoma (HepG2) and normal African green monkey kidney(Vero) cell of ethanol extracts had the activity with IC_{50} as follows: 546±65 and 431±22 µg/ml, respectively. Uys[4] reported the antimalarial activity of the stems of *Parinari capensis* (Chrysobalanceae), and three isolated diterpene lactones possessed antimalarial activity with IC_{50} values of 0.54, 0.67 and 1.57 µg/ml.

Materials and Methods

Plant materials

The stem barks of *P.anamense*. were collected from natural population in Roi-ed Province, Thailand and deposited at the Department of Biology, Faculty of Science and Technology, Rajamangala University of Technology Krungthep, Bangkok.

Extraction

The stem barks of *P.anamense*. were cleaned and washed with distilled water and then chopped into small pieces. The aerial parts (1kg) were dried in an oven at 45 °C for 12 h, and were macerated for 7 days with hexane (2 l) at room temperature. The crude hexane extract was filtered and the filtrate was concentrated under vacuum at 45 °C using a rotary evaporator, to yield a crude hexane extract. The plant residue was then sequentiallly extracted with ethylacetate and methanol to obtain corresponding crude extracts.

Antioxidant activity

DPPH radical scavenging assay

The free radical scavenging was assessed of the stable 1,1-diphenyl-2-picrylhydrazyl (DPPH) free radical method described by Brand-Williams et al., 1995 [5]. with a slight modification. 100 µL of the extract in DMSO was added to 2.9 mL of a DPPH solution (4.5 mg DPPH in 100 mL EtOH) and the mixture was allowed to stand at 30 °C for 30 min. The absorbance was measured at 517 nm. The scavenging effect was determined by comparing the absorbance of the test sample solution and control solution. The percentage of the remaining DPPH against the standard concentration was plotted to obtain the amount of antioxidant that was necessary to decrease by 50% of the initial DPPH concentration (IC_{50}). The standard compound used as positive control was 2,6-di-(tert-butyl)-4-methylphenol (BHT, IC_{50} value of 9.5 µg/mL)

Total phenolics content

The total phenolics content was assessed according to the Folin-Ciocalteu method [6] using gallic acid as standards. Extract powders (1 mg) were dissolved in 1 ml 50% methanol solution. Extract solution (0.5 ml) was mixed with 0.5 ml of 50% Folin-Ciocalteu reagent. After of 2-5 min, 1.0 ml of 20% Na_2CO_3 was added to the mixture and incubated for 10 min at room temperature. The mixture was centrifuged at 150 g for 8 minutes and the absorbance of the supernatant was measured at 730 nm. The total phenolics content was expressed as gallic acid equivalents (GAE) in mg/g sample.

Biological assays

Antimalaria assay

The antimalarial activity of extracts was assessed against *Plasmodium falciparum* (K$_1$ strain) which was cultured according to the method of Trager and Jensen(1976)[7]. The quantitative assessment of malarial activity was determined by means of the microculture radioisotope technique based on the method of Desjardins *et al.*(1979).[8] The inhibitory concentration (IC$_{50}$) represented the concentration causing 50% reduction in parasite growth and it was indicated on [^{3}H]-hypoxanthine by *P. falciparum*. The standard compound used as positive controls was dihydroartemisinin.

Cytotoxic assay

The cytotoxic profile of the extracts was assessed on three cancerous human cell lines using the Resazurin microplate assay (REMA). This assay was previously described by Brien*, et al* [9]. Three cancerous human-cell lines are available for this assay: KB cell line (human mouth carcinoma, ATCC CCL-17), NCI-H187 (human small cell lung cancer, ATCC CRL-5804) and MCF-7 cell line (breast cancer, ATCC HTB-22). In brief, cells at a logarithmic growth phase are harvested and diluted to $7x10^4$ cells/ml for KB and $9x10^4$ cells/ml for NCI-H187 and MCF-7, in fresh medium. Successively, 5 µl of test sample diluted in 5% DMSO, and 45 µl of cell suspension are added to 384-well plates. They were incubated at 37°C in 5% CO_2 incubator. After the incubation period (3 days for KB and MCF-7, and 5 days for NCI-H187), 12.5 µl of 62.5 µg/ml resazurin solution was added to each well, and the plates are then incubated at 37 °C for 4 hours. Fluorescence signal was measured by SpectraMax M5 multi-detection microplate reader (Molecular Devices, USA) at the excitation and emission wavelengths of 530 nm and 590 nm. Percent inhibition of cell growth was calculated by the following equation:

$$\% \text{ Inhibition } = [1- (FU_T / FU_C)]*100$$

Whereas FU_T and FU_C are the mean fluorescent unit from treated and untreated

conditions, respectively. Dose response curves were plotted from 6 concentrations of 2- fold serially diluted test compounds and the sample concentration that inhibited cell growth by 50% (IC$_{50}$) could be devived using the SOFTMax Pro software (Molecular Devices,USA). Ellipticine and doxorubicin were used as positive controls, and 0.5% DMSO was used as a negative control.

Antimicrobial assay

The antimicrobial activity of the extracts was assessed using the method described by Bauer, *et al* [10] on minimum inhibitory concentration (MIC). This assay of plant extracts was tested by the two-fold serial dilution method. The test extract was dissolved in 5% DMSO to obtain 1000 µg/ml stock solution that was incorporated into 0.5 ml of Agar for bacteria to get a concentration of 500 µg/ml and serially diluted by double technique to achieve 250, 125, 62.50, 31.25, 15.55 and 7.80 µg/ml, respectively. The volume was 50 µg of standardized on to each tube. The control tube contained only organism and not the plant extract, and the culture tubes were incubated at 37^{0}C for 24h, the lowest concentration that inhibited microbial growths was MIC value.

Results and Discussion

Table 1 shows the yield of crude extract from the stem bark of *P.anamense*. The yields of crude methanol extract was obtained in higher yields than crude ethylacetate extract and crude hexane extract, respectively. This result presented that crude extracts from the bark of *P.anamense* contain higher amounts of polar bioactive constituents than non-polar.

Table 1. Yield of crude extracts

Solvent	Extract Yield (g/kg dried weight)
hexane	0.0604
ethyl acetate	0.0795
methanol	0.1046

Antioxidant activity

Table 2 shows antioxidant activity of crude extracts from *P. anamense.* Crude methanol extract shows strong DPPH radical scavenging effect with IC$_{50}$ value of 200 µg/ml and total phenolics content of crude hexane extract, ethylacetate extract and methanol extract of 3.19, 12.08 and 42.70 mg GAE/g dw, respectively. This result presents that the extraction over polar solvent is able to extract antioxidant constituents better than non-polar solvent.

Table 2. Antioxidant activity of crude extracts.

Crude extracts	DPPH IC$_{50}$ (µg/ml)	Total phenolic content (mg GAE/g dw)
hexane extract	> 1000	3.19
ethylacetate extract	> 1000	12.08
methanol extract	200	42.70
Standard(BHT)	9.5	-

Biological assays

The results of biological activities of all extracts are shown in Table 3. Among the tested compounds, the crude hexane extract shows strong inhibitory effect against *P.falciparum* with IC_{50} value of 3.25 μg/ml and possesses cytotoxicity against KB cancer cell lines with IC_{50} value of 34.12 μg/ml.

The crude ethylacetate extract possessed cytotoxicity against KB and MCF-7 cancer cell lines with IC_{50} values of 19.03 and 47.70 μg/ml., respectively. The crude methanol extract showed Inhibitory effect against NCI-H187 cancer cell lines with IC_{50} value of 48.51 μg/ml.

Table 3. Biological activity of crude extract of *P. anamense*.

Samples	Antimalarial activity[a] (IC_{50}, μg/ml)	Cytotoxic activity (IC_{50}, μg/ml)		
		KB[b]	NCI-H187[c]	MCF-7[d]
Crude extracts				
Crude hexane	3.25	34.12	-	-
Crude ethylacetate	-	19.03	-	47.70
Crude methanol	-	-	48.51	-
Standard				
Dihydroartemisinine	0.0044	-	-	-
Ellipticine	-	0.325	0.441	-
Doxorubicin	-	0.147	0.041	0.822

[a] = Against *Plasmodium falciparum.* [b] = Human mouth carcinoma. [c] = Human small cell lung cancer. [d] = Breast cancer.

Antimicrobial activity

Table 4 shows Antimicrobial activities of crude extracts from *P. anamens*e. The crude hexane extract of *P. anamens*e shows minimum inhibitory concentrations against *S. mutans* ATCC 27175 *and S. sobrinus* with respective MIC values of 62.50 and 15.55 μg/ml.

The crude methanol extract of *P. anamens*e shows minimum inhibitory concentrations against *S. areus* (MRSA) 20626, *S.areus*(MRSA) 20626 with MIC value of 31.25 μg/ml and *S. milleri* group**,** *S. sobrinus and V. paraheamolyticus* with MIC value of 62.50 μg/ml.

Table 4. Antimicrobial activity of crude extracts.

Microbiology	MIC (μg/ml)		
	Hexane extract	Ethylacetate extract	Methanol extract
S. milleri group	500	1000	62.50
S. mutans ATCC 27175	62.50	> 1000	> 1000
S. sobrinus	15.60	> 1000	62.50
*S. aureus (*MRSA) 20625	> 1000	> 1000	31.25
S. areus (MRSA) 20626	> 1000	1000	31.25
V. paraheamolyticus	> 1000	> 1000	62.50

Conclusions

In summary, crude hexane extracts were active against the malarial parasite and showed inhibitory effect against KB cancer cell lines. Crude ethyl acetate extract showed inhibitory effect against KB and MCF-7 cancer cell lines, and crude methanol extract showed inhibitory effect against NCI-H187 cancer cell lines. It was concluded that the crude extracts form *P. anamense* could be the new source of antimalarial and cytotoxic agents. However, further studies should identify the molecular structure of antimalarial and cytotoxic compounds.

Acknowledgments

References

[1] Chayamaleut, K, *key Characters of Plant Families,* Department of National Park Wildlife and Plant, Bangkok, Thailand (2005).

[2] Chuakul, W., P. Saralamp and S.Prathanturarug, *Thai herbal encyclopedia*, Amarin Printing , Bangkok, Thailand (2000).

[3] Prayong, P., S. Barusrux and N. Weerapreeyakul, *Fitoterapia.* **79** (2008), pp. 598–601.

[4] Uys, A.C.U., S.F. Malan, S.V. Dyka and R.L. Zylb, *Bioorganic & Medicinal Chemistry Letters.* **12** (2002), pp. 2167–2169.

[5] Brand-Williams, W., M. E. Cuvelier, and C. Berset, *Food Science Technology.* **28** (1995), pp. 25 - 30.

[6] Velioglu, Y.S., Mazza, G., Gao, L., & Oomah, B. D. *Journal of Agricutural and Food Chemisty*, **46**(1998), pp. 4113-4117.

[7] Trager, W. and J. B. Jensen, *Science.* **193** (1976), pp. 673 - 675.

[8] Desjardins, R. E., C.J. Canfield, J. D. Haynes and J. D. Chulay, *Antimicrob Agents Chemother.* **16** (1979), pp. 710 - 718.

[9] Brien JO, Wilson I, Orton T, Pognan F, *Eur J Biochem.* **267** (2000), pp. 5421- 5426.

[10] Bauer, A. W., W. M. M. Kirby, J. C. Sherris, and M. Turck, *American Journal Clinical Pathology* .**45** (1966), pp. 493-496.

Pentacyclic Triterpenoids and Steroids from the Rhizomes of *Agapetes Hosseana* Diels

P. Kornwongwan and S. Luangkamin*

Department of Chemistry and Centre for Innovation in Chemistry (PERCH-CIC), Faculty of Science, Chiang Mai University, Chiang Mai 50200, Thailand

*Corresponding Author E-mail Address: *suwaporn@chiangmai.ac.th*

Abstract: *Agapetes hosseana* Diels, locally named Saphaolom, belongs to the family ERICACEAE. Its rhizomes have been use in traditional medicine for nourishment after having a fever. Three pentacyclic triterpenoids (1-3) and two steroids (4 and 5) were isolated from the dichloromethane extract of the dried rhizomes of *Agapetes hosseana* Diels. Their structures were determined to be taraxerone (1), taraxerol (2), 3-acetyl oleanolic acid (3), β-sitosterol (4) and stigmast-4-en-3-one (5), by comparison with the physicochemical and spectroscopic data in the literature. Compounds 1, 3 and 5 were isolated for the first time from this plant.

Introduction

Agapetes hosseana Diels, locally named Saphaolom, belongs to the family ERICACEAE and is widely distributed in the northern area of Thailand. Its rhizomes have been use in traditional Thai medicine for nourishment after having a fever. Previously, there were a few phytochemical investigations carried out on *Agapetes* genus including *A. hosseana* which are rich source of pentacyclic triterpenes [1-4].

As a part of continuing investigation on chemical constituents and bioactive compounds from *Agapetes* genus, the dichloromethane extract of air dried rhizomes of *Agapetes hosseana* Diels exhibited cytotoxicity against human lung (A549) and human breast (MDA-MB-231) cancer cells with IC_{50} values of 22.5 and 79.34 μg/ml, respectively. Therefore, this paper reports the isolation and structural determination of three triterpenoids and two steroids from the rhizomes of *A. hosseana*. The structures of these compounds were determined to be taraxerone (**1**), taraxerol (**2**), 3-acetyl oleanolic acid (**3**), β-sitosterol (**4**) and stigmast-4-en-3-one (**5**), based on the spectral and chemical evidence.

Materials and Methods

General experimental procedures: The melting points were determined on an Electrothermal melting point apparatus using capillary tubes and were uncorrected. The temperature is given in degree Celsius. ^{1}H-NMR (400 MHz), ^{13}C-NMR (100 MHz) spectra were recorded in CDCl$_3$ on Bruker DRX 400 spectrometer. The chemical shifts are given in δ (ppm) and coupling constants in Hz. The high resolution mass spectra were performed on a Q-TOF 2^{TM} mass spectrometer with a Z-spray^{TM} ES source. The electron

impact mass spectra were measured with Agilent-HP 5973 mass spectrometer. The IR spectra were obtained on a Nicolet Magna 510 Fourier transform IR spectrometer using KBr disks. Precoated TLC silica gel 60 F$_{254}$ aluminum sheets and glass plates from Merck were used for thin – layer chromatography (0.21 and 0.25 mm layer thickness for analytical and preparative TLC, respectively). Column chromatography was performed on silica gel 60 with particle size 0.040-0.063 mm.

Plant material: The rhizomes of *A. hosseana* were collected in August, 2008 at Doi Phahompok, Chiang Mai, Thailand. A voucher specimen (QBG-15988) has been deposited at the Herbarium of the Queen Sirikit Botanic garden, Thailand.

Extraction and Isolation: The Dried and powdered rhizomes of *A. hosseana* (304 g) were successively extracted with dichloromethane, ethyl acetate and methanol at room temperature for 7 days. The solvent were removed under vacuum to yield dichloromethane extract as a green viscous oil (2.97 g), ethyl acetate extract as a brownish viscous oil (1.54 g) and methanol extract as a brownish viscous oil (23.74 g). The dichloromethane extract was subjected to column chromatography (CC) over silica gel, eluted with a gradient of *n*-hexane-EtOAc followed by that of EtOAc-MeOH to give 11 fractions. Fraction 2 (243.2 mg) was isolated again by column chromatography (CC), eluted with 2%EtOAc/*n*-hexane to give compound **1** (29.0 mg). Fraction 4 (190.0 mg) was purified by crystallization with dichloromethane to give compound **2** (10.0 mg). The mother liquor was separated again by column chromatography, eluted with *n*-hexane-EtOAc (from 95:5 to 0:100) to give compound **4** (2.1 mg). Fraction 5 (278.9 mg) was purified by a silica gel CC using *n*-hexane-EtOAc (from 80:20 to 0:100) as eluent, yielding 7 subfractions. Subfraction 3 (21.5 mg) was further purified by preparative thin layer chromatography (PTLC) with 2% EtOAc/*n*-hexane to yield compound **5** (1.0 mg). Finally, subfraction 4 (20.2 mg) was subjected to PTLC, with 7% EtOAc/*n*-hexane (3 runs) to give compound **3** (7.1 mg).

Results and Discussion

The dichloromethane extract from the rhizomes of *A. hosseana* was purified to afford five compounds (**1-5**). Compounds **1-5** were identified as

taraxerone [5], taraxerol [6, 7], 3-acetyl oleanolic acid [8], β-sitosterol [9] and stigmast-4-en-3-one [10], respectively, by analysis of the IR, Mass, ^{1}H-NMR, ^{13}C-NMR, ^{1}H-^{1}H COSY, HMQC and HMBC spectra and comparison with the literature. Their structures are shown in Figure1. The physical and spectroscopic data of compound 1-5 are shown below. Compounds 1, 3 and 5 were reported for the first time in this plant. The other compounds had been reported by our group [4] and Deng group [1]. Moreover, the isolated compounds had been reported as bioactive compounds. Compounds 1 and 4 showed potent activity in brine shrimp lethality assay with LC_{50} values of 2.99 and 1.58 μg/ml, respectively [11]. Compound 2 exhibited antibacterial activity against *Staphylococcus aureus, Enteroccus faecalis, Pseudomonas aeruginosa* and *Escherichia coli* with MIC values of 0.04, 0.016, 0.63 and 0.31 mg/ml, respectively [12]. Compound 3 exhibited cytotoxic against NCI-H187 cell line (IC_{50} value of 9.4 μg/ml), anti-malarial (IC_{50} value 5.9 μg/ml) and antituberculosis (MIC value of 50 μg/ml) activities [13].
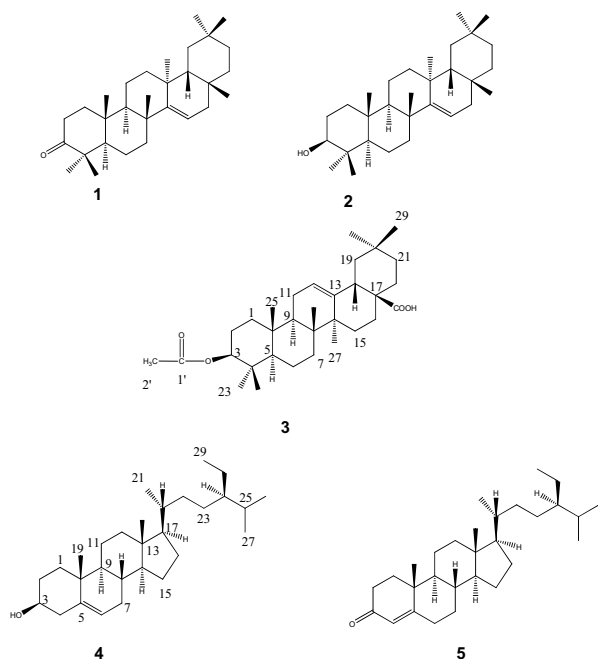

Fig.1 Chemical structure of compounds (1-5) isolated from the rhizomes of *Agapetes hosseana*.

Taraxerone (1) was obtained as white crystals, mp. 241.5-242.0 °C (Lit.[5], 240-243°C); IR (KBr) ν_{max} cm^{-1}: 2937, 1708, 1463, 1377; EIMS, *m/z* (rel. int.): 424 (M$^+$, 21), 300 (82), 285 (63), 204 (100), 133 (60); ^{1}H-NMR (CDCl$_3$, 400 MHz) δ: 0.83 (3H, *s*, H-28), 0.90 (3H, *s*, H-26), 0.91 (3H, *s*, H-30), 0.95 (3H, *s*, H-29), 1.06 (3H, *s*, H-24), 1.08 (3H, *s*, H-23), 1.09 (3H, *s*, H-25) 1.13 (3H, *s*, H-27), 1.00-1.70 (18H, *m*, CH,CH$_2$), 1.86 (1H, *m*, H-1a), 1.92 (1H, *dd*, *J* = 15.2, 3.2 Hz, H-12a), 2.07 (1H, *dt*, *J* = 13.0, 3.2 Hz, H-19a), 2.32 (1H, *m*, H-2a), 2.57 (1H, *m*, H -2b), 5.58 (1H, *dd*, *J* = 8.1, 3.2 Hz, H-15); ^{13}C-NMR (CDCl$_3$, 100 MHz) δ: 14.82 (*q*, C-25), 17.45 (*t*, C-11), 19.68 (*t*, C-6), 21.35 (*q*, C-24), 21.49 (*q*, C-30), 25.58 (*q*, C-27), 26.09 (*q*, C-23),

28.80 (*s*, C-20), 29.86 (*q*, C-26), 29.93(*q*, C-28), 33.07 (*t*, C-22), 33.37 (*q*, C-29), 33.56 (*t*, C-21), 34.15 (*t*, C-2), 35.10 (*t*, C-7), 35.78 (*s*, C-10), 36.66 (*t*, C-16), 37.53 (*s*, C-17), 37.69 (*t*, C-12), 37.74 (*s*, C-13), 38.35 (*t*, C-1), 38.87 (*s*, C-8), 40.62 (*t*, C-19), 47.59 (*s*, C-4), 48.70 (*d*, C-9), 48.77 (*d*, C-18), 55.77 (*d*, C-5), 117.20 (*d*, C-15), 157.59 (*s*, C-14), 217.00 (*s* ,C-3).

Taraxerol (2) was obtained as white needles, mp. 278.7-281.1°C (Lit.[6], 279-281 °C); IR (KBr, cm^{-1}): 3486, 2934, 1472, 1384, 1037; EIMS, *m/z* (rel. int.): 426(M$^+$, 12), 302 (34), 287 (35), 204 (100); ^{1}H-NMR (CDCl$_3$, 400 MHz) δ: 0.75-0.85 (1H, *m*, H-5), 0.80 (3H, *s*, H-24), 0.82 (3H, *s*, H-26), 0.90 (6H, *s*, H-28, H-30), 0.92 (3H, *s*, H-25), 0.94 (3H, *s*, H-29), 0.97 (3H, *s*, H-23), 1.09 (3H, *s*, H-27), 0.98-1.70 (21H, *m*, CH, CH$_2$), 1.92 (1H, *dd*, *J* = 14.7, 2.9 Hz, H-1a), 2.04 (2H, *dt*, *J* = 12.6, 3.0 Hz, H-19a), 3.19 (1H, *dd*, *J* = 11.2, 4.8 Hz, H-3), 5.53 (1H, *dd*, *J* = 8.1, 3.2 Hz, H-15); ^{13}C-NMR (CDCl$_3$, 100 MHz) δ: 15.43 (*q*, C-25), 15.46 (*q*, C-24), 17.50 (*t*, C-11), 18.80 (*t*, C-6), 21.32 (*q*, C-30), 25.91 (*q*, C-27), 27.15 (*t*, C-2), 28.00 (*q*, C-23), 28.81 (*s*, C-20), 29.83 (*q*, C-26), 29.93 (*q*, C-28), 33.09 (*t*, C-22), 33.35 (*q*, C-29), 33.70 (*t*, C-21), 35.12 (*t*, C-7, C-12), 35.80 (*s*, C-10), 36.67 (*t*, C-16), 37.57 (*s*, C-13), 37.71 (*t*, C-1), 37.99 (*s*, C-17), 38.77 (*s*, C-8), 38.98 (*s*, C-4), 41.32 (*t*, C-19), 48.75 (*d*, C-9), 49.28 (*d*, C-18), 55.53 (*d*, C-5), 79.08 (*d*, C-3), 116.88 (*d*, C-15), 158.09 (*s*, C-14).

3-Acetyl oleanolic acid (3) was obtained as white solid, mp. 219.3-222.7 °C (Lit.[8], 220-222°C); IR (KBr) ν_{max} cm^{-1}: 3445, 1695, 1462, 1024; TOFMS *m/z* 521.3518 (M+Na)$^+$; ^{1}H-NMR (CDCl$_3$, 400 MHz) δ: 0.74 (3H, *s*, H-26), 0.77 (1H, *m*, H-5), 0.85 (3H, *s*, H-29), 0.86 (3H, *s*, H-24), 0.88 (3H, *s*, H-23), 0.93 (3H, *s*, H-30), 1.12 (3H, *s*, H-25), 1.25 (3H, *s*, H-27), 1.00-2.00 (21H, *m*, CH, CH$_2$), 2.05 (3H, *s*, H-2′), 2.80 (1H, *dd*, *J*=13.7, 4.0 Hz, H-18), 4.48 (1H, *t*, *J*=7.6 Hz, H-3), 5.27 (1H, *t*, *J* = 3.3 Hz, H-12); ^{13}C-NMR (CDCl$_3$, 100 MHz) δ: 15.38 (*q*, C-25), 16.65 (*q*, C-24), 17.16 (*q*, C-26), 18.18 (*t*, C-6), 21.30 (*q*, C-2′), 22.89 (*t*, C-19), 23.39 (*t*, C-16), 23.53 (*t*, C-11), 23.57 (*q*, C-30), 25.89 (*q*, C-27), 27.67 (*t*, C-2), 28.04 (*q*, C-23), 29.70 (*t*, C-15), 30.67 (*s*, C-20), 32.44 (*t*, C-22), 32.54 (*t*, C-7), 33.05 (*q*, C-29), 33.79 (*t*, C-21), 36.99 (*s*, C-8), 37.70 (*s*, C-10), 38.07 (*t*, C-1), 39.29 (*s*, C-4), 40.95 (*d*, C-18), 41.57 (*s*, C-14), 46.54 (*s*, C-17), 47.55 (*d*, C-9), 55.30 (*d*, C-5), 80.93 (*d*, C-3), 122.57 (*d*, C-12), 143.6 (*s*, C-13), 171.63 (*s*, C-1′), 183.63 (*s*, C-28).

β-Sitosterol (4) was obtained as white crystals, mp. 138.6-140.0 °C (Lit.[9], 138-139 °C); IR (KBr, cm^{-1}): 3450, 2927, 1459, 1050; EIMS *m/z* (rel. int.) 414 (M$^+$, 100), 396 (81), 381 (47), 329 (61), 303 (63), 213 (67); ^{1}H-NMR (CDCl$_3$, 400 MHz) δ: 0.67 (3H, *s*, H-18), 0.81 (3H, *d*, *J*=6.9 Hz, H-27), 0.83 (3H, *d*, *J*=6.9 Hz, H-26), 0.85 (3H, *t*, *J*=7.7 Hz, H-29), 0.91 (3H, *d*, *J* = 6.6 Hz, H-21), 1.00 (3H, *s*, H-19), 1.07-1.92 (25H, *m*, CH, CH$_2$), 1.90-2.05 (2H, *m*, H-7, H-12), 2.18-2.32 (2H, *m*, H-4), 3.52 (1H, *m*, H-3), 5.35 (1H, *d*, *J* = 5.2 Hz, H-6); ^{13}C-NMR (CDCl$_3$, 100 MHz) δ: 11.87 (*q*, C-29), 11.99 (*q*, C-18), 18.79 (*q*, C-21), 19.05

(q, C-27), 19.41 (q, C-19), 19.83 (q, C-26), 21.09 (t, C-11), 23.07 (t, C-28), 24.31 (t, C-15), 26.07 (t, C-23), 28.26 (t, C-16), 29.16 (d, C-25), 31.90 (t, C-2), 31.90 (d, C-8), 31.93 (t, C-7), 33.95 (t, C-22), 36.15 (d, C-20), 36.51 (s, C-10), 37.26 (t, C-1), 39.78 (t, C-12), 42.28 (t, C-4), 42.32 (s, C-13), 45.83 (d, C-24), 50.14 (d, C-9), 56.07 (d, C-17), 56.77 (d, C-14), 70.79 (d, C-3), 121.71 (d, C-6), 140.76 (s, C-5).

Stigmast-4-en-3-one (**5**) was obtained as white powder, mp. 87.0-89.5 $^{\circ}$C (Lit.[10], mp. 87-88 $^{\circ}$C); IR (KBr) ν_{max} cm^{-1} : 2934, 1653, 1450; EIMS m/z (rel. int.) 412 (M^{+}, 25), 370 (11), 229 (42), 124 (100), 95 (20); ^{1}H-NMR (CDCl$_3$, 400 MHz) δ: 0.71 (3H, s, H-18), 0.81 (3H, d, J=6.8 Hz, H-27), 0.83 (3H, d, J=7.1 Hz, H-26), 0.84 (3H, t, J=7.6 Hz, H-29), 0.91 (3H, d, J=6.5 Hz, H-21), 1.18 (3H, s, H-19), 0.95-2.1 (27H, m, CH, CH$_2$) 2.21-2.45 (2H, m, H-2), 5.72 (1H, brs, H-4). ^{13}C-NMR (CDCl$_3$, 100 MHz) δ: 11.98 (q, C-18), 14.13 (q, C-29), 17.40 (q, C-21), 18.71 (q, C-27), 19.03 (q, C-19), 19.83 (q, C-26), 21.04 (t, C-11), 23.07 (t, C-28), 24.20 (t, C-15), 26.07 (t, C-23), 28.20 (t, C-16), 29.15 (d, C-25), 31.93 (t, C-2), 32.06 (t, C-7), 32.96 (d, C-6), 33.99 (t, C-22), 35.64 (d, C-8), 35.69 (t, C-1), 36.12 (d, C-20), 38.62 (s, C-10), 39.63 (t, C-12), 42.4 (s, C-13), 45.83 (d, C-24), 53.82 (d, C-9), 55.88 (d, C-17), 56.01 (d, C-14), 123.70 (d, C-4), 172.00 (s, C-5), 200.00 (s, C-3).

Conclusions

The bioactive triterpenoids, taraxerone (**1**), taraxerol (**2**), 3-acetyl oleanolic acid (**3**) and steroids, β-sitosterol (**4**) and stigmast-4-en-3-one (**5**) were isolated from dichloromethane extract of the rhizomes *Agapetes hosseana* Diels. Compound **1, 3** and **5** were reported for the first time in this plant.

Acknowledgements

References

[1] J. Deng and Y. Chen, *Peop. Rep. China.* **12** (1991), pp. 757-760.

[2] S. H. Huong, Y. Chen, Y. Meng and X. Cheng, *J. Mater Med*. **15** (1990), pp. 549-551.

[3] S. Luangkamin, S. Wongpornchai, P. Phringphrao, W. Thongthae, J. Alongkornsopit and W.Wongkham, *Abstract The 34th Congress Science and Technology of Thailand (STT34)*. (2008), Queen Sirikit National Convention Center, Bangkok.

[4] P. Kornwongwan and S. Luangkamin, *Abstract The 35th Congress Science and Technology of Thailand (STT35)*. (2009), The Tide resort Bangsean, Chonburi.

[5] P.V. Kiem, C.V. Minh, H.T. Huong, N.H. Nam and J. J. Lee, *Arch Pharm Res.* **27** (2004), pp. 1109-1113.

[6] A.C.N. Sacilotto, W. Vichnewski and W. Herz, *Phytochemistry.***44** (1997), pp. 659-661.

[7] W. Jin, X.F. Cai, M. Na, J.J. Lee and K. Bae, *Arch Pharm Res*. **4** (2007), pp. 412-418.

[8] F. Hichri, H.B. Jannet, J.Cheriaa, S. Jegnam and Z. Mighri, *C.R. Chimie*, **6** (2003), pp. 473-483.

[9] U. kolak, G. Topcu, S. Birteksoz, G. Otuk and A. Ulubelen, *Turk J Chem.* **29** (2005), pp. 177-186.

[10]F. Jamaluddin, S. Mohamed and Md. N. Lagis, *Food chem*. **54** (1995), pp. 9-13.

[11]Y. Ahmed, Md. H. Sohrab, S.M. Al-Rezaand and F.S. Tareq, *Food Chem. Toxicol*. **48** (2010), pp. 549-552.

[12]A. Rabie, Ph.D. Thesis, Pretoria University, Preoria, South Afteria (2005), pp. 190.

[13]K. Kanokmedhakul, S. Kanokmedhakul, *J. Ethanopharmacol*. **100** (2005), pp. 284-288

O-Acylation of A 5,6-Dimethoxy-1H-Dibenzo[de,h]Quinolin-7-Ol Derivative as a Route to a Novel Fused Furan System

W. Jaturonrusmee[1*] and J.B. Bremner[2]

[1] Department of Chemistry, Faculty of Science, King Mongkut's University of Technology Thonburi, Bangkok 10140, Thailand
[2] Department of Chemistry, University of Wollongong, Wollongong, NSW 2522, Australia

* E-mail: wasna.jat@kmutt.ac.th

Abstract: Reaction of 1,2,3,11b-tetrahydro-5,6-dimethoxy-1H-dibenzo[de,h]quinolin-7-ol (I) with oxalyl chloride in dry dichloromethane at 0°C gave the novel fused furan derivative 2,3-dihydro-6-hydroxy-5-methoxybenzo[6,7]benzofuro[5,4,3-jih]isoquinoline (II) in 45% yield, together with 1,1′-dicarbonyl-di(2,3-dihydro-5,6-dimethoxy-1H-dibenzo[de,h]quinoline) (III) in 22% yield. The fused product (II) incorporates a new heterocyclic ring system. The characterization of the products was based on spectroscopic evidence. The mechanism of formation of the fused product (II) will be described.

Introduction

In view of the generality and synthetic potential of the acylation of alcohols and amines promoted by oxalyl chloride [1-6], it was planned to investigate an acylation analogue of this type of reaction in case of the 1,2,3,11b-tetrahydro-5,6-dimethoxy-1H-dibenzo-[de,h]quinolin-7-ol (I), which was available [7] from another study. It was then hoped that the N-acylation of the derivative (I) leading to the mono-oxamide derivative (IV) could be effected; this mono-oxamide derivative (IV) was required in turn as part of a synthetic approach to short-bridged (1,8)anthracenophane derivatives. Such compounds are not only of chemical interest but may have potentially useful biological activity. In the event, none of the desired product (IV) was obtained but an interesting alternative reaction was found and is now reported.
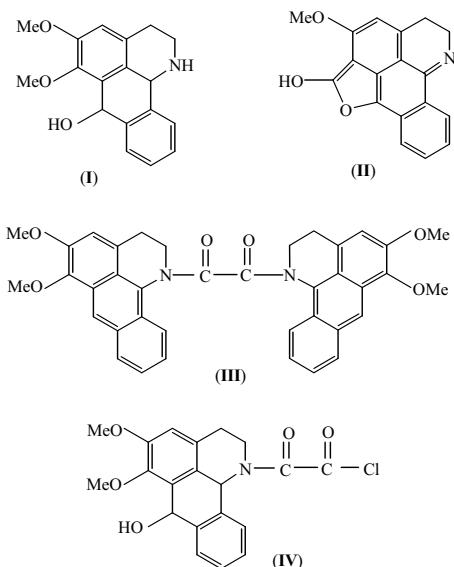
Materials and Methods

The 1,2,3,11b-tetrahydro-5,6-dimethoxy-1H-dibenzo[de,h]quinolin-7-ol (I) was prepared by the method reported [7] previously. Preparative thin-layer chromatography was performed on Camag siliga gel. All chromatographic solvent proportions are volume for volume. Solvents were removed under reduce pressure in a rotatory evaporator; the drying of the organic solvent extracts was done with anhydrous sodium sulfate.

R_f values refer to thin-layer chromatography on Merck silica gel 60 F_{254}.

Mass spectra were determined on VG MM 7070F mass spectrometer operating at 70 eV with source temperature of 200°C (direct insertion); peak intensities, in parentheses, are expressed as a percentage of the base peak.

^{1}H NMR spectra were determined at 300 MHz with a Bruker AM-300 spectrometer, tetramethylsilane being used as internal standard. ^{13}C NMR spectra were recorded at 75.5 MHz with a Bruker AM-300 spectrometer; assignments indicated by superscript letters may be interchanged for the atoms within each group defined by these letters.

Infrared spectra were recorded on a Hitachi 270-30 infrared spectrometer. .

Reaction of 1,2,3,11b-tetrahydro-5,6-dimethoxy-1H-dibenzo[de,h]quinolin-7-ol (I) [7] with oxalyl chloride.

To a solution of 1,2,3,11b-tetrahydro-5,6-di methoxy-1H-dibenzo[de,h]quinolin-7-ol (I) [7] (297 mg, 1.00 mmol) in dry dichloromethane (10 mL) was added oxalyl chloride (0.2 mL, 2.3 mmol) at 0 °C. The solution was stirred at 0°C for 1 hour and then at room temperature for 1 hour. The solution was then evaporated to dryness. The residue was subjected to p.t.l.c. (dichloromethane/3% methanol) to afford four fractions:

Fraction 1 (R_f 0.70) (8 mg), which was not investigated further.

Fraction 2 (R_f 0.60) (10 mg), which was not investigated further.

Fraction 3 (R_f 0.40) yielded 2,3-dihydro-6-hydroxy-5-methoxybenzo[6,7]benzofuro[5,4,3-jih] isoquinoline (II) (130 mg, 0.45 mmol, 45%), as a red

powder which could not be crystallized due to poor solubility in common organic solvents.

Mass spectrum: m/z 291 (M$^{+\cdot}$, 100, accurate mass 291.0884. $C_{18}H_{13}NO_3$ requires 291.0894), 276 (15), 262 (25), 248 (20), 191 (10), 102 (15). ^{1}H NMR δ ((CD$_3$)$_2$SO): 9.254 (broad s, 1H, OH), 8.512 (d, $J = 7.0$ Hz, 1H, H-8*), 8.488 (d, $J = 7.0$ Hz, 1H, H-11*), 7.857 (d of d of d, $J = 7.9, 7.0, 0.9$ Hz, 1H, H-10†), 7.568 (d of d of d, $J = 8.3, 6.9, 1.2$ Hz, 1H, H-9†), 6.867 (s, 1H, H-4), 4.247 (s, 3H, OCH$_3$), 4.075 (t, $J = 6.6$ Hz, 2H, H-3), 3.230 (t, $J = 6.6$ Hz, 2H, H-2), ^{13}C NMR δ ((CD$_3$)$_2$SO): 170.71 (C-6), 154.53 (C-5), 144.44 (C-11b), 139.08, 136.77, 134.57 (C-11$^\#$), 134.31 (C-8$^\#$), 132.83, 128.56, 126.89 (C-10‡), 127.00 (C-9‡), 122.28, 115.60 (C-4), 109.78, 95.45, 62.30 (OCH$_3$), 45.72 (C-2), 29.82 (C-3). IR ν_{max} (Nujol mull): 3360 (sharp, w, OH), 1692 (m), 1644 (sharp, s), 1622 (sharp, s), cm^{-1}.

Fraction 4 (R_f 0.25) yielded 1,1′-dicarbonyl-di(2,3-dihydro-5,6-dimethoxy-1H-dibenzo[de,h] quinoline (**III**) (68 mg, 0.11 mmol, 22%), as a yellow gum.

Mass spectrum: m/z 612 (M$^{+\cdot}$, 95, accurate mass 612.2264. $C_{38}H_{32}N_2O_6$ requires 612.2258), 306 (30), 278 (100), 262 (40). ^{1}H NMR δ (CDCl$_3$): 8.126-8.094 (m, 2H, H-8), 7.727 (s, 2H, H-7), 7.687-7.655 (m, 2H, H-11), 7.447-7.385 (m, 4H, H-9 and H-10), 6.601 (s, 2H, H-4), 4.860 (d of d, $J = 12.1, 4.5$ Hz, 2H), 4.097 (s, 6H, 2 x OCH$_3$), 3.940 (s, 6H, 2 x OCH$_3$), 2.768 (t of d, $J = 13.3, 3.0$ Hz, 2H), 2.199 (broad d, $J = 16.4$ Hz, 2H), 1.311-1.204 (m, 2H). ^{13}C NMR δ (CDCl$_3$): 165.73 (CO), 146.65 (C-5*), 141.08 (C-6*), 131.92, 129.38, 128.68 (ArH), 128.57 (ArH), 127.04, 126.19 (ArH), 125.07 (ArH), 125.00, 123.16, 119.79 (ArH), 119.43, 116.83 (C-4), 61.65 (OCH$_3$), 58.53 (OCH$_3$), 44.21 (CH$_2$N), 29.15 (Ar-CH$_2$). IR ν_{max} (thin film): 1656, 1652 (s, C=O), 1622 (s) cm^{-1}.

Results and Discussion

Reaction of 1,2,3,11b-tetrahydro-5,6-dimethoxy-1H-dibenzo[de,h]quinolin-7-ol (**I**) with oxalyl chloride in dry dichloromethane at 0°C gave the novel fused furan derivative 2,3-dihydro-6-hydroxy-5-methoxy benzo[6,7]benzofuro[5,4,3-jih]isoquinoline (**II**) in 45% yield, together with 1,1′-dicarbonyl-di(2,3-dihydro-5,6-dimethoxy-1H-dibenzo[de,h]quinoline) (**III**) in 22% yield. The fused product (**II**) incorporates a new heterocyclic ring system.

The characterization of the dimeric product (**III**) was based on spectroscopic evidence.

The mass spectrum of (**III**) showed the molecular ion at m/z 612 (95%) with a pominent peak at 306 (30%, M$^{+\cdot}$/2) and a base peak at 278 (M$^{+\cdot}$/2 - CO). The molecular formula, $C_{38}H_{32}N_2O_6$ for (**III**), was established by high-resolution mass spectrometer.

The infrared absorption spectrum showed strong absorption bands at 1656 and 1652 cm^{-1} for (**III**), ascribable to the amide carbonyl groups. The simplicity of the ^{1}H NMR spectrum and the ^{13}C NMR spectrum indicated a high degree of symmetry in the molecule. In the ^{1}H NMR spectrum, H-7 appeared as a singlet at δ 7.73. The positions and multiplicities of

the signals in ^{13}C NMR spectrum was consistent with the proposed structure.

The dimeric product (**III**) is formed by an N-acylation of the second molecule of the amine (**I**) by the intermediate (**IV**) and subsequent aromatization of the central ring.

The structural elucidation of the product (**II**) was based on the following spectroscopic evidence. The mass spectrum displayed a strong molecular ion at m/z 291 which was shown to have the molecular formula $C_{18}H_{13}NO_3$ from high resolution mass spectrometry. The ^{1}H NMR spectrum showed the presence of five aromatic protons, one methoxy group, two methylene groups and a broad singlet at δ 9.25. The last signal was assigned to a hydroxy group and was supported by the infrared spectrum which showed a broad band at 3360 cm^{-1}.

In the ^{13}C NMR spectrum, a quaternary carbon signal at 170.71 ppm was assigned to the olefinic carbon bearing the hydroxy group and attached to oxygen.

The formation of the fused furan product (**II**) probably arises from an initially formed O-acylated intermediate (**a**)[cf. 6] as shown in Scheme 1.
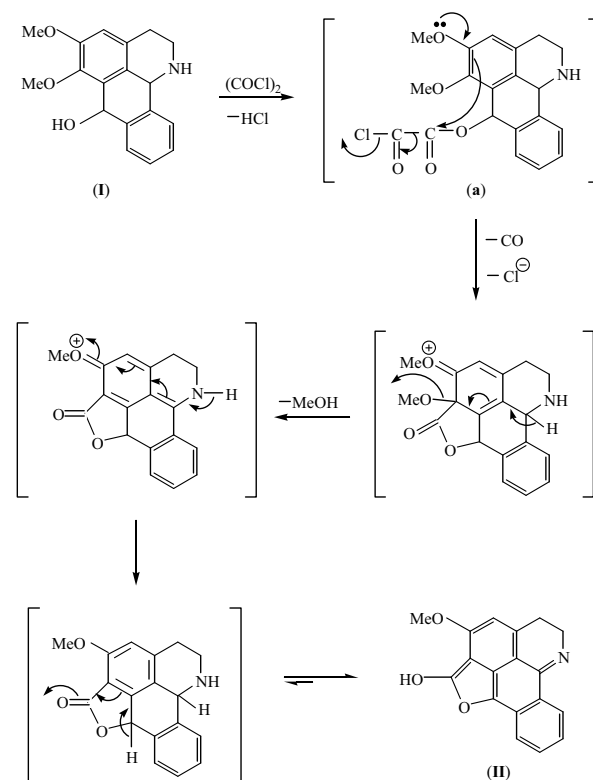
Scheme 1

Conclusions

Opportunities exist for generalization of this O-acylation and followed by cyclization process for the synthesis of other new fused furan systems. Further functional group manipulations should also provide access to fused furan derivatives of potential biological interest.

References

[1] R. Adams, W.V. Wirth and H.E. French, *J. Am. Chem. Soc.* **40** (1918), pp. 424-436.

[2] Y. Mikshich and Z. Pinterovich, *Bull Soc. Chem. Roy Yugoslav.* **1** (1930), p. 9; *Chem. Abstr.* **25** (1931), p. 4246.

[3] C.D. Nenitzescu, I. Necsoiu, and M. Zalman, *Comun. Acad. Rep. Populare Romine.* **8** (1958), p. 659; *Chem. Abstr.* **53** (1959), p. 17092.

[4] S.J. Rhoads and R.E. Michel, *J. Am. Chem. Soc.* **85** (1963), pp. 585-591.

[5] F.R. Jensen and T.I. Moder, *J. Am. Chem. Soc.* **97** (1975)**,** pp. 2281-2296.

[6] D.J. Zwanenburg and W.A.P. Reynen, *Synthesis.* **9** (1976), pp. 624-625.

[7] J.B. Bremner, W. Jaturonrusmee, L.M. Engelhardt and A.H. White, *Tetrahedron Lett.* **30** (1989), pp. 3213-3216.

Aroma volatile composition of *Millingtonia hortensis* Linn. F. flower Growing in Chiang Rai, Thailand

C. Thongpoon [1*], and T. Machan [2]

[1] Program of Chemistry, Faculty of Science and Technology, Pibulsongkram Rajabhat University, Phitsanulok 65000, Thailand
[2] Program of Applied Chemistry, School of Science, Mae Fah Luang University, Chiang Rai 57100, Thailand

*E-mail : cthongpoon@gmail.com

Abstract: This first report on the study of the aroma volatile components of the fresh *Millingtonia hortensis* Linn. F. flower growing in Chiang Rai, Thailand was described. The volatiles of fresh *M. hortensis* flower were extracted by maceration in petroleum ether at room temperature for 12 hours. After removing of the solvent under reduced pressure yielded light yellow semisolid volatile crude. The crude was re-dissolved in ethanol followed by filtration and evaporation to obtain the *M. hortensis* absolute (0.02%). The preliminary sensory evaluation showed that the scent of the obtained absolute was the closest to the fresh flower. The volatile compositions were investigated by GC-MS technique. Twenty seven compounds have been identified and accounted for 86% of the chromatographable components, with solanesol (25.72%), *trans*-farnesol (19.71%), nerolidol (8.54%), palmetic acid (6.77%), vanillin (6.20%), oleic acid (4.54%), linoleic acid (3.87%), L-linalool (3.37%), 1-octen-3-ol (1.67%), α-farnesene (1.22%), and methyl salicylate (1.03%) respectively, as the major constituents.

Introduction

In Thailand, *Millingtonia hortensis* Linn. F. is cultivated as an ornamental tree in yards, gardens and avenues. The plant, commonly known as "Peep" or "Kaa Sa Long" in Thai, belongs to the family Bignoniaceae. The flower of *M. hortensis* has very rich and pleasant scent and has been used as traditional medicine by the natives for treatment of a variety of conditions [1]. Pharmaceutical research revealed that the extract of *M. hortensis* flower has antifungal activity, larvicidal activity [2], antiproliferation activity [3], and antioxidant activity [4]. The general extraction method for the volatile of *M. hortensis* flowers is steam distillation and hydro-distillation. The disadvantage of these extractions is the scent of the obtained extract that is different from the fresh flower. Our report showed the extraction of aroma volatiles from *M. hortensis* flowers using non-polar solvent, petroleum ether, gave the extract that the scent was the closest to the fresh flower. Chemical composition of the extracted aroma volatiles was described.

Materials and Methods

Materials: Fresh flowers of *Millingtonia hortensis* were collected from Mae Fah Luang University, Chiang Rai, Thailand in November 2009. The plant was identified by the CMU herbarium, Faculty of Science, Chiang Mai University, Chiang Mai, Thailand.

Extraction of Essential Oil: Fresh flowers of *M. hortensis* (10 kg) were macerated in petroleum ether (5 L) for 12 h, followed by filtration and then removing of all solvent under reduced pressure to yield semi-solid petroleum ether crude. The crude was re-dissolved in ethanol (25 mL) followed by filtration and evaporation of all solvent to give a light yellow semi-solid *M. hortensis* absolute in a yield of 0.02%. The obtained absolute was dissolved in dichloromethane and adjusted to the concentration of 1 mg/mL.

Analysis of Essential Oil: Chemical compositions in the essential oil were analysed by GC-MS techniques.

GC-MS analysis: The volatile flavour constituents of *M. hortensis* were analysed using an HP model 6890 gas chromatograph equipped with an HP-5MS (5% phenyl-polymethylsiloxane) capillary column (30 m × 0.25 mm i.d., film thickness 0.25 μm; Agilent Technologies, USA) interfaced to an HP model 5973 mass-selective detector. The oven temperature was initially held at 60 °C and then increased by 2 °C /min to 250 °C. The injector and detector temperatures were 250 and 280 °C, respectively. Purified helium was used as the carrier gas at a flow rate 1 mL/min. EI mass spectra were collected at 70 eV ionization voltages over the range of m/z 29–300. The electron multiplier voltage was 1150 V. The ion source and quadrupole temperatures were set at 230 and 150 °C, respectively. Identification of the volatile components was performed by comparison of their Kovat retention indices, relative to C_8–C_{22} *n*-alkanes, and comparison of the mass

spectra of individual components with the reference mass spectra in the Wiley 275, NIST 98 databases and Adams 1989.

Results and Discussion

The volatile absolute of *M. hortensis* was extracted by a maceration of the fresh flower of the plant in petroleum ether. After filtration and removing of the solvent yielded volatile crude of *M. hortensis.* The crude was re-dissolved in ethanol followed by filtration and evaporation to give semi-solid *M. hortensis* absolute in a yield of 0.02%. This extraction procedure showed that the scent of the obtained absolute was the closest to the fresh flower of *M. hortensis.* Identification of the aroma volatile components of *M. hortensis* absolute was performed by a comparison of mass spectra with literature data (Wiley 275, NIST 98) and by comparison of their retention indices (RI) with those reported in the literature [5, 6, and 7]. Table 1 lists the identified compounds in the order of their elution on capillary column. A typical GC-MS TIC profile of the aroma volatiles from *M. hortensis* flower is presented in Figure 1. The most prominent compounds found were solanesol (25.72%), *trans*-farnesol (19.71%), nerolidol (8.54%), palmetic acid (6.77%), vanillin (6.20%), oleic acid (4.54%), linoleic acid (3.87%), L-linalool (3.37%), 1-octen-3-ol (1.67%), *α*-farnesene (1.22%), and methyl salicylate (1.03%) respectively, with integrator raw peak areas expressed as a percentage of the total chromatographable components of the volatiles. These compounds accounted for approximately 85.84% of total volatile components. A number of components could not be identified due to the lack of reference spectra and/or their relatively low abundance.

Conclusions

The aroma volatile components of the fresh flower of *M. hortensis* growing in Chiang Rai, Thailand have been extracted by using the non-polar organic solvent, petroleum ether followed by the polar organic solvent ethanol to yield volatile absolute (0.02%) and analyzed by GC- MS. 27/36 components have been identified. The first three major components were solanesol (25.72%), *trans*-farnesol (19.71%), and nerolidol (8.54%), repectively.

References
[1] R. Ramasubramaniaraja, *Int. J. Pharm. Sci. Rev.Res.*, **4** (2010), pp123-125.
[2] M. Sharma, S. Puri, P.D. Sharma, *Indian J. Pharm. Sci.*, **69** (2007), 599-601.
[3] S. Tansuwanwong, Y. Hiroyuki, I. Kohzoh, U. Vinitketkumnuen, *Asian Pac. J. Cancer Prev.,* **7** (2006), pp 641-644.
[4] P. Leelapornpisid, S. Chansakaow, C. Chaiyasut,N. Wongwattananukul, *International Workshop on Medicinal and Aromatic Plants Acta Horticulturae 786.*
[5] J.C. Leffingwell, E.D. Alford.. *J. Environ. Agric. Food Chem.* **4** (2005), 899-915.
[6] T.Y. Chung, J.P. Eiserich, T. Shibamoto, *J. Agric. Food Chem.,* **41**(1993), 1693-1697.
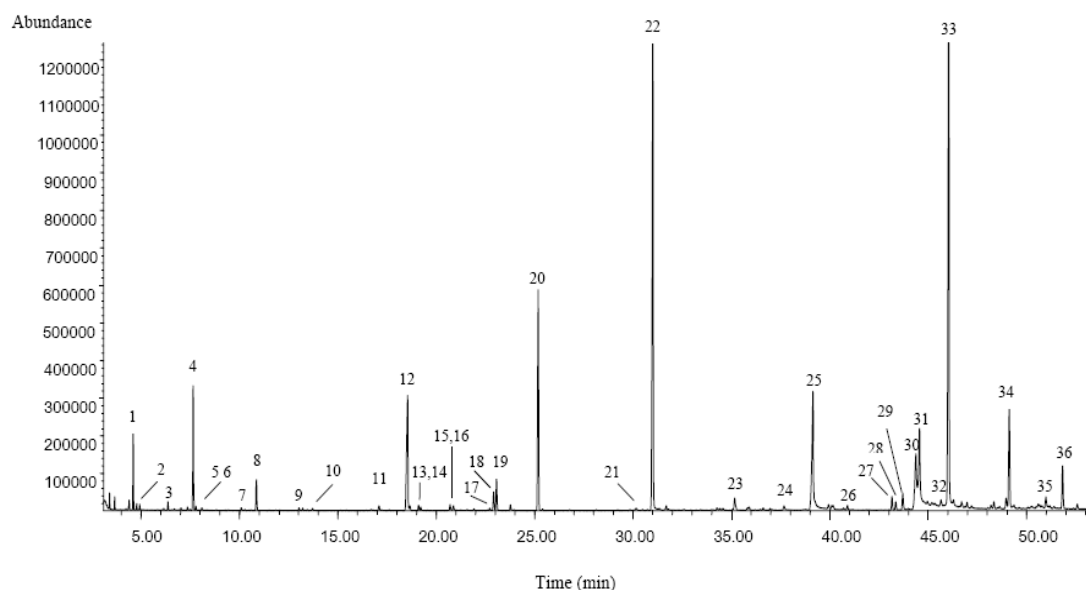[7] J.A. Pino, J. Mesa, Y. Munoz, M.P. Marti, R. Marbot,. *J. Agric. Food Chem.* **53** (2005), 2213-2223.

Figure 1. GC-MS TIC profile of the of the aroma volatile absolute of fresh flower of *M. hortensis.* See experimental for GC-MS condition and **Table 1** for peak identifications.

Table 1: Chemical compositions of the aroma volatile absolute of fresh flower of *M. hortensis*

No	Compounds	RA[a] (%)	RI[b] (exp.)	RI[c] (lit.)	MW	Identification[d]
1	1-Octen-3-ol	1.67	974	974[T]	128	1,2
2	3-Octanol	0.13	993	988[T]	130	1,2
3	*cis*-Linalool oxide (furanoid)	0.09	1039	1067[T]	170	1,2
4	*L*-Linalool	3.37	1043	1095[T]	154	1,2
5	Nonanal	0.13	1104	1100[T]	142	1,2
6	Phenylethyl alcohol	0.07	1112	1106[T]	122	1,2
7	*cis*-Linalool oxide (pyranoid)	0.09	1172	1170[T]	170	1,2
8	Methyl salicylate	1.03	1195	1090[T]	152	1,2
9	Geraniol	0.09	1252	1249[T]	154	1,2
10	2-Methyl naphthalene	tr	1291	1295[T]	142	1,2,3
11	1-Methyl naphthalene	tr	1308	1312[T]	142	1,2,3
12	Unidentified	tr	1391			1,2
13	Vanillin	6.20	1395	1393[T]	152	1,2
14	1,6-Dimethylnaphthalene	0.12	1414		156	1,2
15	Isoeugenol	0.21	1447	1448[T]	164	1,2
16	Unidentified	0.16	1451			
17	Unidentified	0.08	1469			
18	Unidentified	0.72	1478			
19	*α*-Farnesene	1.22	1507	1505[T]	204	1,2
20	Nerolidol	8.54	1563	1561[T]	222	1,2
21	*cis*-Farnesol	0.17	1694	1698[T]	222	1,2
22	*trans*-Farnesol	19.71	1740	1742[T]	222	1,2
23	Unidentified	0.10	1840			
24	Unidentified	0.19	1917			
25	*n*-Hexadecanoic acid	6.77	1967	1959[T]	256	1,2
26	Hexadecanal	0.18	2017		240	1,2
27	Methyl linoleate	0.55	2091	2095[T]	294	1,2
28	Heneicosane	0.32	2097	2100[T]	296	1,2
29	Phytol	0.75	2110	2111[T]	296	1,2,4
30	Linoleic acid	3.87	2133	2132[T]	280	1,2
31	Oleic acid	4.54	2141	2141[T]	282	1,2
32	Stearic acid	0.30	2162	2172[T]	284	1,2,5
33	Solanesol	25.72	2191		631	1
34	Unidentified	4.75	2197			
35	Unidentified	0.47	2210			
36	Unidentified	1.85	2215			

[a]RA, % Relative peak area
[b]RI(exp): Program temperature retention indices as determined on HP-5MS column using a homologous series of n-alkanes (C8-C22) as internal standard and He as carrier gas.
[c]RI(lit): Value from literature data of Adams, R.P. 1995. *Identification of essential oil components by gas chromatography/mass spectrometry*. Allured Publishing Corporation, Carol Stream, IL., using He as carrier gas; T: Program temperature values; MW : Molecular weight.
[d]1, Based on retention index; 2, Based on comparison of mass spectra with literature data (Wiley 275, NIST 98); 3, Leffingwell, J.C., and Alford, E.D. 2005. *J. Environ. Agric. Food Chem*. 4:899-915; 4, Chung, T.Y., Eiserich, J.P., and Shibamoto, T. 1993. *J. Agric. Food Chem*. 41:1693-1697; 5, Pino, J.A., Mesa, J., Munoz, Y., Marti, M.P., and Marbot, R. 2005. *J. Agric. Food Chem*. 53:2213-2223.
Tr : Trace.

Total Synthesis of (±)Aggreceride B

P. Songthammawat[1], J. Amtawong[2], W. Wongkasan[1], C. Hemmara[1], and P. Kuntiyong [1*]

[1] Department of Chemistry, Faculty of Science, Silpakorn University, Nakhon Pathom, Thailand
[2] Phra Pathom Witthayalai School, Nakhon Pathom, Thailand

[*]E-mail: punlop@su.ac.th

Abstract: Aggreceride B, a monoacylglyceride isolated from Actinomyces and Streptomyces strain OM-4209 has been synthesized. This compound inhibits platelet aggregation as well as the activity of Ralstonia solanacearum which causes bacterial wilt in tomatoes. The key steps of the synthesis are malonate alkylation, oxidative cleavage of C=C bond, and Julia-Kocienski olefination.

Introduction

Aggrecerides A-C, isolated from *Streptomyces* strain OM-4209, are monoacylglycerides with inhibitory effect against platelet aggregation, therefore these molecules are potential candidates for therapeutic agent for cardiovascular disease. Aggreceride B isolated from *Actinomyces* also showed potent activity against *Ralstonia solanacearum* which causes bacterial wilt in tomatoes[1].
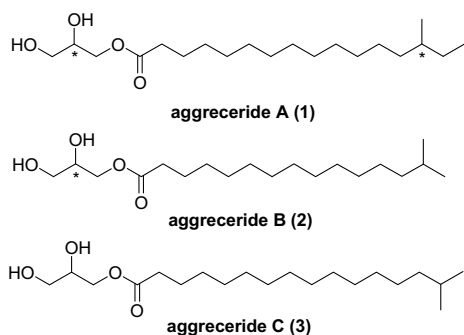

Figure 1. The aggreceride family

To the best of our knowledge, the absolute stereochemistry of the natural form of the aggreceride family has not been conclusively determined although all four diastereomers of aggreceride A have been synthesized [2]. There have been no published report on synthesis of aggrecerides B and C. Herein we report a total synthesis of the fatty acid precursor of aggreceride which is also a natural product known as aseanostatin P1 and its conversion to aggreceride B as a reacemate. Aseanostatin P1, isolated from *Actinomyces* strain from Thailand, inhibits myeloperoxidase (MPO) and regulates the function of polymorphonuclear leukocytes [3].
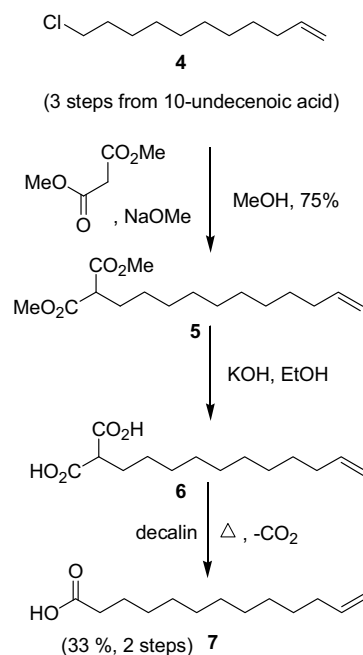

Scheme 1. Synthesis of 12-tridecenoic acid (**7**)

Our synthesis started with known 11-chloro-1-undecene (**4**) which was readily available in 3 steps from commercially available 10-undecenoic acid. Alkylation of chloride **4** with dimethylmalonate gave dimethyl ester **5** in good yield. Subsequent hydrolysis under basic condition and decarboxylation of the resulting dicarboxylic acid gave 12-tridecenoic acid (**7**) in 33% yield over two steps (Scheme 1). This compound was converted into aseanostatin P1 (**12**) over 5 synthetic steps (Scheme 2). Benzylation of the carboxylic acid gave the benzyl ester **8** and subsequent oxidative cleavage of the terminal olefin gave aldehyde **9** in moderate yield. Julia-Kocienski olefination of the aldehyde with phenyltetrazole-sulfone **10**, prepared in 2 steps from isobutyl alcohol, was achieved in good yield to give non-consequential *E/Z* mixture of olefin **11**. Treatment of this compound with hydrogen gas and catalytic palladium on activated charcoal furnished aseanostatin P1 (**12**) quantitatively via simultaneous hydrogenolysis of the benzyl ester and hydrogenation of the C-C double bond.
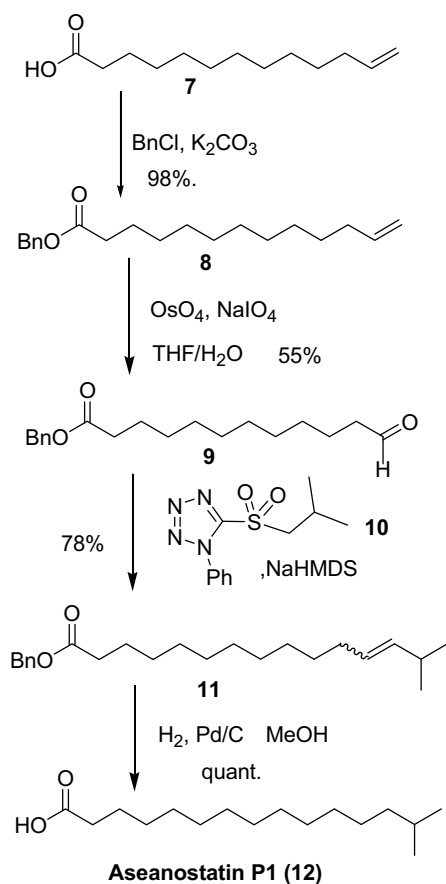
Scheme 2. Synthesis of aseanostatin P1 (**12**)

With the requisite fatty acid in hand, the synthesis of aggreceride B was accomplished in 2 further steps. Ester formation of the fatty acid with glycerol acetonide **13** using DCC and DMAP in dichloeomethane went without incident to give ester **14** and cleavage of the acetonide under acidic condition then completed the synthesis of aggreceride B as a racemic mixture (Scheme 3).
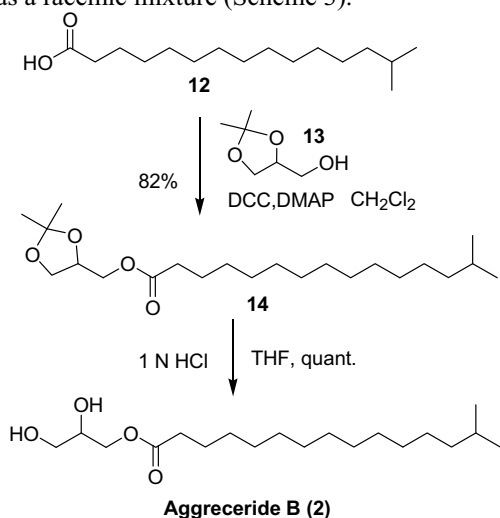
Scheme 3. Completion of aggreceride B (**2**)

Conclusions

In conclusion, we have synthesized aseanostatin P1 and aggreceride B racemate in 10 and 12 synthetic steps, respectively. Total synthesis of both enantiomers of homochiral aggreceride B as well as other members of the family is underway to establish the absolute configuration of the natural forms of aggrecerides as well as to supply enough material for further medicinal studies.

Acknowledgements

References

[1] S. Omura, A. Nakagawa, N. Fukamachi, K. Otoguro and B. Kobayashi, *J. Antibiot.* **39** (1986), pp. 1180–1181.

[2] L. Frydman and J.S. Harwood, *Biosci. Biotech.Biochem* . **59** (1995), pp. 78–82.

[3] A. I. Okawara, Y. Kimoto, K. Watanabe, K. Tokuda, M Shibata, K. Masuda, Y. Takano, K. Kawaguchi, H. Akagawa, N. Nilubol, K. Hotta, K. Yazawa, S. Mizuno, and K. Suzuki, *J. Antibiot.* **44** (1991), pp. 524-532.

Anionic Water Soluble Terphenylene Diethynylene Fluorophores

K. Vongnam[1], T. Vilaivan[2], M. Sukwattanasinit[2], and P. Rashatasakhon[2]*

[1] Program of Petrochemistry and Polymer Science, Faculty of Science, Chulalongkorn University, Phayathai Road, Pathumwan, Bangkok 10330, Thailand

[2] Organic Synthesis Research Unit, Department of Chemistry, Faculty of Science, Chulalongkorn University, Phayathai Road, Pathumwan, Bangkok 10330, Thailand

*E-mail: paitoon.r@chula.ac.th, Tel: +66-2-2187620

Abstract: Dendritic water soluble fluorophores containing terphenylene diethynylene units and carboxylic groups as anionic peripheries are designed and synthesized. The synthesis relies on a regioselective tri-iodination of triphenylamine and a Sonogashira cross-coupling with trimethylsilylacetylene. Removal of the protecting group provides a dendritic core in 78% yield. Starting from hydroquinone, a series of alkylation, iodination, and Sonogashira coupling with methyl 4-ethynylbenzoate afford the dendritic arms in moderate to good yields. The Sonogashira coupling between the core and an excess amount of dendritic arm gives rise to a zeroth generation dendrimer. All of the compounds are characterized by ^{1}H, ^{13}C NMR, and mass spectrometry. One of these anionic water soluble compounds exhibit a selective fluorescence quenching by Fe^{3+} ion in aqueous media.

Introduction

Fluorescence spectroscopy is one of the most sensitive analytical techniques for detecting and imaging of analytes at low concentration. Linear conjugated polyelectrolytes have widely been applied for metal ion detection based on its efficient singlet exciton migration within the polymer chain allowing efficient long-range Förster resonance energy transfer (FRET) between the polymers and a quencher.[1] Despite offering a potentially greater sensivity, the exact number of repeating fluorophores in linear conjugated polymers cannot be precisely controlled and their random conformations are unpredictable. Their large molecular weight distributions are responsible for inconsistent quenching efficiency, which reflects the low sensitivity of the detection. As parts of our research program on designs and syntheses of novel signal transducers for fluorescence sensors, we have demonstrated synthesis and applications of a polyanionic diphenylene ethynylene dendrimer as a selective fluorescence sensor for mercuric ion.[2] Most recently, we also demonstrated a sensor array for protein discrimination from the variously charged

derivatives of this dendrimer.[3] Although those dendritic fluorophores could serve as fluorescent signal transducers, their quantum efficiencies were relatively low which may result from hydrophobicity-induced π-π stacking in aqueous media due to their relatively planar structures. In this paper, we report a new design of polyanionic dendritic terphenylene diethynylenes **1-2** (Figure 1). We hypothesized that the extended conjugation from additional phenylene ethynylene units could result in compounds which have emission maxima at longer wavelengths compared to their diphenylene analogues. More importantly, this should give us an opportunity to incorporate some sterically hindered spacer units to prevent the undesirable molecular stacking.
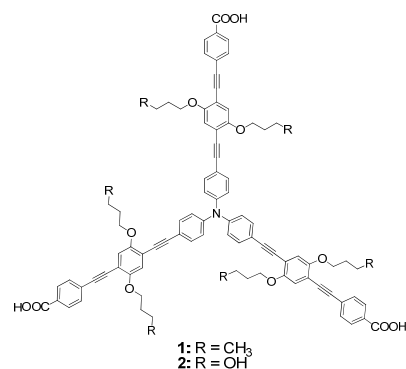
Figure 1. Structures of terphenylene diethynylene **1-2**

Experimental section

All chemicals were purchased from commercial sources and used without purification. All ^{1}H- and ^{13}C-NMR spectra were obtained on a Varian Mercury NMR spectrometer, which operated at 400 MHz for ^{1}H and 100 MHz for ^{13}C nuclei (Varian Company, CA, USA). Mass spectra were recorded on a Microflex MALDI-TOF mass spectrometer (Bruker Daltonics) using doubly recrystallized α-cyano-4-hydroxy cinnamic acid (CCA) and dithranol as a matrix. Absorption spectra were measured by a Varian

Cary 50 UV-Vis spectrophoto-meter. Fluorescence spectra were obtained from a Varian Cary Eclipse spectrofluorometer.

1,4-Dibutoxybenzene (3a)

To a mixture of 10 mL distilled DMF and hydroquinone (13.35 g, 0.12 mol) was added KOH (28 g, 0.5 mol) with violent stirring for half an hour under nitrogen. Then, n-BuBr (44.7 mL, 0.42 mol) was added dropwise to the mixture. After the reaction proceeded for 24 h, the mixture was poured into 100 mL of distilled water. Light yellow solid was filtered and dried under vacuum to afford the product in 17.07 g (64%). ^{1}H NMR (400 MHz, CDCl$_3$) δ ppm 6.81 (4H, s), 3.91 (4H, t, J = 6.5 Hz), 1.80-1.68 (4H, m), 1.55-1.41 (4H, m), 0.97 (6H, t, J = 7.3 Hz). ^{13}C NMR (100 MHz, CDCl$_3$) δ ppm 153.2, 115.4, 68.3, 31.5, 19.2, 13.8.

3,3'-(1,4-Phenylenebis(oxy))dipropan-1-ol (3b)

A mixture of hydroquinone (1.0 g, 9.08 mmol), K$_2$CO$_3$ (4.5 g, 0.033 mol), and 3-chloro-1-propanol (2.28 mL, 0.027 mol) in distilled MeCN (10 mL) was refluxed overnight under nitrogen atmosphere. The reaction was allowed to cool to room temperature and partitioned in CH$_2$Cl$_2$ (50 mL) and water (50 mL). The aqueous layer was separated and extracted with CH$_2$Cl$_2$ (2 × 50 mL). The organic fractions were collected, dried over Na$_2$SO$_4$, filtered and concentrated under reduced pressure to give a white solid residue. The crude product was crystallized from dichloromethane to give a white crystalline solid (1.57 g, 76%). ^{1}H NMR (400 MHz, CDCl$_3$) δppm 6.84 (4H, s), 4.08 (4H, t, J = 5.8 Hz), 3.86 (4H, t, J = 5.8 Hz), 2.03 (4H, p, J = 5.8 Hz). ^{13}C NMR (101 MHz, CDCl$_3$) δ = 153.4, 115.8, 66.9, 60.9, 32.4 ppm.

3,3'-(1,4-Phenylenebis(oxy))bis(propane-3,1-diyl) diacetate (3c)

To a solution of 3b (1.0 g, 4.42 mmol) and a catalytic amount of DMAP in 1:1 mixture of CH$_2$Cl$_2$ and pyridine (40 mL) was slowly added AcCl (1.6 mL, 0.022 mol). The mixture was stirred under N$_2$ at room temperature overnight. The solvent was removed, and the resulting slurry was re-dissolved in EtOAc and neutralized with 1 N NH$_4$Cl. A typical extractive work-up afforded product as light yellow powder (1.28 g, 94%). ^{1}H NMR (400 MHz, CDCl$_3$) δppm 6.81 (4H, s), 4.24 (4 H, t, J = 6.1 Hz), 3.98 (4 H, t, J = 6.1 Hz), 2.08 (4 H, dd, J = 12.61, 6.17 Hz), 2.04 (6H, s). ^{13}C NMR (101 MHz, CDCl$_3$) δ = 171.1, 153.1, 115.5, 64.9, 61.4, 28.7, 20.9 ppm.

1,4-Dibutoxy-2,5-diiodobenzene (4a)

To a cooled solution (< 15 °C) of ICl (1.31 mL, 0.026 mol) in MeOH (20 mL) was added 3a (1.33 g, 5.9

mmol) the mixture was allowed to warm, then heated under refluxing conditions for 4 h. A typical extractive work-up afforded 4a as a pale orange solid (2.08 g, 73%). ^{1}H NMR (400 MHz, CDCl$_3$) δppm 7.17 (2H, s), 3.93 (4H, t, J = 6.3 Hz), 1.85-1.73 (4H, m), 1.60-1.47 (4 H, m), 0.98 (6H, t, J = 7.3 Hz). ^{13}C NMR (101 MHz, CDCl$_3$) δ = 152.8, 122.7, 86.3, 70.0, 31.2, 19.3, 13.9 ppm.

3,3'-(2,5-Diiodo-1,4-phenylene)bis(oxy)bis(propane-3,1-diyl) diacetate (4c)

To a solution of I$_2$ (1.03 g, 4.06 mmol) and KIO$_3$ (0.41 g, 1.94 mmol) in glacial acetic acid (9 mL), H$_2$SO$_4$ (0.6 mL) and DI water (6 mL) was added 3c (1.2 g, 3.87 mmol). The mixture was heated at about 60 °C for 12 h. A typical extractive work-up followed by flash chromatography using hexanes: EtOAc (3:1) as the eluent afforded 4c as a yellow powder (1.45 g, 67%). ^{1}H NMR (400 MHz, CDCl$_3$) δppm 7.18 (2H, s), 4.32 (4H, t, J = 6.1 Hz), 4.02 (4H, t, J = 6.1 Hz), 2.18-2.09 (4H, m), 2.07 (6H, s). ^{13}C NMR (101 MHz, CDCl$_3$) δ = 171.1, 152.7, 122.8, 86.3, 66.7, 61.2, 28.6, 21.1 ppm.

Methyl 4-((2,5-dibutoxy-4-iodophenyl)ethynyl)benzoate (5a)

DBU (0.2 mL, 1.38 mmol) was slowly added to a mixture of 4a (1.18 g, 2.5 mmol), PdCl$_2$(PPh$_3$)$_2$ (17.5 mg, 0.025 mmol) and CuI (9.5 mg, 0.05 mmol) in toluene (30 mL). Then, a solution of methyl 4-ethynylbenzoate (0.2 g, 1.25 mmol) in toluene (2 mL) was added in small portions. The mixture was stirred at room temperature for 12 h. A typical extractive work-up followed by flash chromatography using gradient solvents from pure hexanes to CH$_2$Cl$_2$/hexanes (1:1) as the eluent afforded 5a as a yellow solid (0.34 g, 54 % yield). ^{1}H NMR (400 MHz, CDCl$_3$) δppm 8.02 (2H, d, J = 8.3 Hz), 7.57 (2H, d, J = 8.3 Hz), 7.32 (H, s), 6.91 (1H, s), 3.99 (4H, td, J = 8.19, 6.39 Hz), 3.93 (3H, s), 1.85-1.78 (4H, m), 1.60-1.52 (4H, m), 1.00 (6H, dt, J = 7.4, 1.4 Hz). ^{13}C NMR (100 MHz, CDCl$_3$) δ ppm = 166.5, 154.5, 151.9, 131.4, 129.5, 128.1, 123.9, 115.9, 113.0, 93.4, 88.7, 88.4, 69.8, 52.2, 31.3, 19.3, 13.8 ppm.

3,3'-(2-Iodo-5-((4-(methoxycarbonyl)phenyl)ethynyl)-1,4-phenylene)bis(oxy)bis(propane-3,1-diyl) diacetate (5c)

DBU (0.05 mL, 0.34 mmol) was slowly added to a mixture of 4c (0.37 g, 0.66 mmol), PdCl$_2$(PPh$_3$)$_2$ (4.4 mg, 6.24 µmol) and CuI (2.4 mg, 12.5 µmol) in toluene (10 mL). Then, a solution of methyl 4-ethynylbenzoate (0.05 g, 0.31 mmol) was added in small portions. The mixture was stirred at room temperature for 12 h. A typical extractive work-up

followed by flash chromatography using gradient solvents from pure hexane to CH_2Cl_2/hexane (1:3) as the eluent afforded **5c** as a white solid (91.8 mg, 50 % yield). ^{1}H NMR (400 MHz, CDCl$_3$) δ ppm 8.02 (2H, d, J = 8.2 Hz), 7.58 (2H, d, J = 8.2 Hz), 7.33 (1H, s), 6.93 (1H, s), 4.34 (4H, dt, J = 6.2, 1.7 Hz), 4.08 (4H, td, J = 10.4 and 5.9 Hz), 3.93 (3H, s), 2.20-2.13 (4H, m), 2.07 (6H, s). ^{13}C NMR (100 MHz, CDCl$_3$ δ = 171.1, 166.6, 154.2, 151.8, 131.5, 129.6, 127.9, 123.9, 116.0, 113.2, 93.7, 88.2, 88.1, 66.4, 61.3, 52.3, 28.7, 21.0 ppm.

Tris(4-ethynylphenyl)amine (6)

To a stirred solution of tris(4-iodo phenyl)amine (2.0 g, 3.21 mmol), PdCl$_2$(PPh$_3$)$_2$ (11.3 mg, 0.016 mmol) and CuI (6.0 mg, 0.032 mmol) in toluene (30 mL) was slowly added DBU (2.16 mL, 14.45 mmol). Then, trimethylsilyl acetylene (2.03 mL, 14.45 mmol) was added and the mixture was stirred at room temperature for 24 h. A typical extractive work-up followed by flash chromatography provided a yellow solid, which was mixed with K$_2$CO$_3$ (0.86 g, 6.19 mmol), CH$_2$Cl$_2$ (30 mL) and methanol (30 mL). The mixture was stirred at room temperature for 12 h. A typical extractive work-up followed by flash chromatography afforded brown-yellow solid (0.56 g, 86 % yield). ^{1}H NMR (400 MHz, CDCl$_3$) δppm 7.38 (6H, d, J = 8.5 Hz), 7.01 (6H, d, J = 8.5 Hz), 3.06 (3H, s). ^{13}C NMR (101 MHz, CDCl$_3$) δ = 146.9, 133.2, 123.8, 116.7, 83.3 ppm.

4,4',4''-(4,4',4''-(4,4',4''-nitrilotris(benzene-4,1-diyl)tris(ethyne-2,1-diyl))tris(2,5-dibutoxybenzene-4,1-diyl))tris(ethyne-2,1-diyl)tribenzoic acid (1)

DBU (0.1 mL, 0.63 mmol) was slowly added to a mixture of 5a (0.28 g, 0.55 mmol), PdCl$_2$(PPh$_3$)$_2$ (4.4 mg, 6.3 μmol) and CuI (0.6 mg, 3.2 μmol) in toluene (5 mL). Then, solution of 6 (0.05 g, 0.16 mmol) was added and the mixture was stirred for 12 h. A typical extractive work-up followed by flash chromatography afforded a yellow solid. A mixture of this product (100 mg, 0.069 mmol), saturated KOH aqueous solution (0.1 mL) in THF (5 mL), methanol (5 mL) and water (3 mL) was refluxed with stirring for overnight. Volatile solvents were evaporated and the residue dissolved in water (15 mL). Ice was added to the aqueous layer which is acidified and the mixture was stored in a refrigerator. The suspension was centrifuged to afford 1 as a yellow solid (96.9 mg, 35 % yield). ^{1}H NMR (400 MHz, DMSO) δppm 7.98 (6H, d, J = 7.8 Hz), 7.61 (6H, d, J = 7.8 Hz), 7.47 (6H, d, J = 7.7 Hz), 7.19 (6H, s), 7.16 (6H, s), 7.12 (6H, d, J = 7.7 Hz), 4.05 (12H, s), 1.68-1.63 (12H, m), 1.46-1.41 (12H, m), 0.95 (18H, t, J = 7.3 Hz). [13]C

NMR (101 MHz, CDCl$_3$) δ = 166.6, 153.3, 146.2, 132.7, 130.4, 129.5, 126.8, 124.1, 117.3, 116.4, 113.9, 112.3, 94.9, 93.8, 88.9, 85.9, 68.6, 30.7, 18.7, 13.6 ppm. MS(MALDI-TOF) Calcd for C$_{93}$H$_{87}$NO$_{12}$: 1410.69 Found: 1410.56.

4,4',4''-(4,4',4''-(4,4',4''-nitrilotris(benzene-4,1-diyl)tris(ethyne-2,1-diyl))tris(2,5-bis(3-hydroxypropoxy)benzene-4,1-diyl))tris(ethyne-2,1-diyl)tribenzoic acid (2)

This compound was prepared from **5c** using the same procedure reported for **1**. The product was obtained as a yellow solid (27.1 mg, 34 % yield). 1H NMR (400 MHz, DMSO) δppm 8.03 (7H, d, J = 7.9 Hz), 7.67 (6H, d, J = 7.9 Hz), 7.55 (6H, d, J = 8.0 Hz), 7.27 (6H, s), 7.24 (6H, s), 7.14 (6H, d, J = 8.0 Hz), 4.69-4.54 (6H, m), 4.17 (12H, t, J = 6.5 Hz,), 3.69 (12H, t, J = 5.44 Hz), 1.94 (12H, m). ^{13}C NMR (101 MHz, CDCl$_3$) δ = 166.6, 153.2, 146.3, 132.7, 130.4, 129.5, 126.7, 124.0, 117.3, 116.6, 113.9, 112.3, 94.9, 93.8, 88.7, 85.8, 65.9, 57.2, 32.1 ppm. MS(MALDI-TOF) Calcd for C$_{93}$H$_{87}$NO$_{12}$: 1422.52 Found: 1423.58.

Results and Discussion
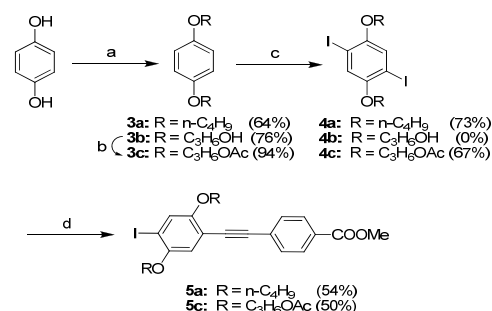
Scheme 1. Reagents and conditions: (a) *n*-BuBr, KOH DMF for **3a** or ClC$_3$H$_6$OH, K$_2$CO$_3$, MeCN for **3b**; (b) AcCl, DMAP, py, CH$_2$Cl$_2$; (c) ICl, MeOH for **4a-b** or I$_2$, KIO$_3$, AcOH, H$_2$O, H$_2$SO$_4$ for **4c**; (d) Methyl 4-ethynyl benzoate, PdCl$_2$(PPh$_3$)$_2$, CuI, DBU, PhMe

Our target dendritic water-soluble terphenylene diethynylene fluorophores were synthesized by mean of Sonogashira coupling. Prior to that key step, the dendritic arms were synthesized by *O*-alkylation of dihydroquinone (Scheme 1). The dibutylated product (**3a**) was successfully iodinated by a reaction with ICl, but the same reaction with **3b** was unsuccessful. We hypothesized that the presence of the hydroxyl groups may interfere with the reaction to some extents. After an acetylation of the hydroxyl groups, **3c** smoothly underwent the iodination upon treatment with I$_2$ and KIO$_3$. A Sonogashira coupling of **3a** and **3c** with methyl 4-ethynylbenzoate gave rise to **5a** and **5c** in moderate yields.

We assembled fluorophore **1** and **2** by a series of Sonogashira couplings (Scheme 2). First, the tris(4-iodophenyl)amine[2] was coupled with trimethylsilyl acetylene, followed by TMS deprotection. A sequential reaction the dendritic arms (**5a** or **5c**) followed by base-hydrolysis led to dendrimer (**1** or **2**) in fair yields.


6: (86%)

b → **1: (35 %)**
        2: (34 %)
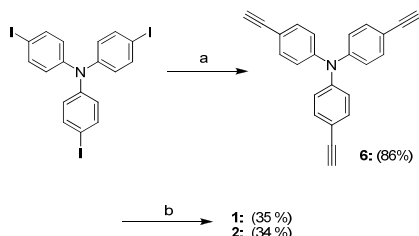
Scheme 2. Reagents and conditions: (a) *i.* trimethylsilyl acetylene, $PdCl_2(PPh_3)_2$, CuI, NEt_3; *ii.* K_2CO_3, CH_2Cl_2, MeOH (1:1); (b) *i.* **5a** or **5c**, $PdCl_2(PPh_3)_2$, CuI, DBU, PhMe; *ii.* KOH, THF, MeOH.

The photophysical properties of **1** and **2** in 50 mM phosphate buffer (pH 8.0) were investigated and the results are shown in Table 1. Both fluorophores exhibit absorption and emission at almost the same wavelength. However, the quantum efficiency of **2** was considerably higher than that of **1**, indicating a better solubility or less aggregation in aqueous media. For a preliminary screening of applications as fluorescence sensors, we investigated the fluorogenic responses of **1** and **2** in the presence of metal ions such as Fe^{3+}, Fe^{2+}, Co^{2+}, Ni^{2+}, Cu^{2+}, Cd^{2+}, Hg^{2+}, Mn^{2+}, Ba^{2+}, Pd^{2+}, Pb^{2+}, Zn^{2+}, Ca^{2+} and Al^{3+}. It was found that **1** exhibit a selective fluorescence quenching by Fe^{3+} ion without showing significant signal changes by Fe^{2+} or other metal ions (Figure 2). This selectivity renders an application of the fluorophore as a sensor for trace analysis and diagnosis of iron-related diseases.

Table 1. Photophysical properties of **1** and **2** in 50 mM phosphate buffer (pH 8.0)

Comp.	Absorption		Emission	
	λ_{max} (nm)	log ε ($M^{-1}cm^{-1}$)	λ_{max} (nm)	$\Phi_F{}^a$
1	396	3.70	490	0.18
2	398	5.10	508	0.33

[a] Quinine sulfate in 0.1 M H_2SO_4 (Φ=0.54) was the reference.
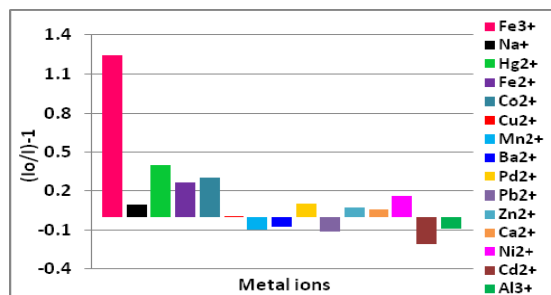
Figure 2. Fluorescence responses of **1** (4 µM) to various metal ions (400 µM) in phosphate buffer (50 mM, pH 8.0).

Conclusion

Two new terphenylene diethynylene dendritic compounds containing negatively charged peripheral groups were successfully synthesized. Both compounds displayed high fluorescent quantum yields in aqueous media, which was rationalized by steric-induced deaggregation. The greater quantum efficiency of **2** may result from the hydrophilic –OH groups facilitating the solubility. Fluorophore **1** exhibited a selective fluorescent quenching by Fe^{3+}. The improvements on sensitivity as well as the exploration of further applications for these fluorophores are currently undertaken.

Acknowledgement

References

1. (a) Chen, L.; McBranch, D. W.; Wang, H.-L.; Helgeson, R.; Wudl, F.; Whitten, D. G. *Proc. Natl. Acad. Sci. U.S.A.* **1999**, *96*, 12287. (b) Wang, D.; Wang, J.; Moses, D.; Bazan, G. C.; Heeger, A. J. *Langmuir.* **2001**, *17*, 1262. (c) Fan, C.; Wang, S.; Hong, J. W.; Bazan, G. C.; Plaxco, K. W.; Heeger, A. J. *Proc. Natl. Acad. Sci. U.S.A.* **2003**, *100*, 6297.

2. Niamnont, N.; Siripornnoppakhun, W.; Rashatasakhon, P.; Sukwattanasinitt, M. *Org. Lett.*, **2009**, *13*, 2768.

3. Niamnont, N.; Mungkarndee, R.; Techakriengkrai, I.; Rashatasakhon, P.; Sukwattanasinitt, M. *Biosens. Bioelectron.* **2010**, *26*, 863.

4. Onitsuka, K.; Ohara, N.; Takei, F.; Tagahashi, S., *Dalton Trans.,* **2006,** 3693.

5. Fang, Z.; Wang, S.; Zhao, L.; Xu, Z.; Ren, J.; Wang, X.; Yang, Q., *Mater. Chem. Phys.*, **2008**, *107*, 305.

6. Wariishi, K.; Morishima, S.; Inagaki, Y., *Org. Process Res. Dev.,* **2003**, *7*, 98.

Synthesis of Chelidamic Acid-Based Photosensitizer for Optoelectronic Devices

S. Seawpakorn[1,2], P. Thamyongkit[2,3] and R. Rojanathanes[2,3*]

[1] Program in Petrochemistry and Polymer Science, Faculty of Science, Chulalongkorn University, Bangkok, Thailand 10330
[2] Department of Chemistry, Faculty of Science, Chulalongkorn University, Bangkok, Thailand 10330
[3] Center of Excellence for Petroleum, Petrochemicals, and Advanced Materials, Chulalongkorn University, Bangkok, Thailand 10330

[*] Email: rojrit@hotmail.com

Abstract: Solar energy is a clean energy empowering our future lives. Efficiency of solar energy conversion depends strongly on the efficiency of the solar cells. This research focuses on the synthesis of "pincer" molecules as optoelectronic converters. Pincers were synthesized from chelidamic acid. Iodo and ethynyl groups were successfully attached onto the 4-pyridinyl position. Then, aminopyridine group can be modified onto both carboxylic ends of the chelidamic acid. The pincers can be dimerised by Sonogashira coupling at the ethynyl group. The pincers were complexed with various transition metal ions. These complexes were tailored for the bulk hetero-junction solar cells. Moreover, benzoic acid was connected onto the 4-pyridinyl position in order to synthesize the pincer dye for the dye-sensitized solar cells. Photophysical and electrochemical properties of dyes will be investigated to evaluate their potential for being used in organic solar cells.

Introduction

Today, global warming is a major problem increasing with energy consumption. The majority of current global energy consumption came from fossil fuels. Future global energy is rise to ~30 TW by 2050, which requires at least an extra 17 TW by 2050 when our fossil fuel reserves are vanishing.[1] The sun is a stable source of energy supplying abundant and clean energy. Currently inorganic semiconductors dominate the solar cell production market, but these materials require high technolygy of production and expensive starting materials, making electricity production in this manner too costly to compete with conventional sources of electricity.[2] Dye-sensitized solar cells (DSSCs) have attracted a great deal of interest because of their relatively higher efficiency and low cost compared with conventional inorganic photovoltalaic devices.[3] Bulk hetero-junction solar cell can be made as a flexible and translucent material and offer more opportunities for application in new markets such as mobile electronics, smart cards, power-generating windows, automotive, home appliance, etc.[2]

Materials and Methods

Chelidamic acid[4], 4-chloropyridine-2,6-dicarcoxylic acid[5] and dimethyl 4-iodopyridine-2,6-dicarboxylate[6] were prepared by following published procedure. 2-(aminomethyl)pyridine, 4-iodobenzoic acid and ethynyltrimethylsilane were purchased from Aldrich. All the solvents used for the synthesis were of analytical grade.

NMR spectra were recorded on a Varian Mercury NMR spectrometer 400 MHz. Mass spectra were obtained using matrix-assisted laser desorption ionization mass spectrometry (MALDI-MS) by using dithranol as a matrix. Absorption spectra were measured in methanol using a Hewlett-Packard 8453 spectrophotometer.
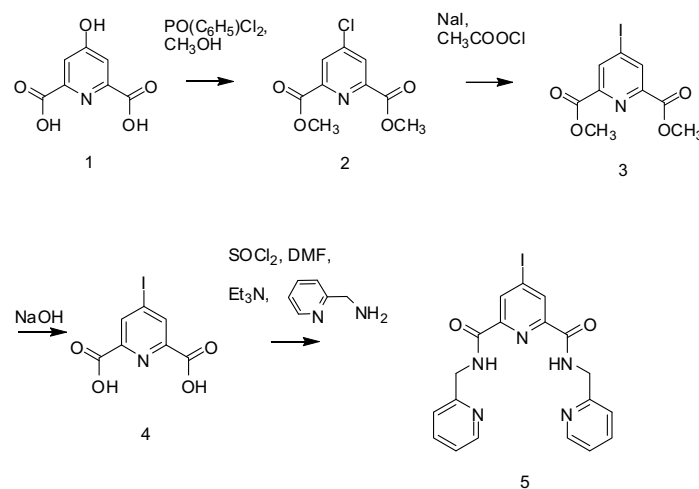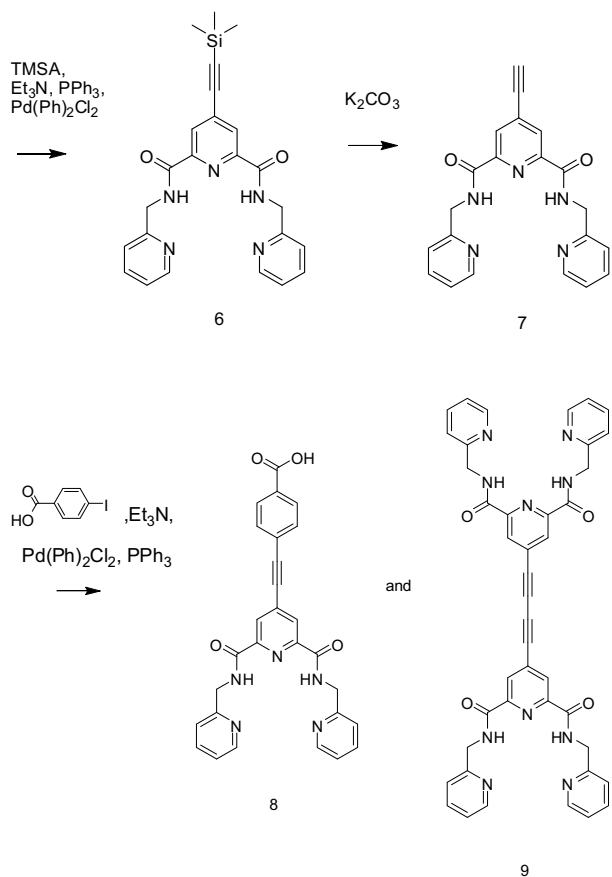
TMSA = Trimethylsillylacethylene

4-iodopyridine-2,6-dicarboxylic acid (4). NaOH (0.660 g, 16.649 mmol, 4 eq) was dissolved in 10 ml of CH_3OH. Methyl 4-iodopyridine-2,6-dicarboxylate **(3)** (1.028 g, 4.162 mmol, 1 eq) was dissolved in 90 ml of CH_2Cl_2. Solution of NaOH was added to solution of **3**, then the mixture was kept stirring at room temperature for 30 min. The crude mixture was then extracted with water. The aqueous phase was adjusted to pH 1 with $HCl_{(aq)}$. The product was collected as a white precipitate (0.9286 g, 98.8 %). ^{1}H NMR (DMSO, 400 MHz) : 8.59 (*s*, 1H, py). ^{13}C NMR (DMSO, 100 MHz) : 108.10, 135.30, 148.27, 163.87.

N,N-bis[2-(pyridinyl)methyl]-4-iodopyridine-2,6-dicarboxamide (5). 4-iodopyridine-2,6-dicarboxylate **4** (1.84 g, 8.402 mmol, 1 eq) was added with excess 15 ml $SOCl_2$ and 1-2 drops of DMF. After refluxing for 2 hours, the excess of $SOCl_2$ was removed. Then, 100 ml of CH_2Cl_2 was added in order to dissolve the crude solid. The 2-(aminomethyl)pyridine (2.17 ml, 21.005 mmol, 2.5 eq) was dissolved into 40 ml of CH_2Cl_2 and slowly added into the reaction. Triethylamine (3.51 ml, 25.21 mmol, 3 eq) was then slowly added. The reaction was kept stirring at room temperature overnight. The solvent was evaporated, the crude product was dissolved in 100 ml of CH_2Cl_2 and washed with 2x20 ml of sat. $NaHCO_3$ and 2x20 ml of water and then dried over Na_2SO_4. The crude product was recrystallized with $CH_2Cl_2/C_2H_5COOCH_3$ giving white solid as the desired product (2.482 g, 74.31 %). ^{1}H NMR (CDCl3, 400 MHz) : 4.81 (*d*, 2H, CH2), 7.23 (*t*, 1H, py), 7.39 (*d*, 1H,

py), 7.70 (*t*, 1H, py), 8.52 (*d*, 1H, py), 8.72 (*s*, 1H, py), 9.10 (*d*, 1H, NH) . ^{13}C NMR (CDCl3, 100 MHz) : 44.63, 108.20, 122.81, 125.21, 134.18, 136.97, 149.17, 150.23, 156.66, 162.60.

N,N-bis[2-(pyridinyl)methyl]-4-[(trimethylsilyl)ethynyl]pyridine-2,6-dicarboxamide (6). Solution of Et3N in THF was added with *N,N*-bis[2-(pyridinyl)methyl]-4-iodopyridine-2,6-dicarboxamide **5** (0.356 g, 0.8946 mmmol, 1 eq), trimethylsilylacetylene (TMSA) (0.2554 g, 1.789 mmol, 2 eq), Pd(Ph)2Cl2 (0.025 g, 0.036 mmol, 0.04 eq) and PPh3 (0.009 g, 0.036 mmol, 0.04 eq), respectively. The reaction mixture was refluxed under nitrogen atmosphere at 120 [0]C for overnight. The reaction mixture was washed with 2x10 ml of sat. NH_4Cl and 2x10 ml of water and was dried over Na_2SO_4. Purification with column chromatography using 1:20 $CH_3OH/C_2H_5COOCH_3$ gave the desired product as white solid (0.316 g, 80 %). ^{1}H NMR (CDCl3, 400 MHz) : 0.27 (*s*, 9H, CH3), 4.81 (*d*, 4H, CH2), 7.22 (*t*, 2H, py), 7.39 (*d*, 2H, py), 7.69 (*t*, 2H, py), 8.38 (*s*, 2H, py), 8.51 (*d*, 2H, py), 9.18 (*d*, 2H, NH). ^{13}C NMR (CDCl3, 100 MHz) : -1.05, 43.94, 100.37, 102.12, 121.49, 121.76, 126.26, 133.72, 136.25, 148.18, 148.37, 156.33, 162.67.

N,N-bis[2-(pyridinyl)methyl]-4-ethynylpyridine-2,6-dicarboxamide (7). *N,N*-bis[2-(pyridinyl)methyl]-4-[(trimethylsilyl)ethynyl]pyridine-2,6-dicarboxamide **6** (0.16 g, 0.036 mmol, 2 eq) was dissolved with 50 ml of CH_3OH and was added with K_2CO_3 (0.011 g, 0.018 mmol, 1 eq), and stirred at room temperature for 30 minutes. CH_3OH was removed with vacuum evaporation. The product was extracted with 50 ml of CH_3Cl_2 and 2x10 ml of water. The organic layer was dried over Na_2SO_4. The solvent was then removed with vacuum evaporation giving the desired product as white solid (0.123 g, 91 %). ^{1}H NMR (CDCl3, 400 MHz) : 3.42 (*s*, 1H, CH), 4.90 (*d*, 4H, CH2), 7.36 (*t*, 2H, py), 7.56 (*d*, 2H, py), 7.84 (*t*, 2H, py), 8.35 (*s*, 2H, py), 8.57 (*d*, 2H, py), 9.59 (*d*, 2H, NH). ^{13}C NMR (CDCl3, 100 MHz) : 44.03, 79.51, 83.57, 121.71, 121.93, 126.71, 133.04, 136.39, 148.47, 148.61, 156.06, 162.44.

Carboxylic derivative (8) and dimer (9). Solution of 30 ml of Et3N in 100 ml of THF was was added with *N,N*-bis[2-(pyridinyl)methyl]-4-ethynylpyridine-2,6-dicarboxamide **7** (0.5 g, 1.348 mmmol, 1 eq), 4-iodobenzoic acid (0.334 g, 1.347 mmol, 1 eq), Pd(Ph)2Cl2 (0.038 g, 0.054 mmol, 0.04 eq) and PPh3 (0.014 g, 0.053 mmol, 0.04 eq), respectively. The reaction mixture was refluxed under nitrogen atmosphere at 120[0]C for overnight. The reaction mixture was washed with 2x15 ml of sat. NH_4Cl and 2x15 ml of water and was dried over Na_2SO_4. Purification with column chromatography by 1/20 : CH_3OH/CH_2Cl_2 gave white solid **8** (0.060 g, 9.1 %) and **9** (0.390 g, 78 %). **8** ^{1}H NMR (DMSO, 400MHz) : 4.68 (*d*, 2H, CH2), 7.27 (*t*, 1H, py), 7.36 (*d*, 1H, py), 7.60 (*d*, 1H, ph), 7.76 (*t*, 1H, py), 7.93 (*d*, 1H, ph), 8.26 (*s*, 1H, py), 8.50 (*d*, 1H, py), 10.10 (*d*, 1H, NH) . **8** ^{13}C NMR (DMSO, 100 MHz) : 44.37, 86.60, 96.02, 121.10, 122.24, 125.58, 129.36, 131.20, 133.52, 136.03, 136.83,

148.89, 149.19, 158.33, 162.88, 169.32. MALDI-MS (dithranol): Found: 492.010 calcd. for $C_{28}H_{21}N_5O_4$ 491.507 **9** ^{1}H NMR ($CDCl_3$, 400 MHz) : 4.81 (*d*, 2H, CH_2), 7.22 (*t*, 1H, py), 7.43 (*d*, 1H, py), 7.71 (*t*, 1H, py), 8.40 (*s*, 1H, py), 8.52 (*d*, 1H, py), 9.42 (*d*, 1H, NH). **9** ^{13}C NMR ($CDCl_3$, 100 MHz) : 44.59, 78.79, 80.32, 122.64, 122.69, 125.51, 127.32, 132.53, 137.22, 149.12, 149.31, 156.73, 162.80. MALDI-MS (dithranol): Found: 741.591 calcd. for $C_{42}H_{32}N_{10}O_4$ 740.784

[Complexs of 8 and 9] . A solution of $Ni(COOCH_3)_2$ (0.030 g, 0.122 mmol, 1eq) in 5 ml of CH_3OH was added dropwise to the solution of **8** (0.060 g, 0.122 mmol, 1eq) in 20 ml of CH_3OH and **9** (0.090 g, 0.122 mmol, 1eq) in 20 ml of CH_3OH at reflux temperature. Brown solid in brown solution was then observed. The reaction was kept refluxing for overnight. After the reaction mixture was allowed to cool down to room temperature, the mixture was filtered and washed with CH_3OH. The product was collected as brown solid (0.031 g and 0.046 g, respectively). A solution of $CuCl_2$ (0.021 g, 0.122 mmol, 1eq) in 5 ml of CH_3OH was added dropwise to the solution of **8** (0.060 g, 0.122 mmol, 1eq) in 20 ml of CH_3OH and **9** (0.090 g, 0.122 mmol, 1eq) in 20 ml of CH_3OH at reflux temperature. Green solid in green solution was then observed. The reaction was kept refluxing for overnight. After the reaction mixture was allowed to cool down to room temperature, the mixture was filtered and washed with CH_3OH. The product was collected as green solid (0.040 g and 0.060 g, respectively).

Results and Discussion

Compound **6** was produced from compound **5** with TMSA using a Sonogashira's coupling**.** The structure was assured from a signal of trimethylene proton at around 0.27 ppm. Other signals remained as can be observed in the starting pincer **5**.

Compound **7** was produced from compound **6** by desillylation of the trimethylsillyl protecting group. Obviously, ^{1}H-NMR spectrometry showed the ethylene proton at 3.42 ppm instead of the trimethylene proton of starting material compound **6**.

Compound **8** and dimer **9** were obtained as a minor and major product from a Sonogashira's coupling of compound **7** with iodobenzoic acid, respectively. The structures of compound **8** and **9** can be confirmed using ^{1}H-NMR spectrometry as the signal of benzoic acid was appeared and ethylene proton was disappeared, respectively. Furthermore, the mass spectrometry can also confirm that the dimer **9** was successfully prepared from this reaction.
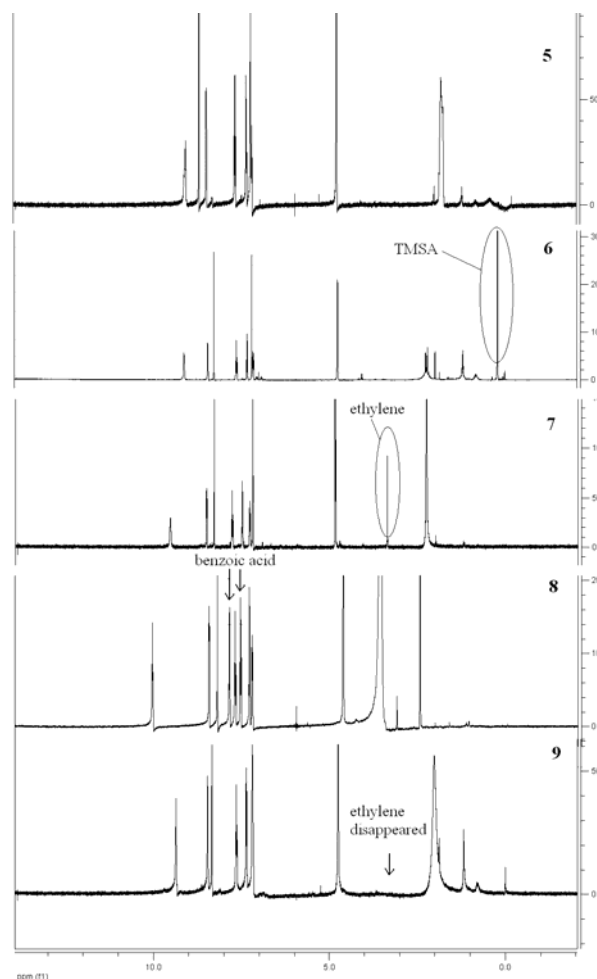

Figue 1. NMR spectra of **5, 6, 7, 8** and **9**

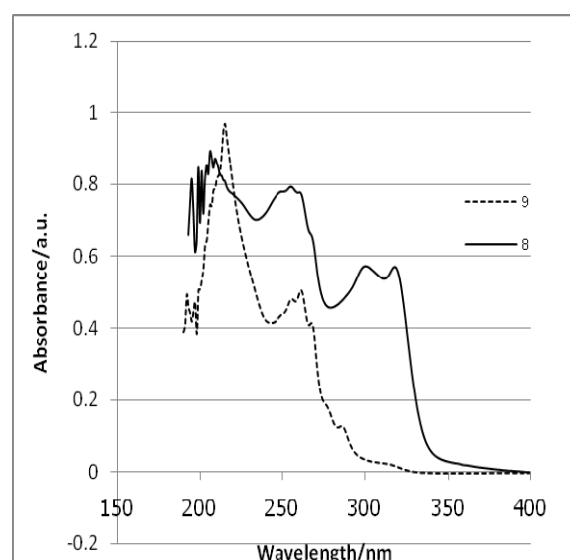Figure 2. Absorbtion spectra of **8** and **9**

Table 1: Photophysical propertie

Samples	λ_{max}(nm)	ε (M^{-1} cm^{-1})
8	214	36000
9	207	71300

UV absorbtion spectra of **8** and **9** are shown in figure 7. The λ_{max} and absorbtion coefficient are concluded in table 1. Absorption bands under 300 nm of both compounds resulted from pyridine rings. For compound **8**, the benzoic moiety exhibit absorption maxima around 310 nm.

Complexes of **8** and **9** with Ni^{2+} and Cu^{2+} had been synthesized. The crystallization of all complexes is now under investigation**.** In future, the crystal structure of the complexes will be characterized and photophysical and electrochemical properties will also be investigated.

Conclusions

Two novel ion pincers had been synthesized from chelidamic acid using Sonogashira's coupling. Under our experimental condition the dimerisation predominated. The benzoic modified pincer can also be obtained. The complexes of both pincers had been synthesized. The single crystal X-ray crystallography, UV spectroscopy, fluorescence spectroscopy, cyclic voltammetry and charge mobility will be observed.

References

[1] R. Elsenberg and G.D. Nocera, *Inorg. Chem.* **44** (2005), pp. 6799-6801.
[2] W. Wong and C. Ho, *Institure of Molecular Functional Materials and Department of Chemistry and Centre for Advanced Luminescence Materials*, Organomet Press, Hong Kong Baptist, China (2010).
[3] X. Ma, J. Hua, W. Wu, Y. Jin, F. Meng, W. Zhan and H. Tian, *Tetrahedron.* **64** (2008), pp. 345-350.

[4] G. Horváth, C. Rusa, Z. Köntös, J. Gerencsėr and P. Huszthy, *Synth. Commun.* **29** (1999), pp. 3791-3731.
[5] M.R. George, C.A. Golden, M.C. Grossel and R.J. Curry, *Inorg. Chem.* **45** (2006), pp. 1739-1744.
[6] G. Chessa, L. Canovese, F. Visentin, C. Santo and R. Seraglia, *Tetrahedron.* **61** (2005), pp. 1755-1763.

Synthesis of A Tetramannoside from Phosphatidylinositol Mannoside as Glycan Analog for Epitope of *Mycobacterium tuberculosis* (*Mtb*)

C. Wattanasiri[1], S. Ruchirawat[1] and S. Boonyarattanakalin[2]*

[1]Laboratory of Medicinal Chemistry, Chulabhorn Research Institute,
and Program in Chemical Biology, Chulabhorn Graduate Institute,
Center of Excellence on Environmental Health, Toxicology and Management of Chemicals,
Vipavadee-Rangsit Highway, Bangkok 10210, Thailand
[2]School of Bio-Chemical Engineering and Technology, Sirindhorn International Institute of Technology,
Thammasat University, Pathum Thani 12121 Thailand

* E-mail: siwarutt@siit.tu.ac.th, and E-mail: siwarutt.siit@gmail.com

Abstract: Tuberculosis (TB) is a serious infectious disease that has been known for centuries. Although there are available protocols for both treatment and prevention, TB still remains a health burden worldwide. Insufficient treatment and poor compliance by patients lead to even more life threatening drug-resistant TB. Efficient TB control by vaccination against TB has been heavily researched. Much attention is drawn to replacing the only available but ineffective bacillus Calmette-Guerin (BCG) vaccine. The developments for new TB vaccines have not been successful. An important obstacle of the vaccine development is undesirable symptoms caused by the vaccine candidates. Synthetic vaccines offer another promising alternative. The logical TB epitopes are within the pathogens' cell surface components. Abundant phosphatidylinositol hexamannoside (PIM$_6$) is an important antigenic glycan found on the cell envelope of *Mycobacterium tuberculosis* (*Mtb*). PIM$_6$ also is involved in many signaling events during the infection and surviving of *Mtb*. We report here the synthesis of a simplified phosphatidylinositol hexamannoside (PIM$_6$) analogue which is designed to be an alternative vaccine candidate or a vaccine adjuvant. The synthesis of PIM$_6$ analogue is made through a series of glycosidation reactions which rely on mannoside building blocks made from the key intermediate 1,2,6 tricyclic orthoester. The tricyclic orthoester is transformed to three main building blocks that are used to construct either 1,6 or 1,2 glycosidic linkages. The reducing end of the glycan is then capped with phosphatidylinositol moiety. Immunological studies of the simplified PIM$_6$ analogue within mammalian host cells may reveal its potential application as a vaccine candidate against TB.

Introduction

Tuberculosis (TB) is a serious infectious disease which has been known for over a century. The disease is similar to the common cold but it can be dormant for years before manifesting the symptoms. The reason the TB bacillus is able to hide in the human body for a long period of time is because of a thick waxy coat. This coat is found to be involved in many signaling events, and immune response during the pathogenesis[9]. Although this disease is known to be curable and preventable, the case reports are still high every year[1]. In 2008, the incidence and mortality cases were 9.3 and 1.3 million cases, respectively[1]. In addition to the burden from TB, multi-drug resistant (MDR-TB) and extensively drug resistant tuberculosis (XDR-TB) are results of the lack of appropriate treatment and compliance issues[2]. TB treatments are complicated and take a long time. Thus, most of the patients would stop the treatment course when they felt well, while the pathogens are not completely eradicated. The current and only TB vaccine available is *Mycobacterium bovis* bacillus Calmette-Guerin (BCG). This live-attenuated vaccine has effectiveness variables depending on geography[2]. The BCG vaccine is prescribed worldwide to every child. It can establish an efficient protection in newborns toward TB, but is not effective in the case of latent TB in adults[2]. Therefore, new research on TB treatment and also vaccines, are a major need worldwide[12,13].

The pathogen that causes tuberculosis is *Mycobacterium tuberculosis (Mtb)*. Its pathogenicity and persistence in human bodies depend upon the cell wall. Lipomannan (LM), phosphatidylinositol mannosides (PIMs) and lipoarabinomannan (LAM), are important soluble molecules found throughout the cell wall layer[6]. These macromolecules are involved in the pathogen interactions with the immune system[10,11]. Many studies about the immune evasion and survival of *Mtb* are based on these molecules.

PIM is a precursor molecule for LM and LAM, which are bigger and have repeating mannose units. PIM consists of about 2-6 mannoses attached to a phosphatidylinositol unit[6]. At the bottom of the myoinositol, there is a phosphate linker group which is attached to lipid groups (Figure 1.). PIM also has a substructure that can be classified by the amount of mannose and type of glycosidic linkage in the mannoside part, such as PIM$_6$ which has 6 mannose connecting sugars. The glycosidic linkages of PIM$_3$ and PIM$_4$ are a 1,6-α linkage, while PIM$_5$ and PIM$_6$ have a 1,2-α linkage[4]. This characteristic maybe involved in different roles of the PIM molecule during the disease progression and immune response.

Chemical synthesis holds many advantages for the study of biological profiles of the PIM series because they are difficult to isolate. PIM appears to be abundant on the cell surface. It is implied that it is not

only a precursor for more complex surface antigens, such as LM and LAM, but it also has unique roles during the infection of TB[9,10]. This molecule could be an important epitope of *Mtb*. The structure of PIM glycans is also feasible for chemical synthesis. Therefore, PIM glycan can be an optional target for a synthetic vaccine or vaccine adjuvant.

Synthetic vaccines have an advantage over ordinary vaccines in terms of both purity of the compound and consistency of production[7,13]. Moreover, the chemically synthetic molecules can be fully characterized which can provide a better insight in immunological studies on a molecular level.
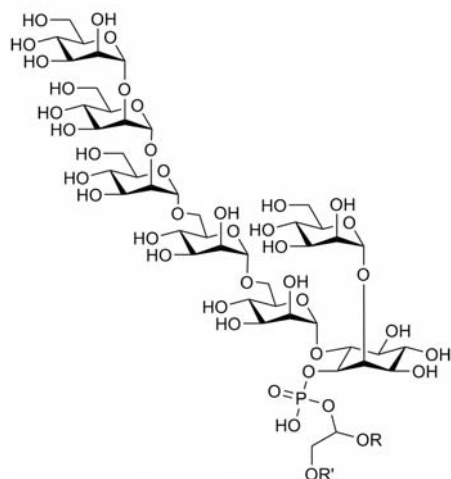
Figure 1. The structure of phosphatidylinositol mannoside (PIM₆). R,R' are lipid groups.

In this research work, we utilize the tricyclic orthoesters as a building block to construct tetrasaccharide glycan unit of the PIM molecule. These building blocks can be modified into various acceptors and donors which can be designed to yield glycosidic

bonds of different linkages. The overall synthesis of the tetrasaccharide glycan was done via a stepwise glycosidation reaction, which also ensures and allows the synthesis of smaller oligosaccharides such as disaccharides and trisaccharides. All of these molecules are essential for the investigation of minimal structure features of the PIM molecule necessary for eliciting sufficient immune response. Information on the epitope structure requirements can be applied to the development of alternative synthetic vaccines against TB.

Materials and Methods

1. Synthesis of mannosyl tricyclic orthoester[3]

The synthesis of building block **1** is shown in (Scheme 1). This synthetic route can provide a gram scale of building block 1 within a week. There were 3 important mannose building blocks (**1,3,4,6**) needed. Build blocks **3** and **6** have a C-2 acyl participating group which would secure an α–linkage of each glycosidic bond in the mannan structure[3].

2. Synthesis of the mannosyl phosphate and building blocks[4,5]

The syntheses of the building blocks including donor **3** and acceptors **4** and **6** are shown in (Scheme 1). The synthesis of mannosyl phosphate **3** and **6** were similar, which can be acquired from the opening of a tricyclic and bicyclic orthoester respectively. Tricyclic orthoester **1** and bicyclic orthoester **5** were stirred with activated 4 Å molecular sieve for 30 minutes prior to reaction. Then, the orthoesters were treated with dibutyl phosphate in dry dichloromethane for 24 hours before quenching with triethylamine (Et₃N). The crude peoduct was purified with a flash column to obtain pure compounds of **2** and **6**.

C-2 hydroxy group of mannosyl phosphate **2** was converted into triisopropylsilyl (TIPS), with the

Scheme 1. Synthesis of the mannose building blocks.[a]
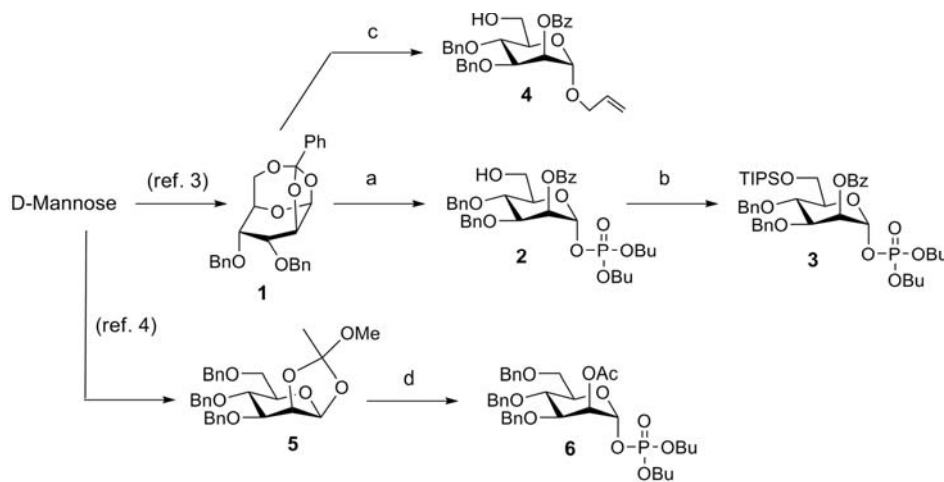
[a]Reagents and conditions: (a) HOP(O)(OBu)₂, 4 Å MS, Et₃N, CH₂Cl₂, quant.; (b) TIPSCl, DMAP, Et₃N, CH₂Cl₂, 78%; (c) AllOH, BF₃-Et₂O, CH₂Cl₂, 76%; (d) HOP(O)(OBu)₂, 4 Å MS, Et₃N, CH₂Cl₂, 77%

addition of chlorotriisopropylsilane (TIPSCl), 4-dimethylaminopyridine (DMAP) and Et₃N. The reaction continued for 48 hours, and was then cleaned with a flash column, providing the pure compound of mannosyl phosphate **3**.

Building block **4** was obtained by the opening of tricyclic orthoester **1** by allyl alcohol (AllOH) with BF₃-Et₂O as the activator. The reaction was done in dichloromethane for 12 hours. Then, the crude product was purified with a flash column.

3. Synthesis of disaccharide glycans

The overall synthesis of the oligosaccharide was done in a stepwise fashion as shown in Scheme 2. First, glycosylation was carried out by trimethylsilyl-trifluoromethanesulfonate (TMSOTf) as an activator to link the donor **3** and acceptor **4**, yielding the disaccharide **7a.** The reaction was done in dichloromethane at 0°C. The reaction was carried out for 2 hours, then quenched with triethylamine (Et₃N). Dissacharide **7a** was purified by a flash column which isolated **7b** as the major product and **7a** as the minor product. The TIPS protecting group on **7a** was cleaved off by treatment of acetyl chloride in dry methanol, which gave **7b** in a high yield. The crude product was purified by a flash column to give the disaccharide acceptor **7b**.

4. Synthesis of trisaccharide glycans

The construction of trisaccharide **8a** was done by extending the disaccharide **7b** at the non-reducing end with mannosyl phosphate **6**. The glycosidation between disaccharide **7b** and mannosyl phosphate **6** was done in dichloromethane at 0°C, with TMSOTf as activator. This reaction was stirred for 2 hours then quenched with Et₃N. Then reaction was purified by a flash column to yield the trisaccharide **8a**. The C-2 acetyl protecting group on the non-reducing end was

removed by acetyl chloride in dry methanol then purified with a flash column to give the clean product of trisaccharide **8b**, which has a free hydroxy group at C-2 of the non-reducing end saccharide unit.

### 5. Synthesis of tetrasaccharide glycans

After acquiring trisaccharide **8b**, it was subjected to a glycosidation reaction with mannosyl phosphate **6.** The activator was TMSOTf in dry toluene at 0°C. The reaction was stirred for 2 hours then stopped by the addition of Et₃N. The crude product was purified by a flash column, giving the pure product of tetrasaccharide **9**.

Results and Discussion

The synthesis of PIM glycan analogues can be done on both the reducing end and non-reducing end[8]. In this study, we performed the synthesis of PIM analogues with a step-wise expansion from the non-reducing end. Each glycosidation can give two types of linkages, an α-linkage and β-linkage. The control of stereoselectivity of the glycosidation reaction, to ensure the desired product and minimize the unwanted side-products, is necessary. The C-2 acyl protecting group of the building blocks is very important because of its neighbour participating group effect. As an example, the synthesis of disaccharide **7a** would require the mannosyl phosphate **3** and building block **4**. In the presence of an activator or TMSOTf, the dibutyl phosphate acts as a leaving group which is pushed out by the electron delocalization from the carbonyl double bond from the C-2 benzoyl group. Consequently, a cyclic orthoester intermediate **10** is formed. This structure would cause steric hindrance on the β-face at the anomeric position. Thus, incoming nucleophiles would preferably attack from the α-face, as shown in Scheme 3.

The protecting groups used for each building block

Scheme 2. Synthesis of tetrasaccharide glycan[a]
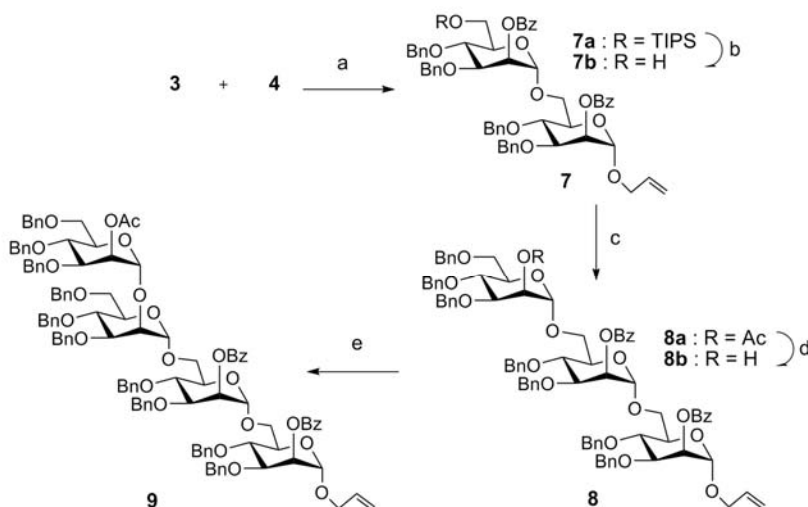

[a]Reagent and conditions: (a) TMSOTf, CH₂Cl₂, Et₃N, 0°C, 22% ; (b) AcCl, MeOH, CH₂Cl₂, Et₃N, 0°C, 85%; (c) **6**, TMSOTf, CH₂Cl₂, 0°C, 86%; (d) AcCl, MeOH, CH₂Cl₂, Et₃N, 0°C, 54%; (e) **6**, TMSOTf, toluene, Et₃N, 0°C, 30%

are designed to tolerate the reaction conditions throughout the synthesis and can be removed selectively at specific steps, which contribute to the regioselectivity of the product. In the building blocks used in this project, the protecting groups on C-1, C-2 and C-6 are different because these positions have been designed to form glycosidic bonds to the adjacent mannose units. Interestingly, the TIPS protecting group on **7a** was was removed prior to the designated reaction, During the glycosidation of dissacharide, we were able to isolate 2 products which were **7a** and **7b**. The stoichiometric amount of the TMSOTf was acidic enough to cleave off the TIPS protecting group. Fortunately, these 2 products are both desired in the synthesis and they were both used in further reactions.

Scheme 3. Synthesis of disaccharide **7a**, illustrating the neighbour participating effect.
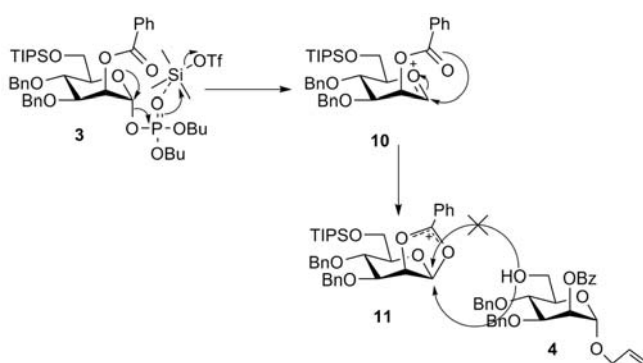
The characterization of the tetramannoside **9** are as follows: HRMS-ESI (m/z) : [M+Na]+ calculated for $C_{113}H_{116}O_{24}$, 1881.1157; Found: 1881.7667 ; ^{1}H NMR (600 MHz, CDCl$_3$) δ 2.04-2.10 (m, 4H), 3.32-4.11 (m, 20H), 4.29-5.24 (m, 22H), 5.46 (dd, 1H), 5.60 (dd, 1H), 5.70-5.84 (m, 2H), 7.01-7.29 (m, 44H), 7.36-7.45 (m, 6H), 8.02-8.09 (m, 4H); ^{13}C NMR (600 MHz, CDCl$_3$) δ 65.91, 66.34, 68.35, 68.64, 69.07, 71.02, 71.35, 71.66, 72.04, 72.31, 73.56, 73.92, 74.28, 74.45, 75.02, 75.34, 77.73, 78.06, 78.34, 78.68, 97.01, 98.24, 118.15, 127.32, 127.40, 127.42, 127.56, 127.60, 127.65, 127.71, 127.80, 127.83, 127.93, 128.11, 128.15, 128.17, 128.21, 128.23, 128.30, 128.32, 128.38, 128.47, 128.59, 128.62, 129.84, 130.00, 133.48, 137.65, 137.96, 138.22, 138.34, 138.50, 165.88, 165.92, 170.53

Conclusion

The tetrasaccharide **9** or 2-O-acetyl-((3,4,6-tri-O-benzyl)-α-D-mannopyranosyl)-(1,2)-((3,4,6-tri-O-ben zyl)-α-D-mannopyranosyl)-(1,6)-(2-O-benzoyl-(3,4-di -O-benzyl)-α-D-mannopyranosyl-(1,6)-(1-O-allyl-2-O-benzoyl-(3,4-di-benzyl)-α-D-mannopyranose was successfully synthesized by the construction of mannose building blocks **3**, **4** and **6**. These building blocks have a C-2 acyl participating group which helps to control the stereoselectivity of the oligomannoside.

Ths tetrasaccharide **9** is a fragment of phosphatidylinositol hexamannoside (PIM$_6$) found on the envelope of *Mtb*. This synthesis can also provide

smaller fragments such as disaccharides and trisaccharides. All of these molecules are important compounds to generate glycan epitopes for immunological studies. The immunological properties of these glycans may reveal interactions between PIM analogues and mammalian immune systems. The obtained information will be important for the development of other synthetic vaccine or adjuvant candidates.

Reference
[1] WHO Fact sheets: Tuberculosis.http://www.who.int/ mediacentre/factsheets/fs104/en/
[2] Colditz G.A. et al. *JAMA*. **271** (1994), pp. 698-702
[3] Yongyat C.; Ruchirawat S.; Boonyarattanakalin S. *Bioorg. Med.Chem.* **18** (2010), pp. 3726-3734
[4] Boonyarattanakalin S.; Liu X.; Michieletti M.; Lepenies B.; Seeburger P.H. *J. Am. Chem. Soc.*, **130** (2008), pp. 16791-16799
[5] Liu X.; Stocker B.L.; Seeburger P.H. *J. Am. Chem. Soc.* **128** (2006), pp. 3638-3648
[6] Brennan P.J. *Tuberculosis*. **83** (2003), pp. 91–97
[7] Verez-Bencomo V. *Science*. **305** (2004), pp. 522-525
[8] Jayaprakash K.N.; Lu J.; Fraser-Reid B. *Angew. Chem. Int. Ed*. **44** (2005), pp. 5894 –5898
[9] Cooper A.M. *Annu. Rev. Immunol*. **27** (2009), pp. 393-422
[10] Harding C.V.; Boom W.H. *Nat. Rev. Microbiol*. **8** (2010), pp. 296-307
[11] Vincent M.S.; Gumperz J.E.; Brenner M.B. *Nat. Immunol*. **8** (2003), pp. 517-523
[12] Comas I.; Gagneux S. *PLoS Pathog*. **5** (2009), pp. 1-7
[13] Barker L.F. et al. *Curr Opin Immunol* **21** (2009), pp. 331–338

Gas Chromatography-Mass Spectrometry and Comprehensive Two-Dimensional Gas Chromatography Analysis of Organic Components in Bio-Oil from Tea Waste

R. Charoenphon[1], S. Chaiklangmuang[2] and S. Wongpornchai[1]*

[1] Department of Chemistry, Faculty of Science, Chiang Mai University, Chiang Mai, Thailand 50200
[2] Department of Industrial Chemistry, Faculty of Science, Chiang Mai University, Chiang Mai, Thailand 50200

* E-mail: scismhth@chiangmai.ac.th

Abstract: Bio-oil is a renewable liquid fuel that is produced from biomass by pyrolysis process. The chemical composition of each bio-oil type relies on many factors, such as biomass type and pyrolysis conditions. In this study, pyrolysis of tea waste using temperature of 600 °C, heating rate of 10 °C/min and hold time of 3 hr yielded two layers of bio-oil samples, which were then subjected to analysis of their chemical compositions by GC-MS and GC×GC technique. Results revealed the detection of 78 and 42 components in the top and bottom layer, respectively. Among these, there were 65 and 36 identified components, respectively. The major components of bio-oil samples from the top layer and the bottom layer were phenolics. However, hydrocarbons that were found only in the top layer of the tea waste bio-oil accounted for 23 % of the total content. When GC×GC was applied to analysis of the tea waste bio-oil samples, additional components were detected which resulted in the total of at least 296 and 136 components found in the top and bottom layer, respectively. In comparison with GC-MS, GC×GC showed greater ability to differentiate the quality of bio-oils in terms of their chemical compositions.

Introduction

Since the energy crisis in the 1970s, the energy utilization from biomass resources has received much attention because biomass is clean. Biomass has negligible content of sulphur, nitrogen and ash, which give lower emissions of SO_2, NO_x and soot than conventional fossil fuels. Zero net emission of CO_2 can be achieved because CO_2 released from biomass will be recycled into the plants by photosynthesis quantitatively [1]. Pyrolysis has been widely used for converting biomasses into liquids and solids. The process is generally described as the thermal decomposition of the organic components in biomass waste in the absence of oxygen at mediate temperature, to yield tar (pyrolysis oil), char (charcoal) and gaseous fractions (fuel gases) [2].

Bio-oils also referred to as biomass pyrolysis liquids, pyrolysis oils, or bio-crude oils. They are dark brown, free flowing liquids with an acrid or smoky odor. The chemical compositions of bio-oils are determined by many factors, such as biomass type, feedstock pretreatment and pyrolysis conditions.

Therefore, bio-oils produced from different materials and by different pyrolysis reactors may differ greatly from one another [3]. Bio-oil can substitute for fuel oil or diesel in many static applications including boilers, furnaces, engines and turbines. Additionally, there are a range of chemicals that can be extracted or derived including food favourings, specialties, resins, agri-chemicals, fertilizers, and emissions control agents. For examples, phenols are used in the resins industry, volatile organic acids are used in formation of de-icers, levoglucosan, hydroxyl acetaldehyde and some additives are applied in the pharmaceuticals, fiber synthesizing or fertilizing industry and flavoring agents in food products [4-5].

Gas chromatography–mass spectrometry (GC–MS) is a suitable method to analyze complex mixtures and to identify their individual components [6]. However, for very complex samples like fragrances, petrochemical products and pyrolysis oils, two-dimensional chromatography may be a good alternative to increase chromatographic resolution [7]. Comprehensive two-dimensional gas chromatography (GC×GC) is a relatively new but powerful technique successfully used for the separation of the volatile constituents in highly complex samples [8] such as petroleum products [9-11], environmental samples [12-13], essential oils [14-15] and flavors and fragrances in food [16-17]. Recently, Fullana *et al*. [18] analyzed pyrolytic products from cellulose, lignin and sewage by GC×GC and over 1000 components were detected. The results showed that more than 70% of total chromatographic peaks could be identified with GC×GC but only 47%, in the best case, with conventional GC. The increase in the number of identified products is due to higher separation efficiency.

In this research, bio-oil samples obtained from pyrolysis of tea waste were analyzed and identified by GC-MS, while GC×GC was also applied to establish the complexity of the samples. The results which show the type and relative quantity of organic components in the bio-oil samples can be used to aid the assessment of their qualities.

Materials and Methods

Sample preparation

The bio-oil samples were prepared in the Department of Industrial Chemistry, Faculty of Science, Chiang Mai University, Thailand. They were produced via pyrolysis of tea waste using temperature of 600 °C, heating rate of 10 °C/min and hold time of 3 hr yielded two layers of bio-oil samples. The top layer was viscous liquid with black color while the bottom layer was liquid with dark brown color.

Approximately 0.05 grams of bio-oil from the top layer and 500 µL from the bottom layer were extracted with hexane using ultrasonication for 60 min. Then, the bio-oil extracts were dehydrated through sodium sulfate anhydrous, filtered and concentrated using vacuum rotary evaporation. Hexane used was analytical grade and obtained from Lab-Scan Analytical Science, Ireland.

GC-MS analysis

GC-MS analysis was performed on a gas chromatograph–mass spectrometer (Agilent 6890 and HP 5973 mass-selective detector, Agilent Technologies) equipped with a fused silica capillary column, Rtx-5MS with dimension of 60 m × 0.25 mm i.d. × 0.50 µm film thickness (Agilent Technologies). GC-MS was operated under a temperature program which was started at 45 °C and ramped to 250 °C at 3 °C/min and hold for 20 min. The injection temperature was 250 °C with an injection volume of 1 µL in the splitless mode. The quadrupole temperature was 150 °C and the transfer-line temperature was 280 °C. A mass range of m/z 29-550 was acquired. Helium was used as carrier gas and was maintained in a constant pressure mode.

GC×GC-FID analysis

A gas chromatograph model HP 6890 equipped with an FID detector and an HP 6890 series auto sampler (Agilent Technologies) was used for the GC×GC-FID experiment. The GC was retrofitted with a longitudinally modulated cryogenic system (LMCS). CO_2 was employed as cryogen, which was thermostatically controlled for the duration of each run. The column set for GC×GC analysis consisted of two capillary columns which were Rtx-5MS (60 m × 0.25 mm i.d. × 0.50 µm film thickness) coupled with BP20 (1.0 m × 0.1 mm i.d. × 0.1 µm film thickness). A temperature program of GC×GC was the same as that in GC-MS experiment. The injection temperature was 250 °C with an injection volume of 1 µL in the splitless mode. A modulation frequency was operated at 5 s per cycle. Helium carrier gas was maintained in constant pressure mode.

Results and Discussion

GC-MS results revealed the detection of 78 and 42 components in the top and bottom layer samples, respectively. Among these, there were 65 and 36 components, respectively, identified based on the mass spectrum matching against those compiled in the mass spectral library (NIST08 Mass Spectral Library, National Institute of Standards and Technology, USA). These identified components are reported in Table 1. The identified compounds were classified in groups of phenolics, hydrocarbons, nitrogenous compounds, aromatic compounds, N-heterocyclic derivatives, O-heterocyclic derivatives, aldehydes, ketones and esters.

Table 1: Relative contents of the identified components in bio-oil obtained from tea waste

Peak No.	RT (min)	Structural Assignment	% Matching	Molecular Formula	% Relative Content	
					Top Layer	Bottom Layer
1	14.596	2-Methylpyridine	91	C_6H_7N	0.2594	0.4705
2	14.947	Methylpyrazine	90	$C_5H_6N_2$		0.4323
3	16.449	2-Furanmethanol	98	$C_5H_6O_2$	0.2772	4.1902
4	16.942	Ethylbenzene	81	C_8H_{10}	0.5205	
5	17.213	N,N-Dimethylacetamide	89	C_4H_9NO		0.5186
6	17.934	2,6-Dimethylpyridine	91	C_7H_9N	0.1287	
7	18.528	Styrene	94	C_8H_8	0.2707	
8	18.659	1,2-Dimethylbenzene	87	C_8H_{10}	0.1914	
9	19.086	2-Ethylpyridine	91	C_7H_9N	0.1189	
10	19.224	2-Methyl-2-cyclopenten-1-one	91	C_6H_8O	0.0347	
11	19.461	1,4-Dimethylcyclohexene	80	C_8H_{14}	0.2291	
12	19.467	2-Acetylfuran	90	$C_6H_6O_2$		1.873
13	19.618	Butyrolactone	96	$C_6H_6O_2$		0.0834
14	20.435	2,5-Dimethylpyridine	94	C_7H_9N	0.7084	0.4252
15	21.272	2,3-Dimethylpyridine	95	C_7H_9N	0.2051	
16	21.866	Propylbenzene	83	C_9H_{12}	0.1455	
17	22.460	3-Methyl-2-cyclopenten-1-one	95	C_6H_8O	0.2970	1.3365
18	23.410	Phenol	94	C_6H_6O	11.9290	24.1778
19	24.349	3-Methoxypyridine	87	C_6H_7NO	0.1881	
20	24.367	Trimethylpyrazine	89	$C_7H_{10}N_2$		0.9699
21	25.044	2-Ethyl-6-methylpyridine	90	$C_8H_{11}N$	0.2202	
22	25.762	1,2,4-Trimethylbenzene	91	C_9H_{12}	0.2070	
23	25.846	2-Hydroxy-3-methyl-2-cyclopenten-1-one	91	$C_6H_8O_2$		0.0898
24	25.857	2-Propenylbenzene	86	C_9H_{10}	0.1591	

Table 1: Relative contents of the identified components in bio-oil obtained from tea waste (continued)

Peak No.	RT (min)	Structural Assignment	% Matching	Molecular Formula	% Relative Content	
					Top Layer	Bottom Layer
25	26.500	2,3-Dimethyl-2-cyclopenten-1-one	94	$C_7H_{10}O$	0.5157	0.7264
26	27.402	2-Methylphenol	97	C_7H_8O	4.2828	3.9081
27	27.716	1-(1H-pyrrole-2-yl)-ethanone	93	C_6H_7NO	0.6219	1.8903
28	28.477	4-Methylphenol	97	C_7H_8O	11.2454	13.1607
29	29.127	N-Methylsuccinimide	87	$C_5H_7NO_2$		0.3723
30	29.284	2-Methoxyphenol	95	$C_7H_8O_2$	2.0889	4.5664
31	30.184	Pentanamide	89	$C_5H_{11}NO$		0.552
32	30.339	6,7-Dihydro-5H-cyclopentapyrazine	87	$C_7H_8N_2$		0.7928
33	31.049	1-Phenyl-1-butene	93	$C_{10}H_{12}$	0.3190	
34	31.429	1-Ethyl-2,5-pyrrolidinedione	91	$C_6H_9NO_2$		1.0876
35	31.720	2-Ethylphenol	95	$C_8H_{10}O$	0.9129	0.1918
36	31.880	Benzeneacetonitrile	95	C_8H_7N	0.6173	1.8833
37	32.296	2,4-Dimethylphenol	96	$C_8H_{10}O$	2.7159	1.5709
38	33.210	4-Ethylphenol	94	$C_8H_{10}O$	5.1239	0.0885
39	33.288	3,5-Dimethylphenol	91	$C_8H_{10}O$	1.5193	2.1829
40	33.793	1-Dodecene	95	$C_{12}H_{24}$	0.8022	
41	34.185	Dodecane	93	$C_{12}H_{26}$	0.4861	
42	34.571	2-Methoxy-4-methylphenol	94	$C_8H_{10}O_2$	0.6798	1.0999
43	34.761	2-Methyl-5H-6,7-dihydrocyclopentapyrazine	90	$C_8H_{10}N_2$		1.1448
44	36.014	2,5-Dimethyl-3-propenylpyrazine	90	$C_9H_{12}N_2$		1.3167
45	36.139	3,5-dimethyl-6,7-dihydro-5H-cyclopentapyrazine	90	$C_9H_{12}N_3$		0.7472
46	36.216	3-Methyl-5-ethylphenol	87	$C_9H_{12}O$	0.9498	
47	36.780	4-Ethyl-3-methylphenol	91	$C_9H_{12}O$	0.9883	
48	37.006	Benzenepropanenitrile	93	C_9H_9N	1.0649	0.2545
49	38.621	1-Tridecene	96	$C_{13}H_{26}$	0.7467	
50	38.770	4-Ethyl-2-methoxyphenol	91	$C_9H_{12}O$	1.3048	0.3574
51	38.960	Tridecane	97	$C_{13}H_{28}$	0.6694	
52	39.910	1H-Indole	95	C_8H_7N	2.3948	1.0686
53	40.059	2-Methylnaphthalene	93	$C_{11}H_{10}$	0.9799	
54	40.920	Vinylidene	86	$C_{11}H_{10}$	1.3271	
55	42.078	2,6-Dimethoxyphenol	96	$C_8H_{10}O_3$	0.5701	1.9495
56	42.720	2-Butyl-2-octenal	99	$C_{12}H_{22}O$	1.8477	0.7038
57	43.159	1-Tetradecene	99	$C_{14}H_{28}$	0.9525	
58	43.468	Tetradecane	98	$C_{14}H_{30}$	1.2238	
59	44.193	3-Methylindole	94	C_9H_9N	1.7473	0.2807
60	45.921	1,6-Dimethylnaphthalene	96	$C_{12}H_{12}$	0.7115	
61	46.562	cis-Isoeugenol	98	$C_{10}H_{12}O_2$	0.6337	
62	46.931	Octylbenzene	87	$C_{14}H_{22}$	0.1826	
63	47.441	1-Pentadecene	99	$C_{15}H_{30}$	1.2948	
64	47.721	Pentadecane	97	$C_{15}H_{32}$	1.5900	
65	51.480	1-Hexadecene	99	$C_{16}H_{32}$	1.0228	
66	51.724	Hexadecane	98	$C_{16}H_{34}$	0.8865	
67	55.317	1-Heptadecene	93	$C_{17}H_{34}$	0.5759	
68	55.519	Heptadecane	99	$C_{17}H_{36}$	0.7386	
69	56.695	2-Isohexyl-6-methyl-1-heptene	93	$C_{14}H_{28}$	1.6869	
70	58.922	1-Octadecene	99	$C_{18}H_{36}$	0.3882	
71	59.130	Octadecane	99	$C_{18}H_{38}$	0.4602	
72	60.615	Neophytadiene	99	$C_{20}H_{38}$	4.2242	
73	60.811	3,7,11,15-Tetramethyl-2-hexadecene	93	$C_{20}H_{14}$	0.5816	
74	62.344	Caffeine	97	$C_8H_{10}N_4O_2$	7.5758	19.7708
75	62.498	Nonadecane	99	$C_{19}H_40$	0.4567	
76	62.955	Hexadecanenitrile	96	$C_{16}H_{31}N$	1.0212	
77	63.526	Methyl hexadecanoate	99	$C_{17}H_{34}O_2$	0.9031	
		$\sum$ % peak area of the identified components			89.7225	96.2351

Component analysis by GC-MS of the bio-oil extracts obtained from different layers showed that hydrocarbons, which have high heating values, were found only in the top layer of the bio-oil. They were accounted for 23 % of the total content. The major components of bio-oil samples found in both top and bottom layers were phenolics such as phenol, 2-methylphenol, 4-methylphenol and 2-methoxyphenol. In group of *N*-heterocyclic derivatives, 1H-indole was found in higher content than the others in the top layer

oil. Caffeine, the key component of tea leaves, was also detected in both bio-oil samples in relatively high contents especially in the bottom layer. Neophytadiene, previously identified as the aroma compound of tea [19], was detected in the top layer with high content. Furthermore, isoeugenol, a propenyl-substituted guaiacol that had been found as tea aroma in partially fermented tea [20] was found in the top layer of the bio-oil. This terpenoid has been documented as having high antioxidant activity,
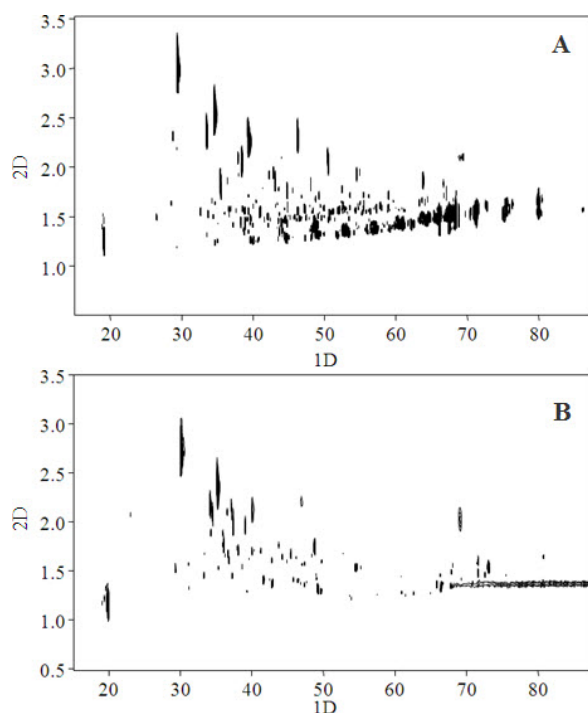
Figure 1. GC×GC-FID contour plots of tea waste bio-oil samples: (A) Top layer (B) Bottom layer

particulary for normalizing antioxidant defense in diabetics [21].

When GC×GC technique was applied to the analysis of organic components in the tea waste bio-oil samples, the obvious complexity of these samples is clearly visible as shown by the GC×GC contour plots in Fig. 1. A number of additional components were detected which resulted in the total of at least 296 and 136 components found in the top and bottom layer, respectively.

Conclusions

Component analysis of the pyrolysis bio-oil samples from tea waste by GC-MS revealed a number of organics present in series such as normal and aromatic hydrocarbons, phenolics, and *N*-heterocyclic derivatives. Two separated layers of the bio-oil could be distinguished by the presence of both normal and aromatic hydrocarbons, which were found only in the top layer oil. An overall of 78 organic components detected by GC-MS was estimated to be only 26% of those shown by the use of GC×GC. This highly efficient technique of separation is thus a promising approach for quality assessment of bio-oils. Further identification of the tea waste bio-oil constituents should be performed by the use of GC×GC-MS in order to obtain a more complete profile of organic constituents especially those that play important role on the bio-oil quality.

References

1] Q. Zhang, J. Chang, T. Wang and Y. Xu, *Energ. Convers. Manage.* **48** (2007), pp. 87-92.
[2] W. T. Tsai, M. K. Lee and Y. M. Chang, *Bioresource Technol.* **98** (2007), pp. 22-28.
[3] Q. Lu, W. Z. Li and X. F. Zhu, *Energ. Convers. Manage.* **50** (2009), pp. 1376-1383.
[4] A. V. Bridgwater, D. Meier and D. Radlein, *Org. Geochem.* **30** (1999), pp. 1479-1493.
[5] A. V. Bridgwater and G. V. C. Peacocke, *Renew. Sust. Energ. Rev.* **4** (2000), pp. 1-73.
[6] J. H. Marsman, G. P. van der Laan and C. M. Beenackers, *J. Process Anal. Chem.* JPAV IV (1999), pp. 39.
[7] J. H. Marsman, J. Wildschut, F. Mahfud and H. J. Heeres, *J. Chromatogr. A* **1150** (2007), pp. 1150, 21-27.
[8] P. Pripdeevech, S. Wongpornchai and P. J. Marriott, *Phytochem. Anal.* **21** (2009), pp. 163-173.
[9] C. V. Muhlen, C. A. Zini, E. B. Caramao and P. J. Marriott, *J. Chromatogr. A* **1105** (2006), pp. 39-50.
[10] J. Beens, J. Blomberg and P.J. Schoenmakers, *J. High. Resolut. Chromatogr.* **23** (2000), pp. 182-188.
[11] G. S. Frysinger and R. B. Gaines, *J. Sep. Sci.* **24** (2001), pp. 87-96.
[12] H. J. Cortes, E. L. Olberding and J. H. Wetters, *Anal. Chim. Acta* **236** (1990), pp. 173-182.
[13] J. F. Focant, A. Sjödin and D. G. Patterson, *J. Chromatogr. A* **1040** (2004), pp. 227-238.
[14] J. Wu, X. Lu, W. Tang, H. Kong, S. Zhou and G. Xu, *J. Chromatogr. A* **1034** (2004), pp. 199-205.
[15] S. Zhu, X. Lu, L. Dong, J. Xing, X. Su, H. Kong, G. Xu and C. Wu, *J. Chromatogr. A* **1086** (2005), pp. 107-114.
[16] R. Shellie, L. Mondello, P. J.Marriott and G. Dugo, *J. Chromatogr. A* **970** (2002), pp. 225-234.
[17] M. Adahchour, L. L. P. van Stee, J. Beens, R. J. J. Vreuls, M. A. Batenburg and U. A. Th. Brinkman, *J. Chromatogr. A* **1019** (2003), pp. 157-172.
[18] A. Fullana, J. A. Contreras, R. C. Striebich and S. S. Sidhu, *J. Anal. Appl. Pyrolysis* **74** (2005), pp. 315-326.
[19] K. Michiko, C. Griangsak and K. Akio, *Agric. Biol. Chem.* **51** (1987), pp. 1683-1687.
[20] T. Yamanishi, M. Kosuge, Y. Tokitomo and R. Maeda, *Agric. Biol. Chem.* **44** (1980), pp. 2139-2142.
[21] F. M. Rauscher, R. A. Sanders and J. B. Watkins, *J. Biochem. Mol. Toxicol.* **15** (2001), pp. 159-16.

Chlorination of *N*-Heteroaromatic Hydroxy Compounds with PPh₃/Chlorinating Agent

W. Kijrungphaiboon[1,2*] and W. Chavasiri[2,3]

[1]Program in Petrochemistry and Polymer Science, Faculty of Science, Chulalongkorn University, Bangkok 10330, Thailand.
[2]Center for Petroleum, Petrochemicals, and Advanced Materials, Chulalongkorn University, Bangkok 10330, Thailand.
[3]Department of Chemistry, Faculty of Science, Chulalongkorn University, Bangkok 10330, Thailand.

* E-mail: auzz_nun@hotmail.com

Abstract: A new methodology for chlorination of *N*-heteroaromatic hydroxy compounds using PPh₃ and a chlorinating agent was disclosed. The effects of type of chlorinating agent, amount of reagents and solvent system were investigated to optimize the reaction conditions. Cl₃CCN in combination with PPh₃ appeared to be a highly reactive reagent for the conversion of *N*-heteroaromatic hydroxy compounds to the corresponding *N*-heteroaromatic chlorides in refluxing toluene within 4 hours. In addition, the scope and the limitation of this developed method were thoroughly examined. Chlorination of 2- and 4-hydroxypyridine gave high yields of 2- and 4-chloropyridine, whereas 3-hydroxypyridine was not reactive under this developed condition.

Introduction

The conversion of *N*-heteroaromatic hydroxy compounds to their corresponding *N*-heteroaromatic chlorides is useful in organic synthesis and pharmaceutical interest. *N*-Heteroaromatic chlorides are often utilized as a phase transfer and are used as an important intermediate for the manufacture of pyrithione-based biocides in cosmetics.[1] They are also used as a starting material in the production of various pharmaceutical products such as antihistamine drug, pheniramine.[2]

N-Heteroaromatic chloride can be prepared from various sources of starting materials. The general protocols mostly stem from the conversion of *N*-heteroaromatic hydroxy compounds because of their commercial availability and easy transformation processes. SOCl₂, POCl₃ or PCl₅[3-5] mostly used as a chlorinating agent in the synthesis of *N*-heteroaromatic chloride. However, such chlorinating agents are harmful, difficult to handle and always generate HCl or SO₂ gases during the reaction. As a result, these reagents cannot be applied to acid-sensitive substrates.

The utilization of the combined reagents between PPh₃ and various chlorinating agents has been extensively reported on the transformation of organic compounds. PPh₃ in the combination with CCl₄,[6] Cl₃CCCl₃,[7] Cl₃CCOCCl₃,[8] Cl₃CCN[9] or Cl₃CCONH₂[10] has been addressed as an efficient reagent for the chlorination of alcohols. The combination of

PPh₃/Cl₃CCN has also been explored to convert sulfonic acids to sulfonyl chlorides for the synthesis of sulfonamides.[11] In addition, the chlorination of carboxylic acids using PPh₃ in combination with CCl₄,[12] cyanuric chloride,[13] Cl₃CCOCCl₃[14] or Cl₃CCN[15] has been reported. Recently, PPh₃/Cl₃CCONH₂ has been introduced as another alternative reagent for the transformation of carboxylic acids to their analogous amides and esters *via* acid chlorides as a reactive intermediate.[16] These aforementioned PPh₃/chlorinating agent systems are attractive since the reaction could perform to produce the desired products in excellent yields under mild conditions with short reaction times.

There are a few reports on the preparation of *N*-heteroaromatic chlorides from *N*-heteroaromatic hydroxy compounds using PPh₃ and a chlorinating agent. Despite the fact that PPh₃/*N*-chlorosuccinimide has been documented for the chlorination of *N*-heteroaromatic hydroxy compounds, the method still have their own disadvantages such as high sociometry amount reagent required and low efficiency.[17,18] Moreover, the combination of PPh₃ with Cl₃CCN has not been applied to *N*-heteroaromatic hydroxy compounds so far. Therefore, the new protocol for the chlorination of *N*-hetero-aromatic hydroxy compounds using PPh₃/Cl₃CCN is described herein.

The objective of this work is to optimize the reaction condition for the preparation of *N*-hetero-aromatic chloride using PPh₃/chlorinating agent by varying the type and amount of chlorinating agents and solvent system, and to investigate the scope and limitation of this developed method.

Materials and Methods

Thin layer chromatography (TLC) was performed of aluminium sheets pre-coated with silica gel (Merck's, Kieselgel 60 PF₂₅₄) and column chromatography was performed on silica gel (Merck's silica gel 60 G Art 7734). The ¹H and ¹³C NMR spectra were performed in deuterated chloroform (CDCl₃) with tetramethylsilane (TMS) as an internal reference on a Varian nuclear magnetic resonance

spectrometer, model Mercury plus 400 NMR spectrometer which operates at 399.84 MHz for ^{1}H and 100.54 MHz for ^{13}C nuclei.

All solvents used in this research were purified prior to use by standard methodology except for those which were reagent grades. The reagents used for synthesis were purchased from Fluka chemical company or otherwise stated and were used without further purification.

General procedure for the conversion of N-hetero-aromatic hydroxy compounds to N-heteroaromatic chlorides: a stirred solution of N-heteroaromatic hydroxy compound (0.25 mmol) and PPh$_3$ 3 equiv. (0.75 mmol) in dry toluene was added selected chlorinating agent 3 equiv. (0.75 mmol) at reflux temperature under N$_2$ atmosphere. After 4 hours, the reaction was quenched by solvent evaporation, and then the yield of the product was determined by ^{1}H NMR on the crude mixture using 1,1,2,2-tetrachloroethane as an internal standard or, alternatively, by gravimetry after being purified by column chromatography on silica gel.

Results and Discussion

To optimize the reaction condition, 2-hydroxy-pyridine, used as a model substrate, was treated with selected chlorinating agents (3 equiv.) and PPh$_3$ (3 equiv.) in refluxing 1,4-dioxane for 4 h to give the desired chloride, and the results are presented (Table 1). Cl$_3$CCN was found as the most reactive reagent for the conversion of 2-hydroxypyridine to 2-chloro-pyridine in 66% yield. On the other hand, other chlorinating agents such as Cl$_3$CCCl$_3$, Cl$_3$CCO$_2$Et, Cl$_3$CCONH$_2$ and NCS provided 2-chloropyridine in low to moderate yield (entries 2-5). This may be because of the better electron-withdrawing effect of the nitrile group compared to the ester and amide groups.

Table 1: Effect of types of chlorinating agent on the formation of 2-chloropyridine


Entry	Chlorinating agent	Yield[a] (%)
1	Cl$_3$CCCl$_3$	58
2	Cl$_3$CCN	66
3	Cl$_3$CCOOEt	34
4	Cl$_3$CCONH$_2$	18
5	NCS	25
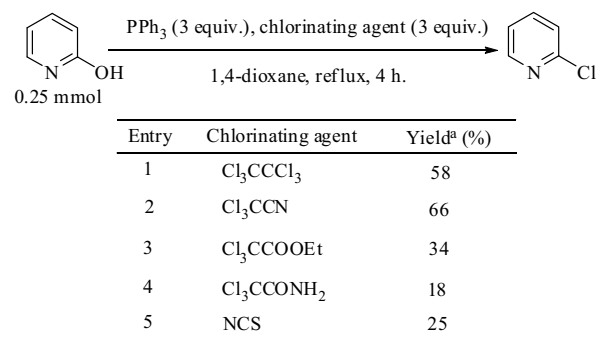
[a] determined by ^{1}H NMR using 1,1,2,2-tetrachloroethane as an internal standard

The effect of solvent and the mole ratio of Cl$_3$CCN:PPh$_3$ was next examined to improve the yield of the desired chloride (Table 2). When the ratio of Cl$_3$CCN:PPh$_3$ was 3:3 and ACN was used as the solvent, the yield of 2-chloropyridine was low (18%,

entry 1) whereas the desired product was obtained in 66-79% yields in other solvents such as 1,4-dioxane, p-xylene and toluene (entries 2-4). In addition, using toluene and increasing the ratio of Cl$_3$CCN:PPh$_3$ to 4:4, the yield of 2-chloropyridine was dramatically increased to 84% (entry 6). However, decreasing the ratio of Cl$_3$CCN:PPh$_3$ to 2:2, the yield of the desired product was significantly decreased (24%, entry 5).

Table 2: Effect of solvent and mole ratio of Cl$_3$CCN:PPh$_3$ on the formation of 2-chloropyridine
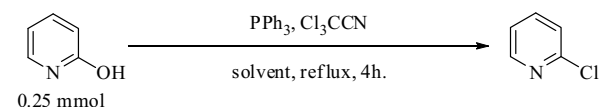
Entry	Solvent	Mole ratio(equiv.)		Yield[a] (%)
		Cl$_3$CCN	PPh$_3$	
1	ACN	3	3	18
2	1,4-dioxane	3	3	66
3	p-xylene	3	3	75
4		3	3	79
5	toluene	2	2	24
6		4	4	84
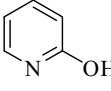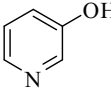
[a] determined by ^{1}H NMR using 1,1,2,2-tetrachloroethane as an internal standard

From aforementioned study, the reaction performed in refluxing toluene was the most efficient yielding the desired 2-chloropyridine in high yield. Although, 4 equiv. of PPh$_3$ and Cl$_3$CCN produced the maximum yield of 2-chloropyridine, it was not much different from using 3 equiv. of PPh3 and Cl3CCN. Hence, the suitable ratio of 2-hydroxypyridine:PPh$_3$:Cl$_3$CCN selected was 1:3:3. This optimal reaction condition was further applied to the synthesis of six N-hetero-aromatic hydroxy compounds to investigate the generality and scope of this method. (Table 3)

In the case of 2-, 3- and 4-hydroxypyridines (entries 1-3), 2- and 4-hydroxypyridines could be converted into the corresponding chloropyridines in high yields while 3-hydroxypyridine was not reactive enough under this condition. This may be because the nitrogen atom at the 3-position could not stabilize the negative charge of reactive intermediate. In addition, 2-chloroquinoline, 2-chloropyrimidine and 4-chloropteridine furnished the corresponding chlorides in 87, 54 and 51%yields, respectively (entries 4-6).

The mechanism for the chlorination of organic compounds such as alcohols and carboxylic acids using PPh$_3$/chlorinating agent has been addressed.[3,19] In this case, the chlorination of N-heteroaromatic hydroxy compounds using PPh$_3$/Cl$_3$CCN was considered to operate via a similar mechanism. PPh$_3$ reacts with Cl$_3$CCN to generate intermediate **1**, which then reacts with N-heteroaromatic hydroxy compound to yield aryloxyphosphonium salt **2**. This salt eventually decomposes to give the desired chloride and triphenylphosphine oxide.

Table 3: Chlorination of selected *N*-heteroaromatic hydroxy compounds

Entry	Substrate	Yield[a](%)
1		79 (65)[b]
2		0
3		71
4		(87)[b]
5		54
6		51

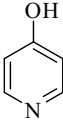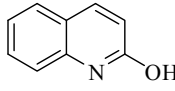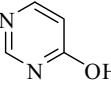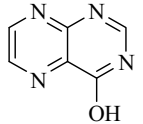[a] determined by ^{1}H NMR using 1,1,2,2-tetrachloroethane as an internal standard

[b] isolated product
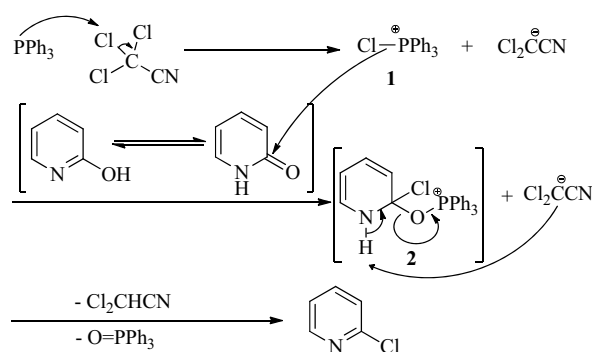
Scheme 1: Proposed mechanism for the chlorination of *N*-heteroaromatic hydroxy compound using PPh$_3$/Cl$_3$CCN

Conclusions

The new and convenient methods for the preparation of *N*-heteroaromatic chlorides from *N*-heteroaromatic hydroxy compounds using PPh$_3$/ chlorinating agent have been explored. PPh$_3$/Cl$_3$CCN has been disclosed to be a suitable combination reagent for the conversion of *N*-heteroaromatic hydroxy compounds to *N*-heteroaromatic chlorides in good yields under mild conditions.

Acknowledgements

References

[1] a) R. Ullrich, C. Dolge, M. Kluge and M. Hofrichter, *FEBS Lett.* **582** (2008), pp. 4100-4106. b) C.B. Andersen, Y. Wan, J.W. Chang, B. Riggs, C. Lee, Y. Liu, F. Sessa, F. Villa, N. Kwiatkowski, M. Suzuki, L. Nallan, R. Heald, A. Musacchio and N.S. Gray, *ACS Chem. Biol.* **3** (2008), pp. 180-192. c) C.W. Am Ende, S.E. Knudson, N. Liu, J. Childs, T.J. Sullivan, M. Boyne, H. Xu, Y. Gegina, D.L. Knudson, F. Johnson, C.A. Peloquin, R.A. Slayden and P.J. Tonge, *Bioorg. Med. Chem. Lett.* **18** (2008), pp. 3029-3033.

[2] B. Armin, Armin. Pharm. **322** (1989), pp. 165-171.

[3] C.A. Busacca, M, Cerreta et al., *Org. Process Res. Dev.* **12** (2008), pp. 603-613.

[4] G. Roma, M. Di Braccio, G. Grossi, D. Piras, V. Ballabeni, M. Tognolini, S. Bertoni and E. Barocelli, *Eur. J. Med. Chem.* **45 (**2010**)**, pp. 352-366.

[5] N.A. Hamdy and A. M. Gamal-Eldeen, *Eur. J. Med. Chem.* **44** (2009), pp. 4547-4556.

[6] E.I. Snyder, *J. Org. Chem.* **37** (1972), pp. 1466.

[7] G. Bringmann and S. Schneider, Synthesis (1986), pp. 139-141.

[8] R.M. Magid, S. Fruchey, W.L. Johnson and T.G. Allen, *J. Org. Chem.* **44** (1979), pp. 359-363.

[9] E.D. Matveeva, A.I. Yalovskaya, I.A. Cherepanov, Yu.G. Bundel and A.L. Kurts, *Organicheskoi Khimii* **27** (1991), pp. 1611-1618.

[10] W. Pluempanupat and W. Chavasiri, *Tetrahedron Lett.* **47** (2006), pp. 6821-6823.

[11] O. Chantarasriwong, D.O. Jang and W. Chavasiri, *Tetraheron Lett.* **47** (2006), pp. 7489-7492.

[12] J.B. Lee, *J. Am. Chem. Soc.* **88** (1996), pp. 3440-3441.

[13] K. Venkataraman and D.R. Wagle, *Tetrahedron Lett.* **20** (1979), pp. 3037-3040.

[14] G.B.Villeneuve and T.H. Chan, *Tetrahedron Lett.* **38** (1997), pp. 6489-6492.

[15] D.O. Jang, D.J. Park and J.Kim, *Tetrahedron Lett.* **40** (1999), pp. 5323-5326.

[16] S. Chaysripongkul, W. Pluempanupat, D.O. Jang and W. Chavasiri, *Bull. Korean Chem. Soc.* **30** (2009), pp. 2066-2070.

[17] O. Sugimoto, M. Mori and K.I. Tanji, *Tetrahedron Lett.* **40** (1999), pp. 7477-7478.

[18] K.I. Tanji, J. Koshio and O. Sugimoto, *Synth. Commun.* **35** (2005), pp. 1983-1987.

[19] W. Pluempanupat, O. Chantarasriwong, P. Taboonpong, D.O. Jang and W. Chavasiri, *Tetrahedron Lett.* **48** (2007), pp. 223-226.

Biologically active alkaloids isolated from the tuber of *Stephania venosa* (Blume) Spreng

A. Makarasen [1], S. Mogkhuntod [2*], N. Khunnawutmanotham [1], N. Chimnoi [1], V. Kongkun [1] and S. Techasakul [1,2]

[1]Chulabhorn Research Institute, Vipavadee-Rangsit Highway, Bangkok 10210, Thailand.
[2] The Center of Innovation in Chemistry (PERCH-CIC), Department of Chemistry, Kasetsart University, 50 Phaholyothin Road, Chatuchak, Bangkok 10900, Thailand.

* Corresponding Author E-Mail Address: fscispt@ku.ac.th

Abstract: The chemical constituents of a methanolic extract of *Stephania venosa* (Blume) Spreng tubers were investigated. The chemical structures of the isolated compounds were characterized using spectroscopic methods. Based on the spectroscopic results obtained, five alkaloids were identified as (-)-tetrahydropalmatine (1), (-)-crebanine (2), dehydrocrebanine (3), (-)-sukhodianine (4), and oxocrebanine (5). Oxocrebanine (5) showed strong activity against cancer cell lines such as acute lymphoblastic leukemia (MOLT-3), cervical carcinoma (HeLa), and hormone-dependent breast cancer (T47-D) with very low cytotoxicity against normal embryonic lung cells (MRC-5). Dehydrocrebanine (3) demonstrated strong activity against acute promyelocytic leukemia (HL-60) together with cytotoxicity against MRC-5. (-)-Tetrahydropalmatine (1), (-)-crebanine (2), and (-)-sukhodianine (4) exhibited weak activity against the cancer cell lines whereas only crebanine (2) showed cytotoxicity against MRC-5. Oxocrebanine (5) also showed activity against Gram-positive bacteria such as *Bacillus cereus* and *Bacillus subtilis*.

Introduction

The genus *Stephania* belongs to the Menispermaceae plant family, which is distributed in Africa, India, and Southeast Asia, as well as Northern and Eastern Australia. This genus is a well-known source of alkaloids, one of the largest groups of natural products with interesting pharmacological activities. Their tuberous roots are widely used in traditional Chinese medicines such as I-roemerine, which was isolated from *Stephania kwangsiensis* Lo tubers and demonstrates inhibitory activity against pathogenic fungi and bacteria [1]. A morphinane alkaloid (6, 7-di-O-acetylsinococuline) from *Stephania cepharantha* tubers also show antiviral activity [2]. Tetrandrine is the major active compound isolated from *Stephania tetrandra* S. Moore, which has been shown to prevent T-cell-mediated liver injure in vivo [3].

Stephania venosa (Blume) Spreng is native to Thailand under the local name "Sabu Leaud". A characteristic feature of the plant is its large tuber, with a long climbing stem and red sap. Tubers of this plant have been used in traditional Thai medicine for treatment of asthma, microbial infection, hyperglycemia, and cancer. Chemical investigation of *S. venosa* revealed a basic yield of a variety of isoquinoline and aporphine alkaloids with different structures such as dehydrocrebanine, liriodenine, (-)-crebanine, (-)-tetrahydropalmatine, oxocrebanine, (-)-O-acetylsukhodianine, oxostephanosine and (-)-kikemanine [4]. The various alkaloids isolated from *S. venosa* have led to numerous studies on their biological activities. However, only incidental reports have been published on the cytotoxicity of the isolated compounds against cancer cells and bacteria [5, 6]. The aim of the current study is to investigate the chemical constituents of *S. venosa* tubers, including their biological activities.

Materials and Methods

Plant Materials: S. venosa tuber was collected from Prachuap Kirikhun Province in the southern part of Thailand in September 2009.

Extraction and Isolation: The fresh tuber of *S. venosa* was cleaned, sliced, and extracted with methanol. The extracts were filtered and were then concentrated using a rotary evaporator, producing a brown semi-solid.

The first portion of methanolic tuber extract (20 g) was subjected to silica gel liquid chromatography using a step gradient of hexane, CH_2Cl_2-hexane, methanol-CH_2Cl_2. The collected fractions were combined based on TLC patterns and concentrated to give twelve fractions. Fraction 2 was repeatedly separated on a silica gel column using the previously described stepwise gradient elution. The collected fractions were combined based on TLC patterns and evaporated to give nine fractions. Pure tetrahydropalmatine **(1),** as yellow needles (14 mg), was obtained by recrystallization from fraction 1 with CH_2Cl_2. Fraction 3 was repeatedly separated on a silica gel column using a step gradient of hexane, hexane-ethyl acetate, and ethyl acetate-methanol. The collected fractions were combined based on TLC patterns and evaporated to give five fractions. Pure dehydrocrebanine **(3),** as yellow needles (10 mg), was obtained through silica gel liquid chromatography of fraction 1 using isocratic elution with ethyl acetate-hexane (1: 4 v/v).

The second portion of the methanolic tuber extract (20 g) was subjected to silica gel liquid chromatography using a step gradient of hexane, CH_2Cl_2-hexane, methanol-CH_2Cl_2. The collected

fractions were combined based on TLC patterns and concentrated to give 12 fractions. Fraction 4 was repeatedly separated on a silica gel column using the step gradient procedure described above. The collected fractions were combined based on TLC patterns and evaporated to give eight fractions. Pure crebanine **(2)**, as colorless needles (76 mg), was obtained from fraction 7 after recrystallization from CH_2Cl_2. Fraction 8 was repeatedly separated on a silica gel column using the step gradient hexane, ethyl acetate-hexane, methanol-CH_2Cl_2, respectively. The collected fractions were combined based on TLC patterns and evaporated to give six fractions. Pure sukhodianine **(4)**, as red needles (11.8 mg), was obtained through silica gel liquid chromatography from fraction 1 using isocratic elution with methanol- CH_2Cl_2 (1: 9 v/v). Fraction 4 was repeatedly separated on a silica gel column using the step gradient procedure described above. The collected fractions were combined based on TLC patterns and evaporated to give nine fractions. Pure oxocrebanine **(5)**, as orange needles (10.6 mg), was obtained by silica gel liquid chromatography from fraction 4 using isocratic elution with methanol-CH_2Cl_2 (1: 4 v/v).

Bacterial Strains: Strains obtained from Thailand Institute of Scientific and Technological Research (TISTR) were as follows: *Staphylococcus aureus* TISTR 517, *Enterococcus faecalis* TISTR 888, *Bacillus cereus* TISTR 687 and *Bacillus subtilis* TISTR 008. Methicillin resistant *Staphylococcus aureus* DMST 20649 obtained from The Department of Medical Sciences, Ministry of Public Health, Thailand.

Precultures of *Staphylococcus aureus*, *Bacillus cereus*, *Bacillus subtilis* and Methicillin resistant *Staphylococcus aureus* were prepared from nutrient agar (NA) at 5 ^{o}C but *Enterococcus faecalis* was grown on Tryptic soy agar (TSA, Difco) and then incubated at 37 ^{o}C. The bacterial suspension (cells in early stationary phase) was subsequently adjusted to 10^6 CFU/ml using MHB and TSB in a shaker incubator for 3-5 h at 150 rpm.

Antibacterial activity assay: Minimum inhibitory concentration (MIC) and minimum bactericidal concentration (MBC) were determined using a modified broth dilution method by the Clinical and Laboratory Standards Institute (CLSI) [7].

Cytotoxicity assay: Quantitative assessment of cytotoxicity was determined using an MTT assay [3(4,5-dimethylthiazol-2-yl)-2-5-diphynyltetrazolium bromide (Sigma-Aldrich, St. Louis, MO, USA)] with hormone-dependent breast cancer cells (T47-D), cervical carcinoma cells (HeLa), and normal embryonic lung cells (MRC-5) based on the method described by Mosman [8], Carmichael [9], Doyly [10], and Tominaga [11]. An XTT assay (3´-[1-[(phynylamino)-carbonyl]-3,4-tetrazolium]-bis(4-methoxy-6-nitro)benzene-sulfonic acid hydrate) was used for acute lymphoblastic leukemia (MOLT-3) and acute promyelocytic leukemia (HL-60) based on the method described by Carmichael et al. [9].

Table 1. Cytotoxic activities of the isolated compounds from *S. venosa* tuber

Cell lines[a]	IC_{50}(µg/mL)						
	Doxorubicin	Etoposide	Tetrahydro palmatine (**1**)	Crebanine (**2**)	Dehydro crebanine (**3**)	Sukhodianine (**4**)	Oxocrebanine (**5**)
MOLT-3	-	0.022±0.001	36.23±1.46	18.06±2.59	3.50±0.33	8.96±0.47	1.10±0.04
T47-D	0.30±0.33	-	Inactive[b]	35.00±2.83	23.5±2.12	45.6±5.131	2.75±0.07
HeLa	0.05±0.00	-	Inactive[b]	36.00±1.41	4.35±0.92	5.0±0.00	2.4±0.152
HL-60	-	0.06±0.07	Inactive[b]	24.85±1.16	2.14±0.11	13.33±0.34	>2.86
MRC-5	-	-	Inactive[b]	35.33±2.52	36.00±1.41	Inactive[b]	Inactive[b]

[a]MOLT-3 (T-lymphoblast: acute lymphoblastic leukemia), T47-D (hormone-dependent breast cancer), HeLa (cervical carcinoma), HL-60 (promyeloblast: acute promyelocytic leukemia), and MRC-5 (Normal embryonic lung cell)
Experiments were performed in triplicate.
[b]Inactive ($IC_{50} \geq 50$ µg/mL)

Table 2. Antibacterial activities of the isolated compounds from *S. venosa* tuber

Bacteria[a]	MIC (MBC) µg/mL					
	Vancomycin	Tetrahydro palmatine (1)	Crebanine (2)	Dehydro crebanine (3)	Sukhodianine (4)	Oxocrebanine (5)
SA	1	>200	200(>200)	128(>200)	200(>200)	200(>200)
MRSA	0.5	200(>200)	200(>200)	128(>200)	128(>200)	200(>200)
EF	2	>200	>200	200(200)	128(200)	>200
BC	2	>200	200(>200)	32(200)	64(200)	32(200)
BS	0.125	>200	200(>200)	32(200)	32(200)	16(200)

[a]SA (*Staphylococcus aureus* TISTR 517), MRSA (Methicillin-resistant *Staphylococcus aureus* DMST 20649), EF (*Enterococcus faecalis* TISTR 888), BC (*Bacillus cereus* TISTR 687), and BS (*Bacillus subtilis* TISTR 008) Vancomycin was used as the positive control.
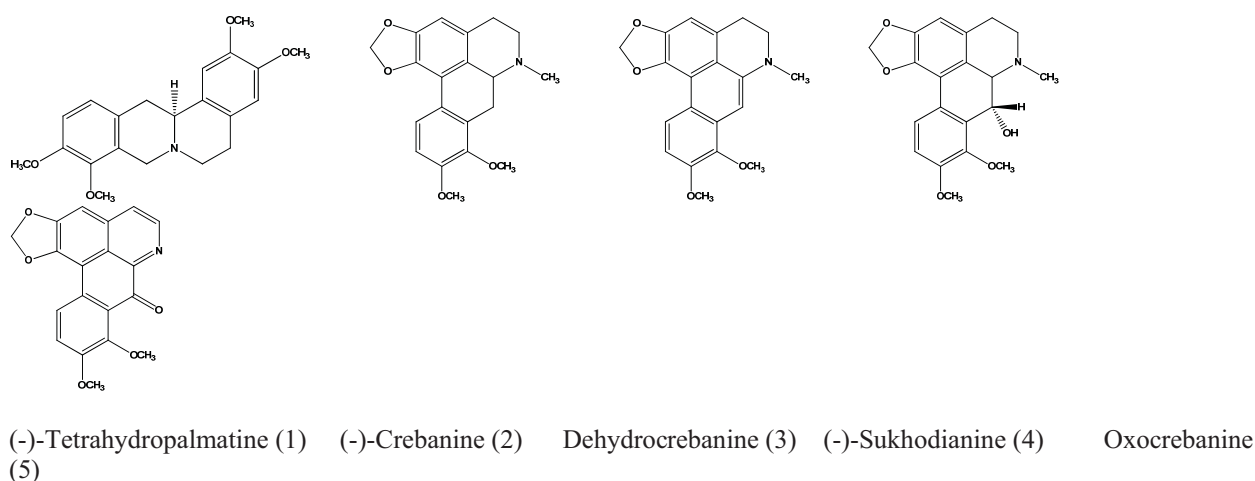

(-)-Tetrahydropalmatine (1)   (-)-Crebanine (2)   Dehydrocrebanine (3)   (-)-Sukhodianine (4)   Oxocrebanine (5)

Figure 1. The chemical structures of the isolated compounds

Results and Discussion

Chromatographic separation of the methanolic extract from the *S. venosa* tuber yielded five known compounds [Figure 1], (-)-tetrahydropalmatine (1), (-)-crebanine (2), dehydrocrebanine (3), (-)-sukhodianine (4), and oxocrebanine (5). Their structures were identified by spectroscopic analysis, as well as by data comparison with those reported in the literature [12-15].

The detailed data of the cytotoxic assay are shown in Table 1. Tetrahydropalmatine (1) and crebanine (2) had weak activities against the various cancer cell lines. Dehydrocrebanine (3) showed strong activity against HL-60 cells with a median inhibitory concentration (IC_{50}) of 2.14 µg/mL. (-)-Sukhodianine (4) displayed moderated activity against MOLT-3 cells (IC_{50} of 8.96 µg/mL) and HeLa cells (IC_{50} of 5.00 µg/mL). Oxocrebanine (5) showed strong activity against the MOLT-3, T47-D, and HeLa cell lines (IC_{50} of 1.10, 2.75, and 2.40 µg/mL, respectively). In addition, 2 and 3 showed cytotoxicity against MRC-5 cells (IC_{50} of 35.33 and 36.00 µg/mL, respectively), whereas 1, 4 and 5 were inactive against MRC-5.

The detailed data of the antibacterial assay are shown in Table 2. Dehydrocrebanine (3), (-)-sukhodianine (4), and oxocrebanine (5) showed moderate activity against *Bacillus cereus* (MIC of 32, 64, and 32 µg/mL, respectively) and *Bacillus subtilis* (MIC of 32, 32, and 16 µg/ mL, respectively) whereas (-)-tetrahydropalmatine (1) and (-)-crebanine (2) showed weak activity.

Conclusions

Five known alkaloids were isolated from tubers of *S. venosa*, and they were evaluated for antibacterial and cytotoxic activities. Oxocrebanine (**5**) has significant cytotoxicity against the cancer cell lines more than the other alkaloids, specifically, **5** showed strong activity against the MOLT-3, HeLa, and T47-D cell lines, and it exhibited antibacterial activity against *Bacillus subtilis* more than the other alkaloids. Only dehydrocrebanine (**3**) showed strong activity against HL-60. Thus, **5** and **3** could potentially be the active compounds in *S. venosa*. Further studies are needed on the detail mechanisms of action for future applications as new drugs.

References

[1] D. Yecheng, L. Jierong, G. Chengwei and Y. Linlin, *Zhiwu Baohu*. **32** (2006), pp. 43–46.

[2] O. Motoki, K. Masahiko, N. As'ari, N. Norio, H. Masao and S. Kimiysu, *Wakan Iyakugaku Zasshi*. **19** (2002), pp. 129-136.

[3] F. Dechun, M. Yunhua, W. Ying, Z. Bianhong, W. Chen and X. Lingyun, *Immunology Letters*, **121** (2008), pp. 127–133.

[4] P. Kalaya, P. Tharadol, T. Bumrung, G. Helene, F. Alan and S. Maurice, *Journal of Natural Products*. **48** (1985), pp. 658-659.

[5] K. Montririttigri, P. Moongkarndi, S. Joongsomboonkusol, B. Chitkul and K. Pattanapanyasat, *Warasan Phesatchasat*. **35(1-4)** (2008), pp. 52-56.

[6] P. Buppachart, K. Tanwarat, L. Pongsatorn, G. Rattanasiri, T. Krittiya, M. Maneerat and B. Yaowaluck, *Acta Horticulturae*, (2005), pp. 57-64.

[7] Clinical and Laboratory Standards Institute. M100-S17, *Performance standards for antimicrobial susceptibility testing, 17th informational supplement*. Wayne, PA: CLSI, 2007.

[8] T. Mosman, Rapid colorimetric assay for cellular growth and survival, application to proliferation and cytotoxicity assay, *J. Immunol Method*. **65** (1983), pp. 55–63.

[9] J. Carmichael, W.G. Degraff, A.F. Gazdar, J.D. Minna and J.B. Mitchell, Evaluation of a tetrazolium-based semi-automated colormetric assay, assessment of chemosensitivity, *Cancer Res*. **47** (1987), pp. 936–942.

[10] A. Doyly, JB. Griffiths, (Eds) Mammalian cell culture-essential techniques, Chichester, Wiley & Sons, 1977

[11] MH. Tominaga, M. Ishiyama, F. Ohseto, K. Sasamoto, T. Hamamoto, K. Suzuki and M. Watanabe, A water-soluble tetrazolium salt useful for colorimetric cell viability assay, *Anal Commun*, **36** (1999), pp. 47–50.

[12] K. Likhitwitayawuid, N. Ruangrungsi and G.A. Cordell, *J. Sci. Soc.* Thailand, **19** (1993), pp. 87–96.

[13] S. Nantapap, C. Loetchutinat, P. Meepowpan, N. Nuntasaen and W. Pompimon, *Am. J. Applied Sci*. **7** (2010), pp.1057-1065.

[14] H. Guinaudeau, M. Shamma, B. Tantisewie and K. Pharadai, *J. Nat. Prod*. **45** (1982), pp. 355-357.

[15] K. Wijeratne, Y. Hatanaka, T. Kikuchi, Y. Tezuka and L. Gunatilaka, *Phytochemistry*. **42** (1996), pp. 1703-1706.

[16] http://paccon2011.swu.ac.th

Synthesis of Triphenylamine-Porphyrin Derivatives as Photo-Sensitizer in Solar Cells

T. Kengthanomma[1,2], P. Rashatasakhon[2,3] and P. Thamyongkit[2,3,*]

[1] Petrochemistry and Polymer Science Program, Faculty of Science, Chulalongkorn University, Bangkok 10330, Thailand
[2] Center of Excellence for Petroleum, Petrochemicals, and Advanced Materials, Chulalongkorn University, Bangkok 10330, Thailand
[3] Department of Chemistry, Faculty of Science, Chulalongkorn University, Bangkok 10330, Thailand

[*] E-mail: patchanita.v@chula.ac.th

Abstract: Three novel porphyrinic compounds were synthesized by a copper-free Sonogashira coupling reaction between tris(4-iodophenyl)amine and 5,10,15-triphenyl-20-(4-ethynylphenyl)porphyrin. The completely coupled product having a triphenylamine core and three peripheral porphyrin moieties will be used as a photo-sensitizer in a bulk heterojunction solar cell. The di-substituted derivative was subjected to a further Sonogashira coupling of the remaining terminal iodo group with a surface anchoring group, i.e. carboxylic acid or cyanoacrylic acid group, to obtain porphyrin products for a dye-sensitized solar cell. Photophysical and electrochemical properties of these photoactive porphyrins are investigated to evaluate the potential for being used in the organic solar cells.

Introduction

Due to the rapid growth of global economies and industries, demand for energy to fuel its impressive industrial expansion is increased. Several sustainable and rational energy plans based on the renewable energy such as wind, natural gas, water, solar energy has been set forth to secure future energy sufficiency.

Solar energy is one of the biggest sources of the available renewable energy on earth and can be harvested by a solar cell that converts it directly into electricity. Nowadays, inorganic solar cells, especially silicon-based one, take the majority part in the market. However, the interests in organic dyes are dractically increasing owing to the possibility of low-cost cell fabrication and the development of extremely light and flexible devices. Some organic compounds such as porphyrins demonstrated satisfactory photochemical and electrochemical properties for being used as photoactive compounds in the optoelectronic devices. At the same time, triphenylamine and its derivatives are widely studied for optoelectronic application due to their excellent charge transfer properties [1-3]. To combine their beneficial properties together, we aim to synthesize a photoactive compound containing both porphyrin and triphenylamine units in the same molecule for a bulk heterojounction organic solar cell. Its photophysical and electrochemical properties will be investigated to evaluate their potential of being used in organic solar cells.

Materials and Methods

All reagents were analytical grade and purchased from Sigma-Aldrich and Merck and used as received without further purification. ^{1}H-NMR and spectrum were obtained in $CDCl_3$ at 400 MHz for [1]H (Varian, USA). Chemical shifts (δ) are reported in parts per million (ppm) relative to the residual $CHCl_3$ peak (7.26 ppm for ^{1}H-NMR). Coupling constant (J) are reported in Hertz (Hz). Mass spectra were obtained using matrix-assisted laser desorption ionization mass spectrometry (MALDI-MS) by using dithranol as a matrix. Absorption spectra were measured in tetrahydrofuran by a Varian Cary 50 UV-Vis spectrophotometer. Emission spectra were recorded in tetrahydrofuran on Varian spectrofluorometer by personal computer data processing unit.

Tris(4-iodophenyl)amine (**3**) was prepared according to the previous literature procedure [4].

*Synthesis of 5,10,15-Triphenyl-20-(4-ethynylphenyl)porphyrin(**2**).* Adapted from a previous published procedure [5], a mixture of benzaldehyde (409.0 mg, 3.858 mmol), pyrrole (351.7 mg, 5.249 mmol) and 4-((trimethylsilyl)-ethynyl)benzaldehyde (267.7 mg, 1.323 mmol) in CH_2Cl_2 (200 mL) was stirred at room temperature until homogeneous solution was obtained. $BF_3 \cdot OEt_2$ (0.25 mL, 2.0 mmol) was added in the solution and the reaction mixture was stirred in room temperature for 1 h. 2,3-dichloro-4,5-dicyanobenzoquinone (DDQ) (500.1 mg, 2.203 mmol) was then added and the reaction was continued for additional 1 h. The resulting mixture was treated with triethylamine (0.5 mL) at room temperature for 5 min and then filtated through a silica pad (CH_2Cl_2). Then solvent was removed and crude product was purified by column chromatography [silica gel, CH_2Cl_2/hexane (1:2)] to give 5,10,15-Triphenyl-20-{4-[2-(trimethylsilyl)ethynyl]phenyl}porphyrin(**1**) as a purple solid. Compound **1** was redissolved in tetrahydrofuran/methanol [3:1] (40.5 mL) and treated with potassium carbonate (90.0 mg, 6.42 mg) at room temperature. After 4 h, solvent was removed under reduced pressure. The reaction mixture was redissolved in CH_2Cl_2 and washed with water. The

organic phase was combined, dried over Na_2SO_4 and concentrated to dryness. After the removal of solvent, the crude mixture was purified by a silica column [CH_2Cl_2/hexane (1:3)], affording compound **2** as a purple solid (75.2 mg, 9% from 4-((trimethylsilyl)-ethynyl)benzaldehyde). ^{1}H-NMR δ ppm –2.87 (s, 2H), 3.25 (s, 1H), 7.64–7.75 (m, 8H), 7.82 (d, J = 8.0 Hz, 2H), 8.11 (d, J = 8.0 Hz, 1H), 8.12–8.15 (m, 8H), 8.72–8.83 (m, 8H). MALDI-TOF-MS m/z calcd 638.760 found 637.689 [M$^+$] (M = $C_{46}H_{30}N_4$).

Synthesis of tris-4,4',4''-(triphenyl-20-(4-ethynylphenyl)porphyrin)triphenylamine (**4**). Following a standard procedure [6], a mixture of compound **2** (296.1 mg, 0.4636 mmol) and **3** (70.8 mg, 0.114 mmol) in toluene/TEA [5:1] (19.6 mL) was stirred under nitrogen atmosphere until a homogeneous solution was obtained. After that, Tris(dibenzylideneacetone)dipalladium(0) (19.0 mg, 0.0207 mmol) and tri(*o*-tolyl)phosphine (35.5 mg, 0.117 mmol) was added and the reaction mixture was stirred under nitrogen atmosphere at 40 °C. After 24 h, the reaction mixture was filtered through a silica pad (toluene). After the removal of solvent under reduced pressure, the crude mixture was separated by a three-column process: a siliga column [CH_2Cl_2/hexane (1:1)], a size-exclusion column [tetrahydrofuran] and then a silica column [CH_2Cl_2/hexane (1:1)] to obtain **4** as a magenta solid (88.6 mg, 36%). ^{1}H-NMR δ ppm –2.82 (s, 6H), 7.58–7.86 (m, 45H), 8.06–8.26 (m, 24H), 8.67–8.93 (m, 24H). MALDI-TOF-MS m/z calcd 2155.542 found 2157.851 [M+] (M = $C_{156}H_{99}N_{13}$).
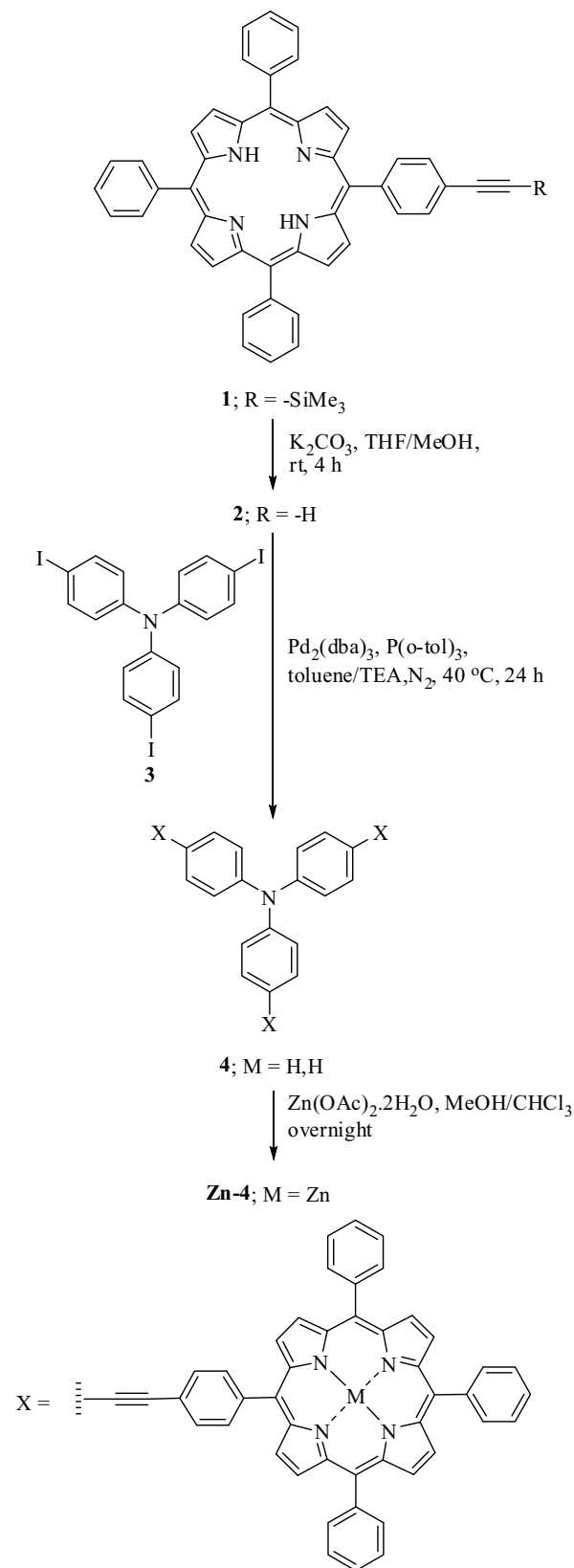
Synthesis of tris-4,4',4''-Zn(triphenyl-20-(4-ethynylphenyl)porphyrin)triphenylamine (**Zn-4**). A solution of compound **4** (88.6 mg, 0.0411 mmol) in $CHCl_3$ (15 mL) was treated with a solution of $Zn(OAc)_2·2H_2O$ (364.8 mg, 1.662 mmol) in methanol (5 mL). After refluxing for 2 h, the reaction mixture was concentrated to dryness, redissolved in CH_2Cl_2 and then washed with water. The organic phase was combined and dried over anydrous $MgSO_4$. After the removal of solvent under reduced presure, the crude product was purified by column chromatography [silica gel, CH_2Cl_2/hexane (2:1)], affording compound **Zn-4** as a maganta solid (90.7 mg, 94%) ^{1}H-NMR δ ppm 7.60–7.98 (m, 45H), 8.06–8.37 (m, 24H), 8.96 (m, 24H). MALDI-TOF-MS m/z calcd 2345.725 found 2348.633 [M+] (M = $C_{156}H_{93}N_{13}Zn_3$).
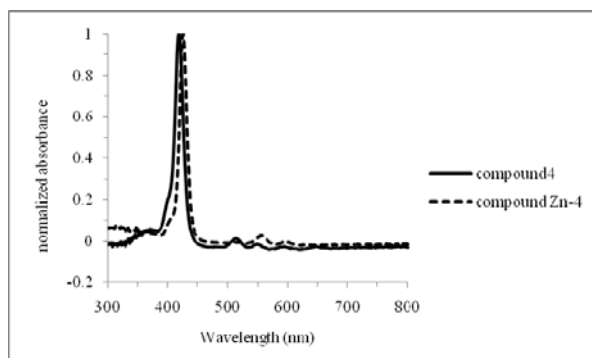
Results and Discussion

A novel porphyrinic compound **Zn-4** was synthesized by a Sonogashira coupling reaction between compounds **2** and **3** followed by zinc-metallation as shown in Scheme 1.

Zn-4 and its freebase precursor **4** were characterized by ^{1}H NMR spectroscopy and mass spectrometry. The ^{1}H NMR spectrum of compound **Zn-4** showed a similar resonating pattern as that of compound **4**, except the disappearance of a resonance due to the internal N-H protons in the porphyrin moiety upon metallation. Data of mass spectra for all compounds are also consistent with their molecular

formulations. UV-vis spectrum of compound **4** exhibited a characterictic absorption maximuum (B band) at 420 nm with Q band at 515, 550 and 590 nm, while that of **Zn-4** showed B band at 425 nm with Q band at 555 and 594 nm. (Fig. 1).


1; R = -SiMe$_3$

K_2CO_3, THF/MeOH, rt, 4 h

2; R = -H

$Pd_2(dba)_3$, P(o-tol)$_3$, toluene/TEA, N$_2$, 40 °C, 24 h

4; M = H,H

$Zn(OAc)_2.2H_2O$, MeOH/CHCl$_3$ overnight

Zn-4; M = Zn

Scheme 1. Synthesis of **Zn-4**

Figure 1. Absorption spectra of compound **4** (solid line) and compound **Zn-4** (dashed line)

Figure 2 shows the emission spectra of compounds **4** and **Zn-4**. Upon the excitation at its maximum absorption (420 nm), the emission of compound **4** appeared at 654 and 719 nm, while that of compound **Zn-4** was observed at 607 and 655 nm upon the excitation at 425 nm. The absence of the emission at about 720 nm in the case of **Zn-4** indicated the complete metallation of the porphyrin ring.
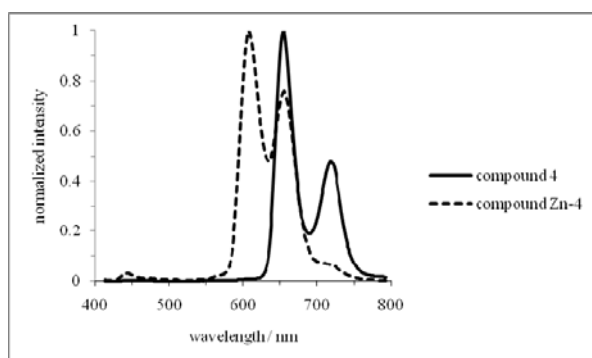
Figure 2. Emission spectra compound **4** (solid line) and **Zn-4** (dashed line)

To evaluate the potential for being used in the organic solar cells, elctrochemical properties by cyclic voltammetry and photovoltaic performance of compound **Zn-4** will be investigated.

Conclusions

In this report, we have successfully synthesized and characterized a novel porphyrinic compound bearing a functionalized triphenylamine core and three porphyrin peripheral moieties. Further photophysical and electrochemical investigation, and solar cell fabrication/evaluation are currently in progress and will be published elsewhere.

Acknowledgement

References

[1] Y. Shirota, *J. Mater. Chem.* **10** (2000), pp. 1–25.
[2] Y. Shirota, *J. Mater. Chem.* **15** (2005), pp. 75–93.
[3] Y. Shirota and H. Kageyama, *Chem. Rev.* **107** (2007), pp. 953–1010.
[4] S.P. McIlroy, E. Cló, L. Nikolajsen, P.K.. Frederiksen, C.B. Nielsen, K.V. Mikkelsen, K.V. Gothelf and P.R. Ogilby, *J. Org. Chem.* **70** (2005), pp. 1134–1146.
[5] J.S. Lindsey, S. Prathapan, T.E. Johnson and R.W. Wagner, *Tetrahedron.* **50** (1994), pp. 8941–8968.
[6] K.-Y. Tomizaki, P. Thamyongkit, R.S. Loewe and J.S. Lindsey, *Tetrahedron.* **59** (2003), pp. 1191–1207.

Synthesis of Magnetic-Molecularly Imprinted Silica Selective to Nicotinamide

B. Khumraksa and M. Pattarawarapan[*]

Department of Chemistry, Faculty of Science, Chiang Mai University,
Huay Kaew Road 239, Chiang Mai, Thailand 50200

[*] E-mail: mookda@chiangmai.ac.th

Abstract: Magnetic nanoparticles (MNPs), Fe_3O_4, have been found numerous applications due to their excellent magnetic property. The participation of a magnetic component in the imprinted silica can build a controllable rebinding process in which they are then easily separated from the matrix by applying an external magnet. Therefore, in this study, the magnetic-molecularly imprinted silicas (M-MIS) were synthesized using a simple sol-gel method to form Fe_3O_4/silica composite materials selective to nicotinamide (NAM). 3-Aminopropyltriethoxysilane (APTS) and tetraethoxy silane (TEOS) were used as the precursor to form imprinted silica. The NAM recognition properties of these M-MISs were investigated by batch rebinding experiment. It was found that the M-MIS having TEOS as a precursor showed the highest percentage NAM bound with good imprinting factor and provided high selectivity in acetonitrile/water mixture.

Introduction

Molecular imprinting is an efficient technique for the creation of synthetic material for molecular recognition [1-8]. Nowadays molecular imprinting technology is considered a convenient approach for the development of molecular recognition systems and have important applications in various areas such as solid phase extraction (SPE) [2, 3], sorbent assays [4], capillary electrochromatography [5], microextraction fibres [6], sensors [7] and catalyst [8].

The molecularly imprinted silica (MIS) are inorganic (siloxane) based polymers formed by the sol-gel method with acid or base catalyzed hydrolysis and condensation of a series of silane monomers [9]. Inclusion of a template species results in the formation of imprinted silica. After template molecule is removed, the cavities are left in the silica matrix which are complementary in both size and functionality arrangement to those of the template molecules. The sol–gel process is a versatile method for preparing transparent optical materials at ambient processing conditions. It enables entrapment of various compounds including organic, organo-metallic and biological molecules (proteins and enzymes). The microporous network of sol–gel derived matrix can be generated with chemical inertness, rigidity, and high porosity. The availability of a wide range of functional silane monomers makes MIS ideally suit for use in various applications [10-12].

Magnetic nanoparticles (MNPs), Fe_3O_4, is a common magnetic iron oxide that are well dispersed in a liquid, normally in water, or form composites with organic or inorganic matrices. The presence of a magnetic component in the imprinted silica allows a controllable rebinding process and ease of their removal from the binding matrix using an external magnet without additional centrifugation or filtration [13].

In this study, a sol-gel method and molecular imprinting technique were employed to synthesize magnetic-molecularly imprinted silica (M-MIS) using NAM as a template molecule. 3-Aminopropyl triethoxysilane (APTS) and tetraethoxysilane (TEOS) were used as the precursor to form imprinted silicas (Fig. 1). Their binding efficiencies in acetonitrile-water (MeCN:H_2O) mixtures were investigated by batch rebinding experiments. The selectivity of selected M-MIS was also evaluated by comparing the NAM rebinding capacities with nicotinic acid (NA) and 3-aminopyridine (3-APY) as NAM structurally related analogues.

Materials and Methods

Materials and reagents: Ferric chloride ($FeCl_3 \cdot 6H_2O$) was purchased from Carlo Erba. Iron(II) sulfate was purchased from POCH. Nicotinamide (NAM), nicotinic acid (NA), 3-aminopyridine (3-APY), tetraethoxysilane (TEOS), and 3-amino propyltriethoxysilane (APTS) were purchased from Sigma–Aldrich and used as received. All other chemicals were purchased from commercial suppliers and used without further purification.
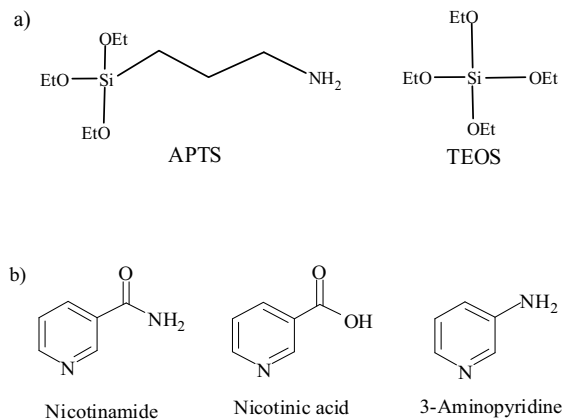

Figure 1. a) Structures of APTS and TEOS precursors b) NAM and its structurally related compounds.
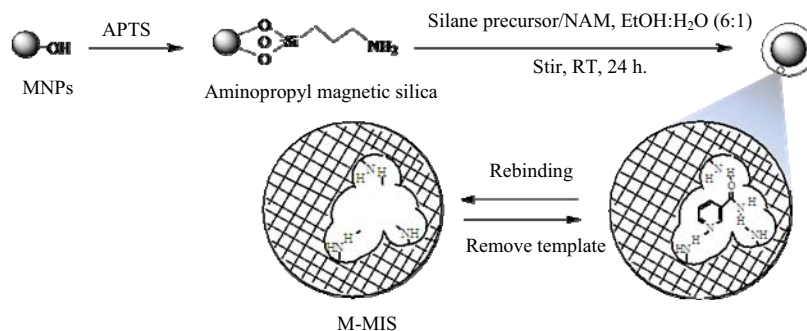
Figure 2. Schematic illustration for preparation of M-MIS.

Preparation of aminopropyl magnetic silica: The synthesis of aminopropyl magnetic silica included two steps which are the preparation of Fe_3O_4 nanoparticles and the synthesis of silica-coated magnetic nanoparticles. Fe_3O_4 magnetic nanoparticles were precipitated in alkali solution of Fe(II) and Fe(III) (molar ratio 2:1) at 80 ºC via the chemical co-precipitation method which reported by Molday [14]. The obtained MNP powders were dispersed in a mixture of ethanol and water by sonication before APTS was added. After agitation for 5 h, the suspended substance was separated by Magnetight™ separation stand (Novagen®) followed by washing several times with water and ethanol, then dried to powders.

Preparation of M-MIS: To prepare the M-MIS, a certain amount of aminopropyl magnetic silica was first dispersed in the mixture of EtOH:H_2O (6:1 v/v). Then, 0.5 ml of ammonia solution and the silane precursor (APTS and TEOS) were added successively under vigorous stirring at room temperature. After 1 h, a stoichiometric amount of NAM was added and stirred at room temperature for 24 h. The resulting M-MIS was separated from the mixture using Magnetight™ separation stand followed by washing with copious ethanol and water. The template was then removed by washed with hot mixture of acetic acid:methanol:water (4:1:1 v/v), then the remained acetic acid was removed by washing with water and methanol. Finally, the M-MIS products were dried at 80 ºC for 24 h. An additional control batch (non-imprinted silica, M-NIS) was prepared following the above described procedure, in the absence of template. The M-MIS and M-NIS were characterized by FT-IR.

Rebinding experiments: 10 mg batched of M-MIS was added to a 0.2 mM solution of NAM in MeCN:H_2O (1:1 v/v) mixture. After incubating for 1 hour at room temperature, the M-MIS was separated by Magnetight™ separation stand. The bound amount of template molecules in M-MIS was determined by measuring the difference between total template amount and residual amount in solution before and after incubation, respectively, with UV-VIS spectro-photometry at the maximum wavelength. This experiment was performed in triplicate.

The molecular selectivity of M-MIS toward NAM was investigated by rebinding study as previously described for NAM rebinding using the NAM structure analogs including nicotinic acid (NA) and 3-aminopyridine (3-APY) (Fig. 1) in comparison with the original template molecule at the selected rebinding conditions. These experiments were done in triplicate for each analogue compound.

Results and Discussion

Preparation and characterization of M-MIS: The synthesis of the M-MIS is illustrated according to Fig. 2. Aminopropyl magnetic silica and silane precursor where incubated with NAM template, after hydrolysis and polycondensation, the three-dimensional polysilicate network can be obtained. Subsequence extraction of the template should generate the recognition site in the microporous silica network which should be able to rebind specifically with the template molecule.

Transmission electron microscopy (TEM) revealed that the MNPs are nearly spherical particles with average diameter about 20 nm (Fig. 3). The distribution curve of the particles size showed the diameter of Fe_3O_4 MNPs in the range of 9–26 nm. Surface modification of the Fe_3O_4 MNPs with APTS yield aminopropyl magnetic silica with 0.64 mmol/g loading of amino group determined by quantitative ninhydrin method [15].
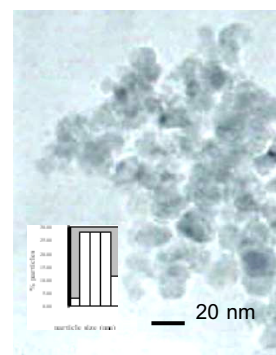

Figure 3. TEM image of MNPs and particle size distribution curve of MNPs.

The modification of aminopropyl magnetic silica with silane precursors produced M-MIS 1 and 2 as brown powder. The compositions and yields of the

obtained M-MISs were shown in Table 1 and the IR absorption spectra of the MNPs, the imprinted-, and the non-imprinted magnetic silicas were shown in Fig. 4. The most distinctive absorption band found in all samples at 3440 cm^{-1} (I) are corresponded to the stretching of O-H and N-H bonds, and it was attributed to non-condensed silanols, residual water and to the aminopropyl groups linked to the silica network. In the spectrum of all samples, the observed features around 630 cm^{-1}(IV) and 460 cm^{-1} (V) indicated Fe–O bond vibration of bulk Fe$_3$O$_4$ [16], while absorption band associated to Si-O stretching is at 1075 cm^{-1} and Si-O bending at 460 cm^{-1} (V). In case of aminopropyl magnetic silica (b), the band that locate around 1550-1620 cm^{-1} (II) is the N-H bending which suggested that aminopropylsilane has been coated onto the surface of MNPs. This characteristic band of N-H was also observed in M-MIS 1 and M-NIS 1 which can be attributed to the incorporation of the primary amines from the APTS into the silica matrices of M-MIS.

For M-MIS and M-NIS, there is no substantial difference in the IR absorption bands; any possible difference between these materials, specially their sorptive properties, should be due to the morphological differences caused by the molecular imprinting process.

Table 1. Compositions and yield of M-MIS and M-NIS

M-MIS/ M-NIS	Template	Silane precursor	% yield
M-MIS 1	NAM	TEOS/APTS	43.9 %
M-NIS 1	-	TEOS/APTS	59.5 %
M-MIS 2	NAM	TEOS	55.1%
M-NIS 2	-	TEOS	59.6 %

Rebinding experiment: The rebinding experiment is used to evidence the imprinting effect of M-MIS by comparing the rebinding efficiency of M-MIS to the corresponding M-NIS. Rebinding efficiency of the M-MISs were evaluated from the quantity of template bound to M-MIS which can be calculated in term of percentage bound (%Bound) according to equation 1.

$$\%Bound = (Q/ Q_{initial}) \times 100 \quad (1)$$

Where Q is the amount of analytes bound to the M-MIS and Q$_{initial}$ is the initial amount of analytes before incubating with the M-MIS.

The imprinting effect of M-MIS related to non-imprinted one can be evaluated from the imprinting factor (α) which can be calculated according to equation 2. The imprinting effect is evidenced when the α value is >1.

$$\alpha = \frac{\%Bound\ M\text{-}MIS}{\%Bound\ M\text{-}NIS} \quad (2)$$

Where %Bound$_{MIS}$ and %Bound$_{NIS}$ represent the percentage of bound analyte by M-MIS and M-NIS, respectively.
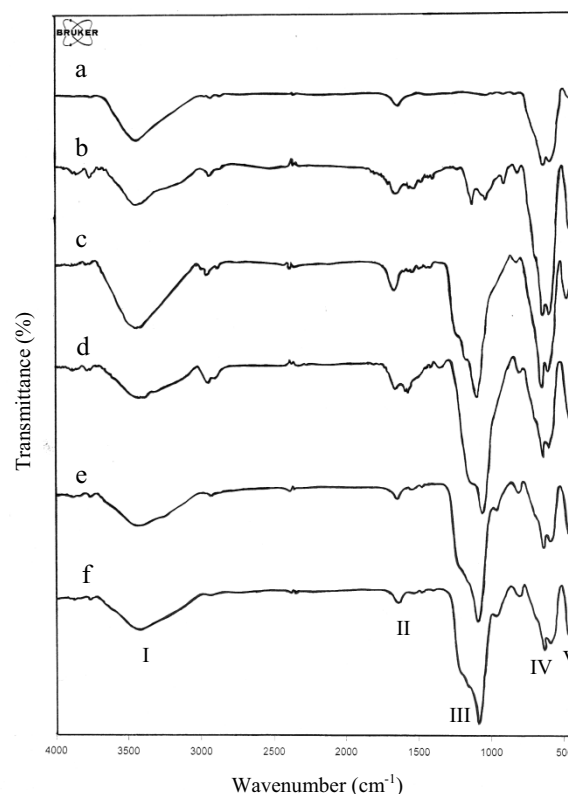

Figure 4. FT-IR spectra of the (a) MNPs, (b) Aminopropyl magnetic silica , (c) M-MIS 1 (d) M-NIS 1, (e) M-MIS 2 and (f) M-NIS 2. See text for band assignment

In this study, the rebinding efficiency of M-MIS 1 and M-MIS 2 were investigated in MeCN:H$_2$O system. As shown in Table 2, M-MIS 2 gave higher %Bound than M-MIS 1, while its α value was slightly lower.

For NAM, the previously reported %Bound in aqueous media were found in range of 9-47%, with the α values of 1.0 - 2.3 [3, 17, 18]. Thus, the binding efficiency of both M-MISs were in acceptable range.

It is noted that the only difference between M-MIS 1 and M-MIS 2 is that M-MIS 2 contains higher amount of APTS. This observation is in agreement with previous study in which it was found that adding too much APTS can interfere with the template rebinding process of M-MIS [19].

Table 2. Percent NAM bound onto M-MIS 1 and 2 in MeCN:H$_2$O system and their imprinting factor.

M-MIS	%Bound	α
1	6.41	2.28
2	22.41	1.90

Since M-MIS 2 gave much higher %Bound than M-MIS 1, the binding selectivity of M-MIS 2 was thus

further investigated. When the rebinding study was performed using NAM's structurally related compounds, including NA and 3-APY, it was found that both NA and 3-APY were not bound to M-MIS 2 (data not shown). This data indicates that M-MIS 2 can bind to NAM more preferentially than other structurally related substrates.

Conclusions

A simple molecular imprinting procedure was adopted to synthesize the molecularly magnetic-imprinted silicas (M-MISs) by combining a surface molecular imprinting technique with a sol-gel process. The synthesized M-MIS can be rapidly and easily separated under a magnetic field allowing facile rebinding process. The rebinding experiments indicate that the M-MIS 2 exhibit the greatest binding affinity and selectivity toward NAM.

Acknowledgements

References

[1] C. J. Tan and Y. W. Tong, *Anal. Bioanal*. Chem. **389** (2007), pp. 369-376.

[2] W. M. Mullett , M. F. Dirie, E. P.C. Lai, H. Guo and X. He, Anal. *Chim. Acta* **414** (2000), pp. 123-131.

[3] W. Kareuhanon, V. S. Lee, P. Nimmanpipug, C. Tayapiwatana and M. Pattarawarapan, *Chromato graphia* **70** (2009), pp. 1531-1537.

[4] C.J. Allender, K.R. Brain and C.M. Heard, *Prog. Med. Chem.* **36** (1999), pp. 235-291.

[5] L. Schweitz, L.I. Andersson, S. Nilsson, *Anal. Chem.* **69** (1997), pp. 1179-1183.

[6] W.M. Mullett, P. Martin, *J. Pawliszyn, Anal.. Chem.* **73** (2001), pp. 2383-2389.

[7] D. Kriz, O. Ramstrom, A. Svensson, K. Mosbach, *Anal. Chem.* **67** (1995), pp. 2142-2144.

[8] A. Visnjevski, E. Yilmaz, and O. Bruggemann, *Appl. Catal., A* **260** (2004), pp. 169-174.

[9] W. Stőber, A. Fink and E. Bohn, *J. Colloid Interface Sci.* **26** (1968), pp. 62-69.

[10] R.G. da Costa Silva and F. Augusto, *J. Chromatogr., A,* **1114** (2006), pp. 216-223.

[11] S. Marx and A. Yazaltsman, *Int. J. Environ. Anal. Chem.* **83** (2003), pp. 671-680.

[12] R. Gupta and A. Kumar, *Biotechnol. Adv.* **26** (2008), pp. 533-547.

[13] C. Zhao, H. Huang, H. Zhang and C. Wang, *Anal. Bioanal. Chem.* **395** (2009), pp. 1125-1133.

[14] R.S. Molday, *US Patent* **4**, 452, (1984), pp. 773.

[15] I. Taylor and A.G. Howard, *Anal. Chim. Acta* **271** (1993), pp.77-82.

[16] M. Ma, Y. Zhang, W. Yu, H-Y. Shen, H-Q. Zhang and N. Gu, *Colloids Surf., A* **212** (2003), pp. 219-226.

[17] R.D. Sole, M.R. Lazzoi and G. Vasapollo, *Drug Deliv.* **17** (2010), pp. 130-137.

[18] M. Pattarawarapan, S. Komkham, W. Kareuhanon and C. Tayapiwatana, *e-Polymers* **091** (2008), pp. 1-9.

[19] Z. Xue, H. Xi-Wen, C. Lang-Xing, L. Wen-You and Z. Yu-Kui, *Chin. J. Anal. Chem.* **37** (2009), pp.174-180.

Silica Supported Base in Organic Synthesis

P. Rattanaburi and M. Pattarawarapan[*]

Department of Chemistry, Faculty of Science, Chiang Mai University,
Huay Kaew Road 239, Chiang Mai, Thailand 50200

* Email: mookda@chiangmai.ac.th

Abstract: A silica-supported base reagent (Si-DIEA) containing a structure similarity to diisopropylethylamine (DIEA) has been developed for use as base reagent in the synthesis of sulfonamide. The Si-DIEA base was prepared by immobilization of commercial grade silica gel with 3-aminopropyltrimethoxysilane, followed by reacting with chloroacetyl chloride which was then reacted with diisopropylamine. The advantage of using Si-DIEA includes excellent yield (94% yield) and purities without any further purification steps, mild reaction conditions, short reaction period, and ease of product isolation.

Introduction

Solid supported reagents are commonly used in solution phase organic synthesis to facilitate product purification. This technique requires the attachment of reagents to solid support to facilitate their isolation and enable the chemist to monitor reaction using common analytical techniques. The use of solid-supported reagents means that excess reagent can be employed in order to drive the reaction to completion, while the reagent can be easily removed from the reaction mixture simply by filtration [1].

Reaction with solid-supported reagents does not suffer from such disadvantages as difficult product isolation and low yield due to loss of product in purification step. Spreading reagents on a finely divided solid support is also known to produce an enhanced reaction rate, greater efficiency. In addition, the lower mobility of supported reagents makes them safer to handle.

Polymers are widely used in the preparation of solid supported reagents, while other materials such as zeolites, clays, alumina and silica have also been investigated. Recently, silica gel has been considered as a new alternative material for use as a solid support [2,3]. This support becomes popular reagent due to the advantages over other organic supports such as high loading, ease of chemical modification or attachment with reagents. Unlike certain polymers, silica exhibits no swelling in organic solvents and is thermally, chemically and mechanically stable. Due to the non-porous nature of the support, functionalization of silica is only limited to the surface. Thus, the reaction rate is not limited by reagent diffusion whilst enabling controlled, reproducible loading in order to prevent any undesired effects [4,5].

Diisopropylethylamine or so called Hünig's base, DIPEA or DIEA is a tertiary amine commonly used in organic synthesis as a base. Because the nitrogen atom is shielded by the two isopropyl groups and an ethyl group, only a proton is small enough to easily fit. This compound is thus a good base but a poor nucleophile, which makes it a useful organic reagent. So far, DIEA has been successfully applied in various reactions. For example, it is used as a selective reagent in the alkylation of primary amine or secondary amines with alkyl halides. No formation of quaternary ammonium salt side product is obtained when using this base [6]. DIEA is also commonly used in peptide synthesis to prevent racemization of amino acids during peptide coupling.

In this study, amine functionalized silica gel was modified with diisopropylamine to give silica-supported base reagent (Si-DIEA) that consists of structure similar to diisopropylethylamine. Its application was investigated in the synthesis of sulfonamides.

Materials and Methods

Silica gel and triethylamine were purchased from MERCK. 3-Aminopropyltriethoxysilane and benzenesulfonyl chloride were purchased from Fluka. Benzylamine and diisopropylethylamine (DIEA) were purchased from Sigma-Aldrich. All other solvents and chemicals were obtained from commercial sources and used without prior purification.

Silica Pretreatment

Silica gel (10 g) was added with a mixture of nitric acid and sulfuric acid (1:1, 700 ml), followed by sonicating for 10 min. The mixture was then refluxed for 3 h, and washed with deionized water until pH ~ 7. The pre-purified silica gel was then oven dried at 120°C for 24 h and kept in desiccators [7].

*Synthesis of 3-Amino propyl Silica **1***

3-Aminopropyltriethoxysilane (3 ml) was dissolved in 50 ml of toluene in a round-bottomed flask. Whilst the solution was stirred vigorously, 3 g of the silica gel was slowly added. After sonicating for 10 min, the reaction mixture was refluxed for 3 h. The silica gel was then rinsed with toluene, followed by methanol and acetone, respectively to obtain Silica **1**. The Silica **1** was oven dried at 80°C for 12 h and kept in desiccator. The amount of the amino group on silica was 0.8 mmol/g, estimated from quantitative ninhydrin test [8].

Synthesis of Silica 2

3-Amino functionalized Silica **1** (1 g) was added as a powder into a 100 ml round-bottomed flask containing chloro-acetyl chloride (10 eq) in dichloromethane (50 ml), the reaction mixture was cooled and triethylamine (5 eq) was added. After stirring for 1 h at 0°C, the reaction mixture was stirred at room temperature overnight. After the completion of the reaction as indicated by negative ninhydrin test of the resulting silica, the solid was then filtered and washed with dichloromethane, followed by deionized water, acetone and dichloromethane, respectively. The Silica **2** was oven dried at 80°C for 12 h and kept in desiccator [9].

Synthesis of Silica-Supported Base (Si-DIEA)

The Silica **2** (2 g) was added as a powder into a 100 ml round-bottomed flask containing diisopropylamine (10 eq), K_2CO_3 (5 eq) in dichloromethane 100 ml, the solution was stirred vigorously at room temperature for overnight. The silica-supported base (Si-DIEA) was then filtered and washed with dichloromethane, followed by deionized water, acetone and dichloromethane, respectively. The Si-DIEA was oven dried at 80°C for 12 h and kept in desiccator. The loading capacity of diisopropylamine on Si-DIEA, calculated from the starting aminated Silica **1,** was 0.73 mmol/g.
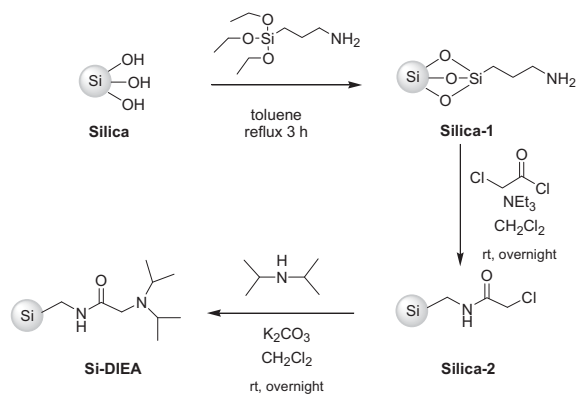
Scheme 1. Synthesis of Si-DIEA

Synthesis of Sulfonamide

Benzenesulfonyl chloride (25 mg) was added into a stirred solution containing benzylamine (1.2 eq) and Si-DIEA (5.0 eq) in dichloromethane. The reaction mixture was stirred at room temperature for 30 minute. After the reaction was completed, Si-DIEA was filtered and washed with dichloromethane. The combined reaction mixture was evaporated to give *N*-benzylbenzenesulfonamide as a white solid (94% yield). ^1H NMR (400 MHz, CDCl$_3$) δ 4.2 (1H, s), 4.9 (1H, s) and 7.5-7.9 (10H, m).
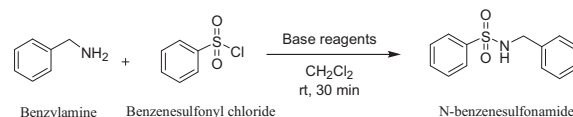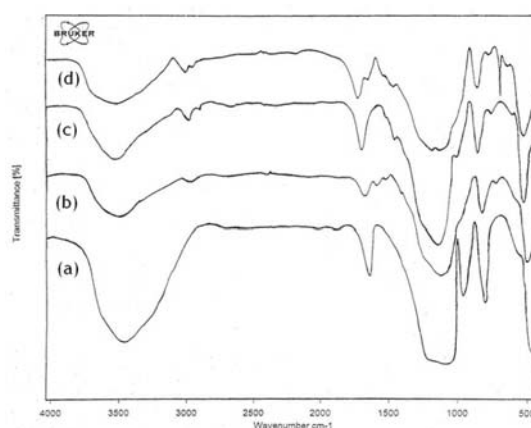

Scheme 2. Synthesis of *N*-benzylbenzene-sulfonamide.

Results and Discussion

Silica-supported base reagent (Si-DIEA) was prepared by surface modification of silica gel with 3-aminopropyltrimethoxysilane which can then be further acylated and connected to diisopropylamine, leading to modified surface of silica that has structure similar to DIEA base (Scheme 1).

The Si-DIEA was structurally characterized by Fourier Transform Infrared Spectroscopy (FT-IR). Figure 1 showed the FT-IR spectrum of the silica gel before and after surface modification. The O-H stretching band occurs at 3300-3500 cm^{-1} for starting silica gel (a). The N-H stretching bands occur at 3424 cm^{-1} and 1551 cm^{-1} for Silica **1** (b). The C-Cl stretching band at 800-785 cm^{-1}, C=O stretching band at 1655 cm^{-1} and C=O symmetry stretching at 1384 cm^{-1} were obtained from Silica **2** (c). For Si-DIEA base reagent (d), the C-N stretching band occurs at 1050-1230 cm^{-1} C-H stretching band at 2950-2800 cm^{-1} and C=O banding at 1630-1690 cm^{-1}.

**Figure 1.** IR spectra of Silica (a), Silica **1** (b), Silica **2** (c), Si-DIEA (d)

To demonstrate the applicability of the obtained Si-DIEA, it was applied as base reagent in the synthesis of *N*-benzylbenzenesulfonamide (Scheme 2). The same reaction using Silica **2** and DIEA was also performed for comparison. 1.2 equiv. of DIEA was used in the solution phase synthesis, while 5.0 equiv. of Si-DIEA or Silica **2** was applied in the solid supported reagent mediated reaction. Typical aqueous work up and product purification by column chromatography was

performed when using DIEA reagent. When using silica reagent, the sulfonamide product was isolated by concentrated the crude reaction mixture after the silica reagent was filtered off. Table 1 showed the yield obtained from the reactions. It was found that when using solution- and supported- DIEA as base, comparable yields of the product was obtained. However, only 47.2% of product was observed when using Silica 2 suggesting that this support did not act as base. When Si-DIEA was reused in the sulfonamide synthesis, high yield of product can be achieved up to five repeated run.

Table 1. The percentage yields obtained from the synthesis of *N*-benzylbenzenesulfonamide

Reagent	%yield				
	Run No.				
	1	2	3	4	5
DIEA base solution	96.5	-	-	-	-
Silica-2	47.2	-	-	-	-
Si-DIEA	94.6	90.5	91.6	92.4	92.5

Considering the purity of the sulfonamide, NMR was used to analyze the purity of the crude reaction mixtures obtained from the reaction using DIEA and Si-DIEA as base (Figure 2). The chemical shift at 4.2 ppm is corresponded to the –CH$_2$ of the benzyl group of sulfonamide product while at δ 3.92 ppm belong to the –CH$_2$ group of benzyl amine. After 30 minute, both reactions using DIEA and Si-DIEA were completed as indicated by the disappearance of NMR peaks at δ 3.92 ppm. While the crude mixture from DIEA mediated reaction contains significance amount of DIEA (δ 3.92, 2.91, 1.56 ppm), no trace of this base can be found using Si-DIEA.
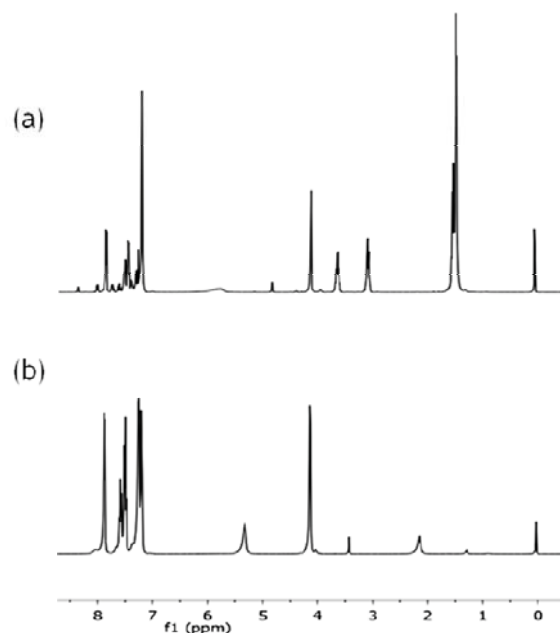
Figure 2. Stack plot of NMR spectra of the crude reaction mixtures from *N*-benzylbenzenesulfonamide synthesis using DIEA base (a) and Si-DIEA (b).

Conclusions

Silica-supported base reagent (Si-DIEA) has been synthesized and can be used as an effective base reagent in the synthesis of sulfonamide. This procedure is fast, produces excellent yield, and allows easy isolation of product without any aqueous work up and/or column chromatography.

References
[1] L. N. H. Arakaki, L. M. Nunes, J. A. Simoni and C. Airoldi, J. Colloid Interface Sci. **228** (2000), pp.46-51.
[2] S. Bhattacharyya, Molecular Diversity **9** (2005), pp.253-257.
[3] I. R. Baxendale, S. V. Ley and M. Martinelli, Tetrahedron **61** (2005), pp.5323-5349.
[4] I. R. Baxendale and S.V. Ley. Current Org. Chem. **9** (2006), pp.1521-1534.
[5] C. Wiles, P. Watts and S. J. Haswell, Tetahedron **60** (2004), pp.8421-8427.
[6] J. L. Moore, S. M. Taylor, and V. A. Soloshonok, ARKIVOC **6** (2005), pp.287-292
[7] M. Pattarawarapan and S. Singhatana, Chiang Mai J. Sci. **33** (2006), pp.203-209
[8] I.Taylor, A. Howard and G. Anal. Chim. Acta. **271** (1993), pp.77-82.
[9] B. C. Hamper, S. A., Kolodziej, A. M. Scates, R. G. Smith and E. Cortez, Org. Chem. **63** (1998), pp. 708-718.

Partial Synthesis of Lupeol and *β*-Sitosterol Esters

P. Phringphrao and S. Luangkamin[*]

Department of Chemistry and Centre for Innovation in Chemistry (PERCH-CIC), Faculty of Science, Chiang Mai University, Chiang Mai 50200, Thailand

*Corresponding Author E-mail Address: *suwaporn@chiangmai.ac.th*

Abstract: Lupeol (1) and *β*-sitosterol (2) were isolated from the hexane and ethyl acetate extracts of the rhizomes of *Agapetes megacarpa*. Lupeol cinnamate (3) and three new esters, lupeol benzoate (4), *β*-sitosterol cinnamate (5) and *β*-sitosterol benzoate (6) were successfully synthesized in good yield by esterification of lupeol or *β*-sitosterol with cinnamic acid or benzoic acid using dicyclohexylcarbodiimide (DCC) and 4-dimethylaminopyridine (DMAP) as a coupling reagent. The synthetic compounds were characterized by spectroscopic data.

Introduction

Agapetes megacarpa W.W. Smith, in Thailand commonly known as Prathat doi, belong to the family ERICACEAE. It is a shrub or epiphytic shrub, widely distributed in the north of Thailand, especially, Doi Tung (Chiang Rai), Doi Phukha (Nan), Doi Angkang (Chiang Mai) and Doi Inthanon (Chiang Mai). The rhizomes of *A. megacarpa* have been used in traditional Thai medicine for roborant. Prevously, our group have been reported the chemical constituents of *A. megacarpa* which are rich sources of lupeol and *β*-sitosterol [1]. Both compounds have been reported various biological activities. Lupeol has been reported to have anti-inflammatory activity against TPA induced inflammation in mice, human Topoisomerase II inhibitory, cytotoxicities against human non-small-cell bronchopulmonary carcinoma cell line and human HT1080 fibrosarcoma cell and protective against cyclophosphamide induced cardiac mithocondria toxicity [2-6]. *β*-Sitosterol is known as phytosterol. It has been reported to exhibit cytotoxicities against bowes, Hela cervical, MCF-7 breast, CasKi cervical and A549 lung cancer cell lines with their IC_{50} of 36.5, 46.22, 42.10, 72.0 and 78.0 *μ*M, respectively [7-9]. Moreover, it has been reported to have antihypercholesterolemic, anti-inflammatory antibacterial, antifungal properties [10]. Furthermore, some triterpenoid esters have been reported their biological activity. Lupeol cinnamate has been reported to have insecticidal activity against *Cylas formicaruis* [11]. *Cis*-3-*O*-*p*-Hydroxy cinnamoyl ursolic acid has been reported to exhibit tumor cell growth inhibition in MCF-7 breast, ME 180 cervical and PC 3 prostate cell lines [12]. 3-(Z)-Caffeoyl lupeol has been reported to exhibit antimalarial activity with an ED_{50} value of 8.6 mg/ml [13].

As a result of the bioactive lupeol, *β*-sitosterol and triterpenoid esters, the synthesis of new triterpenoid esters are interesting for further biological investigation. This paper reported the synthesis of lupeol esters and *β*-sitosterol esters by esterification of lupeol and *β*-sitosterol. The lupeol and *β*-sitosterol starting were isolated from the rhizomes of *Agapetes megacarpa*.

Materials and Methods

General experimental procedures: The melting points were determined on an Electrothermal melting point apparatus using capillary tubes and were uncorrected. The temperature is given in degree Celsius. ^{1}H-NMR (400 MHz), ^{13}C-NMR (100 MHz) spectra were recorded in $CDCl_3$ on Bruker DRX 400 spectrometer. The chemical shifts are given in δ (ppm) and coupling constants in Hz. The electron impact mass spectra were measured with Agilent-HP 5973 mass spectrometer. The IR spectra were obtained on a Nicolet Magna 510 Fourier transform IR spectrometer using KBr disks. Precoated TLC silica gel 60 F_{254} aluminum sheets and glass plates from Merck were used for thin – layer chromatography (0.21 and 0.25 mm layer thickness for analytical and preparative TLC).

Plant material: *Agapetes megacarpa* was collected from Doi phahompok, Chiang Mai province in May 2007. A voucher specimen (QBG-21548) has been deposited at the Herbarium Queen Sirikit, Botanic Garden, Chiang Mai, Thailand.

Isolation of Lupeol and β-sitosterol: The air-dried powdered rhizomes of *A. megacarpa* (772.72 g) were extracted with methanol using Soxhlet extraction. After evaporation of methanol, the extract was suspended in water and partitioned with *n*-hexane, ethyl acetate and *n*-butanol, respectively. Removal of solvents from each fractions yielded *n*-hexane (26.76 g, 3.5%), ethyl acetate (18.46 g, 2.4%) and *n*-butanol extracts (17.20 g, 2.2 %).

The hexane and ethyl acetate extracts were subjected to a silica gel column chromatography, eluted with gradient condition start from 100% *n*-hexane, a mixture of *n*-hexane - EtOAc, a mixture of EtOAc – MeOH and 100% MeOH. Selected fractions were further purified by column chromatography and/or preparative TLC to give lupeol (**1**) 376.8 mg and *β*-sitosterol (**2**) 164.0 mg (Fig. 1), the starting material for synthesis of their esters. The physical and spectroscopic data of lupeol and *β*-sitosterol are shown below.
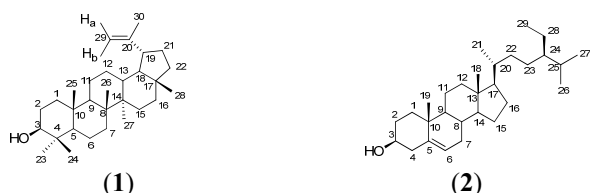
Fig. 1 The structures of lupeol (**1**) and *β*-sitosterol (**2**)

Lupeol (**1**) was obtained as white powder, mp. 210.3 – 212.5 °C (lit. [14], 212 – 214 °C); IR (KBr, cm⁻¹): 3450, 2910-2820, 1500, 1050; EIMS *m/z* (rel. int.) 426 (M⁺, 411 (9), 207 (100), 189 (27); ¹H-NMR (CDCl₃, 400 MHz) *δ*: 0.68 (1H, *m*, H-5), 0.75 (3H, *s*, H-24), 0.79 (3H, *s*, H-28), 0.83 (3H, *s*, H-25), 0.93 (3H, *s*, H-27), 0.97 (3H, *s*, H-23), 1.02 (3H, *s*, H-26), 1.68 (3H, *s*, H-30), 0.8-1.70 (22H, *m*, CH, CH₂), 1.90 (2H, *m*, H-21), 2.37 (1H, *dt*, *J* = 11.1, 5.9 Hz, H-19), 3.19 (1H, *dd*, *J* = 11.1, 5.0 Hz, H-3), 4.57 (1H, *dd*, *J* = 2.3, 1.3 Hz, H$_b$-29), 4.68 (1H, *d*, *J* = 2.3 Hz, H$_a$-29); ¹³C-NMR (CDCl₃, 100 MHz) *δ*: 14.56 (*q*, C-27), 15.38 (*q*, C-24), 15.98 (*q*, C-26), 16.13 (*q*, C-25), 18.01 (*q*, C-28), 18.33 (*t*, C-6), 19.31 (*q*, C-30), 20.94 (*t*, C-11), 25.17 (*t*, C-12), 27.42 (*t*, C-15), 27.45 (*t*, C-2), 28.00 (*q*, C-23), 29.85 (*t*, C-21), 34.29 (*t*, C-7), 35.59 (*t*, C-16), 37.18 (*s*, C-10), 38.06 (*d*, C-13), 38.71 (*t*, C-1), 38.87 (*s*, C-4), 40.01 (*t*, C-22), 40.84 (*s*, C-8), 42.84 (*s*, C-14), 43.01 (*s*, C-17), 48.00 (*d*, C-19), 48.31 (*d*, C-18), 50.45 (*d*, C-9), 55.33 (*d*, C-5), 79.02 (*d*, C-3), 109.33 (*t*, C-29), 150.99 (*s*, C-20).

β-sitosterol (**2**) was obtained as white crystals, mp. 138.6-140.0 °C (lit. [15], 138-139 °C); IR (KBr, cm⁻¹) : 3450, 1050 ; EIMS *m/z* (rel. int.) 414 (M⁺, 100), 396 (81), 381 (47), 329 (61), 303 (63), 213 (67); ¹H-NMR (CDCl₃, 400 MHz) *δ*: 0.67 (3H, *s*, H-18), 0.80 (3H, *d*, *J* = 6.9 Hz, H-27), 0.82 (3H, *d*, *J*= 6.9 Hz, H-26), 0.84 (3H, *t*, *J* = 7.8 Hz, H-29), 0.92 (3H, *d*, *J* = 6.6 Hz, H-21), 1.00 (3H, *s*, H-19), 1.07-1.92 (25H, *m*, CH, CH₂), 1.90-2.05 (2H, *m*, H-7, H-12), 2.18-2.32 (2H, *m*, H-4), 3.52 (1H, *m*, H-3), 5.35 (1H, *d*, *J* = 5.2 Hz, H-6); ¹³C-NMR (CDCl₃, 100 MHz) *δ*: 11.87 (*q*, C-29), 11.99 (*q*, C-18), 18.79 (*q*, C-21), 19.05 (*q*, C-27), 19.41 (*q*, C-19), 19.83 (*q*, C-26), 21.09 (*t*, C-11), 23.07 (*t*, C-28), 24.31 (*t*, C-15), 26.07 (*t*, C-23), 28.26 (*t*, C-16), 29.16 (*d*, C-25), 31.64 (*t*, C-2), 31.90 (*d*, C-8), 31.93 (*t*, C-7), 33.95 (*t*, C-22), 36.15 (*d*, C-20), 36.51 (*s*, C-10), 37.26 (*t*, C-1), 39.78 (*t*, C-12), 42.28 (*t*, C-4), 42.32 (*s*, C-13), 45.83 (*d*, C-24), 50.14 (*d*, C-9), 56.07 (*d*, C-17), 56.77 (*d*, C-14), 70.79 (*d*, C-3), 121.71 (*d*, C-6), 140.76 (*s*, C-5).

General method for the synthesis of Lupeol and β-sitosterol [16]: Lupeol or *β*-sitosterol (20 mg) was added to a stirred solution of cinnamic acid or benzoic acid (8 mg) and 4-(dimethylamino)-pyridine (DMAP) (2 mg) in dry dichloromethane (2 mL). The reaction mixture was stirred at room temperature for 5 minutes and then a solution of dicyclohexylcarbodiimide (DCC) (11 mg) in dry dichloromethane (1 mL) was added to the reaction mixture. After that, it was

continuously stirred for 17 hour at room tempeture. The precipitate of dicyclohexylurea was filtered off and the filtrate washed with saturated ammonium chloride solution (2x5 ml) and water, dried over anhydrous sodium sulfate, filtered and the filtrate concentrated in vacuo. The crude product of lupeol or *β*-sitosterol esters were purified by preparative TLC to afford the ester **3** (6.0 mg), ester **4** (5.1 mg,), ester **5** (7.7 mg) and ester **6** (5.2 mg) (Fig. 2). The percentage yield of ester products **3-6** after recover lupeol or *β*-sitosterol starting were 36.8, 31.0, 50.9 and 29.7, respectively. The physical and spectroscopic data of four esters are shown in below.
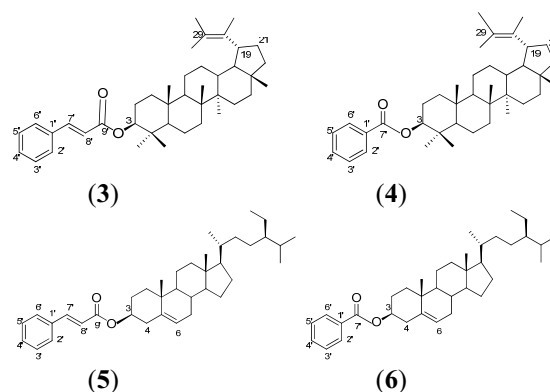

Fig. 2 The structures of lupeol cinnamate (**3**), lupeol benzoate (**4**), *β*-sitosterol cinnamate (**5**) and *β*-sitosterol benzoate (**6**)

Lupeol cinnamate (**3**) was obtained as white powder, mp. 272.8-274 °C; IR (KBr, cm⁻¹) : 1709, 1647, 1590, 1233; ¹H-NMR (CDCl₃, 400 MHz) *δ*: 0.79 (3H, *s*), 0.89 (3H, *s*), 0.90 (3H, *s*) 0.92 (3H, *s*), 0.95 (3H, *s*), 1.04 (3H, *s*), 1.69 (3H, *s*), 0.95-1.80 (23H, *m*), 1.85-2.0 (1H, *m*, H-21A), 2.38 (1H, *dt*, *J* = 11.0, 5.8 Hz, H-19), 4.58 (1H, *d*, *J* = 1.3 Hz, H$_b$-29), 4.62 (1H, *dd*, *J* = 10.5, 5.9 Hz, H-3), 4.71 (1H, *m*, H$_a$-29), 6.45 (1H, *d*, *J* = 16.0 Hz, H-8'), 7.38 (3H, *m*, H-3', 4', 5'), 7.52 (2H, *m*, H-2', 6'), 7.67 (1H, *d*, *J* = 16.0 Hz, H-7'); ¹³C-NMR (CDCl₃, 100 MHz) *δ*: 14.54 (*q*), 16.00 (*q*), 16.21 (*q*) 16.67 (*q*), 18.01 (*q*), 18.24 (*t*), 19.00 (*q*), 20.95 (*t*), 23.90 (*t*), 25.00 (*t*), 27.45 (*t*), 28.02 (*q*), 29.70 (*t*), 34.24 (*t*), 35.50 (*t*), 37.13 (*s*, 2C), 38.07 (*d*), 38.43 (*t*), 40.01 (*s*), 41.00 (*s*), 42.86 (*s*), 43.01 (*s*), 48.02 (*d*), 48.31 (*d*), 50.37 (*d*), 55.44 (*d*), 81.08 (*d*), 109.36 (*t*), 118.90 (*d*), 128.05 (*d*, 2C), 128.85 (*d*, 2C), 130.13 (*d*), 134.80 (*s*), 144.25 (*d*), 151.00 (*s*), 167.00 (*s*).

Lupeol benzoate (**4**) was obtained as white powder, mp. 258.2-260.5 °C; IR (KBr, cm⁻¹) : 1697, 1642, 1545, 1235; ¹H-NMR (CDCl₃, 400 MHz) *δ*: 0.80 (3H, *s*), 0.90 (3H, *s*), 0.92 (3H, *s*), 0.96 (3H, *s*), 1.00 (3H, *s*), 1.05 (3H, *s*), 1.57 (3H, *s*), 0.85-1.80 (23H, *m*), 1.90 (1H, *m*, H-21A), 2.38 (1H, *m*, H-19), 4.58 (1H, *dd*, *J* = 2.3, 1.3 Hz, H$_b$-29), 4.70 (1H, *d*, *J* = 2.3 Hz, H$_a$-29), 4.71 (1H, *dd*, *J* = 11.0, 5.2 Hz, H-3), 7.42 (2H, *dd*, *J* = 7.8, 7.4 Hz, H-3', 5'), 7.54 (1H, *t*, *J* = 7.4 Hz, H-4'), 8.10 (2H, *dd*, *J* = 8.2, 1.1 Hz, H-2', 6');

^{13}C-NMR (CDCl$_3$, 100 MHz) δ: 14.56 (*q*), 16.01 (*q*), 16.20 (*q*) 16.80 (*q*), 18.02 (*q*), 18.25 (*t*), 19.30 (*q*), 20.99 (*t*), 23.78 (*t*), 25.13 (*t*), 27.46 (*t*), 28.13 (*q*), 29.86 (*t*), 34.24 (*t*), 35.59 (*t*), 37.16 (*s*), 38.08 (*d*), 38.22 (*s*), 38.42 (*t*), 40.02 (*t*), 40.90 (*s*), 42.87 (*s*), 43.02 (*s*), 48.03 (*d*), 48.32 (*d*), 50.38 (*d*), 55.47 (*d*), 81.64 (*d*), 109.37 (*t*), 128.31 (*d*, 2C), 129.53 (*d*, 2C), 131.04 (*s*), 132.68 (*d*), 150.97 (*s*), 166.30 (*s*).

β-sitosterol cinnamate (**5**) was obtained as white crystals, mp. 248.3-250 $^\circ$C; IR (KBr, cm^{-1}) : 1710, 1642, 1208; ^{1}H-NMR (CDCl$_3$, 400 MHz) δ: 0.69 (3H, *s*), 0.82 (3H, *d, J* = 6.9 Hz), 0.83 (3H, *d, J* = 6.9 Hz), 0.85 (3H, *t, J* = 7.6 Hz), 0.93 (3H, *d, J* = 6.5 Hz), 1.05 (3H, *s*), 0.95-2.07 (27H, *m*), 2.40 (2H, *d, J* = 7.6 Hz, H-4), 4.75 (1H, *m,* H-3), 5.41 (1H, *d, J* = 4.3 Hz, H-6), 6.42 (1H, *d, J* = 16.0 Hz, H-8'), 7.41 (3H, *m*, H-3', 4', 5'), 7.52 (2H, *m*, H-2', 6'), 7.68 (1H, *d, J* = 16.0 Hz, H-7'); ^{13}C-NMR (CDCl$_3$, 100 MHz) δ: 11.87 (*q*), 11.99 (*q*), 18.79 (*q*), 19.04 (*q*), 19.36 (*q*), 19.82 (*q*), 21.05 (*t*), 23.08 (*t*), 24.31 (*t*), 26.11 (*t*), 27.90 (*t*), 28.26 (*t*), 29.17 (*d*), 31.90 (*d*), 31.94 (*t*), 33.96 (*t*), 36.17 (*d*), 36.65 (*s*), 37.04 (*t*), 38.24 (*t*), 39.75 (*t*), 42.34 (, *s*), 45.86 (*d*), 50.07 (*d*), 56.06 (*d*), 56.71 (*d*), 74.12 (*d*), 118.73 (*d*), 122.73 (*d*), 128.04 (*d*, 2C), 128.87 (*d*, 2C), 130.16 (*d*), 134.56 (*s*), 139.71 (*s*), 144.43 (*d*), 166.43 (*s*).

β-sitosterol benzoate (**6**) was obtained as white crystals, mp. 223.5-224.2 $^\circ$C; IR (KBr, cm^{-1}) : 1697, 1642, 1545, 1235; ^{1}H-NMR (CDCl$_3$, 400 MHz) δ: 0.69 (3H, *s*), 0.82 (3H, *d, J* = 6.9 Hz), 0.83 (3H, *d, J* = 6.9 Hz), 0.85 (3H, *t, J* = 7.6 Hz), 0.93 (3H, *d, J* = 6.5 Hz), 1.07 (3H, *s*), 0.95-2.07 (27H, *m*), 2.46 (2H, *d, J* = 7.6 Hz, H-4), 4.88 (1H, *m,* H-3), 5.41 (1H, *d, J* = 3.8 Hz, H-6), 7.41 (2H, *t, J* = 7.8 Hz, H-3', 5'), 7.55 (1H, *t, J* = 7.4 Hz, H-4'), 8.02 (2H, *dd, J* = 7.9, 1.4 Hz, H-2', 6'); ^{13}C-NMR (CDCl$_3$, 100 MHz) δ: 11.87 (*q*), 11.99 (*q*), 18.79 (*q*), 19.04 (*q*), 19.38 (*q*), 19.82 (*q*), 21.06 (*t*), 23.08 (*t*), 24.31 (*t*), 26.11 (*t*), 27.90 (*t*), 28.26 (*t*), 29.18 (*d*), 31.90 (*d*), 31.95 (*t*), 33.96 (*t*), 36.17 (*d*), 36.67 (*s*), 37.05 (*t*), 38.23 (*t*), 39.75 (*t*), 42.34 (*s*), 45.86 (*d*), 50.07 (*d*), 56.06 (*d*), 56.72 (*d*), 74.60 (*d*), 122.79 (*d*), 128.27 (*d*, 2C), 129.54 (*d*, 2C), 130.87 (*s*), 132.71 (*d*), 139.69 (*s*), 166.03 (*s*).

Results and Discussion

Lupeol (**1**) and β-sitosterol (**2**), the starting for esterification were obtained from the hexane and ethyl acetate extracts of the rhizomes of *Agapetes megacarpa*. Both compounds were identified by spectroscopic data and comparison with the literature [14,15]. Lupeol esters (**3**, **4**) were prepared in 36.8 % and 31.0 %yield by esterification of lupeol with cinnamic acid and benzoic acid, in the presence of dicyclohexylcarbodiimide (DCC) and 4-(dimethylamino)-pyridine (DMAP) (Scheme 1). β-Sitosterol esters (**5**, **6**) were also achieved in 50.9 % and 29.7% yield by esterification of β-sitosterol with both acids (Scheme 2).

Lupeol benzoate (**4**), β-sitosterol cinanmate (**5**) and β-sitosterol benzoate (**6**) are reported for the first time whereas lupeol cinnamate (**3**) has

been reported as bioactive natural product which was isolated from the plants, *Rhizophora mangle, Himatanthus sucuuba* and *H. articulate* [11-12,17-18]. Lupeol and β-sitosterol esters were evaluated for anti-mycobacterium tuberculosis (Anti-TB) against H37Ra strain. The results revealed that all esters were inactive. The cytotoxicity of these compounds will be further study.
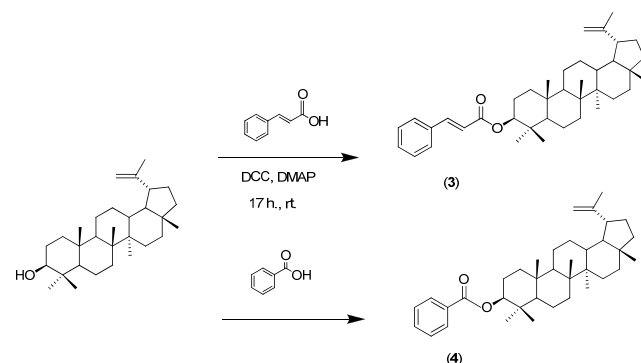
Scheme 1. Synthesis of lupeol cinnamate (**3**) and lupeol benzoate (**4**)
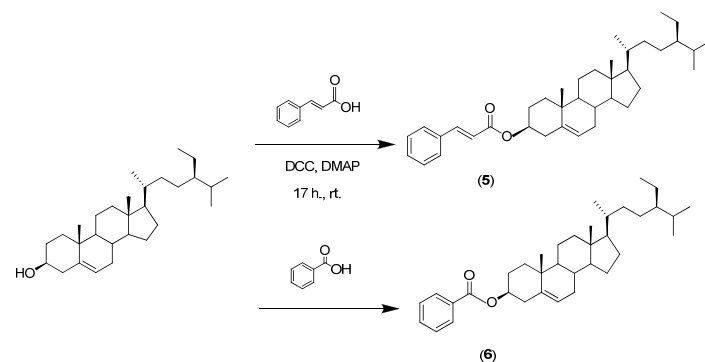
Scheme 2. Synthesis of β-sitosterol cinanmate (**5**) and β-sitosterol benzoate (**6**)

Conclusions

Lupeol cinnamate (**3**) and three new esters, lupeol benzoate (**4**), β-sitosterol cinanmate (**5**) and β-sitosterol benzoate (**6**) were successfully synthesized by esterification of lupeol or β-sitosterol with cinanmic acid or benzoic acid using dicyclohexylcarbodiimide and DMAP as a coupling reagent.

Acknowledgements

Conservation Department for to collection the plant material.

References

[1] Luangkamin, S.; Wongpornchai, S.; Phringphrao, P.; Thongthae, W.; Alongkornsopit, J.; Wongkham, W. *Abstract The 34th Congress Science and Technology of Thailand,* **2008**, Queen Sirikit National Convention Center, Bangkok.

[2] Akihisa, T.; Yasukawa, K.; Oninuma, H.; Kasahara, Y.; Yamanouchi, S.; Takido, M.; Kumaki, K.; Tamura, T. *Phytochemistry.* **1996**, 43(6): 1255-1260.

[3] Wada, S.; Iida, A.; Tanaka, R. *J. Nat. Prod.* **2001**, 64: 1545-1547.

[4] Mutai, C.; Abatis, D.; vagias, C.; Moreau, D.; Roussakis, C.; Roussis, V. *Phytochemistry.* **2004**, 65: 1159-1164.

[5] Nakanishi, T.; Inatomi, Y.; Murata, H.; Shigeta, K.; Iida, A.; Murata, J.; Farrera, M.A.P.; Iinuma, M.; Tanaka, T.; Tajima, S.; Oku, N. *Chem. Pharm. Bull.* **2005**, 53(2): 229-231.

[6] Sudharsan, P.T.; Mythili, M.Y.; Selvakumar, E.; Varalakshmi, P. *J. Cardiovasc. Pharmacol*. **2006**, 47(2): 205-210.

[7] Nguyen, A. T.; Malonne, H.; Duez, P.; Vanhaelen-Fastre, R.; Vanhaelen, M.; Fontaine, *J. Fitoterapia.* **2004**, 75: 500-504.

[8] Ding, Y.; Nguyen, H. T.; Kim, S. I.; Kim, H. W.; Kim, Y. H. *Bioorg. Med. Chem. Lett*. **2009**, 19: 3607-3610.

[9] Malek, S. N. A.; Shin, S. K.; Wahab, N. A.; Yaacob, H. *Molecules.* **2009**, 14: 1713-1724.

[10] Chai, J. W.; kuppusamy, U.R.; Kanthimathi, M.S. *Malay. J. Biochem. Mole. Biol*. **2008**, 16(2): 28-30.

[11] Williams, L. A.D. *Naturwissenschaften.* **1999**, 86: 450-452.

[12] Wood, C.A.; Lee, K.; Vaisberg, A. J.; Kingston, D. G. I; Neto, C.C.; Hammond, G. B. *Chem. Pharm. Bull.* **2001**, 49(11): 1477-1478.

[13] Murphy, B. T.; Mackinnon, S. L.; Yan, X.; Hammond, G. B.; Vaisberg, A. J.; Neto, C.C. *J. Agric. Food. Chem.* **2003**, 51: 3541-3545.

[14] Imam, S.; Azhar, I.; Hasan, M. M.; Ali, M. S.; Ahmed, S.W. *Pak. J. Pharm. Sci*. **2007**, 20(2): 125-127.

[15] Kolak, U.; Topcu, G.; Birteksoz, S.; Otuk, G.; Ulubelen, A. *Turk. J. Chem.* **2005**, 29: 177-186.

[16] Kongkathip, N.; Luangkamin, S.; Kongkathip, B.; Sangma, C.; Grigg, R.; Kongsearee, P.; Prabpai, S.; Pradidphol, N.; Piyaviriyagul, S.; Siripong, P. *J. Med. Chem.* **2004**, 47(18): 4427-4438.

[17] Barreto, A.S.; Carvalho, M. G.; Nery, I. A.; Gonzaga, L.; Kaplan, M. A. G. *J. Braz. Chem. Soc.* **1998**, 9(5): 430-434.

[18] Silva, J.R.A.; Pinto, C.M.R.C.; Pinheiro, M.L.B.; Timborini, M.C.C.E.; Young, C.M.; Bolzani, V.S. *Quim. Nova*. **1998**, 21(6): 702-704.

Characterization of chemically modified chitosan with phthalic anhydride prepared by spray drying and solvent precipitation techniques

S. Khawthong[1,2] , P. Sriamornsak[1,2], S. Limmatvapirat[1,2], M. Luangtana-anan[1,2], S. Niratisai[3], J. Nunthanid[1,2] and P. Laopoonpat[*3]

[1]Department of Pharmaceutical Technology and [2]Pharmaceutical Biopolymer Group (PBiG), Faculty of Pharmacy, Silpakorn University, Nakhon pathom, 7300, Thailand
[3]Department of Pharmaceutical Chemistry, Faculty of Pharmacy, Silpakorn University, Nakhon pathom, 7300, Thailand

*E-mail: panjapol@su.ac.th

Abstract: The aim of this study was to develop chitosan derivatives via ring-opening reactions of phthalic anhydride with amino groups of chitosan by two different methods of preparation, spray drying and solvent precipitation techniques. The chemical structure of the modified chitosan was characterized by FTIR spectroscopy. Moreover, their physical properties were analyzed by powder X-ray diffractometry (PXRD). The solubility of the derivatives in various pH media was also determined by measurement of the %transmission of the solution using UV spectrophotometry. The result of the FTIR spectrum of the spray dried derivative (SDCS-Der) demonstrated the new peaks attributed to an asymmetric and a symmetric carboxylate anion stretching (-COO⁻) of the phthalate functional groups and the carbonyl stretching of carboxylic groups indicating the structure of chitosan monophthalate. The FTIR spectrum of the precipitated derivative (PCS-Der) demonstrated the peaks assigned to the C=O stretching of the phthaloyl groups and an asymmetric and a symmetric carboxylate anion stretching (-COO⁻) indicating the structure of chitosan sodiumbiphthalate via ring-opening reactions of phthalic anhydride with the amino groups of chitosan. PXRD analysis showed that both derivatives were amorphous solids. The solubility of SDCS-Der was improved in wider acidic to neutral pH regions (pH<6) while PCS-Der was soluble only at pH above 5.

Introduction

Chitosan (CS) is a cationic natural biopolymer composed of $\beta(1 - 4)$-D-glucosamine units generally prepared from chitin by chemical or enzyme reaction. It has a number of properties, such as biocompatibility, biodegradability and non toxicity, which are suitable for many usages in biomedical and pharmaceutical formulations [1]. However, its applications are restricted since CS is soluble only in some dilute acidic media (pH<5) due to the presence of free amino groups along the polymer chain. To expand the application of CS, attempts have been made to develop many different CS salts and derivatives via substitution reactions at the free amino groups of CS such as alkylation, acylation, sulfation, thiolation, quaternarization, etc., [2-5]. Among those reactions, substitutions of CS via ring-opening reactions with various cyclic acid anhydrides are the most attractive technique used to improve CS solubility and widen its applications [6-9].

The aim of this study was to develop CS derivatives by modification of the chemical structure of the polymer via ring-opening reactions of phthalic anhydride with amino groups of CS. Two different preparation techniques, spray drying and solvent precipitation were used for comparison reason. The chemical structure of the modified CS was characterized by FTIR spectrophotometry. Moreover, their physical properties were analyzed using powder X-ray diffractometry (PXRD). The solubility of the derivatives in various pH media was also determined by measurement of the %transmission of the solution using UV spectrophotometry.

Materials and Methods

CS, average molecular weight of 20 kDa with 87% degree of deacetylation was purchased from Seafresh Chitosan Co., Ltd. (Lab.), Thailand. Phthalic anhydride (PA, lot no. S5335992917) was purchased from MERCK, Germany. All other chemicals were of reagent grade.

Spray drying

CS flakes was dissolved in 1% v/v aqueous acetic acid to make a 5% w/v CS solution. The CS solution was mixed together with 5% w/v phthalic anhydride (PA) in acetone (CS:PA ; 1:1 mole ratio) under stirring at 40 °C for 4 h and left overnight at room temperature. The mixture was sprayed at an inlet temperature of 130±2 °C using a spray dryer (LabPlant SD-06 Laboratory Scale Spray Dryer, UK). The obtained powders were collected for further investigation.

Solvent precipitation

CS powder, 10% w/v, was dissolved in 2.5% v/v aqueous acetic acid. The CS solution was mixed with 5% w/v phthalic anhydride (PA) in acetone (CS:PA ; 1:1 mole ratio) under stirring at 40 °C for 4 h and left overnight at room temperature. The mixture was adjusted to pH 6.0 with 0.5 N sodium hydroxide solution and dispersed in acetone followed by filtration and then washed the precipitate with excess acetone. Finally, the precipitate was dried in vacuum oven at 40 °C for 24 h.

Physicochemical characterization

CS and the derivatives were characterized by FTIR spectroscopy (model Magna-IR system 750, Nicolet

Biomedical, Madison, WI, USA) and powder X-ray diffractometry (Miniflex II, Rigaku, Japan). The solubility of CS and the derivatives in various pH media were evaluated from the turbidity of the sample. The % transmittance of the solution was measured at wavelength of 600 nm using a UV spectrophotometer (Lambda 2, Perkin Elmer, USA) [10].

Results and Discussions
FTIR spectroscopy

The FTIR spectra of CS and the derivatives are illustrated in Figure 1. The characteristic peaks at 1650 and 1600 cm^{-1} in the spectrum of CS were assigned to the C=O stretching (amide I) and the –NH$_2$ bending (amine), respectively [1]. The absorption bands at 1155 cm^{-1} (asymmetric stretching of the C–O–C bridge), 1082 and 1033 cm^{-1} (skeletal vibration involving the C–O stretching) are characteristics of its saccharine structure [11]. In the spectra of the derivatives, the absorption bands of stretching vibration of –OH and -NH at 3500-3400 cm^{-1} became narrower and shifted to lower wave number after introducing substitution groups [9]. The spectrum of the spray dried derivative (SDCS-Der) showed the new peaks at 1560 and 1385 cm^{-1} attributed to an asymmetric and a symmetric carboxylate anion stretching (-COO$^-$), respectively while the absorption bands at 1600 cm^{-1} (–NH$_2$ bending) and 1650 cm^{-1} (amide I) disappeared. The weak asymmetric NH$_3^+$ bending at 1660-1590 cm^{-1} region and the fairly strong symmetrical NH$_3^+$ bending near 1550-1485 cm^{-1} were hardly observed because they were overlapping with the asymmetric and symmetric carboxylate anion stretching [12]. In addition, the peak at 1714 cm^{-1} assigned to the carbonyl stretching of carboxylic groups was also observed indicating the structure of chitosan monophthalate (Figure 2a.). Since there were excess water content and no adding of NaOH to neutralize phthalic acid from the hydrolysis of phthalic anhydride in the spray drying process, the interaction between the acid and the protonated CS resulted in the formation of the phthalate salt.

In the spectrum of the precipitated derivative (PCS-Der), the peak of the carbonyl stretching (amide I) of CS was shifted to 1645 cm^{-1} indicating the amide I of the phthaloyl group and the peak of -NH$_2$ bending at 1600 cm^{-1} disappeared. In addition, the strong peak at 1560 cm^{-1} and 1383 cm^{-1} regions attributed to an asymmetric and a symmetric carboxylate anion stretching (-COO$^-$), respectively were observed indicating the structure of biphthalate salt (Figure 2b.). It was in accordance with the very less water content in the precipitation technique that could prevent the hydrolysis of PA to phthalic acid and the adding of NaOH also restricted the residual acid. Thus, the substitution of CS via ring-opening reaction with PA to form N-phthaloyl chitosan was occurred. Furthermore, NaOH also interacted with the carboxylic groups at another end of the phthaloyl groups and chitosan sodiumbiphthalate was formed.
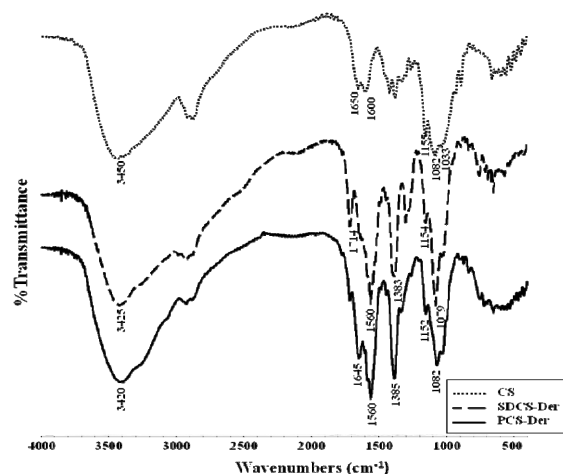

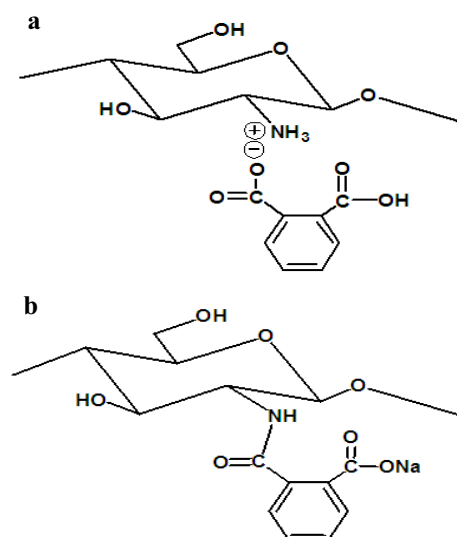Figure 1. FTIR spectra of CS, SDCS-Der and PCS-Der.

Figure 2. Estimated chemical structure of (a) SDCS-Der and (b) PCS-Der.

Powder X-ray Diffractometry

Powder X-ray diffraction (PXRD) patterns of CS, SDCS-Der, PCS-Der and physical mixture (PM) of CS and PA at 1:1 mole ratio are demonstrated in Figure 3. The semi-crystalline peaks at around 11° and 20° (2θ) were observed in the PXRD pattern of CS. It was reported that the peak at 11° (2θ) was assigned to the crystal forms I and the strongest peak appears at 20° (2θ) corresponded to the crystal forms II [11, 13]. A lot of strong intermolecular and intramolecular hydrogen bonds (H-bonds) made CS easily formed crystalline regions and resulted in being water insoluble [9]. The PXRD pattern of PM also showed the semi-crystalline peaks of CS and the crystalline peaks of PA (Figure 3d). After modification by both techniques, the halo diffraction patterns of SDCS-Der and PCS-Der were observed. It was suggested that the subsitution at the amino groups of CS made both derivatives became amorphous solids.
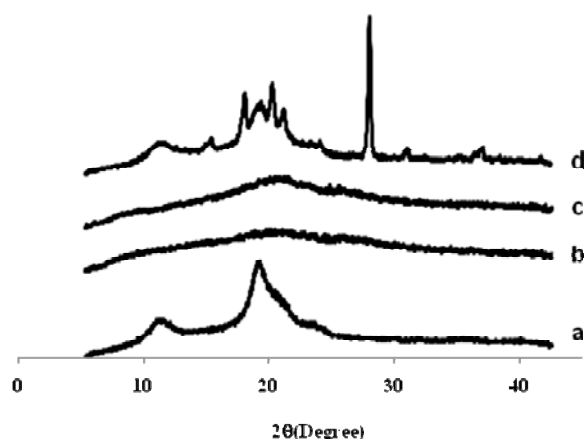
PACCON2011 (Pure and Applied Chemistry International Conference 2011)

Figure 3. Powder X-ray diffraction patterns of a. CS b. SDCS-Der c. PCS-Der and d. physical mixture of CS:PA at 1:1 mole ratio).

Solubility study

The %transmittance of CS, SDCS-Der and PCS-Der in various pH media are shown in Figure 4. CS which is the starting material in this study was soluble in the acidic region at pH below 5 according to the %transmittance higher than 80% but it was insoluble in neutral and alkaline solutions above pH 5. This was expected due to the presence of amino groups along the polymer chain which were protonated at low pH resulted in increasing the solubility [14]. SDCS-Der, chitosan monophthalate, expressed the better solubility than that of CS in wider acidic to neutral regions at pH below 6 because the %transmittance was nearly 90% and higher. In addition, it was still insoluble and precipitated at alkaline pH.

The modification of PCS-Der decreased its solubility in acidic regions at pH below 5 since the %transmittance was lower than 80%. It was according to the transformation of the amino groups of CS to amide forms. At pH 5 and higher, the solubility was improved as the %transmittance was around and higher than 80%. The improved solubility was caused by the deprotonation of carboxylate anions since the precipitated derivative was sodiumbiphthalate salt.
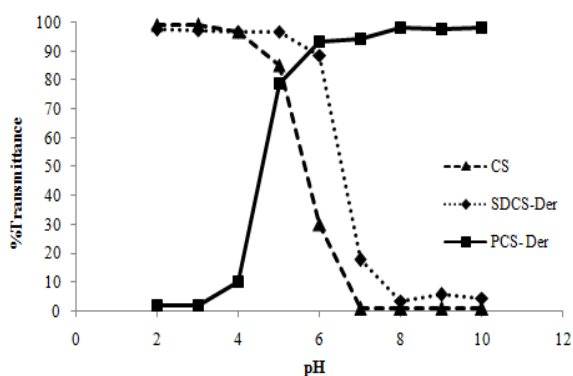
Figure 4. The %transmittance of CS, SDCS-Der and PCS-Der in various pH media.

Conclusions

In this study, CS derivatives were successfully modified by chemical reaction between CS and phthalic anhydride. In the spray drying technique, chitosan monophthalate was formed by the interaction between phthalic acid from the hydrolysis of phthalic anhydride and the amino groups of CS. Chitosan sodium biphthalate was also developed by solvent precipitation techniques via ring-opening reactions of phthalic anhydride with the amino groups of chitosan. Both derivatives were amorphous solids. The solubility of the phthalate salt was improved in wider acidic to neutral pH regions while the biphthalate salt was soluble at only pH above 5. The improved solubility provides the derivatives to be suitable for the application in many pharmaceutical fields, especially in enteric coating process and enhancement of the solubility of chitosan polymers.

References

[1] J. Nunthanid, M. Laungtana-anan, P. Sriamornsak, S. Limmatvapirat, S. Puttipipatkhachorn, L.Y. Lim and E. Khor, *Journal of Controlled Release*. **99** (2004), pp.15-26.
[2] B. Xiao, Y. Wan, M. Zhao Y. Liu and S. Zhang, *Carbohydrate Polymers* **83** (2011), pp. 144–150.
[3] K.V. H. Prashanth and R.N. Tharanathan, *Trends in Food Science & Technolog*. **18** (2007), pp. 117-131.
[4] V.K. Mourya and N.N. Inamdar, *Reactive & Functional Polymers*. **68** (2008), pp. 1013–1051.
[5] G. Ma, D. Yang, Y. Zhou, M. Xiao, J. F. Kennedy and J. Nie, *Carbohydrate Polymers* **74** (2008) pp. 121-126.
[6] Greg T. Hermanson. *Bioconjugate Techniques*. Academic Press, San Diego, 1996, pp. 91-95
[7] H. Sashiwa and S. Aiba. *Progress in Polymer Science* **29** (2004), pp. 887–908.
[8] Y. Shigemasa, H. Usui, M. Morimoto, H. Saimoto, S. Okamoto and H. Sashiwa, *Carbohydrate Polymers*. **39** (1999), pp. 237–243.
[9] J. Q. Zhou, and J. W. Wang, *Enzyme and Microbial Technology*. **45** (2009), pp. 299–304.
[10] C. Qin, H. Li, Q. Xiao, Y. Liu, J. Zhu and Y. Du, *Carbohydrate Polymers*. **63** (2006), pp. 367-374.
[11] C. Zhang, Q. Ping, H. Zhang and J. Shen**,** *European Polymer Journal*, **39** (2003) pp. 1629–1634
[12] R. M. Silverstein, G. Clayton Bassler and T. C. Morrill, *Spectrometric identification of organic compounds*, New York, 5th Ed., John Wiley & Sons, Inc., Publication, 1991, pp. 91-142.
[13] Y. Q. Zhang, C. H. Xue, Y. Xue, R. C. Gao, and X. L. Zhang, *Carbohydrate Research*. **340** (2005), pp. 1914–1917.
[14] K. Mello, L. Bernusso, R. Moraes Pitombo and B. Polakiewicz, *Brazilian Archives of Biology and Technology* **49** (2006) pp. 665-668.

Copper Catalyzed Aromatization of Conjugated and Skipped Dienes

N. Ngamsomprasert[*] and W. Chavasiri

Department of Chemistry, Faculty of Science, Chulalongkorn University, Bangkok 10330, Thailand

[*] Email niti_ngam@hotmail.com

Abstract: Aromatization is one of important reactions in organic synthesis. This research aims to develop a mild and efficient catalytic system for aromatization of conjugated and skipped dienes. A system consisting of copper salts as a catalyst coupled with *tert*-butylhydroperoxide (TBHP) as an oxidant was selected. Various parameters including type of ligands, solvent, temperature, reaction time and type of dienes display significant effects on the efficiency of the reaction. Skipped dienes such as γ-terpinene and 9,10-dihydroanthracene could be aromatized in high yields at room temperature in 15 minutes. On the other hand, conjugated dienes such as α-terpinene and 9,10-dihydrophenanthrene needed more severe conditions or longer reaction time to produce high yield of their corresponding aromatized products.

Introduction

Dehydrogenation is an important reaction to remove hydrogen molecule from the substrate. Aromatization is one of dehydrogenations. Various catalysts have previously been reported including sulphur, selenium [1], platinum metal [2] and quinone compounds such as chloranil [3] and 2,3-dichloro-5,6-dicyanobenzoquinone (DQQ) [4]. However, some reagents required long reaction time, high temperature, yet yielded little amount of product. In addition, a stoichiometric amount of quinones must be used in certain reports. Therefore, alternative procedures should be sought.

The interesting catalytic system is consisted of peroxide as an oxidant coupled with a metal catalyst such as Fe [5], Co [6], Cu [7] and Ti [8]. Many previous researches addressed the use of various metal complexes giving high yields, but still needed long reaction time and most of them were expensive. Copper salts and complexes [9], on the other hand, were also employed in many researches. We report herein the finding of a suitable catalytic system utilizing copper catalysts in aromatization of conjugated and skipped dienes.

Materials and Methods

Chemicals: The substrates and reagents for synthesizing the precursors and products employed in this work were purchased from Fluka, Aldrich and TCI chemical companies and were used without further purification.

Instruments: The ^{1}H and ^{13}C-NMR spectra were obtained on the Varian nuclear magnetic resonance spectrometer, model Mercury plus 400 NMR spectrometer which operated at 399.84 MHz for ^{1}H and 100.54 MHz for ^{13}C nuclei. Gas chromatograph was performed on Varian CP-3800 instrument using CP-sil8 column, FID as a detector and N_2 as carrier gas.

Conditions optimization for aromatization of γ-terpinene: In a pear-shaped flask consisting of a solution of copper salt 1 mL (Table 1) was added γ-terpinene (1 mmol) and TBHP. The mixture was stirred at room temperature (Figure 1). After the reaction was completed, water (0.5 mL) and brine (0.2 mL) were added. The upper layer was removed and analyzed by GC with the addition of cyclohexanone (0.25M in EtOAc) as an internal standard.
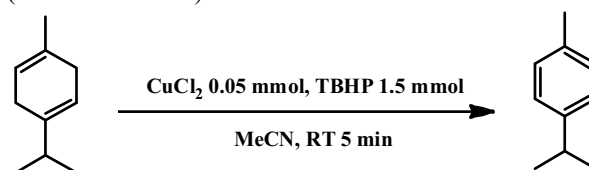

Figure 1: Aromatization of γ-terpinene

Table 1: Solvent and catalyst screening

Entry	Solvent	Cu-salt[a]	Conversion	%Yield
1	EtOAc	$CuCl_2$	92	90
2	MeOH	$CuCl_2$	83	82
3	CH_2Cl_2	$CuCl_2$	40	37
4	*n*-Hexane	$CuCl_2$	20	17
5	MeCN	$CuCl_2$	>99	99
6	MeCN	CuCl	98	95
7	MeCN	$CuSO_4$	91	86
8	MeCN	CuCN	82	63
9	MeCN	$Cu(OAc)_2$	93	90
10	MeCN	$CuCl_2$[b]	>99	99

[a] Cu-salt 0.05 mmol
[b] $CuCl_2$ 0.01 mmol

General procedure for aromatization of dienes using copper catalysts: The procedure was under the same conditions as those for the optimization studies,

but used copper salts in 0.02 mmol, TBHP 1.5 mmol. Skipped dienes were stirred at room temperature for 5-15 minutes. Conjugated dienes such as α-terpinene were stirred at 60°C for 15-60 minutes (Table 2). This procedure was applied to various dienes shown in Table 3.
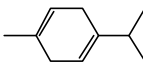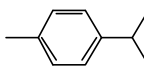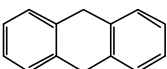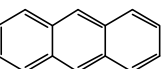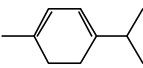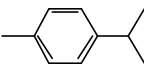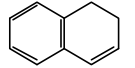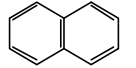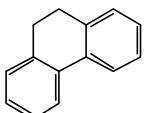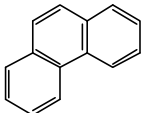
Table 2: Aromatization of α-terpinene[a]

Entry	Temp	Time (min)	Conversion[b]	%Yield[b]
1	RT	15	60	24
2	RT	30	68	26
3	RT	60	64	26
4	60°C	15	97	93
5	60°C	30	99	95
6	60°C	60	99	96

[a] α-terpinene 1 mmol
[b] determined by GC

Table 3: Aromatization of dienes

Entry	Substrate	Product	%Yield[a]
1			Quant.
2			Quant. (95)[b]
3			93
4			60
5			65

[a] determined by GC
[b] isolated yield

Results and Discussion

Finding an optimal condition for Cu-salt and TBHP catalytic system, γ-terpinene was used as a substrate following the reaction in figure 1. A preliminary screening of solvent and Cu-salt as a catalyst for aromatization of γ-terpinene to p-cymene was shown in table 1. The solubility of the catalyst is very important to produce p-cymene. For the screening of solvent, non-polar solvent such as n-hexane (entry 4) did not give high yield of product, presumably due to the low solubility of the catalyst. On the other hand, the total dissolution of the catalyst in polar solvent such as ethyl acetate and acetonitrile resulted in good yields and excellent %conversion. Catalyst screening, in addition, was shown that Cu-salts produced p-cymene in good yields. Moreover, the catalysts bearing chloride ion as ligands were superb especially CuCl$_2$.

Entry 10 in table 1 shows that decreasing the amount of CuCl$_2$ to 0.01 mmol still gave excellent yield and good %conversion.

The investigation on a conjugated dienes using α-terpinene as a chemical model was also conducted (figure 2). Under the same condition, only 20% yield was attained. Therefore, some parameters such as temperature and reaction time were adjusted as shown in table 2, because of a hydrogen atom in skipped dienes was more acidic than conjugated diene.
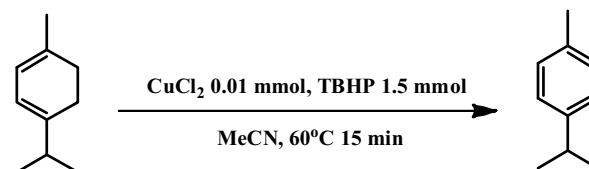

CuCl$_2$ 0.01 mmol, TBHP 1.5 mmol

MeCN, 60°C 15 min

Figure 2: Aromatization of α-terpinene

This catalytic system was also applied to other dienes as shown in table 3. 9,10-Dihydroanthracene, produced the corresponding product in an excellent yield. After the reaction was completed (15 minutes), the product was crystallized (95% yield) with high purity. In the case of 1,2-dihydronaphthalene (entry 4), low yield of naphthalene was obtained perhaps due to its high volatility. Moreover, TLC of this reaction mixture exhibited another substance. This compound was finally separated by silica gel column chromatography and was identified by ^{1}H and ^{13}C NMR. ^{1}H-NMR (CDCl$_3$) δ 7.09-7.17 (m, 4H), δ 6.63-6.65 (d, 1H, J = 9.6 Hz), δ 6.01-6.05 (dd, 1H, J = 9.6, 4.8 Hz), δ 4.74-4.78 (ddd, 1H, J = 6.4, 5.6, 4.8 Hz), δ 3.27-3.33 (dd, 1H, J = 16.8, 5.6 Hz), δ 2.94-3.00 (dd, 1H, J = 16.8, 6.4 Hz) and δ 1.21 (s, 9H)

From the NMR data, the structure of this compound was elucidated as a new peroxide as presented in figure 3. The structure of this new peroxide was further confirmed by COSY technique and HRMS.
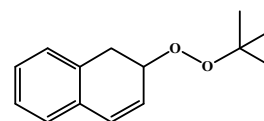

Figure 3: Structure of new peroxide compound

Conclusions

The CuCl$_2$–TBHP is a mild and efficient aromatization catalyst for skipped and conjugated dienes. This system provides an excellent yield of the corresponding product, particularly for the aromatization of skipped dienes. For conjugated diene, this system needed higher temperature and required more reaction time than that for skipped dienes.

References

[1] P.P. Fu, and R.G. Harvey. *Chem. Rev.,* **1978**, *78*, 317-361.

[2] H. Adkins, L.M. Richards, and J.W. Davis. *J. Am. Chem. Soc.*, **1941**, *63*, 1320-1325.

[3] E.J. Agnello, and G.D. Laubach. *J. Am. Chem. Soc.*, **1960**, *82*, 4293-4299.

[4] H.J. Pi, H. Liu, W. Du, and W.P. Deng. *Tetrahedron Lett.,* **2009**, *50*, 4529-4531.

[5] A. Dhakshinamoorthy, M. Alvaro, and H. Garcia. *J. Catal.,* **2009**, *267*, 1-4.

[6] A.G. Oblad, R.F. Marschner, and L. Heard. *J. Am. Chem. Soc.,* **1940**, *62*, 2066-2069.

[7] S. Rayati, S. Zakavi, M. Koliaei, A. Wojtczak, and A. Kozakiewicz. *Inorg. Chem. Commun.*, **2010**, *13*, 203-207.

[8] G. Srinivas, and M. Periasamy. *Tetrahedron Lett.,* **2002**, *43*, 2785-2788.

[9] K. Yamamoto, Y.G. Chen, and F.G. Buono. *Org. Lett.,* **2005**, *21*, 4673-4676.

Synthesis of Benzoquinolizine Alakloids; Application for Synthesis of Natural Emetine

T. Chaiwon[1,4], A. Namsa-aid[2*] and S. Ruchirawat[3]

[1]Chemical Biology Program, Chulabhorn Graduate Institute, Vibhavadee- Rangsit, Bangkok 10210, Thailand
[2] Laboratory of Natural Products, Chulabhorn Research Institute, Vibhavadee- Rangsit, Bangkok 10210, Thailand
[3] Laboratory of Medicinal Chemistry, Chulabhorn Research Institute, Vibhavadee- Rangsit, Bangkok 10210, Thailand
[4]The Center of Excellence on Environmental Health, Toxicology, and Management of Chemicals, Faculty of Science, Mahidol University, Bangkok 10400, Thailand
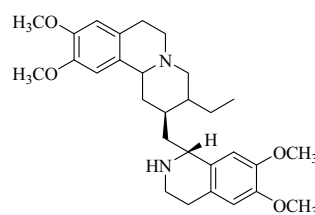
[*]E-mail: anucha@cri.or.th

Abstract: Several alkaloids in plants contain benzoquinolizine as a core structure which exists in natural products. In this study, we designed a new method for the synthesis of the benzoquinolizine. The construction of the benzoquinolizine was performed in four steps *via* ring closing metathesis (RCM) reaction as a key step. Benzoquinolizine can be used as a key intermediate in the synthesis of emetine, which is one of the benzoquinolizine-isoquinoline compounds. Emetine shows a potent inhibitor of protein synthesis including antitumor, antiviral and antiamoebic activities for future development as commercialized natural products.

Figure 1 Emetine alkaloid structure

Introduction

Emetine ($C_{29}H_{40}N_2O$, 1) is one of the benzoquinilizine-isoquinoline dimeric alkaloid. The structure shows pentacyclic compound containing four aromatic methoxy groups.[1,2]

Emetine (1) was isolated from *Cephaelis ipecacuanha* or from *Cephaelis acuminata.* the extraction with benzene-heptane mixture afforded the ipecac powder. After purification by recrystallization, the expected emetine (1) was obtained as a hydrochloride derivative.[3]

Biological Activity of Emetine

The identification of emetine (1) as a more potent agent improved the treatment as amoebiasis. Such as in 1976 study of 27 patients treated with dehydroemetine and various other drugs suggested that all drug combinations were successful at treating amoebic liver abscesses.

In 1993, the treatment of cutaneous amoebiasis in a 7-year old girl was accomplished with dehydroemetine and metronidazole in Mexico.[4]

Table 1: Example of pharmaceutically import alkaloids extracted from plants[5]

Natural Products	Pharmaceutical Activity
Reserpine	Central nervous system
Caffeine	Autonomic nervous system
Physostigmine, Pilocarpine	Cholinergic
Atropine, Hyoscyamine, Scopolamine	Cholinergic blocking
Ephedrine	Adrenergic
Emetine	Antiamoebic
Quinine	Antimalarial

Materials and Methods

Preparation of Compound 5

Homoveratylamine (6) (3.0 g, 0.0166 mol) and ethyl formate (20 mL, 0.2487 mol) were combined in a 100 mL round-bottom flask fitted with a reflux condenser. The mixture was heated to 55-60 ^{o}C for 8 h. After cooling to room temperature, the reflux condenser was removed. The mixture was evaporated under reduced pressure. Chromatography of the crude gave a product as a light yellow oil (3.3 g, 95%).

Preparation of Isoquinoline derivative (3)

A mixture of compound 5 (3.3 g, 0.0158 mol) and phosphorus oxychloride (3 mL, 0.0322 mol) in acetonitrile (20 mL) were stirred of 85-90 ^{o}C under argon for 2 h. The mixture was evaporated under reduced pressure. Crystallization of a crude by ethanol and diethyl ether gave a product as a brown crystal (2.8 g, 0.0148 mol, 94%).

Preparation of Compound 4

A solution of isoquinoline derivative (3) (296 mg, 1.53 mmol) in dry dichloromethane (10 mL) was stirred at -78 ^{o}C for 5 min before allyltributylstannane (0.47 mL, 1.53 mmol) was added. The mixture was stirred at -78 ^{o}C for 10 min. Acryloyl chloride (0.13 mL, 1.60 mmol) was added and the reaction mixture was stirred at -78 ^{o}C under argon for 1 h. The mixture was heated to 0 ^{o}C for 1 h and room temperature for 4 h. Since the mixture has already been stirring at room temperature, the mixture was evaporated under reduced pressure. The crude was purified by PLC by PLC to give the product as a yellow oil (309 mg, 1.08 mmol, 70%).

Preparation of Benzoquinolizine derivative (2)

Compound 4 (1.5 g, 0.0052 mol) and Grubb's catalyst the 1st generation (0.44 g, 0.53 mmol) were combined in a 100 mL round-bottom flask fitted with a reflux condenser. The mixture was replaced under an argon atmosphere and heated to 55-60 ^{o}C for 4 h. After cooling to room temperature, the reflux condenser was removed and the mixture was evaporated under reduced pressure. Column chromatography of the crude gave a product as a gray solid (1.14 g, 0.0044 mol, 85%).

Preparation of Compound 7

1,3-dithiane (55.68 mg, 0.46 mmol) and n-BuLi (0.23 mL, 0.46 mmol) were stirred in THF under an argon atmosphere in a 25 mL round-bottom flask at -78 ^{o}C for 1 h. After warming to room temperature, benzoquinolizine derivative (2) (60mg, 0.23 mmol) was added and stirred for 30 min. Iodoethane (0.04 mL, 0.46 mmol) was added. The reaction was stirred overnight. The reaction was quenched by adding saturated ammonium chloride. The mixture was evaporated under reduced pressure. Extraction and crystallization of the crude gave yellow crystal of product (25 mg, 0.06 mmol, 26%).

Preparation of Compound 8

Compound 7 (50 mg, 0.12 mmol) and n-BuLi (0.12 mL, 0.25 mmol) were stirred in THF under an argon atmosphere in a 25 mL round-bottom flask at -78 ^{o}C for 1 h. After warming to room temperature, isoquinoline derivative (47.04 mg, 0.25 mmol) was added. The reaction was monitored by TLC and no reaction was observed.

Results and Discussion

Emetine (1) was isolated from *Cephaelis ipecacuanha* or *Cephaelis acuminate* and a variety of interesting biological activities.[6] We studied its synthesis to design the reaction pathways for a natural emetine (1) synthesis as a future antiamoebic agent. The strategy we chose to develop is outlined in retro-synthetic format in Scheme 1. Emetine (1) is constructed from the combinaton between benzoquinolizidine (2) and isoquinoline derivative (3). Both of these part are generated by the concise synthesis.
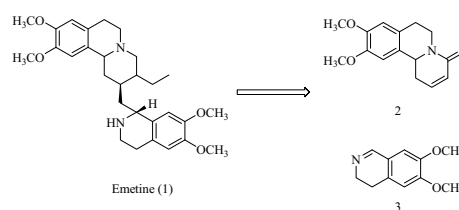

Scheme 1 Retro-synthetic plan of emetine (1)

We envisaged benzoquinolizine derivative (2) arising from ring-closing metathesis of amide compound (4) by using Grubbs' catalyst. The amide (4) could be prepared from the addition of allyl and acryloyl group[7] together into an isoquinoline derivative (3) which could be synthesized form the commercially avialable homoveratrylamine (6). The Bischler-Napieralski reaction would introduce for isoquinoline synthesis by closing of formamide derivative (5) as shown in Scheme 2.
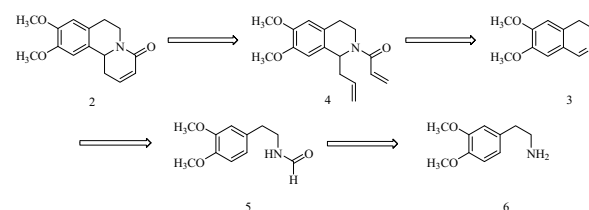
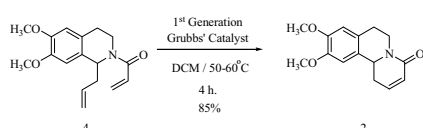Scheme 2 Retro-synthetic plan of benzoquinolizine derivative (2)

A synthetic plan in emetine (1) synthesis can be shown as following;
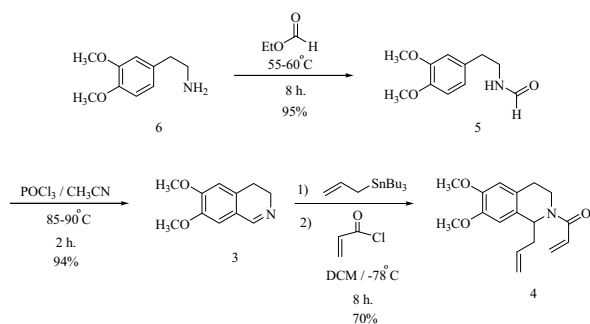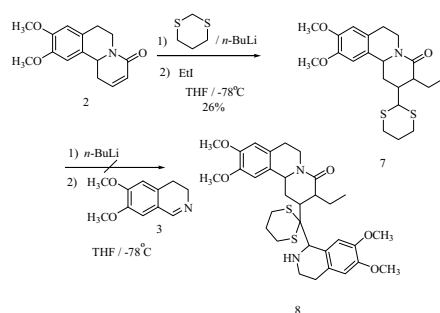

Scheme 3 Synthetic plan of compound 4

Homoveratylamine was treated with ethyl formate under thermal condition to give formamide compound (5) in high yield. Then, Bischler-Napieralski reaction was applied for ring closure of formamide derivative (5) to obtain the desired dimethoxy isoquinoline (3) which was continuously transformed to the amide compound (4) by addition of tributylallylstannane to position 1 of isoquinoline. Then, treatment of acryloyl chloride in the same condition provides the key intermediate amide compound (4) in good yield as shown in Scheme 3.

To synthesize the tricyclic alkaloid (2), benzoquinolizine, the key step ring-closing metathesis was treated the amide compound (4) with the first generation Grubbs' catalyst in the presence of dichloromethane under refluxing condition affording the expected benzoquinolizine (2) as a major product as shown in Scheme 4.


Scheme 4 Synthetic plan of tricyclic alkaloid (2)

In present, we have got dimethoxy isoquinoline (3) and benzoquinolizine compound (2) as the major precursors in hand. For construction of the emetine (1), both of major precursors would be connected together with dithiane molecule functioned as a linker.

Scheme 5 Synthetic plan of compound 8

1,3–Dithiane anion prepared by treatment of n-BuLi in presence of THF at -78 °C was added benzoquinolizine (2) which was performed by Michael addition reaction after that the ethyliodide was added to a solution mixture trapped the carbanion intermediate to give the desired Michael addition product, benzoquinolizine derivative (7).[8] To generate the dithiane carbanion of compound (7) again, the n-BuLi was introduced into the compound (7) in the presence of THF at -78 °C. Then, the dimethoxyisoquinoline was added to the solution mixture. After quenching the mixture, it obtained the starting material compound (7) and lacked the expected product (8) as shown in Scheme 5.
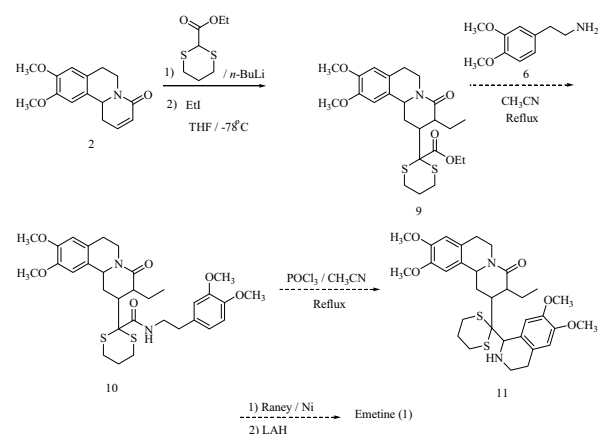
Scheme 6 New synthetic plan of emetine (1)

From the failure of the synthesis of compound (8) as depicted in Scheme 6, we investigated the new synthetic plan by changing the 1,3-dithiane to a ethyl-1,3-dithiane-2-carboxylate, which could be generated the more stable carbanion intermediate reacted to the benzoquinolizine as the Michael addition reaction. The homoveratrylamine (6) would be introduced to afford the intermediate (10). Bischler-Napieralski reaction was performed for ring closure to get the isoquinoline derivative (11). Finally, the reduction of both dithiane and amide group would be taken place to provide the emetine (1).

Conclusions

The experiment has obtained the key intermediate benzoquinolizine as expected. The transformation of the key benzoquinolizine to emetine (1) has not accomplished. The re-experiment to find out a suitable condition for emetine (1) synthesis has also suggested, because the included addition of isoquinoline moiety has complicated.

References

[1] S. Nobuko, N. Kyoko, I. Junko, S. Yojiro, N. Yuka, B. F. Kenneth, C. Gordon, L. Kuo-Hsiung, *Phytochemistry* **67** (2006), pp. 894 – 897.

[2] W. Kenneth and Bentley, *The Isoquiniline Alkaloids*, **vol. 1** (1998), harwood academic publishers.

[3] C. Tringali, *Bioactive Compounds from Natural Sources; Isolation, Characterization and Biological Properties*, CRC Press, (2000).

[4] M. Magana-Garcia, A. Arista-Viveross, **10** (1993) *Pediatric dermatology* pp. 352-355.

[5] Margaret F. Roberts, Michael Wink, Alkaloids: Biochemistry, Ecology and Medicinal Application, Springer, (1998).

[6] Pual, *Medicinal Natural Products A Biosynthetic Approach*, Second Edition, JOHN WILEY & SONS, LTD, (2002).

[7] S. Ruchirawat, A. Namsa-aid, *Tetrahedron Letters* **42** (2001) pp. 1359-1361.

[8] C. Jung-Kai, C. Bo-Rui, C. Yu-Hsio, C. Nein-Chen, *Tetrahedral* **64** (2008) pp. 9685-9688.

Inhibitory Effect of *Phyllanthus emblica* Lin. Fractional Extracts on *in vitro* Oxidation and Protein Glycation

J. Kritsana[1], O. Siriporn[1] and Y. Songwut[1*]

[1] Department of Pharmaceutical Science, Faculty of Pharmacy, Chiang Mai University,
Suthep Road, Chiang Mai, Thailand 50200

[*] E-mail : songwut_y@yahoo.com

Abstract: The inhibitory effect on *in vitro* oxidation and protein glycation of the fractional extracts of *P. emblica* were investigated in this study to screen the suitable fraction with the highest biological activities for further medicinal product development. Fresh fruits of *P. emblica* were dried and macerated with 95% ethanol. The concentrated crude extract was then fractional extracted with different organic solvents; hexane, chloroform, ethyl acetate, and butanol, respectively. The antioxidant potentials of the crude and the organic fractions of *P. emblica* extracts were evaluated using different model systems including ferric reducing antioxidant power and scavenging of 1,1-diphenyl-2-picrylhydrazyl radical. The results indicated that the ethyl acetate fraction of *P. emblica* processed the highest antioxidant activity with EC1 value of 177.91±22.43 mM/mg and IC$_{50}$ value of 12.08±2.62 µg/ml. Its antioxidant activity was higher than that of α-tocopherol (vitamin E). The ethyl acetate fraction exhibited the highest total phenolic contents with GAE value of 51.65±7.69 mg/g dry extract. The high correlations between antioxidant activity and the total phenolic content were obtained. The HPLC chromatograms demonstrated that active compounds from ethyl acetate fraction were gallic acid and ascorbic acid, respectively. The inhibitory effect of *P. emblica* crude and fractional extracts on bovine serum albumin (BSA) glycation was measured in terms of advanced glycation end products (AGEs). The ethyl acetate fraction also showed the greatest inhibitory activity on a glycation reaction. These results demonstrated that the ethyl acetate fraction of *P. emblica* was capable of suppressing protein glycation and was suitable for further pharmaceutical dosage form development in the future.

Introduction

The extract of *Phyllanthus emblica* Linn. shows many pharmacological effects against many diseases such as cancer, diabetes, liver injury, heart disease, ulcer and anemia[1]. It is a medicinal plant that has a long period used in Indian traditional[2] and Thai folk medicines. *P. emblica* fruits enrich with vitamin C and polyphenolic compounds such as gallic acid, emblicanin A, emblicanin B, pedunculagin and punigluconin[3] which have high antioxidant activity. In addition, the effect of *P. emblica* in lowering blood glucose levels in diabetic patients and reducing diabetic complications in rats have been reported.[4; 5]

It is known that a glycation reaction occurred between reducing sugars and amino groups of proteins can form Advanced Glycation End-products (AGEs).[6; 7] These products can not retain the protein function and can cause pathogenesis of diabetic complications and ageing.[8] The previous study showed that there was a relationship between antioxidant activity and anti-diabetic activity of 'Triphala' (equal proportions of three plant extracts include *P. emblica*)[9]. Although crude extract of *P. emblica* demonstrates various pharmacological activities, its unpleasant characteristic makes it difficult to obtain a good formulation. Fractionated extraction of *P. emblica* was carried out in this study in order to improve the appearance, antioxidant and antiglycation activities. The appropriate fraction will be selected for tablet formulation in the future.

Materials and Methods

P. emblica fractional extraction: Fresh fruits of *P. emblica* were dried and ground to powder then extracted with 95% ethanol. The macerated solvent was evaporated to dryness and the yield value of the crude extract obtained was 21.23±1.04%. The crude extract was then dissolved in water and fractional extracted with hexane, chloroform, ethyl acetate and butanol, respectively. The solvent fractions were collected and evaporated. The yield values of the hexane, chloroform, ethyl acetate, butanol fractions and water residue were 5.37±0.33%, 1.24±0.64%, 16.00±1.75%, 26.78±0.85%, and 14.55±1.85%, respectively.

Ferric reducing antioxidant power (FRAP) assay: The reducing ability of the crude and fractional extracts were determined by FRAP assay.[10] The FRAP reagent containing 1 ml of 10 mM tripyridyltriazine (TPTZ) solution in 40 mM HCl plus 1 ml of 20 mM FeCl$_3$ and 10 ml of acetate buffer pH 3.6, was freshly prepared. The crude or the fractional extracts were dissolved in ethanol to a concentration of 150 µg/ml. An aliquot (20 µl) of the extract solution was mixed with 180 µl of the FRAP reagent, and the absorbance of the mixture was measured at 540 nm using Microplate reader (Bio-Rad Model 680, USA). The FeSO$_4$ solutions were used to obtain the calibration curve. The reducing power was expressed as equivalent concentration (EC$_1$); the concentration of

antioxidant having a ferric reducing ability equivalent to that of 1 mM $FeSO_4$.

DPPH radical scavenging activity: The free radical scavenging activity of the crude extract and its fractions was determined by DPPH method.[11] The samples were dissolved in ethanol to prepare various concentration solutions. 20 µl of each sample solution was added with 180 µl of the ethanolic solution containing 100 mM DPPH (1,1-diphenyl 2-picrylhydrazyl) radicals and kept in the dark for 30 min at room temperature. The absorbance was measured at 540 nm using Microplate reader (Bio-Rad Model 680, USA). The IC_{50} value, the effective concentration of sample to obtain 50% antioxidant activity, was determined.

Total phenolic content (TPC): The total phenolic contents of *P. emblica* crude and fractional extracts were determined with Folin-Ciocalteu method.[12] An aliquot of 20 µl of the crude and the fractional extract solutions (400 µg/ml) were mixed with 45 µl of the Folin-Ciocalteu Reagent followed by 135 µl of 2% w/v Na_2CO_3 solution. The absorbance was then measured at 790 nm using Microplate reader (Bio-Rad Model 680, USA) after incubation at room temperature for 2 hr. Gallic acid was used as a standard. Results were expressed in terms of gallic acid equivalent (GAE) mg/g dry extract.

HPLC analysis: The crude and the fractions of *P. emblica* extract were characterized by HPLC (Hewlett packard/hp1100, USA) analysis on a reverse phase C_{18} column (5 µm, 4.0×250 mm, Hypersil ODS, Agilent, USA) using a UV-detector operating at 220 nm. A solvent system was acetonitrile: 0.05% phosphoric acid (isocratic; 10:90) at a flow rate of 0.5 ml/min. All extracts were dissolved in methanol (1 mg/ml) and filtered through a membrane filter (0.45 µm) before injection (10 µl) into the HPLC system. Gallic acid and ascorbic acid were used as standards.

Antiglycation assay: The antiglycation activity of *P. emblica* crude and fractional extracts was investigated following Matsuura and coworkers[13] with some modifications. One milliliter of the reaction mixture containing 1 mg/ml bovine serum albumin (BSA), 200 mM glucose with either aminoguanidine (positive control) or the plant extract as an inhibitor in phosphate buffer saline (PBS) pH 7.4 with sodium azide 0.02% w/v as a preservative was prepared. The negative control was the unreacting solution that used PBS instead of an inhibitor. The mixtures were incubated at 60°C for 30 hr. After cooling, the reaction mixtures were added with 100 µl of 100% w/v trichloroacetic acid (TCA) and then centrifuged at 10000 rpm, 4 °C for 10 min to obtain AGEs precipitates. The obtained precipitates were dissolved with 500 µl alkaline PBS and the fluorescence intensity (ex. 360 nm, em. 465 nm) was monitored by using Multimode reader (Backman Coulter, DTX 880, USA). The percentage inhibitory activity was calculated by the equation $[(A-B)/A] \times 100$, where A is the value derived from the fluorescence intensity of the control and B is that with the inhibitor treatment.[8]

Results and Discussion

Appearance of P. emblica extracts: The crude extract was viscous semi-solid with dark brown in colour. The butanol and water fractions were dark brown solid. The ethyl acetate fraction was light brown semi-solid, whereas the hexane extract was green semi-solid because of chlorophyll.

Antioxidant activity of P. emblica extracts: The antioxidant activity of *P. emblica* crude and fractional extracts was expressed in term of IC_{50} and EC1 values for free radical scavenging activity and reducing ability as shown in Table 1. The fraction of ethyl acetate showed the highest reducing ability (EC1 value of 177.91±22.43 mM/mg). The EC1 values of ethyl acetate fraction and crude extract were significantly higher than other fractions. The ethyl acetate fractional extract also had the highest antioxidant activity with the lowest IC_{50} value of 12.08±2.62 µg/ml. Its value was equivalent to 75.45% and 67.14% of the IC_{50} of the crude extract and α-tocopherol. All other fractions had higher IC_{50} value than that of the crude extract and α-tocopherol.

Table 1: Antioxidant activity of the fractional extracts

Samples	EC1 (mM/mg)	IC_{50} (µg/ml)
Crude extract	121.08±7.68*	16.01±1.83
Hexane	31.58±5.72	265.58±63.98
Chloroform	29.96±0.88	196.88±37.18
Ethyl acetate	177.91±22.43**	12.08±2.62
Butanol	74.30±4.86	23.71±1.76
Water residue	51.83±13.14	61.66±13.20
α-Tocopherol	N.A.	17.99±0.04

*p<0.05 and **p<0.01 (ANOVA and Multiple comparison with LSD)
N.A. = not available

Total phenolic contents of P. emblica extracts: The total phenolic contents of *P. emblica* crude and fractional extracts were determined in this study and the results are shown in Figure 1. The ethyl acetate fraction had the highest total phenolic content with the GAE value of 51.65±7.69 mg/g dry extract. The previous studies showed that the extract of *P. emblica* is composed of phenolic compounds, namely Emblicanin A, Emblicanin B, Punigluconin and Pedunculagin with gallic acid as substituent groups.[14] Thus, it can be indicated that the high antioxidant activity of ethyl acetate fraction resulted from the high total phenolic content.

Correlations between antioxidant activity and total phenolic content: In this study, the correlations between individual antioxidant activity and the total phenolic content of the crude and fractional extracts were evaluated and the results are shown in Table 2. The correlation coefficients (r) of all relationships were greater than 0.9 or less than -0.7, indicating good correlations between these parameters.
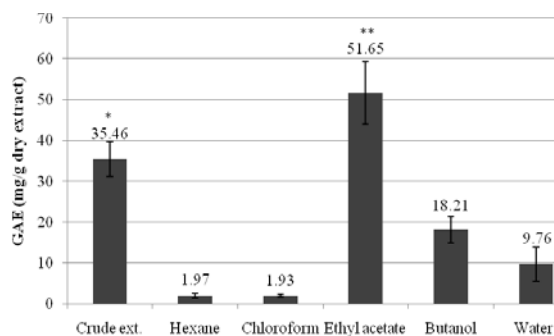
*p<0.05 and **p<0.01
(ANOVA and Multiple comparison with LSD)

Figure 1. GAE value of *P. emblica* fractions

It was previously reported that polyphenols found in dietary and medicinal plants are able to inhibit oxidative stress, [15; 16] and the direct linear relationship between the total phenolic content and total antioxidant activity was observed [17]. From the results, it was highly possible that polyphenolic compounds in *P. emblica* extracts were responsible for the antioxidation activity via two mechanisms i.e., free radical scavenging and reducing ability.

Table 2: The correlation coefficients of antioxidant activity and total phenolic content of crude and fractional extracts

Relationship	Correlation coefficients (r)
IC_{50} and EC1	-0.704**
GAE and IC_{50}	-0.750**
GAE and EC1	0.981**

**p<0.01

HPLC analysis of the fractional Extracts: The HPLC chromatogram of *P. emblica* crude extract (Figure 3) demonstrated 2 major peaks at the retention times of 4.470 min and 6.339 min, corresponding to ascorbic acid and gallic acid, respectively. The HPLC chromatograms of the ethyl acetate fraction showed that polyphenols, particularly gallic acid were substantially extracted by ethyl acetate. The chromatogram of the water fraction demonstrated the large peak of ascorbic acid, indicating that this substance remained in the water after organic solvent extraction due to its high polarity. There was no gallic acid or ascorbic acid peaks in the chromatograms of hexane and chloroform fractions, while only the small peak of gallic acid was observed in the chromatogram of butanol fraction.

Antiglycation activity of P. emblica extracts: The inhibitory activity of *P. emblica* fractional extracts on AGEs formation was studied and the results were shown in Figure 2. In this study, the hexane and the chloroform fractions were not included because of their low yield value and defect in solubility in PBS, the solvent used for in vitro antiglycation study. The ethyl acetate fraction of *P. emblica* had the highest % inhibitory activity on the glycation reaction and it

value was higher than that of the positive control, aminoguanidine (AG).
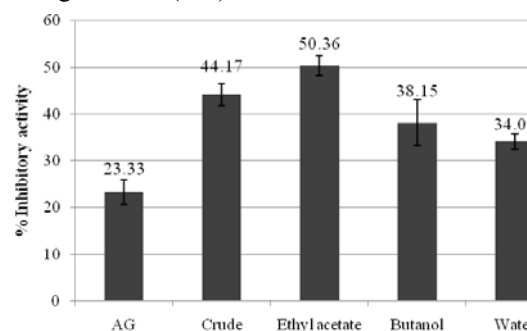

Figure 2. % Inhibitory activity of AG and *P. emblica* crude and fractional extracts
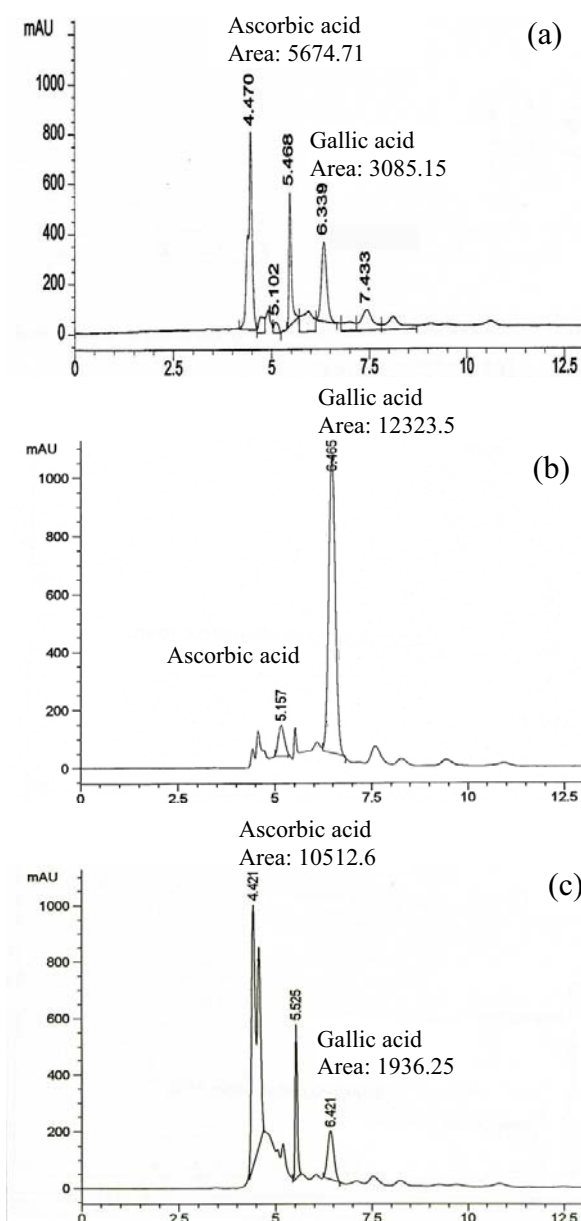

Figure 3. HPLC chromatograms of *P. emblica* crude extract (a), ethyl acetate (b) and water (c) fractions

Conclusions

It was obviously demonstrated in this study that the ethyl acetate fractional extract of *P. emblica* is a good candidate for further product formulation because it had the highest polyphenolic compound content, antioxidation activity and antiglycation activity. Its appearance was lighter in color and less viscous than that of the crude extract.

Acknowledgements

References

[1] K.H. Khan, *Bot. Res. Intl.* **4** (2009), pp. 218-228.

[2] P. Scartezzini, and E. Speroni, *J. Ethnopharmacol.* **71** (2000), pp. 23-43.

[3] S.K. Bhattacharya, A. Bhattacharya, K. Sairam, and S. Ghosal, *Phytomedicine.* **9** (2002), pp. 171-174.

[4] P. Faizal, S. Suresh, R.S. Kumar, and K.T. Augusti, *Indian J. Clin. Biochem.* **24** (2009), pp.82-87.

[5] P. Suryanarayana, M. Saraswat, J.M. Petrash, and G.B. Reddy, *Mol. Visio.* **13** (2007), pp. 1291-1297.

[6] R. Singh, A. Barden, T. Mori, and L. Beilin, *Diabetologia.* **44** (2001), pp. 129-146.

[7] M.S. Ahmad, and N. Ahmed, *J. Nut.* **136** (2006), pp. 769S-799S.

[8] T. Kiho, S. Usui, K. Hirona, K. Azawa, and T. Inakuma, *Biosci. Biotechnol. Biochem.* **68** (2004), pp.200-205.

[9] M.C. Sabu, and R. Kuttan, *J. Ethnopharmacol.* **81** (2002), pp. 155-160.

[10] A. Ardestani, and R. Yazdanparast, *Food Chem. Toxicol.* **45** (2007), pp. 2402-2411.

[11] B. Yang, J. Wang, M. Zhao, Y. Liu, W. Wang, and Y. Jiang, *Carbohydr. Res.* **341** (2006), pp. 634–638.

[12] K. Takuya, T. Hiromasa, O. Yukari, Y. Yukikazu, A. Erdembileg, S. Kuninori, and Y. Yosuke, *J. Agric. Food Chem.* **52** (2004). pp. 2391-2396.

[13] N. Matsuura, T. Aradate, C. Sasaki, H. Kojima, M. Ohara, J. Hasegawa, and M. Ubutaka, *J. Health Sci.,* **48** (2002), pp. 520-526.

[14] K. G. Suresh, N. Harish, D. Shylaja, and. P.V. Salimach, *J. Food Comp. Anal.* **19** (2006), pp. 446-452.

[15] C. Manach, A. Scalbert, C. Morand, C. Rémésy, and L. Jime´nez, *Am. J. Clin. Nutr.* **79** (2004), pp. 727-747.

[16] C.A. Rice-Evans, N. J. Miller, and G. Paganda, *Free Radic. Biol. Med.* **20** (1996), pp. 933-956.

[17] M. Rudnicki, M. Roberto de Oliveira, T.d.V. Pereira, F.v.H. Reginatto, F. Dal-Pizzol, and J.C.u.F. Moreira, *Food Chem.* **100** (2007), pp.719-724.

[18] R. Singh, A. Baeden, T. Mori, and L. Beilin, *Diabetologia.* **44** (2001), pp. 129-146.

Chemical Constituents of *Globba reflexa* Rhizomes

N. Manokam[1] and N. Nuntawong[1]*

[1]Department of Chemistry, Faculty of Science, Chiang Mai University, Chiang Mai, Thailand

E-mail: nuchnipa@chiangmai.ac.th

Abstract: The ground dried rhizomes of *Globba reflexa* were successively extracted with hexane and dichloromethane at room temperature. The crude extracts were separated and purified by column chromatography. Three compounds; villosin (1), (*E*)-15,16-bisnorlabda-8(17),11-dien-13-one (2) and a mixture of stigmasterol (3) and β-sitosterol (4) were isolated from the hexane and dichloromethane extracts. The structures of the compounds were identified by spectroscopic techniques and by comparison of spectroscopic data with those of reported values. All identified compounds were reported for the first time in this plant.

Introduction

The genus *Globba* is the third largest genus of the Zingiberaceae. *Globba* species are distributed throughout tropical (and parts of subtropical) Asia, ranging from India to southern China, south and east to the Philippines and New Guinea [1], the *Shorea robusta* Gaertn.f. forests of Nepal [2], with the center of distribution in monsoonal Southeast Asia, especially Thailand [3] and Myanmar [4]. They comprise about seventy species growing in tropical areas and forty species have been found in Thailand [5]. The crude extract of *Globba sp.* showed biological activities such as *Globba marantina* showed antimicrobial activity [6] and *Globba wintii* exhibited inhibitory effect on 2,2'-azobis (2-amidinopropane) dihydrochloride (AAPH)-induced protein oxidation and protein glycation [7]. Phytochemical investigation on *Globba sp.* resulted in the isolation of naturally occurring sesquiterpenoids, curcumenoids and diterpenoids. Some of them showed moderate to high inhibitory activites against cyclic adenosine monophosphate (cAMP) phosphodiesterase [8] and strong cytotoxic properties towards a panel of cancer cell lines (MCF-7 (human breast adenocarcinoma cell line), PC-3 (human prostate cancer cell line) and H-460 (human lung cancer cell line) [9].

Globba reflexa, commonly known as Kaopansa is one of the forty species of *Globba* found in Thailand, ranging from northern to midland such as Chiang Mai, Lampang and Saraburi. Morphological of rhizomes is light tan outside, whitish and slightly aromatic inside, corolla is orange, inflorescence is nodding and leaves is blades dull dark green above, pale light green below [10].

In our preliminary investigation on the bioactivities of the rhizomes of *Globba reflexa*, we found that the crude hexane and dichloromethane extracts exhibited cytotoxicity against BC (human breast cancer) and NCl-H187 (small cell lung cancer) cell lines with IC_{50} values ranging from 15.58-44.02 µg/mL. Since there has no report on phytochemical and biological study on this plant, the present study is therefore aimed to investigate the chemical constituents from the rhizomes of *Globba reflexa* with respect to seeking some potential drug leads. Moreover, the isolated compounds from *Globba reflexa* may be used for further chemotaxonomic studies on the genus.

Materials and Methods

2.1. Collection and Preparation of Plant Materials

The rhizomes of *Globa reflexa* were collected from Doi Sutep-Pui National Park in May 2008. The rhizomes were air died.

2.2. Extraction and Isolation

Air dried rhizomes of *Globba reflexa* (0.75 kg) were successively extracted at room temperature three time with hexane and dichloromethane. The solvents were evaporated under reduced pressure to yield crude hexane (25.25 g) and dichloro- methane (19.96 g) extracts.

2.3. Chromatographic Separation

The crude hexane extract (25.25 g) was separated by silica gel column chromatography using hexane-dichloromethane gradient (from 100:0 to 0:100), dichloromethane-ethyl acetate gradient (from 100:0 to 0:100) and ethyl acetate-ethanol gradient (from 100:0 to 0:100) to give six fractions (F_1-F_6). Fraction F_4 was further purified by repeated silica gel column chromatography to give compound **1**.

The crude dichloromethane extract (19.96 g) was purified using the same procedure as the crude hexane extract to give five fractions (F_1-F_5). Fraction F_2 was further purified by repeated silica gel column chromatography to give compounds **2, 3** and **4**.

The structures of all isolated compounds were identified by interpretation of their spectral data including EIMS, IR, ^{1}H NMR and ^{13}C NMR as well as by comparison of spectroscopic data with those of reported values.

Results and Discussion

Chomatographic separation of the hexane and dichloromethane extracts of the rhizomes of *Globba reflexa* yielded three know compounds. These compounds were identified as villosin (**1**), (*E*)-15,16-bisnorlabda-8(17),11-dien-13-one (**2**) and a mixture of stigmasterol (**3**) and β-sitosterol (**4**)

Compound **1** was obtained as a colorless amorphous solid with optical rotation $[\alpha]_D^{29}$-1.61 (*c* 1.05, CHCl$_3$). The molecular formula was assigned as C$_{20}$H$_{28}$O$_2$ based on the molecular ion peak at *m/z* 300 in the EIMS. The IR spectrum indicated the presence of an α,β-unsaturated-γ-lactone from absorption band at 1754 cm^{-1}. The structure of compound **1** was determined from ^{1}H, ^{13}C, ^{1}H-^{1}H COSY, DEPT 135, HMQC and HMBC experiments. The ^{1}H NMR indicated the presence of three methyl groups at δ 0.80 (3H, *s*, H-20), δ 0.87 (3H, *s*, H-19) and 0.89 (3H, *s*, H-18), as well as *exo*-methylene protons at δ 4.50 (1H, *br s*, H-17a) and 4.76 (1H, *br s*, H-17b). In addition, the signals of two *trans*-olefinic proton were observed at δ 6.11 (1H, *d*, *J*=15.8 Hz, H-12) and 6.90 (1H, *dd*, *J*=10.1, 15.8 Hz, H-11) (Table 1). These characteristic signals suggested that compound **1** has a labdane diterpenoid skeleton. It was further supported by the peak at *m/z* 137 in the EIMS (Fig 1).

The ^{13}C NMR spectrum of **1** showed signals of three methyls at δ 33.66 (C-18), 22.03 (C-19), 15.14 (C-20), seven methylenes at δ 19.19 (C-2), 23.45 (C-6), 36.83 (C-7), 40.89 (C-1), 42.29 (C-3), 69.69 (C-15), 108.49 (C-17), five methines at δ 54.75 (C-5), 62.28 (C-9), 120.75 (C-12), 136.92 (C-11), 142.55 (C-14) and five quarternary carbons at δ 33.66 (C-4), 39.31 (C-10), 129.56 (C-13), 149.50 (C-8) and 172.46 (C-16). The structure was further confirmed by HMBC correlations of singlet olefinic proton at δ 7.15 (1H, *br s*, H-14) with the carbonyl at δ 172.46 as well as with the signals at δ 69.69 (C-15), 120.75 (C-12) and 129.56 (C-13). In addition, long-range correlation between H-12 (δ 6.11, *d*, 15.8) and the carbonyl carbon (δ 172.46) indicated that this functional group was located at C-16 rather than at C-15. All the HMBC correlations are depicted in Fig 2.
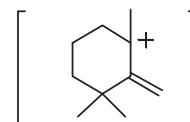

Figure 1 Characteristic fragment of labdane-type Diterpenoid

Table 1
^{1}H NMR and ^{13}C NMR data of compound **1** and **2**

position	Compound 1		Compound 2	
	δ$_C$	δ$_H$ (multiplicity)	δ$_C$	δ$_H$ (multiplicity)
1	40.89	α1.00 (m)	40.86	α1.05 (obscured signal)
		β1.41 (m)		β1.37 (m)
2	19.19	α1.46 (m)	18.99	α1.42 (m)
		β1.51 (m)		β1.54 (m)
3	42.29	α1.17 (m)	42.09	α1.20 (m)
		β1.35 (m)		β1.44 (m)
4	33.66		33.54	
5	54.75	1.09 (dd,12.5, 2.5)	54.45	1.10 (dd,12.5, 2.6)
6	23.45	β1.38 (m)	23.23	β1.39 (m)
		α1.70 (m)		α1.71 (m)
7	36.83	α2.08 (dt,13.4,5.1)	36.61	α2.09 (dt, 1.25, 4.8)
		β2.44 (ddd, 13.4, 4.0, 2.0)		β2.45 (overlapping signal)
8	149.50		148.61	
9	62.28	2.37 (br d, 10.1)	60.79	2.48 (br d,10.0)
10	39.31		39.33	
11	136.92	6.90 (dd, 10.1, 15.8)	146.72	6.87 (dd, 10.0, 15.8)
12	120.75	6.11 (d, 15.8)	133.57	6.07 (d, 15.8)
13	129.56		198.18	
14	142.55	7.15 (br s)	27.21	2.27 (s)
15	69.69	4.81 (br s)		
16	172.46			
17a	108.49	4.50 (br s)		4.40 (br d, 1.3)
17b		4.76 (br s)	108.61	4.79 (br d, 1.3)
18	33.66	0.89 (s)	33.57	0.89 (s)
19	22.03	0.87 (s)	21.92	0.84 (s)
20	15.14	0.80 (s)	15.11	0.89 (s)

From these data, the structure of **1** was assigned as villosin by the above evidences and by comparison of spectroscopic data with those of the literature values [11],[12]. This compound has also been isolated from *Hedychium villosum* [11], *Hedychium coronarium* [13], *Hedychium gardnerianum* [14] and *Curcuma comosa* [15].
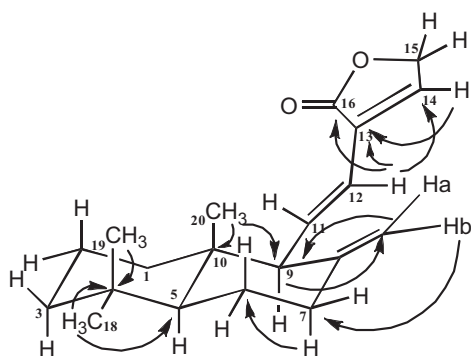
**Figure 2** HMBC correlations of compound 1

Compound **2** was obtained as a colorless amorphous solid with optical rotation $[\alpha]_D^{29}$ -8.50 (*c* 0.67, CHCl$_3$). The molecular formula was assigned as C$_{18}$H$_{28}$O based on the molecular ion peak at *m/z* 260 in the EIMS. The ^{1}H and ^{13}C NMR spectra showed similar patterns to those of compound **1**, with the only difference in the absence of a singlet signal of an olefinic proton at δ 7.15 (1H, *br s*, H-14) and a signal of methylene proton at δ 4.81 (2H, *br s*, H-15). The ^{13}C NMR signals of methine carbon at δ 142.55 (C-14), methylene carbon at δ 69.69 (C-15) and quarternary carbon at δ 172.46 (C-16) were also absence. However, the signal at δ 198.18 (C-13) was assigned to a carbonyl group, the presence of which was supported by the absorption band at 1664 cm^{-1} observed in the IR spectrum. In the HMBC spectrum, olefinic proton signal at δ 6.87 (1H, *dd, J*=10.0, 15.8 Hz, H-11) and δ 6.07 (1H, *d, J*=15.8 Hz, H-12) showed correlation with the carbonyl at δ 198.18. Long-range correlation between H-12 (δ 6.07) and C-14 (δ 27.21) were also observed. From these data, the structure of **2** was assigned as (*E*)-15,16-bisnorlabda-8(17),11-dien-13-one by the above evidences and by comparison of spectroscopic data with those reported values [16]. This compound has been previously isolated from *Alpinia apeciosa* [16], *Alpinia calcarata* [17] and *Curcuma mangga* [18].

A mixture of compounds **3** and **4** was obtained as a colorless crystals. EIMS spectrum showed a parent molecular ion peak at *m/z* 412 and 414 respectively which corresponds to molecular formula C$_{29}$H$_{48}$O and C$_{29}$H$_{50}$O. The IR spectrum showed absorption peaks at 3424 cm^{-1}(O-H str.), 2939 cm^{-1} and 1675 cm^{-1} (C=O in aliphatic carbonyl compound), 1512 cm^{-1} and 1608 cm^{-1} (C=C), 1119 cm^{-1} (C-OH), 1036 cm^{-1} (C-O). In ^{1}H NMR spectrum of compounds **3** and **4** showed signals at δ

3.53 (1H, *m*, H-3), olefinic proton at 5.36 (1H, *d, J=* 5.1, H-6), two olefinic proton at δ 5.16 (1H, *dd, J*=15.2, 8.6 Hz, H-22) and 5.00 (1H, *dd, J*=15.2, 8.6 Hz, H-23) which were identical with the chemical shift of H-22 and H-23 respectively of stigmasterol [18] and showed six methyl group at δ 0.68 (3H, *s*, H-18), δ 0.83 (3H, *d*, H-27), δ 0.85 (3H, *d*, H-29), δ 0.86 (3H, *d*, H-26), δ 0.93 (3H, *s*, H-19), δ 1.02 (3H, *d*, H-21). The ^{13}C NMR signals of C$_{22}$=C$_{23}$ double bond in stigmasterol and C$_{22}$-C$_{23}$ single bond in β-sitosterol were also similar to the data in the literature of stigmasterol [19, 20] and β–sitosterol [19], respectively.

Conclusions

Three compounds (Fig 3) were isolated from the rhizomes of *Globba reflexa*. They were identified to be villosin (**1**), (*E*)-15,16-bisnorlabda-8(17),11-dien-13-one (**2**) and a mixture of stigmasterol (**3**) and β-sitosterol (**4**). All compounds were reported for the first time from *Globba reflexa.*
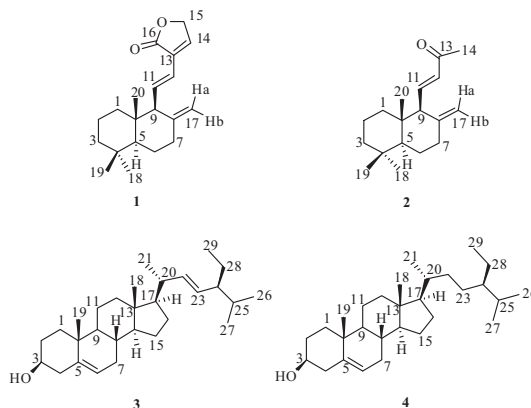
Figure 3 Compounds 1-4 isolated from the rhizomes of *Globba reflexa*

References
[1] K. Schumann, *Zingiberaceae*. Das Pflanzenreich, Wilhelm Engelmann. **vol 4**, Leipzig, German (1904), pp 1–458.
[2] E. L.Webb, R. N. Sah, *Forest Ecology and Management*. **176** (2003), pp. 337-353.
[3] K. Larsen, *Thai Forest Bulletin (Botany)*, **24** (1996), pp. 35-49.
[4] W. J. Kress, R. A. DeFilipps, E. Farr and Yin Yin Kyi. *Contributions from the United States National Herbarium*. **Vol 45**, Department of Systematic Biology – Botany, National Museum of Natural History , Washington, DC (2003), pp.1-590.
[5] P. Sirirugsa, *Thai Zingiberaceae : Species Diversity And Their Use,* International Conference on Biodiversity and Bioresources: Conservation and Utilization, Phuket, Thailand. (1999), 23-27 November 1997.
[6] A. J. Ram, L. Md. Bhakshu and R. R. V. Raju, *J. Ethno. pharmacol.* **90** (2004), pp. 353–357.
[7] C. Chaiyasut, and S. Chansakaow, *Naresuan University Journal* . **15** (2007), pp. 35-41.

[8] S. Onanong, Chemical constituents and their inhibitions of cyclic AMP phosphodiesterase of the rhizomes of *Globba malaccensis* Ridl, Master's Thesis, Chulalongkorn University, 2005.

[9] Maulidiani, K. Shaari, C. Paetz, J.Abas F and NH. Lajis*, Nat Pro Com*. **4** (2009), pp. 1031-1036.

[10] J.F.Mexwell, Flora Of Thailand. CMU Herbarium. (2008), Department of Biology, Faculty of Science, Chiang Mai University.

[11] P. Xiao, C. Sun, M. Zahid, O. Ishrud, Y. Pan, *Fitoterapia*. **72** (2001). pp. 837-838.

[12] Q. Zhao, C. Qing, X. Jiang and G. Li Xu, *Chem. Pharm. Bull*. 56 (2008), pp.210-212.

[13] C. Nitirat, P. Somchai ,N. Lukana, D. Decha, C. Daranee,K. Nisachon, M. Chulabhorn and T. Supanna, *Nat Pro Res*. **22**(2008). pp. 1249–1256.

[14] I. Kumrit, A. Suksamrarn, P. Meepawpan, S. Songsri and N. Nuntawong, *Phytother Res*.24 (2010). pp.1009-1013.

[15] C. Ratchanaporn, C. Nattawara, S. Saovaros, F. Suthat, V. Jim and S. Apichart, *J. Nat. Prod*. **73** (2010), pp. 724-728.

[16] I. Hideji, M. Makoto, M. Susumu, *Chem. Pharm. Bull*. **28** (1980). pp.3452-3454.

[17] K. Ling-Yi, Q. Min-Jian and N. Masatake, *J. Nat. Prod*. **63** (2000). Pp. 939-942.

[18] M. Kunlanat, Chemical constituents of the *curcuma mangga* rhizome. Master's Thesis, Chulalongkorn University, 2000.

[19] H. M. Rowshanul, N. Farjana, R. Mayiar, H. M. Ekramul and K. M. Rezaul, *Pakistan J Biol Sci*. **10** (2007). pp. 4174-4176.

[20] P. S. Jain and S. B. Bari, *Asian J Plant Sci*. **9** (2010). pp.163-165.

Triphenylbenzene-Ethynylene Dendritic Fluorophores

S. Sirilaksanapong [1], M. Sukwattanasinitt [2] and P. Rashatasakhon [2*]

[1] Program of Petrochemical and Polymer Science, Faculty of Science, Chulalongkorn University, Pathumwan, Bangkok 10330, Thailand
[2] Organic Synthesis Research Unit, Department of Chemistry, Faculty of Science, Chulalongkorn University, Pathumwan, Bangkok 10330, Thailand

* E-mail: paitoon.r@chula.ac.th

Abstract: A series of water soluble anionic dendritic fluorophores composed of triphenylbenzene-ethynylene repeating units and anionic carboxylate peripheries are synthesized. Two compounds are zeroth generation dendrimers which have 3 and 6 carboxylic acid groups. An example of first generation dendrimer containing 9 phenylene-ethynylene units and twelve carboxylic acid groups is also successfully synthesized. Their photophysical properties are thoroughly investigated using solutions in aqueous phosphate buffer. The first generation dendrimer exhibits a selective fluorescence quenching by Cu^{2+} ion.

Introduction

During the past few decades, the importance of fluorescence chemo- and biosensors has been well recognized which is evident by the exponential development of the research in these fields. In most of the pioneer works,[1] linear conjugated polymers such as poly(phenyleneethynylene) or poly(phenylenevinylene) were used as fluorescence signal transducer. For sensibility accessment, the changes in fluorescent intensities or emission wavelengths were monitored as the amounts of analytes were gradually increased. However, the linear conjugated polymers are usually prepared by Pd-catalyzed reactions; i.e. Heck,[2] Suzuki,[3] or Sonogashira couplings[4]. The resulting polymers are usually polydispersed and their conformation in liquid medium cannot be confidently predicted, which may lead to uncertainty in the interpretation of fluorescent signal change. In an attempt to develop more sensitive and efficient fluorescent sensors, our group has previously reported the synthesis of monodispersed and conformationally rigid dendritic polyelectrolytes which could be utilized as signal transducer for mercuric ion detection[5] and protein sensor array[6].

As parts of our continuing research in design and synthesis of dendritic polyelectrolytes, we envision the incorporation of 1,3,5-triphenylbenzene into the phenyleneethynylene fluorophores since it could provide a strong fluorescent signal and can be easily prepared or functionalized.[7] Consequently, compound **1** and **2** were designed to have the same conjugate backbone but a different number of hydrophilic carboxylate peripheries. With the increased fluorophore units, compound **3** was expected to emit fluorescent signal at a longer wavelength compared the others. Although this first generation dendrimer

appeared to be hydrophobic, its water solubility should be facilitated by the twelve carboxylic acid groups.
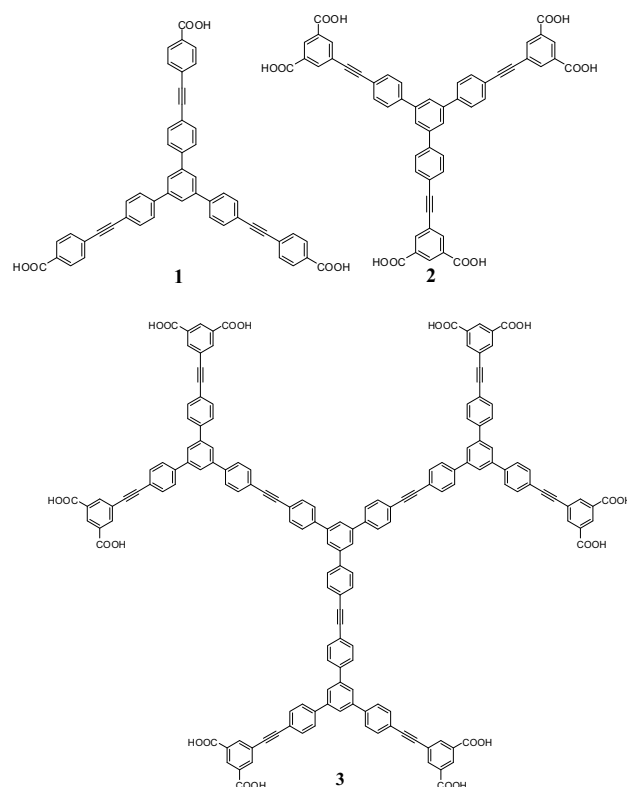
Figure1. Structures of dendritic fluorophores **1-3**.

Materials and Methods

Reactions were carried out under a nitrogen atmosphere. The starting materials and reagents were purchased from commercial sources and used without further purification. The synthesis compounds were characterized by ^{1}H-NMR Varian mercury nmr spectrometer 400 MHz. and 100 MHz. for ^{13}C (Varian company, Ca, USA.) using $CDCl_3$ and DMSO as the solvent. Chemical shifts were recorded in parts per million (ppm), and splitting patterns are designated as s (singlet), d (doublet), t (triplet) and m (multiplet). The molecular weights of compound were evaluated by Microflet Muldi-TOF mass spectroscopy (Bruker daltonics). The UV/Vis spectra were recorded on a Varian Carry 50 UV/Vis spectrophotometer And Fluorescence measurements were carried out on a

Varian Carry Eclipse spectrofluorometer with a xenon lamp as the light source**Experimental**

***1,3,5-Tris-(4-iodophenyl)-benzene* (4)**: A solution of 4-Iodoacetophenone (1.0 g, 4.08 mmol) and CF_3SO_3H (90 μL, 1.00 mmol) in toluene were stirred under reflux conditions for 3 h. The crude solid was washed with EtOH and Et_2O and then recrystallized from EtOH and CH_2Cl_2 (1:1) to afford **4** as white needles (0.65 g, 60 %): mp >260 °C; ^{1}H NMR δ 7.78 (d, J = 8.1 Hz, 6H), 7.67 (s, 3H), 7.39 (d, J = 8.1 Hz, 6H); ^{13}C NMR δ 141.6, 140.1, 138.0, 129.1, 124.9, 93.6. Anal. Calcd. for $C_{24}H_{15}I_3$: C, 42.12; H, 2.21. Found: C, 42.13; H, 2.20.

Compound 5: To a degassed solution of **4** (100 mg, 0.14 mmol) in THF (10 mL) and Et_3N (10 mL) were added $Pd(PPh_3)_2Cl_2$ (15 mg, 22 μmol), PPh_3 (12 mg, 44 μmol) and CuI (8.4 mg, 44 μmol). A solution of ethyl 4-ethynylbenzoate (100 mg, 0.58 mmol) in THF (2 mL) was added dropwise then stirred at rt overnight. After removal of solvents under reduced pressure, the residue was extracted with H_2O/CH_2Cl_2. The organic phase was washed with brine and dried over sodium sulfate. The CH_2Cl_2 was removed under reduced pressure and the residue was purified by column chromatography on siliga gel using hexane/CH_2Cl_2 (1:4) as the eluent. The tri-ester **5** (93 mg, 78%) was obtained as a pale yellow solid. ^{1}H NMR (400 MHz, $CDCl_3$): δ 8.05 (d, J = 8.4 Hz, 6H), 7.82 (s, 3H), 7.69 (dd, J = 8.17 and 20.26 Hz, 12H), 7.62 (d, J = 8.4 Hz, 6H), 4.39 (q, J = 7.1 Hz, 6H), 1.41 (t, J = 7.1 Hz, 9H); ^{13}C NMR (100 MHz, $CDCl_3$): δ = 166.1, 141.7, 141.0, 132.3, 131.5, 129.9, 129.5, 127.8, 127.3, 125.3, 122.2, 92.1, 89.7, 61.2, 14.3.

Compound 6: This compound was prepared from **4** (100 mg, 0.14 mmol) and diethyl-5-(ethynyl)iso-phthalate (120 mg, 0.51 mmol) using the same procedure described for **5**. After a purification by a column chromatography using hexane/CH_2Cl_2 (1:9) as the eluent, hexa-ester **6** (110 mg, 87%) was obtained as a pale yellow solid. ^{1}H NMR (400 MHz, $CDCl_3$): δ = 8.66 (t, J =1.8 Hz, 3H) 8.41 (t, J = 1.8 Hz, 6H), 7,86 (s, 3H), 7.77 (t, J = 1.8 Hz, J = 6.6 Hz, 6H), 7.70 (dd, J = 1.8 and 6.6 Hz, 6H), 4.46 (q, J = 7.2 Hz, 12H), 1.46 (t, J = 7.2 Hz, 18H); ^{13}C NMR (100 MHz, $CDCl_3$): δ 165.2, 141.7, 141.1, 136.4 ,132.3, 131.3, 130.1, 127.4, 125.3, 124.2, 122.0, 90.9, 88.5, 61.6, 14.3.

Compound 1: To a solution of **5** (93 mg, 0.69 mmol) in THF (4 mL) and EtOH (4 mL) was added saturated KOH aqueous solution (0.1 mL) and the mixture was refluxed for 6 h. The volatile solvents were evaporated and the residue dissolved in water (5 mL). The solution was cooled with ice and acidified to pH 3 by 1 M HCl. The suspension was centrifused to afford **1** as a yellow solid (79 mg, 90%). ^{1}H NMR (400 MHz, DMSO-d_6): δ 8.04 (s, 3H), 8.00 (dd, J = 8.4 and 17.5 Hz, 12H), 7.71 (t, J = 8.4 Hz, 12H). ^{13}C NMR (100 MHz, DMSO-d_6): δ 166.7, 140.7, 140.3, 132.1, 131.8, 131.5, 130.6, 129.6, 127.6, 126.6, 124.8, 121.2, 115.2, 91.9, 89.5.

Compound 2: This compound was prepared by hydrolysis of **6** (110 mg) under the method described

above. After the suspension was centrifused, **2** was obtained as a brown solid (95 mg, 96%). ^{1}H NMR (400 MHz, DMSO-d_6): δ 8.46 (t, J = 1.5 Hz, 3H), 8.29 (d, J = 1.5 Hz, 6H), 8.07 (s, 3H), 8.04 (d, J = 8.4 Hz, 6H), 7.77 (d, J = 8.4 Hz, 6H). ^{13}C NMR (100 MHz, DMSO-d_6): δ 166.0, 140.7, 140.3, 135.3, 132.7, 132.2, 129.2, 127.6, 124.8, 123.1, 121.1, 90.7, 88.5.

***1,3,5-Tris-(4-ethynyl-phenyl)-benzene* (7)**:
To a degassed solution of **4** (1 g, 1.46 mmol) in THF (50 mL) and Et_3N (50 mL) were added $Pd(PPh_3)_2Cl_2$ (154 mg, 220 μmol), PPh_3 (116 mg, 440 μmol) and CuI (84 mg, 440 μmol). Trimethylsilylacetylene (0.7 mL, 4.8 mmol) was slowly added and the reaction mixture was stirred for 5 hours at rt. Then the solution was partitioned between CH_2Cl_2 (300 mL) and 6 M HCl (200 mL). The organic phase was separated, washed with saturated NH_4Cl and dried over Na_2SO_4. After evaporation of CH_2Cl_2, the crude product was purified by column chromatography using hexane/ CH_2Cl_2 (5:1) as the eluent to afford 1,3,5-Tris-(4-trimethylsilylethynyl-phenyl)-benzene (850 mg, 97%) as colorless crystals. ^{1}H NMR (400 MHz, $CDCl_3$): δ = 7.80 (s, 3H), 7.67 (d, J = 8.4 Hz, 6H), 7.56 (d, J = 8.4 Hz, 6H), 0.27 (s, 27H); ^{13}C NMR (100 MHz, $CDCl_3$): δ = 142.0, 141.2, 132.8, 127.5, 125.5, 123.0, 105.0, 95.6, 0.0. Anal. Calcd. for $C_{39}H_{42}Si_3$: C 79.72, H 7.11; found: C 78.89, H 7.15. The compound was then dissolved in THF (20 mL) and EtOH (80 mL). After adding K_2CO_3 (1.2 g, 8.7 mmol), the reaction mixture was stirred for 3 hours then CH_2Cl_2 (300 mL) was added. The organic phase washed with water and dried over Na_2SO_4. After evaporating the solvent, the crude product was purified by column chromatography (hexane / CH_2Cl_2; 10:3) to afford **7** (460 mg, 85%) as colorless solid. ^{1}H-NMR (400 MHz, $CDCl_3$): δ = 7.81 (s, 3H), 7.70 (d, J = 8.4 Hz, 6H), 7.62 (d, J = 8.4 Hz, 6H), 3.23 (s, 3H); ^{13}C NMR (100 MHz, $CDCl_3$): δ = 142.0, 141.5, 133.0, 127.6, 125.6, 121.9, 83.6, 78.4. Anal. Calcd. for $C_{30}H_{18}$: C 95.21, H 4.79, Found: C 95.08, H 4.83.

Compound 8: This compound was prepared from **4** (500 mg, 0.73 mmol) and diethyl-5-(ethynyl)iso-phthalate (370 mg, 1.53 mmol) using the same procedure described for **5**. A column chromatography on silica gel with hexane/CH_2Cl_2 (1:2) afforded yellow solid (0.25 g, 37%) ^{1}H NMR (400 MHz, $CDCl_3$): δ 8.65 (m, 2H), 8.37 (dd, J = 1.5 and 10.2 Hz, 4H), 7.82 (m, 2H), 7.76 (d, J = 1.5 Hz, 3H), 7.70 (q, J = 8.5 Hz, 8H), 7.41 (d, J = 7.45 Hz, 2H), 4.43 (m, 8H), 1.43 (dd, J^l = 7.0 and 13.28 Hz, 12H). ^{13}C NMR (100 MHz, $CDCl_3$): δ = 165.4, 165.3, 142.0, 141.8, 141.2, 140.5, 138.2, 136.9, 136.6, 132.5, 131.6, 131.4, 130.4, 130.3, 129.3, 128.7, 127.5, 125.3, 125.2, 124.4, 124.3, 122.2, 103.1, 96.7, 93.8, 91.1, 88.7, 14.5, 14.5.

Compound 3: This compound were prepared by a Sonogashira coupling between dendron **6** (190 mg, 0.21 mmol) and tri-yne **7** (23 mg, 0.062 mmol) using the same procedure described in the synthesis of **5**. iPr_2NH was used instead of Et_3N and the reaction was stirred at 50°C overnight. Column chromatography on

silica gel with CH_2Cl_2 and a small amount of EtOH as an eluent yielded dodeca-ester as a pale brown crystal (82 mg, 48%) ^{1}H NMR (400 MHz, CDCl3): δ 8.60 (s, 6H), 8.36 (s, 12H), 7.75 (s, 12H), 7.66 (m, 48H), 4.42 (q, J = 7.0 Hz, 24H), 1.43 (t, J = 7.0 Hz, 36H), ^{13}C NMR (100 MHz, DMSO-d6): δ = 165.1, 141.6, 141.5, 140.9, 140.4, 140.4, 136.4, 134.6, 133.1, 132.3, 132.2, 131.3, 131.0, 130.0, 128.9, 127.3, 127.2, 125.1, 124.2, 122.7, 122.6, 121.9, 91.0, 90.4, 90.3, 88.5, 61.6, 34.4, 32.0, 29.7, 29.4, 29.1, 28.9, 25.0, 23.0, 22.7, 14.6, 14.2. Anal. Calcd. for $C_{186}H_{138}O_{24}$: C, 81.03, H, 5.05. Found: 81.02, 5.06. This dodeca-ester (82 mg) was dissolve in THF (7 mL) and EtOH (7 mL), then saturated KOH aqueous solution (0.2 mL) was added and the mixture was refluxed for 6 h. After the usual work up and acidification to pH 3 by 1 M HCl, the suspension was centrifused to afford **3** as a brown solid (68 mg, 96% yield). ^{1}H NMR (400 MHz, DMSO-d6): δ 13.56 (s, 12H), 8.43 (s, 6H), 8.26 (s, 12H), 7.98 (m, 33H), 7.72 (m, 27H) ^{13}C NMR (100 MHz, DMSO-d6): δ 165.8, 140.6, 140.3, 135.5, 132.1, 132.0, 131.9, 129.7, 127.4, 124.7, 123.3, 121.0, 90.9, 88.3.

Results and Discussion
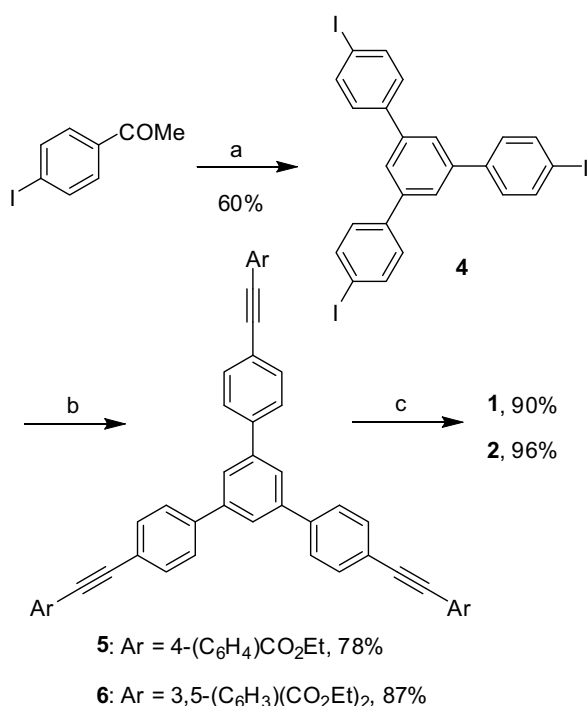
Scheme 1. Reagents and conditions: (a) CF_3SO_3H, PhMe, reflux; (b) ethyl 4-ethynylbenzoate or diethyl-5-(ethynyl)isophthalate (3.6 eq.), $Pd(PPh_3)_2Cl_2$, CuI, PPh3, THF, Et3N (c) KOH, EtOH, THF, reflux.

Our synthesis began with a cyclo-trimerization of 4-iodoacetophenone using trifluoromethanesulfonic as a catalyst. The resulting triiodo triphenylbenzene (**4**) was then reacted with aryl acetylenes under a Sonogashira coupling conditions to

afford the zeroth generation dendrimers bearing ester groups (**5** and **6**), which were hydrolyzed to provide fluorophore **1** and **2** in excellent yields.

The first generation dendrimer was synthesized in a convergent approach, in which the triyne core (**7**) was prepared from the Sonogashira coupling of **4** with trimethylsilyl acetylene followed by a base-catalyzed desilylation. Dendron **8** was obtained using the method described for **6**, but the amount of aryl acetylene was limited to 2.1 molar equivalents. The coupling of **7** with **8** followed by a hydrolysis of the ester groups gave rise to the first generation dendritic fluorophore in moderate yield.

8: Ar = 3,5-$(C_6H_3)(CO_2Et)_2$
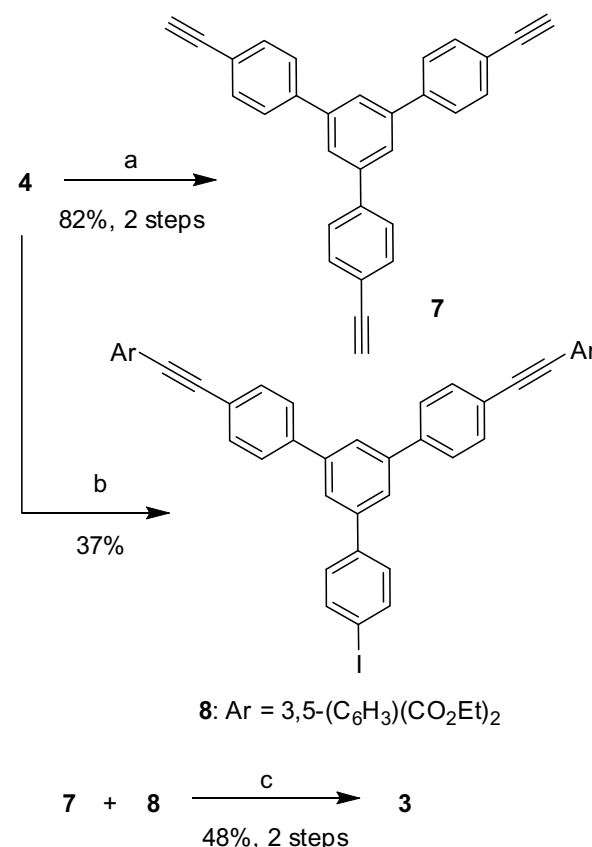
Scheme 2. Reagents and conditions: (a) *i.* trimethylsilylacetylene, $Pd(PPh_3)_2Cl_2$, CuI, PPh3, THF, Et3N; *ii.* K_2CO_3, THF, MeOH; (b) diethyl-5-(ethynyl)isophthalate (2.1 eq.), $Pd(PPh_3)_2Cl_2$, CuI, PPh3, THF, Et3N; (c) *i.* $Pd(PPh_3)_2Cl_2$, CuI, PPh3, THF, *i*Pr2NH, 50 °C; *ii.* KOH, MeOH, THF, reflux.

The absorption and emission spectra of each fluorophore were shown in Figure 2 and the related data were summarized in Table 1. All of the compounds have maximum wavelength of absorption around 310-318 nm. The effect of substitution patterns at the peripheries could be observed as **1** and **2** exhibited significantly different Stokes shifts. The emission band of **1** appeared at a longer wavelength, which indicated that the three carboxylate groups at the *para* positions may cause an intra-molecular charge transfer (ICT). Therefore, the excited state geometry of

1 could be much different from its ground state. On the other hand, the carboxylate groups in **2** were positioned at the *meta* positions where the electron-withdrawing groups played less prominent roles. The emission band of **3** was much broader, which may result from the higher degree of aggregation in aqueous media caused by a large hydrophobic moiety. It could also be due to many possible conformations of **3** which led to various geometrical relaxation.
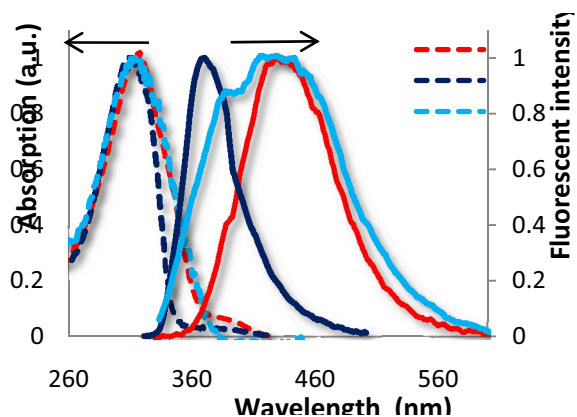
Figure 2: Normalized absorption and fluorescent spectra of **1-3** in 10 mM phosphate buffer pH 8.

Table 1: Photophysical properties of **1-3** in 10 mM phosphate buffer pH 8.0.

Cmpd.	Absorption		Emission	
	λ_{abs} (nm)	ε (M^{-1} cm^{-1})	λ_{ems} (nm)	Φ
1	318	47000	426	0.214 [a]
2	310	19600	365	0.472 [a]
3	314	16600	444	0.050 [b]

[a] 2-Aminopyridine in 0.1 M H_2SO_4 (Φ = 0.60) and [b] Quinine sulphate in 0.1 M H_2SO_4 (Φ = 0.54) were used as references.

In a preliminary screening on sensing applications, we tested an aqueous solution of each fluorophore with a number of metal ion solutions. We were gratified that **3** exhibited a strong fluorescence quenching by Cu^{2+} (Figure 3). However, it was also observed that Fe^{2+} and Hg^{2+} could also quench the fluorescent signals to some extents. Enhancements of the selectivity of **3** toward Cu^{2+} are currently undertaken.

Conclusions

We have accomplished the synthesis of dendritic triphenylbenzene-ethynylene fluorophores. Possibly due to their superior water solubilities, the zeroth generation dendrimers displayed stronger fluorescent signals than the first generation. With substitutents at the *para* positions in **1**, the intramolecular charge transfer caused by the electron-withdrawing carboxylate group and electron-releasing triphenylbenzene core could be more pronounced and may lead to a larger Stokes shift. The first generation dendrimer exhibit some selectivity toward Cu^{2+} ion.

The improvement of the selectivity and the investigation of other sensing ability of the fluorophores are currently being studied.
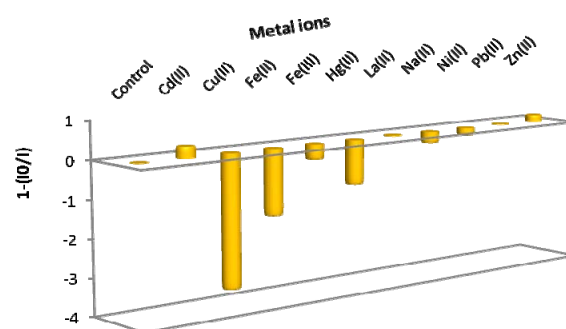
Figure 3: Fluorescent quenching efficiencies of **3** (1 μM) in the presence of various metal ions (50 μM).

References

[1] a) U. H. F. Bunz, *Chem. Rev*. **100**, (2000), pp. 1605-1644. b) B. Liu, W. L. Yu, J. Pei, S. Y. Liu, Y. H. Lai, W. Huang. *Macromolecules*. **34**, (2001)**,** pp. 7932-7940. c) I. B. Kim; A. Dunkhorst; J. Gilbert; U. H. F. Bunz *Macromolecules*. **38** (2005), pp. 4560-4562.

[2] M. Pan, S. Bao, L. Yu, *Macromolecules*. **28**, (1995), pp. 5151-5153.

[3] T. Yokozawa, H. Kohno, Y. Ohta, A. Yokoyama *Macromolecules*. **43**, (2010), pp. 7095-7100.

[4] C. Wang, A. S. Batsanov, M. R. Bryce *J. Org. Chem*. **71,** (2006), pp.108-116.

[5] N. Niamnont, W. Siripornnoppakhun, P. Rashatasakhon, M. Sukwattanasinitt, *Org. lett*. **11**, (2009), pp. 2768-2771.

[6] N. Niamnont, R. Mungkarndee, I. Techakriengkrai, P. Rashatasakhon, M. Sukwattanasinitt, *Biosens. Bioelectron.* **26,** (2010), pp 863-867.

[7] a) J. Brunel, O mongin, A. Jutand, I. Ledoux, J. Zyss, M. B. Desce, *Chem. Mater.* **15**, (2003), pp. 4139-4148. b) L.Yu, J.S. Lindsey, *J. Org. Chem*. **66**, (2001), pp.7402-7419.

Design of Chromone-based Compounds as Potential DPP-4 Inhibitors

W. Swainoi[1], A. Keawnoi[1], S. Jankan[1], and O. Vajragupta[2*]

[1]Program of Chemistry, and Center of Excellence for Innovation in Chemistry, Faculty of Science and Technology, Bansomdejchaopraya Rajabhat University, Isaraphab15, Bangkok 10600, Thailand
[2]Department of Pharmaceutical Chemistry, Faculty of Pharmacy, Mahidol University
447 Sri-Ayudhya Road, Bangkok 10400, Thailand

*E-mail: pyovj@mahidol.ac.th

Abstract: In this study, dipeptidyl peptidase IV (DPP-4) was selected as a drug target in searching for new antidiabetic drugs. Novel DPP-4 inhibitors were developed based on the information of medicinal herbs and structure based drug design. The DPP-4 template was prepared from human DPP-4 crystal structure bound with sitagliptin (PDB: 1X70) and validated. The structure-based drug design is the methodology for searching the novel structures of DPP-4 inhibitors. The combinatory library of 254 structures containing two main fragments linked with hydrazone or amide functions was prepared. Two main fragments are chromone (P1) and the varied side chains (P2). Molecular docking of the structures in the library against DPP-4 template was conducted to identify the hit structures of increased binding capacity and consequently leading to potent inhibitory action. Twenty-two top ranking compounds or hit compounds were identified which are 13 hydrazone derivatives and 9 amide derivatives. Twenty-two identified hit compounds were synthesized and screened for their DPP-4 inhibitory action in vitro at 100 μM. Most compounds showed weak inhibitory action at 100 μM. The IC$_{50}$ of two most potent compounds were determined, the IC$_{50}$ of 6-methyl-3-((2-phenylhydrazono)methyl)-4H-chromen-4-one and N-(3,5-dimethoxyphenyl)-4-oxo-4H-chromene-3-carboxamide were found to be 153.53 μM and 397.66 μM, respectively. These two compounds are considered as leads, further leads optimization is currently in progress to increase the potency.

Introduction

Diabetes mellitus (DM) currently affects an estimated 20.8 million people within the US population. The World Health Organization estimates the number of people with diabetes to be approximately 180 millions. This number is projected to double by 2030 [1]. An entirely novel therapeutic principle for the treatment of type-2 diabetes mellitus (2DM) was introduced onto the incretin-based therapies. The incretin effect is mediated by mainly two incretin hormones: glucose dependent insulinotropic polypeptide (GIP) and glucagon-like peptide-1 (GLP-1). Both GIP and GLP-1 also promote β-cells proliferation and inhibit apoptosis, leading to expansion of β-cells mass. GLP-1, but not GIP, controls glycemia via additional actions on glucose sensors, inhibition of gastric emptying, food intake and glucagon secretion. However, GLP-1 as well as GIP are rapidly degraded in plasma by the serine protease dipeptidyl peptidase IV. Inhibition of DPP-4 increases the levels of endogenous intact circulating GLP-1 and GIP. Consequently, the development of DPP-4 inhibitors is rapidly emerging as a novel therapeutic approach to the treatment of type 2 diabetes [2-6].

Chromone naturally occurring compounds in nature especially in plants and interesting structure was found to be the important component or pharmacophores of many biologically active molecules such as antimycobacterial, antifungal, anticonvulsant, antimicrobial and anticancer agents [7,8]. Hence, chromone was selected to be and core structure for the designed compounds. Molecular docking of the hit structures with DPP-4 were conducted to identify with increasing binding capacity which leads to potent inhibitory action. The identified hit compounds were synthesized and tested for its inhibition action against DPP-4.

Methodology

Molecular Design: The chromone function (P1) was modified by different side chains (P2) to fit DPP-4 was active binding site. There two main fragments (P1 and P2) were linked by two functions: hydrazone and amide leading to a combinatorial library of 256 compounds hydrazone and amide.

DPP-4 Template Preparation: A template of protein target (DPP-IV) was prepared from a crystallographic structure of human dipeptidyl peptidase IV (DPP-4, PDB entry code: 1x 70) bound to the inhibitor 715 (sitagliptin). The template 1 x 70 was added hydrogen and Gasteiger charges using AutoDockTools (ADT).

Ligand Preparation: The combinatory library of 254 structures containing two main fragments linked with hydrazone or amide functions was prepared. The 3D structures of all ligands were initially drawn, cleaned up by the ChemDraw Ultra version 11.0 and Chem 3D Ultra 11.0. program and then energy was minimized by MM2. All hydrogens were added and Gasteiger charges were assigned to each pdb file by using ADT 1.5.2 Gasteiger charge was nonpolar hydrogen was merged, aromatic carbons identified, Later, the rigid root and rotatable bonds were defined. The compounds in the library were docked with the contructed DPP-4 template.

Docking protocols: The running parameters used are as follows: number of Genetic Algorithm (GA) runs: 100, population size: 150, Maximum number of evaluation: 15,000,000 and maximum number of generation: 27000.

Synthesis: Thirteen chromone hydrazones (A1 – A13) were synthesized by condensation of chromones and 8 hydrazines in ethanol as shown in Scheme 1.
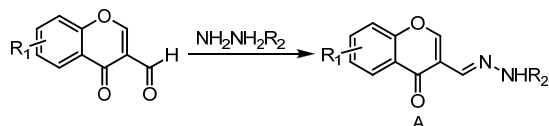
Scheme 1. Synthesis of chromone hydrazons A1-A13. Chromone derivatives with various hydrazines in ethanol. stir 2-4 hr., RT.

Chromone amides (B1-B8) were synthesized by condensation of chromones and amines with the aid of peptide coupling agents, CDI and DIC as shown in Scheme 2.
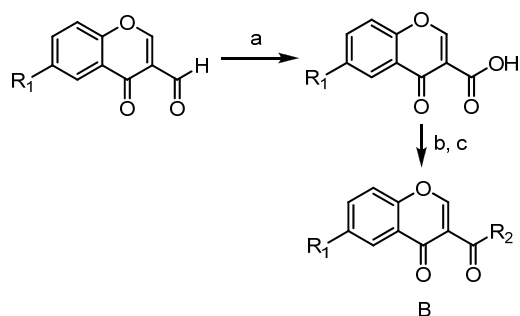
Scheme 2. Synthesis of chromone amides B1- B9 (a) NaOClO, H_2NSO_3H, H_2O, CH_2Cl_2, 0°C, 30mins or 5 hr. (b) CDI, DMAP, dried CH_2Cl_2, stir 1hr. (c) add R_2NH_2, stir overnight, RT.

The structure of synthesized compound was characterized by their melting points, FTIR, 1H NMR, 13C NMR, MS, and elemental analyses of C, H and N. Spectral data (FTIR, NMR, GC-MS and LC-MS) were compatible with the assigned structures in all cases.

DPP-4 inhibitory activity assay: The effects of synthesized compounds on the DPP-4 activity were evaluated in vitro. A fluorometric assay was employed to measure the DPP-4 activity by using gly-pro-aminomethylcoumarin (Gly-Pro-AMC) as substrate. The substrate was cleaved by the enzyme to release the fluorescent aminomethylcoumarin (AMC). The amount of the liberated AMC was measured by the fluorescent emission at wavelength of 460 nm after an excitation at wavelength of 380 nm. The assay was performed in a 96-black well plate and the sequential addition of reagent was buffer, enzyme, and sitagliptin (positive control) or test compounds. The assay mixtures were mixed well, and incubated at 37°C for 1 hr. The substrate was added in the final step, the fluorescent intensity (F) was measured and recorded.

The percent inhibition was determined using below equation.

$$\% \text{ Inhibition} = \frac{(F_{control} - F_{test\ compound}) \times 100}{F_{control}}$$

For IC_{50}, % inhibitions of test compounds in 3 -5 varied concentrations were determined. The IC_{50} value was obtained from linear regression plot between % inhibitions and concentrations of test compounds.

Results and Discussion

A combinatorial library of 254 Chromone-based compounds were designed and docked against DPP-4 template. The obtained nergies from docking were ranked. Twenty-two top ranking compounds or hit compounds were identified which are 13 chromone hydrazones and 9 chromone amides. Twenty-two identified hit compounds were synthesized and screened in vitro at 100 μM for their inhibitory action against extracted from human plasma. The result in Table 1 and Table 2 showed that chromone hydrazone A3 and chromone amide B3 were the most potent compounds. The IC_{50} of these two compounds were determined as shown in Table 3.

Table 1. Effect of chromone hydrazones on DPP-4

Cpd	R₁	R₂	Binding energy (kcal/mol)	% inhibition
A1	H	4-CF₃OPh	-6.53	15.36
A2	6-CH₃	4-CF₃OPh	-6.63	5.12
A3	6-CH₃	Ph	-6.86	37.12
A4	6-CH₃	4-FPh	-6.92	-4.22
A5	7-OAc	4-FPh	-7.49	9.13
A6	6-CH₃	4-CNPh	-7.93	1.83
A7	7-OAc	4-CNPh	-8.28	7.74
A8	H	2-COOHPh	-6.58	-4.45
A9	6-CH₃	2-COOHPh	-6.79	6.31
A10	H	4-COOHPh	-6.81	-2.01
A11	6-CH₃	4-COOHPh	-6.94	4.76
A12	H	2-ClPh	-6.94	-1.95
A13	6-CH₃	2-ClPh	-.7.36	-3.36

The binding modes of A3 and B3 were shown in Figure 1. The docked poses of A3 and B3 locate in the active DPP-4 binding site close to the catalytic triad Ser630 but the chromone cores are in the opposite direction. The un-substituted chromone core of B3 was able to locate in the small P1 pocket whereas the more bulky chromone nucleus of A3 from 7-methyl substitution is unable to locate in the P1 pocket.

Therefore the chromone core of A3 flips horizontally to occupy the bigger P2 pocket. Both compounds form one H-bonding interaction with Arg669 in chromone A3, the oxygen in chromone in Arg669. The chromone rings of A8, A9 and A12 flip vertically from these two pockets leading to weak interaction.

Table 2. Effect of chromone amides on DPP-4

Cpd	R_1	R_2	Binding energy (kcal/mol)	% inhibition
B1	6-CH$_3$		-7.74	7.44
B2	6-CH$_3$		-8.16	12.57
B3	H		-8.00	21.35
B4	6-CH$_3$		-8.54	7.36
B5	6-CH$_3$		-7.71	48.86**
B6	H		-6.46	-2.68
B7	6-CH$_3$		-6.74	3.92
B8	H		-8.84	8.69
B8	6-CH$_3$		-8.78	9.14

** High blank

Table 3. IC$_{50}$ and docking results

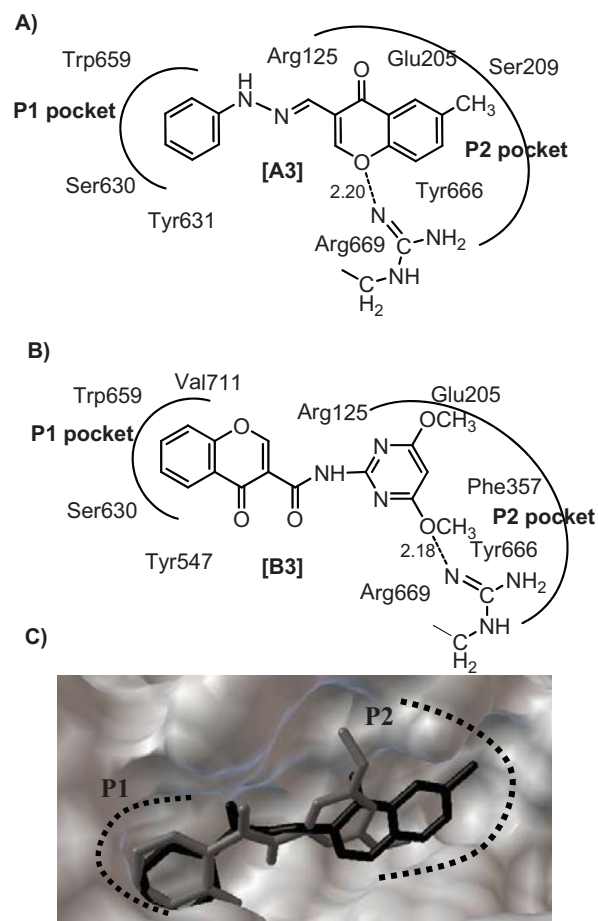|	A3	B3
Binding energy (kcal/mol)	-6.86	-8.00
% Member in cluster	60	79
Interacted amino acids (hydrophobic)	Ser209, Phe357, Ser630, Tyr631, Tyr662,Tyr666	Arg125, Phe357, Ser630, Tyr631, Val656, Tyr666, Val711
H-bond (distance Å)	Arg669(2.20)	Arg669(2.18)
IC$_{50}$ (μM)	153. 53	397.66

Figure 1. The binding modes of (A) chromone hydrazone A3, (B) chromone amide B3 and (C) the overlay docked poses of A3 (black) and B3 (gray) showing the opposite orientation of chromone nucleus.

Conclusions

In summary, two series of chromone hydrazones (A) and chromone amide derivatives (B) were designed and screened in silico. Thirteen identified hit compounds from docking were synthesized and evaluated for the inhibitory action against DPP-4. 6-Methyl-3-((2-phenyl hydrazono)methyl)-4H-chromen-4-one (A3) and N-(3,5-di methoxyphenyl)-4-oxo-4H-chromene-3-carboxamide (B3) were found to be the promising leads with IC$_{50}$ of 153.53 μM and 397.66 μM, respectively. These two compounds are considered as new leads for further to increase the potency to nM level.

Acknowledgements

References

[1] J.J. Neumiller, P.S. Odegard, J.R White, S.M.Jr. Setter and R.K. Campbell, *The Diabetes Educator.* **34** (2008), pp. 183-200.

[2] J.J. Holst, C.F. Deacon, T. Vilsboll, T. Krarup and S. Madsbad, *Trends Mol Med.* **14** (2008), pp. 161-168.

[3] E.J. Verspohl, *Pharmacol Therapeut.* **124** (2009), pp. 113–138.

[4] D.J. Drucker, *Cell Metab.* **3** (2006), pp. 153–165.

[5] L.L. Baggio and D.J. Drucker, Gastroenterology. **132** (2007), pp. 2131-2157.

[6] M..M. Combettes, *Curr Opin Pharmacol.* **6** (2006), pp. 598-605.

[7] K.M. Khan, N. Ambreen, S. Hussain, S. Perveen and M.I. Choudhary, *Bioorgan Med Chem.* **17** (2009), pp. 1–26.

[8] B.D. Wang, Z.Y. Yang and Tr. Li, *Bioorgan Med Chem.* **14** (2006), pp. 6012-6021.

Design and Synthesis of Chromone Derivatives as Topoisomerase I Inhibitors

C. Maicheen[1], J. Jittikoon[2] and J. Ungwitayatorn[1]*

[1] Department of Pharmaceutical Chemistry, Faculty of Pharmacy, Mahidol University, 447 Sri-Ayudhya Road,
Rajathevi, Bangkok 10400, Thailand
[2] Department of Biochemistry, Faculty of Pharmacy, Mahidol University, 447 Sri-Ayudhya Road,
Rajathevi, Bangkok 10400, Thailand

* E-mail: pyjuw@mahidol.ac.th

Abstract: The new chromone structures were designed based on the docking simulation study using AutoDock program. From the docking simulation study, a flavonoid compound, the known topoisomerase inhibitor, myricetin showed good binding interaction with DNA topoisomerase I. The docking result supported the agarose gel assays, which showed that myricetin was the most potent topoisomerase I and II inhibitor (IC$_{50}$ 11.9 μg/ml against both enzymes) among several studied flavonoids [1]. In order to obtain the better binding inhibitor, the structures of myricetin-related chromone compounds were modified by adding the steric substituent consisting of substituted benzyl group and substituted benzoyl group to form hydrogen bond to the surrounding amino acids. Compound 11c was the best docked ligand for DNA topoisomerase I with binding energy -11.39 kcal/mole. The hydrogen bonding between compound 11c and Arg364, Lys425 and Thr718 was observed. The designed structures were synthesized using 2 main steps. Firstly, the chromone structure was prepared by one-pot cyclization using 1,8-diazabicyclo[5.4.0]undec-7-ene (DBU) as catalyst. Secondly, the steric group was added by esterification or etherification reactions. The synthesized compounds will be tested for their inhibitory activity against topoisomerase I by gel electrophoresis using eukaryotic topoisomerase drug screening kit.

Introduction

Topoisomerases are enzymes which relieve the torsional stress in the DNA helix that is generated as a result of replication, transcription, and other nuclear processes [2]. Topoisomerases are classified as type I and II on the basis of two different sequences and functions [3]. All topoisomerases act through an active-site tyrosine residue to cleave the phosphodiester backbone and form a covalent phosphotyrosine intermediate with the DNA. Type I topoisomerase is a 100 kDa monomeric enzyme, which acts by introducing transient single-stranded breaks, whereas type II topoisomerase is a 106-108 kDa dimeric enzyme which introduces transient double-stranded breaks and requires ATP as a cofactor [3-6].

Human topoisomerase I cleaves a single DNA strand through transesterification of Tyr723. This reaction is carried out via a nucleophilic attack of an active site tyrosine OH group which becomes covalently bound to the 3'-phosphate of DNA at the site of nicking and forms the cleavage complex (Figure 1). This transient break allows helical supertension to be released by the unwinding of positively supercoiled DNA or the rewinding of the negatively supercoiled DNA [2,3,7].

The natural product camptothecin, an alkaloid extracted from *Camptotheca acuminate* which exhibits potent antitumor activity, has been shown to target topoisomerase I by binding to the covalent topoisomerase I-DNA complex with Arg364, Asp533 and Asn722 using hydrogen bonding interactions [2, 3, 8-10].
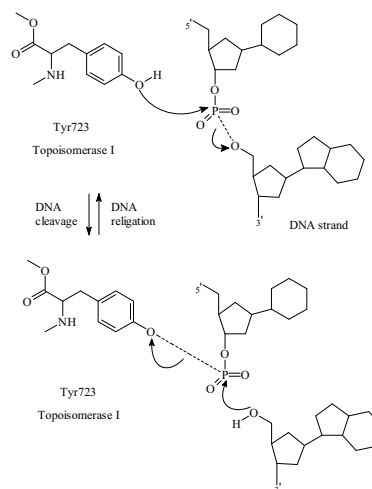

Figure 1. DNA strand breaking by topoisomerase I.

Among a large number of flavonoids, only certain flavones are potent and selective inhibitors of topoisomerase I-catalyzed DNA religation. Their ability to stabilize the covalent topoisomerase I-DNA complex *in vitro* and in living cells is similar to that of the known topoisomerase I inhibitor camptothecin, although the mechanism of interaction appears to be different. Thus, flavonoids seem to be an ideal model for the study of structural requirements for selective interaction with DNA cleavage and religation reactions catalyzed by topoisomerase I that may serve for the development of new anti-cancer drugs [11].

From the program docking simulation study using AutoDock, a flavonoid compound, myricetin showed good binding interaction with DNA topoisomerase I.

The binding and docking energy values were -11.70 and -12.00 kcal/mole, respectively. In order to find more potent inhibitor, the structure of myricetin was modified by adding steric substituent at ring A. The obtained modified compound, M31 exhibited both binding energy (-14.50 kcal/mole) and docking energy (-14.30 kcal/mole) better than myricetin. The hydrophobic interaction between the added phenyl ring of M31 and Ile535 was observed (Figure 2) [12].
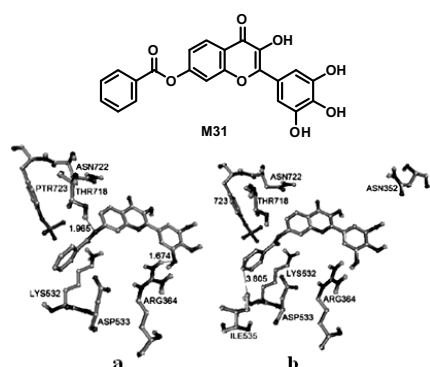

Figure 2. The interaction between DNA topoisomerase I (1T8I) and M31 showing: (a) hydrogen bonding interaction; (b) hydrophobic interaction.

Since myricetin contains six OH groups (Figure 3), the attempt to add the steric substituent to the OH might result in obtaining many undesired products, therefore chromone compounds with only one OH group are used as a starting material in this study.
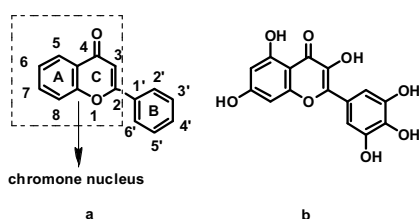
Figure 3. (a) General flavonoid structure. (b) Myricetin structure.

Materials and Methods

1. Docking study of chromone derivatives with topoisomerase I

The molecular structures of all compounds were modeled with SYBYL 8.0 molecular modeling program (Tripos Associates, Saint Louis, MO) on an Indigo Elan workstation (Silicon Graphics Inc., Mountain View, CA) using the sketch approach. Firstly, each structure was energy minimized using the standard Tripos force field (Powell method and 0.05 kcal/mol.Å energy gradient convergence criteria) and electrostatic charge was assigned by the Gasteiger-

Hückel method. These conformations were used as starting conformations to perform docking. The crystal structures of topoisomerase I complexed with inhibitor were obtained from the Brookhaven Protein Database (PDB). The inhibitor structures were firstly removed from the complex structures, and added polar hydrogen parameters. The grid maps representing the protein in the actual docking process were calculated with AutoGrid. The docking calculations were performed using AutoDock program version 4.0 [13]. The docking study was carried out using the Lamarckian genetic algorithm, applying a standard protocol, with an initial population of 150 randomly placed individuals, a mutation rate of 0.02, and a crossover rate of 0.80. One hundred independent docking runs were carried out for each ligand. Results differing by less than 2.0 Å in positional root mean-square deviation (rmsd) were clustered together and represented by the result with the most favorable free energy of binding.
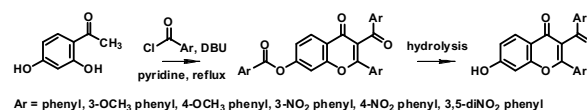
2. Synthesis

The synthetic pathway was carried out in 2 main steps. The first step was to construct the chromone structure by one-pot cyclization reaction [14]. The second step was for adding steric group to the chromone via esterification or etherification (O-alkylation) reaction.

Step 1:
Cyclization (Scheme 1)

The cyclization of phenolic ketones was carried out in one step by reacting with aroyl chloride in the presence of 1,8-diazabicyclo[5,4,0]undec-7-ene (DBU), outline as shown in Scheme 1. The intermediate chromone ester was then hydrolyzed to yield the desired chromone derivatives.
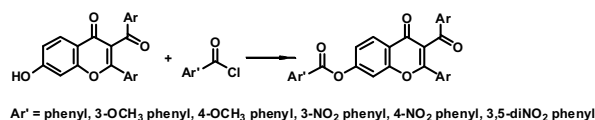

Ar = phenyl, 3-OCH₃ phenyl, 4-OCH₃ phenyl, 3-NO₂ phenyl, 4-NO₂ phenyl, 3,5-diNO₂ phenyl

Scheme 1. Synthesis of chromone derivatives.

Step 2:
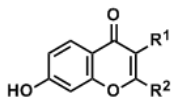Esterification (Scheme 2)

The esterification was performed by the reaction of chromone compound and acid chloride [15].

Ar' = phenyl, 3-OCH₃ phenyl, 4-OCH₃ phenyl, 3-NO₂ phenyl, 4-NO₂ phenyl, 3,5-diNO₂ phenyl

Scheme 2. Esterification of chromone derivatives.

Table 1: Structures of the designed chromone derivatives (compounds 1-12) and their binding energies.

Cpd	R^1	R^2	Binding energy* (kcal/mole)
1	H	phenyl	-5.01
2	H	3′-(OCH$_3$)-phenyl	-5.81
3	H	4′-(OCH$_3$)-phenyl	-5.86
4	H	3′-(NO$_2$)-phenyl	-5.43
5	H	4′-(NO$_2$)-phenyl	-5.88
6	H	3′,5′-(diNO$_2$)-phenyl	-5.90
7	benzoyl	phenyl	-5.97
8	3″-(OCH$_3$)-benzoyl	3′-(OCH$_3$)-phenyl	-6.16
9	4″-(OCH$_3$)-benzoyl	4′-(OCH$_3$)-phenyl	-6.68
10	3″-(NO$_2$)-benzoyl	3′-(NO$_2$)-phenyl	-7.09
11	4″-(NO$_2$)-benzoyl	4′-(NO$_2$)-phenyl	-6.36
12	3″,5″-(diNO$_2$)-benzoyl	3′,5′-(diNO$_2$)-phenyl	-7.14

Table 2: Structures of the designed chromone derivatives (compounds in series 7-12) and their binding energies.
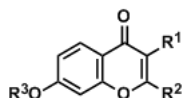

Cpd	R^1	R^2	R^3	Binding energy * (kcal/mole)
7	benzoyl	phenyl	H	-5.97
7a	benzoyl	phenyl	benzyl	-8.26
7b	benzoyl	phenyl	3‴-(OCH$_3$)-benzyl	-8.33
7c	benzoyl	phenyl	4‴-(OCH$_3$)-benzyl	-8.21
7d	benzoyl	phenyl	3‴-(OCH$_3$)-benzoyl	-8.77
7e	benzoyl	phenyl	4‴-(OCH$_3$)-benzoyl	-8.82
7f	benzoyl	phenyl	3‴-(NO$_2$)-benzoyl	-8.62
7g	benzoyl	phenyl	4‴-(NO$_2$)-benzoyl	-8.56
7h	benzoyl	phenyl	3‴,5‴-(diNO$_2$)-benzoyl	-7.25
8	3″-(OCH$_3$)-benzoyl	3′-(OCH$_3$)-phenyl	H	-6.16
8a	3″-(OCH$_3$)-benzoyl	3′-(OCH$_3$)-phenyl	benzyl	-7.62
8b	3″-(OCH$_3$)-benzoyl	3′-(OCH$_3$)-phenyl	3‴-(OCH$_3$)-benzyl	-7.50
8c	3″-(OCH$_3$)-benzoyl	3′-(OCH$_3$)-phenyl	4‴-(OCH$_3$)-benzyl	-7.64
8d	3″-(OCH$_3$) benzoyl	3′-(OCH$_3$)-phenyl	benzoyl	-8.42
8e	3″-(OCH$_3$)-benzoyl	3′-(OCH$_3$)-phenyl	3‴-(OCH$_3$)-benzoyl	-8.72
8f	3″-(OCH$_3$)-benzoyl	3′-(OCH$_3$)-phenyl	4‴-(OCH$_3$)-benzoyl	-6.91
9	4″-(OCH$_3$)-benzoyl	4′-(OCH$_3$)-phenyl	H	-6.68
9a	4″-(OCH$_3$)-benzoyl	4′-(OCH$_3$)-phenyl	benzyl	-7.50
9b	4″-(OCH$_3$)-benzoyl	4′-(OCH$_3$)-phenyl	3‴-(OCH$_3$)-benzyl	-7.95
9c	4″-(OCH$_3$)-benzoyl	4′-(OCH$_3$)-phenyl	4‴-(OCH$_3$)-benzyl	-7.86
9d	4″-(OCH$_3$)-benzoyl	4′-(OCH$_3$)-phenyl	benzoyl	-8.11
9e	4″-(OCH$_3$)-benzoyl	4′-(OCH$_3$)-phenyl	3‴-(OCH$_3$)-benzoyl	-7.97
9f	4″-(OCH$_3$)-benzoyl	4′-(OCH$_3$)-phenyl	4‴-(OCH$_3$)-benzoyl	-8.93
10	3″-(NO$_2$)-benzoyl	3′-(NO$_2$)-phenyl	H	-7.09
10a	3″-(NO$_2$)-benzoyl	3′-(NO$_2$)-phenyl	benzyl	-7.30
10b	3″-(NO$_2$)-benzoyl	3′-(NO$_2$)-phenyl	benzoyl	-7.70
10c	3″-(NO$_2$)-benzoyl	3′-(NO$_2$)-phenyl	3‴-(NO$_2$)-benzoyl	-9.35
10d	3″-(NO$_2$)-benzoyl	3′-(NO$_2$)-phenyl	4‴-(NO$_2$)-benzoyl	-9.39
10e	3″-(NO$_2$)-benzoyl	3′-(NO$_2$)-phenyl	3‴,5‴-(diNO$_2$)-benzoyl	-6.94
11	4″-(NO$_2$)-benzoyl	4′-(NO$_2$)-phenyl	H	-6.36
11a	4″-(NO$_2$)-benzoyl	4′-(NO$_2$)-phenyl	benzyl	-8.81
11b	4″-(NO$_2$)-benzoyl	4′-(NO$_2$)-phenyl	benzoyl	-9.29
11c	4″-(NO$_2$)-benzoyl	4′-(NO$_2$)-phenyl	3‴-(NO$_2$)-benzoyl	-11.39
11d	4″-(NO$_2$)-benzoyl	4′-(NO$_2$)-phenyl	4‴-(NO$_2$)-benzoyl	-10.54
11e	4″-(NO$_2$)-benzoyl	4′-(NO$_2$)-phenyl	3‴,5‴-(diNO$_2$)-benzoyl	-6.67
12	3″,5″-(diNO$_2$)-benzoyl	3′,5′-(diNO$_2$)-phenyl	H	-7.14
12a	3″,5″-(diNO$_2$)-benzoyl	3′,5′-(diNO$_2$)-phenyl	benzyl	-6.92
12b	3″,5″-(diNO$_2$)-benzoyl	3′,5′-(diNO$_2$)-phenyl	benzoyl	-6.75
12c	3″,5″-(diNO$_2$)-benzoyl	3′,5′-(diNO$_2$)-phenyl	3‴-(NO$_2$)-benzoyl	-8.87
12d	3″,5″-(diNO$_2$)-benzoyl	3′,5′-(diNO$_2$)-phenyl	4‴-(NO$_2$)-benzoyl	-7.56
12e	3″,5″-(diNO$_2$)-benzoyl	3′,5′-(diNO$_2$)-phenyl	3‴,5‴-(diNO$_2$)-benzoyl	-5.56

* The binding energy values are obtained from AutoDock 4.0.

PACCON2011 (Pure and Applied Chemistry International Conference 2011)

Etherification (Scheme 3)

The etherification was carried out by Williamson ether synthesis using chromone compound and substituted benzyl chloride [16].

Ar' = phenyl, 3-OCH$_3$ phenyl, 4-OCH$_3$ phenyl
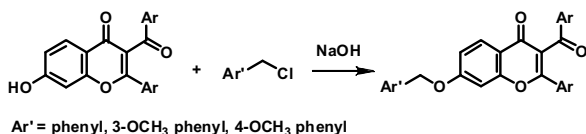
Scheme 3. The Williamson ether synthesis of chromone derivatives.

Results and Discussion

The docking simulation technique was performed using AutoDock 4.0 program with designed compounds. Table 1 summarizes the result of the docking study presented as binding energy.

Compounds 7-12 (R_1 = substituted benzoyl) showed the better binding energy than compounds 1-6 (R_1 = H), therefore compounds 7-12 were selected for further modification by adding steric group at the OH group as shown in Table 2.

Introduction of steric group at R_3 such as compound 7e (R_3 = 4'''-(OCH$_3$)-benzoyl), compound 8e (R_3 = 3'''-(OCH$_3$)-benzoyl), compound 9f (R_3 = 4'''-(OCH$_3$)-benzoyl), compound 10d (R_3 = 4'''-(NO$_2$)-benzoyl), compound 11c (R_3 = 3'''-(NO$_2$)-benzoyl) and compound 12c (R_3 = 3'''-(NO$_2$)-benzoyl) led to the higher binding energy than unmodified compound 7, 8, 9, 10, 11 and 12 (R_3 = H), respectively.

Compound 11c was the best docked ligand for DNA topoisomerase I with binding energy -11.39 kcal/mole. The hydrogen bondings between compound 11c and Arg364, Lys425 and Thr718 were observed (Figure 3).
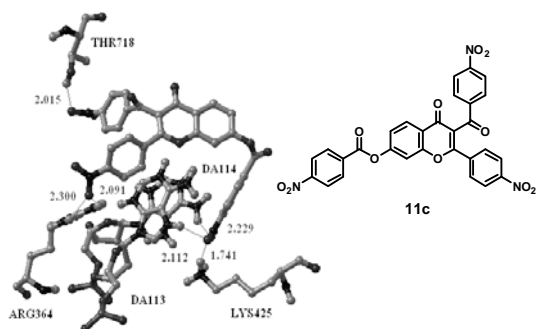

Figure 3. The hydrogen bonding between compound 11c and DNA topoisomerase I (1T8I).

Compounds 7a, 7d-7g, 8a, 8b, 8d, 8e, 9b, 9d, 9e, 9f, and 11b have been successfully synthesized and their structures verified by spectroscopic techniques. These compounds will be tested for their inhibitory activity against topoisomerase I by gel electrophoresis using eukaryotic topoisomerase drug screening kit in order to confirm the docking results.

Conclusions

In this study the docking simulation technique was used to predict the inhibitory activity against the target macromolecule, additionally the binding mode of designed compounds were observed. The binding energies of the designed compounds-enzyme interactions are important to describe how fit the ligand binds to the target macromolecule. The obtained results are useful to understand the structural features required to enhance the inhibitory activity.

References

[1] A. Constantinou, R. Mehta, C. Runyan, K. Rao, A. Vaughan and R. Moon, *J Nat Prod.* **58**(1995), pp.217-25.

[2] B.L. Staker, M.D. Feese, M. Cushman , Y. Pommier, D. Zembower, L. Stewart, et al, *J Med Chem.* **48**(2005), pp. 2336-2345.

[3] A. Lauria, M. Ippolito and A. Almerico, *J Mol Model.* **13**(2007), pp.393-400.

[4] Y. Pommier, *Nat Rev Cancer.* **10**(2006), pp.789-802.

[5] K. Padget, R.Carr, A.D.J. Pearson, M.J. Tilby and C.A. Austin, *Biochem Pharmacol.* **59**(2000), pp.629-38.

[6] D.A. Burden and N. Osheroff, *Biochim Biophys Acta.* **1400**(1998), pp.139-154.

[7] C. Bailly, *Crit Rev Oncol Hematol.* **45**(2003), pp.91-108.

[8] M.R. Redinbo, L. Stewart, P. Kuhn, J.J. Champoux and W.G. Hol, *Science.* **279**(1998), pp.1504-13.

[9] C. Marchand, S. Antony, K.W. Kohn, M. Cushman, A. Ioanoviciu, B.L. Staker, et al, *Mol Cancer Ther.* **5**(2006), pp.287-95.

[10] B.L. Staker, K. Hjerrild, M.D. Feese, C.A. Behnke, A.B. Burgin and L. Stewart, *Proc Natl Acad Sci.* **99**(2002), pp.15387-15392.

[11] F. Boege, T. Straub, A. Kehr, C. Boesenberg, K. Christiansen, A. Andersen, et al, *J Biol Chem.* (1996), pp.2262-2270.

[12] N. Phosrithong and J. Ungwitayatorn, *Med Chem Res.* **19**(2009), pp.817-835.

[13] http://autodock.scripps.edu

[14] C. Riva, C. De Toma, L. Donadel, C. Boi, R. Pennini, G. Motta, et al, *Synthesis.* (1997), pp.195-201.

[15] J. McNulty, V. Krishnamoorthy and A. Robertson, *Tetrahedron Lett.* **49**(2008), pp. 6344-6347.

[16] R.G. Stabile and A.P. Dicks, *J Chem Educ.* **80**(2003), pp.313-315.

Syntheses of TADDOL–Anthracene Adduct as Chiral Catalyst for Use in Asymmetric Addition Reactions

D. Nim-anussornkul, P. Wiriyasuksawat and P. Meepowpan*

Department of Chemistry, Faculty of Science, Chiang Mai University, Chiang Mai, Thailand.

* Corresponding Author E-Mail Address: puttinan@chiangmai.ac.th

Abstract: The new chiral catalyst, TADDOL–anthracene adduct (–)-(11R)-1, is easily synthesized through the use of enantiomerically pure form of the versatile dimethyl itaconate–anthracene adduct [(+)-(11S)-2] as starting material. The key steps of these syntheses are the tandem aldol–lactonization and reduction with LAH to obtain the adduct in moderate yields. This catalyst will be used as chiral catalysts in reduction with NaBH₄ to the β-keto diester [(±)-3].

Introduction

The chiral diols which were acquired from the optically active tartaric acid and Grignard reagents, TADDOLs (α,α,α',α'-tetraaryl-1,3-dioxolane-4,5-di methanols), are the most effective chiral catalysts for asymmetric synthesis[1], for instance, hetero Diels–Alder reactions[2], vinylogous Mukaiyama–aldol reactions[3], oxidation reaction[4], nucleophilic addition to C=O double bonds. In 2009, Ajay and co-workers have reported the efficient catalyst, racemic anthracene–based diol [(±)-4], for Ullmann coupling for the formation of diaryl and alkyl aryl ethers through C–O bond formation in acetonitrile under very mild conditions[5]. Furthermore, Sanhes and coworkers have reported the synthesis of the novel chiral diphosphite ligands (5) and their complexes of rhodium and palladium which have anthracene group as the main skeleton. These two novel ligands, palladium and rhodium, were examined in asymmetric allylic alkylation of rac-3-acetoxy-1,3-diphenyl-propene and asymmetric hydroformylation in 90% and 51% ee respectively[6].
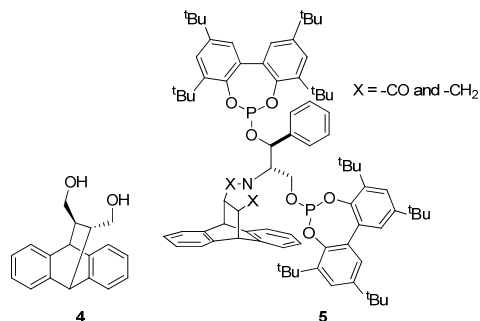

Figure 1. Chemical structure of (±)-diol CuI complex (4)[5] and chiral diphosphites ligands (5)[4]

The goal of this research is to design and synthesize the new chiral catalyst, TADDOL–anthracene adduct (11R)-1 which were prepared by

modification of the versatile dimethyl itaconate–anthracene adduct [(+)-(11S)-2] in enantio-merically pure form. This new chiral catalyst will be applied in reduction of the β-keto diester [(±)-3] by using NaBH₄.
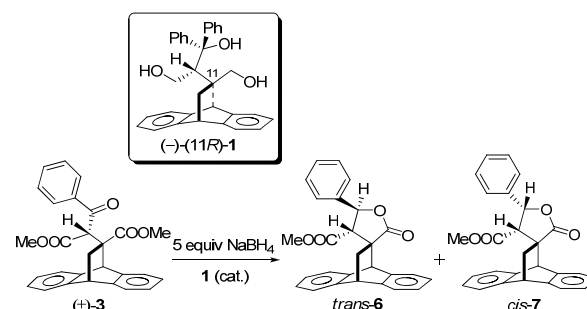

Figure 2. The reduction of the β-keto diester [(±)-3] using TADDOL–anthracene 1 catalyst

Materials and Methods

General materials and experiments: All reactions were carried out under nitrogen. Unless otherwise noted, materials were obtained from commercial suppliers and used without further purification. Melting points were determined by using a Gallenkamp Electrothermal apparatus and were uncorrected. The ¹H and ¹³C NMR spectra were recorded on Bruker DRX 400 MHz spectrometers and chemical shifts were given in ppm downfield from tetramethylsilane (TMS). All NMR spectra were measured in CDCl₃ and chemical shifts were reported as δ-values in parts per million (ppm) relative to residue CHCl₃ as internal reference (¹H: δ 7.26, ¹³C: δ 77.00) and coupling constants (J values) were reported in hertz (Hz). Peak multiplicities are indicated as follows: s (singlet), d (doublet), t (triplet), dt (doublet of triplets), ddd (doublet of doublet of doublets) and m (multiplet). Infrared spectra were taken with a FT-IR model TENSER 27 (Bruker) spectrometer and absorption frequencies were reported in reciprocal centimeters (cm⁻¹). Mass spectra (electrospray ionization mode, ESI-MS) were measured on a micromass Q-TOF-2™ (Waters) spectrometer. Flash column chromatography was performed employing Merck silica gel 60 and Merck silica gel 60H. Preparative thin layer chromatography (PLC) plates were carried out using Merck silica gel 60 PF₂₅₄. Analytical thin layer chromatography was performed with Merck silica gel 60 F₂₅₄ aluminum plates. Solvents were dried over CaH₂ and distilled before

used. Tetrahydrofuran (THF) was freshly distilled from sodium and benzophenone ketyl under nitrogen. Diisopropylamine was distilled over CaH_2 and stored under nitrogen. n-Butyllithium was purchased from Fluka and Across as solution in hexane and titrated periodically according to the 2,5-dimethoxybenzyl alcohol method. Ethyl bromide was distilled over P_2O_5 and distilled before used.

Synthesis of tetrahydro-4′-carbomethoxy-5′-diphenyl-2′-furanone-3′-spiro-11-9,10-dihydro-9,10-ethanoanthracenes: To a 100 mL round-bottomed flask equipped with a magnetic stirrer bar, fitted with a three-way stopcock and nitrogen inlet. n-Butyllithium (1.30 mL, 1.82 mmol, 1.4 M in hexane) was added to a stirring solution of diisopropylamine (0.30 mL, 2.18 mmol) in THF (5 mL) at –78 °C, then stirred at 0 °C for 1 h. To the LDA solution, dimethyl itaconate–anthracene adduct [(+)-(11S)-2] (1.52 mmol) in THF (10 mL) was added at –78 °C and stirred at 0 °C for 2 h. At –78 °C, benzophenone (1.2 equiv) was added to the reaction mixture and left stirring at room temperature for overnight. The resulting mixture was quenched with 10% HCl and extracted with CH_2Cl_2 (3x15 mL). The combined organic layer were dried ($MgSO_4$), filtered and concentrated *in vacuo*. Purification of the residue by flash column chromatography (EtOAc /CH_2Cl_2/hexane = 0.5 : 1 : 8.5 as eluent) afforded two diastereomers adducts, (+)-(11R)-8 as major product and (–)-(11R)-9 as minor product.

Tetrahydro-4′-carbomethoxy-5′-diphenyl-2′-fura none-3′-spiro-11-9,10-dihydro-9,10-ethanoanthra cenes (8 and 9). Compound (+)-(11R)-8 (64%): white crystals; mp 248.8–250.4 °C (CH_2Cl_2/hexane); R_f (EtOAc/ CH_2Cl_2/hexane = 0.5 : 1 : 8.5) 0.19; δ_H (400 MHz, $CDCl_3$) 1.40, 1.58, 4.12 (3H, ABX system, J = 13.2, 3.1, 2.3 Hz, CH_2, ArCH), 3.30 (3H, s, COOMe), 3.40 (1H, s, CHCOOMe), 4.70 (1H, s, ArCH), 6.98–7.46 (18H, m, ArH); δ_C (100.6 MHz, $CDCl_3$) 42.9, 43.9, 48.1, 50.5, 51.3, 64.7, 86.1, 122.3, 123.8, 124.9, 125.0, 125.6, 125.8, 126.2, 126.7, 127.4, 127.5, 127.9, 128.8, 139.5, 140.1, 140.7, 143.0, 143.1, 143.5, 169.8, 176.2.

Compound (–)-(11R)-9 (2%): white crystals; mp 245.9–246.2 °C (CH_2Cl_2/hexane); R_f (EtOAc/CH_2Cl_2/ hexane = 0.5 : 1 : 8.5) 0.17; δ_H (400 MHz, $CDCl_3$) 1.52, 2.44, 4.29 (3H, ABX system, J = 13.5, 3.5, 2.7 Hz, CH_2, ArCH), 3.07 (3H, s, COOMe), 3.72 (1H, s, CHCOOMe), 3.92 (1H, s, ArCH), 6.83–7.84 (18H, m, ArH); δ_C (100.6 MHz, $CDCl_3$) 38.5, 43.8, 48.7, 51.4, 52.9, 62.4, 86.5, 123.2, 123.8, 124.5, 125.0, 125.2, 125.5, 125.9, 126.8, 127.0,127.4, 128.1, 128.6, 129.3, 138.2, 138.8, 142.0, 143.0, 144.1, 144.4, 170.1, 175.7.

Reduction of tetrahydro-4′-carbomethoxy-5′-di phenyl-2′-furanone-3′-spiro-11-9,10-dihydro-9,10-ethanoanthracenes and their derivatives: The major product (+)-(11R)-8 (1.5259 g, 3.14 mmol) was added to a cooled (–78 °C) solution of LAH (20 equiv,

2.5720 g, 67.77 mmol) in THF (10 mL). The reaction mixture was stirred at room temperature for 3 days and then quenched by dropwise addition of acetone (5 mL). After that, the resulting solution was extracted with EtOAc (3x15 mL) and the combined organic portions were dried ($MgSO_4$), filtered and concentrated *in vacuo*. Purification of the residue by flash column chromatography (EtOAc/hexane = 1 : 9 as eluent) gave the TADDOL–anthracene adducts [(–)-(11R)-1] as the major products.

TADDOL–anthracene adduct (–)-(11R)-1 (42%): white solid; mp 202.7–204.2 °C (CH_2Cl_2/hexane); R_f (10% EtOAc/hexane) 0.08; δ_H (400 MHz, $CDCl_3$) 0.52, 1.36, 3.91 (3H, ABX system, J = 13.5, 3.0, 2.6 Hz, CH_2, ArCH), 2.25 (1H, s, CHCH2OH), 2.55, 4.25 (2H, d, J = 8.70 Hz, CH_2OH), 2.60 (1H, s, CHCH2OH), 3.97, 4.51 (2H, d, J = 12.90, 2.69 Hz, CHCH_2OH), 4.69 (1H, s, ArCH), 4.97 (1H, s, CHCH2OH), 5.69 (1H, s, Ph2COH) 7.05–7.36 (18H, m, ArH); δ_C (100.6 MHz, $CDCl_3$) 38.2, 44.6, 48.2, 49.6, 53.8, 61.6, 66.4, 82.2, 123.3, 123.3, 124.8, 125.4, 125.6, 126.0, 126.4, 126.3, 127.7, 128.3, 140.5, 141.5, 142.5, 145.0, 146.00, 149.6.

General procedure for the reduction of 11-carbomethoxy-11-(1′-benzoyl)methoxyacetyl-9,10-di hydro-9,10-ethanoanthracene by using $NaBH_4$: To a cooled solution (0 °C) of $NaBH_4$ (5 equiv) in THF was added the β-keto diester (3) and catalyst, respectively. The resulting mixture was stirred at 0 °C for 4 h and then quenched by addition of acetone (1 mL). After that, the resulting solution was extracted with CH_2Cl_2 (3x15 mL) and the combined organic portions were dried ($MgSO_4$), filtered and concentrated *in vacuo*. Purification of the residue by flash column chromatography (EtOAc/hexane = 1 : 9 as eluent) obtained *trans*-6 as the major product and *cis*-7 as the minor product.

Tetrahydro-4′-carbomethoxy-5′-phenyl-2′-fura none-3′-spiro-11-9,10-dihydro-9,10-ethanoanthra cenes (trans-6 and cis-7). Compound *trans*-6: white solid; mp 228.9–229.9 °C (CH_2Cl_2/hexane); R_f (10% EtOAc/hexane) 0.12; δ_H (400 MHz, $CDCl_3$) 2.11, 2.55, 4.38 (3H, ABX system, J = 12.5, 3.0, 2.4 Hz, CH_2, ArCH), 2.96 (3H, s, COOMe), 3.05 (1H, d, J = 10.2 Hz, CHCOOMe), 4.66 (1H, s, ArCH), 6.05 (1H, d, J = 10.2 Hz, CHO), 7.05–7.44 (13H, m, ArH); δ_C (100.6 MHz, $CDCl_3$) 37.4, 43.8, 46.7, 51.5, 51.8, 59.0, 78.4, 123.2, 123.4, 124.8, 125.2, 126.0, 126.3, 126.6, 126.7, 127.6, 128.6, 128.9, 137.2, 137.8, 139.9, 143.3, 168.1, 176.0.

Compound *cis*-7: white solid; mp 220–221 °C (CH_2Cl_2/hexane); R_f (10%EtOAc/hexane) 0.09; δ_H (400 MHz, $CDCl_3$) 2.20, 2.26, 4.49 (3H, ABX system, J = 12.4, 3.1, 2.3Hz, CH_2, ArCH), 2.54 (1H, d, J = 5.6 Hz, CHCOOMe), 3.28 (3H, s, COOMe), 4.77 (1H, s, ArCH), 5.51 (1H, d, J = 5.6 Hz, CHO), 6.97–7.56 (13H, m, ArH); δ_C (100.6 MHz, $CDCl_3$) 40.8, 43.8, 46.9, 50.9, 51.4, 61.0, 76.9, 124.0, 124.4, 125.4, 126.0,

126.3, 126.8, 127.5, 128.2, 128.5, 139.3, 140.7, 142.0, 169.3,176.7.

Results and Discussion

The TADDOL–anthracene adduct (−)-(11R)-**1** was synthesized by using dimethyl itaconate–anthracene adduts [(+)-(11S)-**2**] as starting materials *via* tandem aldol−lactonization to give the adduct (+)-(11R)-**8** as the major product and followed by reduction with LAH affording to the target catalyst, as shown in Scheme 1.
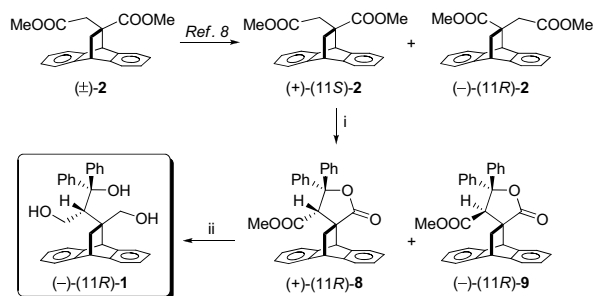
Scheme 1. Synthesis of TADDOL–anthracene adduct. *Reagents and conditions:* (i) a. 1.2 equiv LDA, THF, −78 °C to 0 °C, 2 h, b. 1.2 equiv benzophenone, 0 °C to rt, 2 h, c. 10% HCl; (ii) a. 20 equiv LiAlH$_4$, THF −78 °C to rt, 3 days, b. 10% HCl.

The stereochemistry of the major products **8** and minor products **9** can be explained through the chair–like transition states **C** and **D** wherein the steric repulsion between phenyl group and the anthracene ring are as shown in Scheme 2. Transition state **D** led to the minor product **9** from this steric effect, so transition state **C** which is stable more than **D** led to the major product **8**. The stereochemistry at proton H$_c$ position was determined by NOE experiment. In the case of the adduct **8**, the proton H$_c$ (δ 3.40 ppm) enhanced with H$_a$ more than H$_y$.
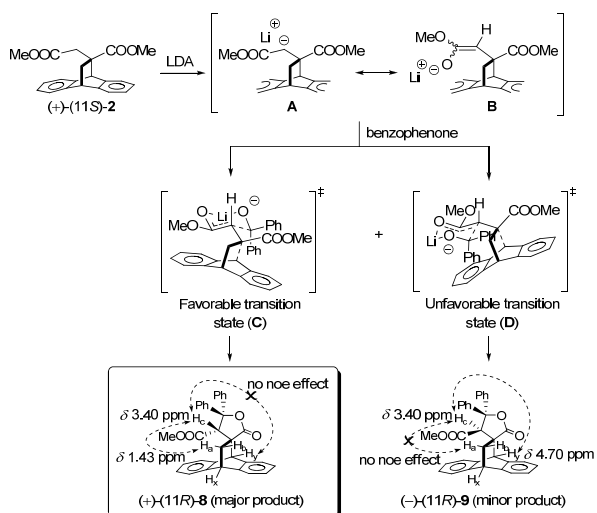
Scheme 2. Proposed mechanism of the adducts (+)-(11R)-**8** and (−)-(11R)-**9**.

Thus, the orientation of H$_c$ was on the upper face as

H$_a$. In the same way, NOE result of H$_c$ (δ 3.72 ppm) of adduct **9** showed the enhancement with H$_y$ but no NOE effect with H$_a$. It indicated that the orientation of H$_c$ was on the lower face as H$_y$ (Scheme 2).

The structure of TADDOL–anthracene catalyst (−)-(11R)-**1** could be confirmed by MM2 force field calculations for energy minimization from modeling program ChemBio3D Ultra 11.0 program. Besides, the orientation of the proton H$_c$ and H$_a$ were affirmed by the NOE experiment. The proton H$_c$ (δ 2.25 ppm) show the greatest interaction with H$_a$ more than H$_y$. Thus, the NOE correlation indicated that the proton H$_c$ oriented at the same face as H$_a$ (Figure 3).
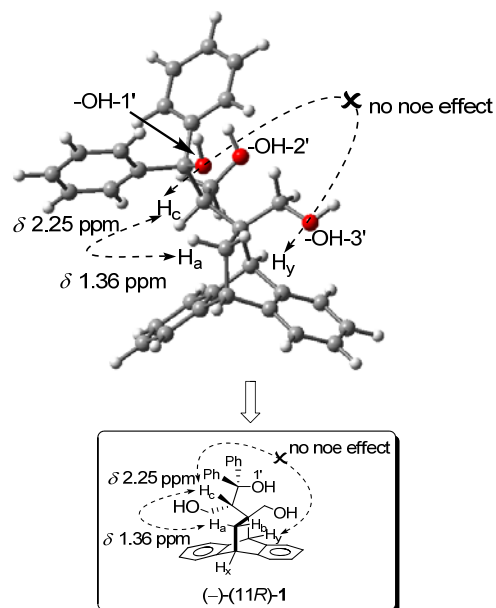

Figure 3. 3D structural conformation of TADDOL–anthracene adduct (−)-(11R)-**1** generated by MM2 force field calculations for energy minimization from modeling program ChemBio3D Ultra 11.0 and GaussView 3.09 program

From the study of the effect of TADDOL–anthracene (−)-(11R)-**1**, as catalyst, in reduction reaction of the β-keto diester by using NaBH$_4$ as the reducing agent gave the results as shown in Table 1.

Table 1. Reduction of the β-keto diester adduct **3** with various mol% of TADDOL–anthracene (−)-(11R)-**1**

Entry	conditions	n mol% of **1** (cat.)	Yield (%)[a]		Ratio trans:cis	%conversion
			trans-**6**	*cis*-**7**		
1	THF:MeOH (1:3)	–	61	17	3.5:1.0[b]	87
2	THF	1	18	9	2.0:1.0	87
3	THF	5	10	12	0.8:1.0	91
4	THF	10	14	10	1.4:1.0	98

[a] Isolated yield.
[b] Jongkol, R.; Choommongkol, R.; Tarnchompoo, B.; Nimmanpipug, P.; Meepowpan, P. *Tetrahedron* **2009**, *65*, 6382–6389.

In 2009, Jongkol and co-workers has reported the reduction of the β-keto diester adduct by NaBH$_4$ in THF:MeOH systems that obtained *tran*-**6** and *cis*-**7** in the highest diastereoselectivity (entry 1)[7]. Thus, we are interested to apply our catalyst, TADDOL–anthracene adduct (–)-(11*R*)-**1**, as catalyst instead of using MeOH in this reaction. The low concentration of catalyst (entry 2) afforded the ratio of *trans:cis* isomers in 2:1. On the other hand, when concentration of catalysts were increased (entry 2 and 3), the ratio of *trans:cis isomers* decreased to 1:1 of *trans:cis* isomers. On the contrary, percent conversion increased when the concentration of catalysts increased too. Surprisingly, the high concentration of catalyst will be obtained the percent yield of *cis*- more than *trans*- isomer.

Conclusions

The new chiral catalyst, TADDOL–anthracene adduct (–)-(11*R*)-**1**, would be applied as catalyst in low concentration (1 mol% of catalyst) for reduction of the β-keto diester. This catalytic system was successfully which increased the ratio of *cis*-isomer when decreasing of mol% of catalyst was used. On the other hand, we can expect that the use of other optically active form of TADDOL–antrhracene adduct (+)-(11*S*)-**1** will be increase the ratio of *trans*-isomer. In the future work, these two catalysts will be applied for asymmetric1,2-addition reaction of EtMgBr to benzaldehyde.

References

[1] For the reviews of the applications of TADDOLs and their derivatives: (a) D. Seebach, A. K. Beck, And A. Heckel, *Angew. Chem. Int. Ed.* **40** (2001), pp. 92–138; (b) H. Pellissier *Tetrahedron* **64** (2008), pp. 10279–10317.

[2] H. Du, D. Zhao, and K. Ding, *Chem. Eur. J.* **10** (2004), pp. 5964–5970.

[3] V. Bhasker Gondi, M. Gravel, and V. H. Rawal, *Org. Lett.* **7** (2005), pp. 5657–5660.

[4] W. Adam, A. K. Beck, A. Pichota, C. R. Saha-Moller, D. Seebach, N. Vogl, and R. Zhang, *Tetrahedron: Asymmetry* **14** (2003), pp. 1355–1361.

[5] A. B. Naidu, E. A. Jaseer, G. *J. Sekar, J. Org. Chem.* **74** (2009), pp. 3675–3679.

[6] D. Sanhes, A. Gual, S. Castillon, C. Claver, and M. Gomez, *Tetrahedron: Asymmetry* **20** (2009), pp. 1009–1014.

[7] R. Jongkol, R. Choommongkol, B. Tarnchompoo, P. Nimmanpipug, P. Meepowpan, *Tetrahedron* **65** (2009), pp. 6382–6389.

[8] P. Kongsaeree, P. Meepowpan, Y. Thebtaranonth, *Tetrahedron: Asymmetry* **12** (2001), pp. 1913–1922.

ฤทธิ์ทางชีวภาพและองค์ประกอบทางเคมีจากเหง้าประทัดดอย

BIOLOGICAL ACTIVITIES AND CHEMICAL CONSTITUENTS FROM THE RHIZOME OF *AGAPETES MEGACARPA*

สุวพร เหลืองขมิ้น [*1], สุกัญญา วงศ์พรชัย[1], พันทิวา พริ้งเพราะ[1], วรวิทย์ ทองแท้[2], จริยา อลงกรณ์โสภิต[3] และ วีระ วงศ์คำ[3]

Suwaporn Luangkamin*[1], Sugunya Wongpornchai[1], Phantiwa Phringphrao[1], Worawit Thongthae[2] Jariya Alongkornsopit[2] and Weerah Wongkham[3]

[1] Department of Chemistry, Faculty of Science, Chiang Mai University, Chiang Mai, 50200
email : suwaporn@chiangmai.ac.th
[2] Protected Area Regional Office 16, National Park Wildlife and Plant Conservation Department, Chiang Mai, 50100
[3] Department of Biology, Faculty of science, Chiang Mai University, Chiang Mai, 50200

บทคัดย่อ: นำส่วนสกัดหยาบเฮกเซน ส่วนสกัดหยาบเอทิลอะซิเตต และส่วนสกัดหยาบบิวทานอล ที่สกัด จากเหง้าของประทัดดอย (Agapetes megacarpa) ทดสอบความเป็นพิษต่อเซลล์ พบว่าส่วนสกัดหยาบ ทั้งหมด ออกฤทธิ์ยับยั้งเซลล์ไลน์ของมะเร็งเต้านม (MCF-7) ได้ดีมาก มีค่า ED_{50} อยู่ในช่วง 0.89-4.1 μg/mL และออกฤทธิ์ยับยั้งเซลล์ไลน์ของมะเร็งปอด (NCI-H1299) ได้ปานกลาง ในขณะที่ไม่แสดงความ เป็นพิษกับเซลล์ปกติ เมื่อนำส่วนสกัดหยาบนี้มาศึกษาองค์ประกอบทางเคมี โดยนำมาแยกด้วยวิธีทางโคร มาโทกราฟี ได้สารบริสุทธิ์ 5 สาร ได้แก่ 2,7-dihydroxyxanthone, lupeol, lupenone , 3-ketooleanane และ β-sitosterol ซึ่งพิสูจน์โครงสร้างโดยใช้เทคนิคทางสเปกโทรสโคปีและเปรียบเทียบข้อมูลกับสารที่ ทราบโครงสร้างแล้ว

Abstract: The crude hexane, ethyl acetate and butanol, extracted from the rhizome of *Agapetes megacarpa*, were screened for cytotoxic activities. All extracts exhibited high cytotoxicity against MCF-7 cell line with ED_{50} values between 0.89-4.1 μg/mL and showed medium activity against NCI-H1299 cell line whereas cytotoxicity against vero cell was not found. Chemical investigation of these extracts utilizing chromatographic separation and purification, afforded five compounds: 2,7-dihydroxyxanthone, lupeol, lupenone, 3-ketooleanane and β-sitosterol. The structures of these compounds were elucidated by analyzing their spectroscopic data and comparing with those of the known compounds.

Keywords: *Agapetes megacarpa*, Prathat Doi, cytotoxicity, triterpene, xanthone

สารไตรเทอร์พีนจากใบสะเภาลม *(Agapetes hosseana* Diels*)*

# TRITERPENES FROM THE LEAVES OF *AGAPETES HOSSEANA* DIELS.

พรพนา กรวงษ์วาล และสุวพร เหลืองขมิ้น*

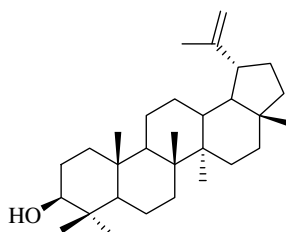Pornpana Kornwongwan and Suwaporn Luangkamin*
Department of Chemistry, Faculty of Science, Chiang Mai University, Chiang Mai, 50200

บทคัดย่อ: สะเภาลมเป็นพืชสมุนไพรที่อยู่ในวงศ์ Ericaceae เมื่อศึกษาองค์ประกอบทางเคมีในสารสกัด หยาบไดคลอโรมีเทนของใบสะเภาลม โดยนำมาแยกและทำให้บริสุทธิ์ด้วยเทคนิคทางโครมาโทกราฟี ได้ สารบริสุทธิ์ในกลุ่มเพนตะไซคลิกไตรเทอร์พีน 7 สาร คือ friedelin (**1**), epifriedelanol (**2**), friedelanol (**3**), lupeol (**4**), α-amyrin (**5**), β-amyrin (**6**) และ taraxerol (**7**) โครงสร้างของสารดังกล่าว วิเคราะห์ โดยใช้เทคนิคสเปกโทรสโคปีและเปรียบเทียบกับข้อมูลกับสารที่ได้มีรายงานมาแล้ว
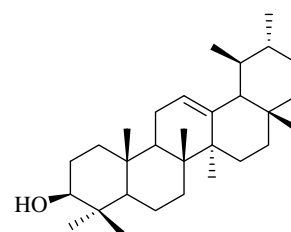
Abstract: *Agapetes hosseana* Diels, locally named Saphaolom, belongs to the family Ericaceae and has been used in traditional medicine.Chemical investigation of dichloromethane extract from the leaves of *Agapetes hosseana* Diels using chromatographic purification, afforded seven pentacyclic triterpenes which are friedelin (**1**), epifriedelanol (**2**), friedelanol (**3**), lupeol (**4**), α-amyrin (**5**), β-amyrin (**6**) and taraxerol (**7**). The structures of these compounds were elucidated by analysis of their spectroscopic data and compared with those of the known compounds.
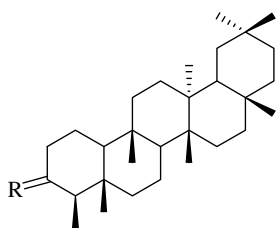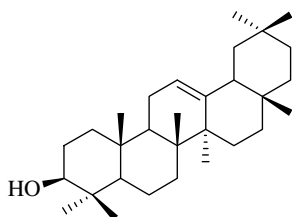
(**1**) friedelin, R= O
(**2**) epifriedelanol, R=3α–OH, 3β–H
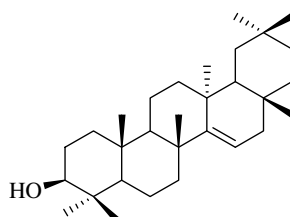(**3**) friedelanol, R=3β–OH, 3α–H

lupeol (**4**)

α–Amyrin (**5**)

β–Amyrin (**6**)

taraxerol (**7**)